Department of Electronic and Electrical Engineering

Cooperative Communication in Wireless Local Area Networks

by

Samir Gaber Sayed Abdel Gawad

A Thesis submitted in fulfilment of requirements for the degree of
Doctor of Philosophy of University College London

Communications and Information Systems Group
Department of Electronic and Electrical Engineering
University College London

Statement of Originality

I hereby declare that the research recorded in this thesis and the thesis itself was composed and originated by myself in the Department of Electronic and Electrical Engineering, University College London, except where otherwise indicated.

Samir Gaber Sayed

Acknowledgements

I would like to express my deepest thanks to my supervisor, Dr. Yang Yang, for his valuable advice, encouragement, patience, and his suggestions and constant support during this research.

I would like to thank the Egyptian Government for the generous scholarship which was awarded to me. Many thanks also go to the staff of the Egyptian Educational and Cultural Bureau at London for their help and support during the period of my study at the University College London.

I would like to express my sincere gratitude to Professor Izzat Darwazeh for his valuable comments and insightful advice. I also would like to thank my friends and colleagues, especially Ryan Grammenos and Ioannis Kanaras, in the Department of Electronic and Electrical Engineering at the University College London for their continuous help and encouragement.

I am grateful to Professor Mohamed Eladawy for his support and help. I would like to thank Prof. Ahmed Abdelwahab for his help and support during my MSc degree. I am also very much indebted to my friend Saad Roushdy for his help, support, understanding and friendly advice. My thanks also go to my friend Eltayeb Abass for his help and support during my stay in England.

Of course, my eternal thanks go to my parents, my wife, and my sons Zyad and Gasser for their patience, support and *love*. Without their

aid this work would never have come into existence. I dedicate this study to them.

Last but certainly not least, I wish to thank the following close friends: Amr Elsayed, Asem Shalaby, Ayman Ragab, Mohamed Saad, Raafat Elshaer, Sameh Salah, Sameh Salem, and Walid Al-atabany.

Abstract

The concept of cooperative communication has been proposed to improve link capacity, transmission reliability and network coverage in multiuser wireless communication networks. Different from conventional point-to-point and point-to-multipoint communications, cooperative communication allows multiple users or stations in a wireless network to coordinate their packet transmissions and share each other's resources, thus achieving high performance gain and better service coverage.

According to the IEEE 802.11 standards, Wireless Local Area Networks (WLANs) can support multiple transmission data rates, depending on the instantaneous channel condition between a source station and an Access Point (AP). In such a multi-rate WLAN, those low data-rate stations will occupy the shared communication channel for a longer period for transmitting a fixed-size packet to the AP, thus reducing the channel efficiency and overall system performance.

This thesis addresses this challenging problem in multi-rate WLANs by proposing two cooperative Medium Access Control (MAC) protocols, namely Busy Tone based Cooperative MAC (BTAC) protocol and Cooperative Access with Relay's Data (CARD) protocol. Under BTAC, a low data-rate sending station tries to identify and use a close-by intermediate station as its relay to forward its data packets at higher data-rate to

the AP through a two-hop path. In this way, BTAC can achieve cooperative diversity gain in multi-rate WLANs. Furthermore, the proposed CARD protocol enables a relay station to transmit its own data packets to the AP immediately after forwarding its neighbour's packets, thus minimising the handshake procedure and overheads for sensing and reserving the common channel. In doing so, CARD can achieve both cooperative diversity gain and cooperative multiplexing gain. Both BTAC and CARD protocols are backward compatible with the existing IEEE 802.11 standards.

New cross-layer mathematical models have been developed in this thesis to study the performance of BTAC and CARD under different channel conditions and for saturated and unsaturated traffic loads. Detailed simulation platforms were developed and are discussed in this thesis. Extensive simulation results validate the mathematical models developed and show that BTAC and CARD protocols can significantly improve system throughput, service delay, and energy efficiency for WLANs operating under realistic communication scenarios.

Contents

List of Figures

List of Tables

List of Abbreviations

ABI	Allied Business Intelligence
ACK	Acknowledgment
AP	Access Point
ARF	Auto Rate Fallback
BEB	Binary Exponential Backoff
BER	Bit Error Rate
BSS	Basic Service Set
BSSID	Basic Service Set Identifier
BTAC	Busy Tone based Cooperative MAC
BTS	Busy Tone Signal
CACK	Cooperative ACK
CARD	Cooperative Access with Relay's Data
CCA	Clear Channel Assignment
CCK	Complementary Code Keying
CCTS	Cooperative CTS
CFP	Contention Free Period
CoopMAC	Cooperative MAC
CRC	Cyclic Redundancy Code
CRTS	Cooperative RTS
CTS	Clear To Send
CW	Contention Window

DA	Destination Address
DBPSK	Differential Binary Phase Shift Keying
DCF	Distributed Coordination Function
DFS	Dynamic Frequency Selection
DIFS	Distributed Interframe Space
DQPSK	Quadrature Phase Shift Keying
DS	Distributed System
DSSS	Direct Sequence Spread Spectrum
EBTAC	Enhanced BTAC
EDCF	Enhanced Distributed Coordination Function
EIFS	Extended Interframe Space
ESS	Extended Service Set
FCC	Federal Communications Commission
FCS	Frame Check Sequence
FHSS	Frequency Hopping Spread Spectrum
GHz	Giga Hertz
HA	Helper Address
HIPERLAN	High-Performance Radio Local Area Network
HOL	Head-Of-Line
HTS	Helper-ready To Send
IBSS	Independent Basic Service Set
IFS	Interframe Space
IR	Infrared
ISM	Industrial, Scientific, and Medical
Kbps	Kilo bit per second
LBT	Listen Before Talk
MAC	Medium Access Control
Mbps	Mega bit per second

MF	Mobile Framework
MHz	Mega Hertz
MIMO	Multiple Input Multiple Output
MPDU	MAC Protocol Data Unit
MRTS	Modified Request To Send
MSDU	MAC service Data Unit
NACK	Negative Acknowledgment
NAV	Network Allocation Vector
OAR	Opportunistic Auto Rate
OFDM	Orthogonal Frequency Division Multiplexing
OMNET++	Objective Modular Network Testbed in C++
PBCC	Packet Binary Convolutional Code
PC	Point Coordinator
PCF	Point Coordination Function
PDAs	Personal Digital Assistants
pdf	probability density function
PER	Packet Error Rate
PHY	Physical layer
PIFS	Point Coordination Function Interframe Space
PLCP	Physical Layer Convergence Procedure
PMD	Physical Medium Dependent
PPDU	PLCP Protocol Data Unit
PSDU	PLCP Service Data Unit
PSM	Power Saving Mechanism
QoS	Quality of Service
RA	Receiver Address
RAAR	Relay-based Adaptive Auto Rate

RBAR	Receiver Based Auto Rate
rDCF	relay-enabled Distributed Coordination Function
rPCF	relay-enabled Point Coordination Function
RRTS	Relay Ready To Send
RSSI	Received Signal Strength Intensity
RTH	Ready To Help
RTS	Request To Send
SA	Source Address
SAP	Service Access Point
SFD	Frame Delimiter
SIFS	Short Interframe Space
SNR	Signal to Noise Ratio
TA	Transmitter Address
TI	Texas Instruments
TPC	Transmitter Power Control
WEP	Wired Equivalent Privacy
WFA	Wi-Fi Alliance
WLANs	Wireless Local Area Networks

List of Symbols

$ACK_{timeout}$	Time out of an ACk packet.
BER_{rd}	Bite error rate at data-rate R_{rd}.
BER_{sd}	Bite error rate at data-rate R_{sd}.
BER_{sr}	Bite error rate at data-rate R_{sr}.
BER_b	Bit error rate at base data-rate R_b.
$CTS_{timeout}$	Time out of a CTS packet.
CW_{max}	Maximum contention window size.
CW_{min}	Minimum contention window size.
D_{CTS}	Duration field of a CTS packet in BTAC protocol.
D_{data1}	Duration field of a data packet from a source to a relay in BTAC protocol.
D_{MRTS}	Duration field of a MRTS packet.
$DATA_{timeout}$	Time out a data packet.
$E[D_{b,i}]$	Average delay in the backoff stages.
$E[D_{c,i}]$	Average delay due to packet collision.
$E[D_{e,i}]$	Average delay due to erroneous transmission.
$E[D_{o,i}]$	average delay of overhearing during backoff.
$E[D_{s,i}]$	Average delay due to a successful transmission.
$E[D_i]$	Average packet delay of node i, where $i = 1, 2, ...N$.
$E[D_T]$	Average total delay of the network.
$E[PL]$	Average payload size in octets.

$E[T_{C_i}]$	Average collision duration at node i.
$E[T_{C_i}]$	Average erroneous transmission duration at node i.
$E[T_{S_i}]$	Average successful transmission duration at node i.
$E[T_C]$	Average time that the channel is sensed busy due to a collision.
$E[T_E]$	Average time the channel is sensed busy due to an erroneous transmission.
$E[T_I]$	Average duration of an empty slot time.
$E[T_S]$	Average time during which the channel is sensed busy due to a successful transmission.
$E_C^{(i)}$	Average energy consumption due to collision period of a node i.
$E_E^{(i)}$	Average energy consumption due to erroneous transmission of a node i.
$E_O^{(i)}$	Average energy consumption due to an overhearing transmission of a node i.
$E_S^{(i)}$	Average energy consumption due to a successful transmission of a node i.
E_{e1}^c	Energy consumption of a MRTS corruption.
E_{e2}^c	Energy consumption of a CTS corruption under cooperative transmission.
E_{e3}^c	Energy consumption of a data packet (source-relay) corruption.
E_{e4}^c	Energy consumption of a data packet (relay-AP) corruption.
E_{e5}^c	Energy consumption of an ACK corruption under BTAC protocol.

E_{e1}^{d}	Energy consumption of RTS corruption.
E_{e2}^{d}	Energy consumption of CTS corruption.
E_{e3}^{d}	Energy consumption of a data packet (source-AP) corruption.
E_{e4}^{d}	Energy consumption of ACK corruption.
$E_{B}^{(i)}$	Average energy consumption during backoff period.
$E_{C}^{(i)}$	Average energy consumption during collision period.
$E_{E}^{(i)}$	Average energy consumption during erroneous transmission period.
E_{e1}	Energy consumption of RTS corruption.
E_{e2}	Energy consumption of CTS corruption.
E_{e3}	Energy consumption of a data packet (source-AP) corruption.
E_{e4}	Energy consumption of an ACK corruption.
$E_{O}^{(i)}$	Average energy consumption during overhearing transmission period.
$E_{S}^{(i)}$	Average energy consumption during successful transmission period.
G_R	Rate gain.
K	Maximum queue length of node i.
L_{ACK}	ACK packet length in octets.
L_{CACK}	CACK packet length in octets.
L_{CCTS}	CCTS packet length in octets.
L_{CRTS}	CRTS packet length in octets.
L_{CTS}	CTS packet length in octets.

L_{MRTS}	MRTS packet length in octets.
L_{PLCP}	Physical Layer Convergence Procedure header in octets.
L_{RRTS}	RRTS packet length in octets.
L_{RTS}	RTS packet length in octets.
L_r	Data packet length of relay node in octets.
L_s	Data packet length of a source node in octets.
$N_{f,i}$	Average number of slots during which node i freezes its backoff counter due others transmissions.
$N_{s,i}$	Average number of time slots represents the successful transmission period of node i.
$N_{u,i}$	Average number of time slots represents the unsuccessful transmission period of node i.
$P(t)$	Stochastic transition matrix.
$P'(t)$	Derivative of $P(t)$.
p_{e1}^c	Corruption probability of a MRTS packet.
p_{e2}^c	Corruption probability of a CTS packet.
p_{e3}^c	Corruption probability of a data packet from a source to a relay.
p_{e4}^c	Corruption probability of a data packet from a relay to the AP.
p_{e5}^c	Corruption probability of an ACK packet in BTAC.
p_{e1}^d	Corruption probability of a RTS packet.
p_{e2}^d	Corruption probability of a CTS packet.
p_{e3}^d	Corruption probability of a data packet from a source to the AP.

p_{e4}^{d}	Corruption probability of an ACK from the AP to a source.
$P_{b,i}$	Probability the channel is sensed busy by a node i.
$P_{c,i}$	probability of collision of node i.
$P_{e,i}$	Total packet error rate probability of node i.
$P_{E,i}$	Probability that at least one packet arrives in the MAC queue during the following time slot conditioning that the queue is empty at the beginning of the slot.
$p_{i,j}(t_0)$	Transition probability from state i to state j after t_0 sec.
P_{IX}	Average power consumption in idle/sensing.
P_{RX}	Average power consumption in reception.
$P_{s,i}$	Successful transmission probability of a node i.
$P'_{s,k}$	Successful transmission probability of node $k \neq i$ of remaining $N-1$ nodes.
P_{tr}	Probability of at least one transmission occurs in a slot time.
P_{TX}	Average power consumption in transmission.
$P_{u,i}$	probability of unsuccessful packet transmission from node i.
P_s	Total successful transmission probability.
Q	Infinitesimal generator or transition rate matrix.
q_{e1}^{c}	probability that CRTS is corrupted given that no CRTS collision.
q_{e2}^{c}	probability that CCTS is corrupted and CRTS is correct given that no CRTS collision.

q_{e3}^{c}	probability that RRTS is corrupted and both CRTS and CCTS are correct given that no CRTS collision.
q_{e4}^{c}	probability that DATA-S(source-relay) is corrupted and CRTS, CCTS, and RRTS are correct given that no CRTS collision.
q_{e5}^{c}	probability that DATA-S (relay-destination) is corrupted and CRTS, CCTS, RRTS, and DATA-S (source-relay) are correct given that no CRTS collision.
q_{e6}^{c}	probability that DATA-R is corrupted and CRTS, CCTS,RRTS, and DATA-S (source-relay) are correct given that no CRTS collision.
q_{e7}^{c}	probability that CACK is corrupted and CRTS, CCTS,RRTS, DATA-S (source-relay), and at least one of both DATA-S (relay-destination) and DATA-R are correct given that no CRTS collision.
q_i	Probability that the there is at least one packet available at the queue at the post-backoff stage.
R_{rd}	Data-rate from a relay node to the AP in Mbps.
R_{sr}	Data-rate from a source node to a relay node in Mbps.
R_b	Base data-rate in Mbps.
S	Saturated throughput.
$T_{s,i}^{c}$	Successful time duration due to cooperative transmission of node i.
$T_{s,i}^{d}$	Successful time duration due to direct transmission of node i.
T_{ACK}	Time duration of an ACK packet.
T_{BTS}	Duration of a BTS signal.

T_{CACK}	Duration of a CACK.
T_{CCTS}	Duration of a CCTS.
T_{CRTS}	Duration of a CRTS.
T_{CTS}	Duration of a CTS.
T_{DIFS}	Duration of a DIFS slot.
T_{MRTS}	Duration of a MRTS.
T_{rd}	Duration of a data packet from a relay to the AP.
T_{RRTS}	Duration of RRTS.
T_{RTS}	Duration of a RTS.
$T^c_{s,i}$	Successful transmission period of node i under cooperative transmission.
$T^d_{s,i}$	Successful transmission period of node i under direct transmission.
T_{sd}	Duration of a data packet from a source to the AP.
T_{SIFS}	Duration of SIFS.
T_{sr}	Duration of a data packet from a source to a relay.
$T_{u,i}$	Unsuccessful transmission period of node i due to packet errors.
T_{ACK}	Duration of ACK packet.
T_B	Average sojourn time in bad state.
T_c	Collision time duration.
T_G	Average sojourn time in good state.
u^d_1	Corruption probability of a RTS packet given no RTS collision in 802.11b.
u^d_2	Corruption probability of a CTS packet given no RTS corruption and collision in 802.11b.
u^d_3	Corruption probability of a data packet given no CTS and RTS corruption, and no RTS collision in 802.11b.

u_4^d	Corruption probability of an ACK packet given no RTS and CTS and data packets corruption, and no RTS collision in 802.11b.
U_F	Final state probability vector.
U_I	Initial state probability vector.
v_1	Probability a MRTS is corrupted given that a single MRTS is transmitted.
v_2	Probability a CTS is corrupted given that a MRTS is received correctly.
v_3	Probability a data packet from a source to a relay is corrupted given that a CTS is received correctly.
v_4	Probability a data packet from a relay to the AP is corrupted given that a data packet from a source to a relay is received correctly.
v_5	Probability an ACK packet is corrupted given that a data packet from a relay to the AP is received correctly.
w_1	Probability that CRTS is corrupted given that no CRTS collision.
w_2	Probability that CCTS is corrupted given that CRTS is correct and no CRTS collision.
w_3	probability that RRTS is corrupted given that both CRTS and CCTS are correct and no CRTS collision.
w_4	Probability that a data packet (source-relay) is corrupted given that CRTS, CCTS, and RRTS are correct and no CRTS collision.

w_5	Probability that a data packet (relay-AP) is corrupted given that CRTS, CCTS, RRTS, and a data packet (source-relay) are correct and no CRTS collision.
w_6	Probability that a data packet of a relay node is corrupted given that CRTS, CCTS, RRTS, and a data packet (source-relay) are correct and no CRTS collision.
w_7	probability that CACK is corrupted given that CRTS, CCTS, RRTS, DATA-S (source-relay), and at least one packet of both the source data packet (relay-AP) and a relay data packet are correct and no CRTS collision.
α_k	Probability that the channel is busy due to a transmission from node k.
δ	Channel propagation delay.
η	Energy efficiency.
λ	Packet arrival rate in packets per second.
λ_b	Transition rate constant from bad state to good state.
λ_g	Transition rate constant from good state to bad state.
$\overline{N_{ek}^c}$	Average number of retries due to collisions.
$\overline{N_{o,i}}$	Average number of transmissions overheard by the a node i.
$\overline{N_{r,i}}$	Average total number of retries.
$\overline{N}_{e1}^c$	Average number of retries due to MRTS corruption.
$\overline{N}_{e2}^c$	Average number of retries due to CTS corruption.

$\overline{N}_{e3}^{c}$	average number of retries due to data packet (source-relay) corruption.
$\overline{N}_{e4}^{c}$	Average number of retries due to data packet (relay-AP) corruption.
$\overline{N}_{e5}^{c}$	Average number of retries due to ACK corruption under BTAC.
$\overline{N}_{e1}^{d}$	Average number of retries due to RTS corruption.
$\overline{N}_{e2}^{d}$	Average number of retries due to CTS corruption.
$\overline{N}_{e3}^{d}$	Average number of retries due to DATA-S (source-AP) corruption.
$\overline{N}_{e4}^{d}$	Average number of retries due to ACK corruption.
$\overline{N}_{b,i}$	The average number of time slots during the backoff duration.
$\overline{N}_{e1}$	Average number of retries due to RTS corruption.
$\overline{N}_{e2}$	Average number of retries due to CTS corruption.
$\overline{N}_{e3}$	Average number of retries due to data packet (source-AP) corruption.
$\overline{N}_{e4}$	Average number of retries due to ACK corruption.
$\overline{N}_{idle,i}$	Average number of consecutive idle slots between two consecutive busy slots.
$\pi_{j,k}$	Steady state probability of Markov chain in the state (j, k).
π_B	Steady state probability for being in bad state.
π_G	Steady state probability of being in good state.
ρ_i	Utilization factor.
σ	Slot time duration.
τ_i	Probability of successful transmission of node i in a randomly chosen time slot.

Chapter 1

Introduction

In 1985, the United States Federal Communications Commission (FCC) opened the experimental Industrial, Scientific and Medical (ISM) spectral bands for license-free commercial applications of spread wireless spectrum technologies. During the last 20 years, Wireless Local Area Networks (WLANs) have been widely deployed in educational institutions, business buildings, public areas and even our homes to provide wireless broadband access services, thanks to the popularity of Internet applications and the proliferation portable communication devices (such as laptops and smart mobile phones). The dominant industrial standards for WLANs are the IEEE 802.11 family (1) and its European counterpart High-Performance Radio Local Area Network (HIPERLAN) (2). The key advantages of WLANs technologies include low costs (in deployment and maintenance), small size, ease of deployment and use, high speed, and cheap and portable devices. According to the Allied Business Intelligence (ABI) research (3), the world wireless market is predicted to grow from over 1.2 billion chipset unit shipments in 2009 to nearly 2.25 billion unit shipments in 2014.

1.1 Problem Statement

According to the IEEE 802.11 standards, a WLAN can support multiple transmission data rates depending on the instantaneous wireless channel condition between a device/station and an Access Point (AP). To achieve the target Packet Error Rate (PER) in data transmission, a device/station transmits its packets to an AP at a low date rate when the channel quality is poor. Heusse et al (4) show that the IEEE 802.11 WLANs presents a *performance anomaly* whereby the presence of a low data-rate device/station degrades the performance of a high data-rate devices/stations. This is because, relative to the high data-rate stations, a low data-rate station occupies the shared communication channel for a longer period for transmitting the same size packet to the destination, thus reducing the channel efficiency and overall system performance. To demonstrate this negative effect, we evaluate the overall throughput and delay performance of an IEEE 802.11b WLAN (5) consisting of 20 stations, each with either a high transmission data rate of 11 Mbps or a low data rate of 1 Mbps. When the number of low data-rate stations increases, the overall throughput and delay performance degrades. For example, when the number of low-data rate stations is three, the throughput decreases by 34% and the delay increases by 39% relative to the values when the number of low-data rate stations in zero.

1.2 Motivations and Objectives

The ubiquitous WLAN systems, based on the multi-rate IEEE 802.11 standards, lead to degradations in the performance of such networks. As

shown in pervious section, the overall system performance of a multi-rate WLAN is determined by those low data-rate stations in the network. Recent studies indicate that the IEEE 802.11 Medium Access Control (MAC) protocol is the main reason for this performance anomaly effect. Therefore, it is fundamentally important to design or improve these MAC protocols to utilise efficiently limited bandwidth and provide reliable system performance, thus enabling WLANs to support many new applications such as real-time multimedia communications. On the other hand, the IEEE 802.11 standards have been widely accepted and is now ubiquitous, it is then difficult to design a completely new MAC protocol that can succeed commercially. Our aim in this thesis is to design backward compatible MAC protocols, which can improve WLAN system performance with no significant changes to current IEEE 802.11 standards.

The concept of cooperative communications has been recently proposed to allow multiple users, devices or stations in a wireless network to coordinate their packet transmissions and share each other's resources and capabilities, thus achieving cooperative diversity gain or cooperative multiplexing gain. Specifically, cooperative diversity gain can be obtained by using intermediate stations, termed relays, to forward a sender's data packets to its destination (an AP in WLANs). While cooperative multiplexing gain can be achieved by enabling the relays to combine their own data transmissions with those forwarding packets, i.e. reserve the medium for additional data transmissions from the relays. In contrast to previous work, mainly focusing on physical (PHY) layer performance optimisation, our objective in this thesis is to understand the impact of cooperative communications on MAC layer performance and then design new cooperative MAC protocols to improve WLAN performance, in terms of system through-

put, latency, and energy efficiency.

1.3 Thesis Contributions

The research reported here addresses a new area of engineering. This research has resulted in several novel contributions outlined below:

- Design and verification of a new Busy Tone based Cooperative MAC protocol, namely BTAC, is designed. BTAC has the advantage of improving the system performance in terms of throughput, delay, and energy efficiency, through achieving *cooperative diversity gain*. The BTAC is detailed in Chapter 3.

- Design and verification of a novel cooperative medium access control (MAC) protocol, termed "Cooperative Access with Relay's Data" (CARD). CARD can achieve both *cooperative diversity* and *cooperative multiplexing* gains and significantly improve the system throughput, delay, and energy efficiency of multi-rate WLANs. The CARD protocol is detailed in Chapter 4.

- Development of mathematical models to evaluate the performance of both BTAC and CARD protocols taking into account dynamic wireless channel conditions.

- Development of a new analytical energy efficiency model for both BTAC and CARD protocols. This model consider the multi-rate, channel conditions, cooperative transmission, and saturated traffic load.

- Development of a new mathematical model to study the perfor-

mance of both BTAC and IEEE 802.11b protocols under unsaturated traffic load and ideal channel conditions.

1.4 Publications

The work reported in this thesis resulted in the publications listed below:

1. S. Sayed and Yang Yang, " A new Cooperative MAC Protocol for Wireless LANs" in London Communication Symposium (LCS), September 2007.

2. S. Sayed and Yang Yang, "BTAC: A busy tone based cooperative MAC protocol for wireless local area networks," in Proc. Third International Conference on Communications and Networking in China ChinaCom 2008, 2008, pp. 403-409.

3. S. Sayed and Yang Yang,"RID: Relay with integrated data for multi-rate wireless cooperative networks," in Proc. 5th International Conference on Broadband Communications, Networks and Systems BROADNETS '08, 2008, pp. 383 - 388.

4. S. Sayed, Yang Yang, and Honglin Hu, "CARD: Cooperative Access with Relay's Data for Multi-Rate Wireless Local Area Networks," in Proc. IEEE International Conference on Communications ICC '09, 2009, pp. 1-6.

5. S. Sayed, Yang Yang, and Honglin Hu, "Throughput Analysis of Cooperative Access Protocol for Multi-Rate WLANs," in Proc. IEEE Wireless

Communications and Networking Conference (WCNC'09), 2009, pp. 1-6.

6. S. Sayed, Yang Yang, and Honglin Hu, "Throughput Analysis of Cooperative Access with Relay's Data Protocol for Unsaturated WLANs," in Proc. of the 2009 International Conference on Wireless Communications and Mobile Computing 2009 (IWCMC'09), 2009, pp. 790-794.

7. S. Sayed, Yang Yang, Haiyou Guo, and Honglin Hu, "Energy Efficiency Analysis of Cooperative Access with Relay's Data Algorithm for Multi-rate WLANs," in Proc. IEEE Personal, Indoor and Mobile Radio Communications Symposium 2009 (PIMRC'09), 2009.

8. S. Sayed, Yang Yang, Haiyou Guo, and Honglin Hu, "Analysis of Energy Efficiency of a Busy Tone Based Cooperative MAC Protocol for Multi-rate WLANs," accepted for publication in Proc. IEEE Wireless Communications and Networking Conference 2010 (WCNC'10), 2010.

9. S. Sayed, Yang Yang, Haiyou Guo, and Honglin Hu, "BTAC: A busy tone based cooperative MAC protocol for wireless local area networks," accepted for publication in Mobile Networking and Applications (MONET), 2009.

10. Chi-Kin Chau, Fei Qin, Sayed Samir, Muhammad Husni Wahab and Yang Yang, "Harnessing Battery Recovery Effect in Wireless Sensor Networks: Experiments and Analysis," to appear in IEEE Journal on Selected Areas in Communications (JSAC), Special Issue on Simple Wireless Sensor Networking Solutions, 2010.

Also another paper titled "CARD: Cooperative Access with Relay's Data for Multi-Rate Wireless Local Area Networks" is submitted to the IEEE

Transaction on Wireless Communication.

1.5 Thesis Organisation

The thesis is organised as follows.

Chapter 2 reviews the background material and provides an overview of the dominant IEEE 802.11 standards, specifically the standards that have a common MAC protocol. The IEEE 802.11 WLANs structure is then presented, including frequency bands, frame formats and MAC layer access mechanisms. Some related work on the design and analysis of 802.11 MAC protocols is also reviewed.

Chapter 3 proposes and analyses a Busy Tone based cooperative MAC protocol, namely BTAC, for multi-rate WLANs. The BTAC transmission protocol is explained in detail and compared with the IEEE 802.11b (5) standard to show its compatibility with the latter. A cross-layer analytical model under dynamic channel conditions is developed to evaluate the performance of BTAC in terms of throughput, energy efficiency, and service delay. The proposed models and system performance are validated by computer simulations.

Chapter 4 proposes a novel cooperative MAC protocol, namely Cooperative Access with Relay's Data (CARD), which comprises the design of three algorithms for sender nodes, relay nodes and the AP, respectively. Analytical models are then derived to analyse the throughput, delay, and energy efficiency performance of the CARD protocol under different channel conditions. The models are validated by computer simulations.

Chapter 5 presents an analytical model under ideal conditions and

unsaturated traffic load. Subsequently, throughput, energy efficiency, and delay analyses are given in details and computed for both IEEE 802.11b and BTAC protocols. Furthermore, the analytical model is validated using computer simulations.

Chapter 6 concludes this thesis and proposes some research directions for future work.

Chapter 2

Background and State of the Art

Nowadays, the IEEE 802.11 standards have been widely accepted for deploying WLAN services. This chapter reviews Physical (PHY) layer and Medium Access Control (MAC) layer defined in IEEE 802.11 standards, as well as some related work on performance evaluation of WLANs.

The remainder of the chapter is organised as follows. Section 2.1 reviews the IEEE 802.11 standards. In Section 2.2 the WLAN network structure is presented. Section 2.3 explains the main features of the MAC layer in the IEEE 802.11. The function of the PHY layer and the frame format of the IEEE 802.11 are explained in Section 2.4. The critical requirements of an efficient MAC protocol are given in Section 2.5. The related work is given in Section 2.6, followed by summary in Section 2.7.

2.1 IEEE 802.11 Standards

In 1985, the United States Federal Communications Commission (FCC) opened the experimental industrial, scientific, and medical (ISM)

bands for commercial applications of spread spectrum technology without a government licence. There are different parts for the IEEE 802.11 standard that are briefly outlined below.

- **IEEE 802.11-legacy**

  The 802.11 study group was established under the IEEE Project 802 to recommend the first international standard of the IEEE 802.11 (1) protocol, called IEEE 802.11 legacy. It was released in 1997 and clarified in 1999. Due to the increasing commercial interest, the Wi-Fi Alliance (WFA) was formed in 1999 to certify interoperability of WLANs devices based on the IEEE 802.11 specifications. The legacy IEEE 802.11 (1) specifies two data rates of 1 and 2 Mbps. It defines three PHY layers: Infrared (IR) operating at 1 Mbps, Frequency Hopping Spread Spectrum (FHSS) operating at 1 or 2 Mbps, and Direct Sequence Spread Spectrum (DSSS) operating at 1 or 2 Mbps. The FHSS and DSSS technologies use the 2.4 GHz frequency band.

- **IEEE 802.11a**

  The IEEE 802.11a (6) was ratified in 1999. It operates in the 5 GHz band using Orthogonal Frequency-Division Multiplexing (OFDM) techniques in PHY layer at a transmission data-rate up to 54 Mbps.

- **IEEE 802.11b**

  The IEEE 802.11b standard (5) was released in 1999. The IEEE 802.11b extended the transmission data-rate up to 11 Mbps using a DSSS PHY layer at 2.4 GHz frequency band as the original IEEE 802.11. Despite the 802.11a provides a transmission data-rate up to 54 Mbps, the IEEE 802.11b has become the most popular standard operating in the 2.4 GHz ISM band.

- **IEEE 802.11d**

  The IEEE 802.11d (7) was ratified in 2001. It is employed in some countries where systems using other standards in the IEEE 802.11 family are not allowed to operate. It provides procedures to let the IEEE 802.11 networks operate compliantly to the regulations of these countries by introducing regulatory domains.

- **IEEE 802.11e**

  The IEEE 802.11 Working Group certified the IEEE 802.11e (8), in 2005, to enhance the current standards. The IEEE 802.11e is based upon IEEE 802.11a and supports applications with Quality of Service (QoS) mechanisms.

- **IEEE 802.11g**

  In order to provide a high data-rate as the 802.11a and a relatively large coverage area as 802.11b, the IEEE 802.11g standard (9) was released in 2003. The IEEE 802.11g operates in the 2.4 GHz band and employs OFDM physical layer at a transmission data-rate up to 54 Mbps. It is fully compatible with the IEEE 802.11b standard.

- **IEEE 802.11h**

  The IEEE 802.11h (10) is employed to provide Dynamic Frequency Selection (DFS) and Transmitter Power Control (TPC). TPC protocol is used to adapt the transmission power based on regulatory requirements.

- **IEEE 802.11i**

  The IEEE 802.11i (11) is released to provide effective data security by enhancing the Wired Equivalent Privacy (WEP) protocol.

- **IEEE 802.11j**

  The IEEE 802.11j (12) is released to allocate the Japanese spectrum in the 4.9 to 5 GHz band for indoor, outdoor and mobile applications.

- **IEEE 802.11-2007**

  The IEEE 802.11-2007 (13) standard was released, in 2007, to enhance the existing MAC protocol and PHY layer functions such as data link security. It also incorporates eight amendments which are IEEE 802.11a (6), IEEE 802.11b (5), IEEE 802.11d (7), IEEE 802.11e (8), IEEE 802.11g (9), IEEE 802.11h (10), IEEE 802.11i (11), and IEEE 802.11j (12).

- **IEEE 802.11n**

  Recently, the IEEE 802.11n (14) standard has been released to improve the transmission data-rate (up to 600 Mbps) and the coverage area range over the previous standards, such as the IEEE 802.11a and IEEE 802.11b/g. The IEEE 802.11n standard employs the Multiple-Input Multiple-Output (MIMO) technique in the PHY layer and the frame aggregation scheme to the MAC layer.

Comparisons for the most popular IEEE 802.11 standards, such as 802.11a, 802.11b, 802.11g, and 802.11n are illustrated in Table 2.1 (15–17).

2.2 Network Architecture

As shown in Fig. 2.1, a WLAN may contain several Basic Service Sets (BSSs), each of them consists of an Access Point (AP) and a group of neighbouring user stations. The function of the AP is to form a bridge between wireless and wired network. When a station needs to communicate with

	802.11a	802.11b	802.11g	802.11n
Release date	1999	1999	2003	2009
Data-rate	54 Mbps	11 Mbps	54 Mbps	248 Mbps
Throughput	20 Mbps	5 Mbps	22 Mbps	144 Mbps
Frequency	5 GHz	2.4 GHz	2.4, 5 GHz	2.4, 5 GHz
Channel BW	20 MHz	20 MHz	20 MHz	20, 40 MHz
Modulation	OFDM	DSSS, CCK	DSSS,CCK,OFDM	DSSS,CCK,OFDM
Coverage	15-30m	45-90 m	45-90 m	75-150 m

Table 2.1: Dominant IEEE 802.11 standards

another station in the same BSS, the station sends first to the AP and then the AP sends to the other station. The BSSs may be interconnected via their APs through the Distributed System (DS). The whole interconnected network including the BSSs and the DS is called an Extended Service Set (ESS). As a basic 802.11 network type, Independent BSS (IBSS) supports at least two stations to directly communicate with each other in an ad hoc mode (i.e. without AP). Consequently, the medium access coordination is distributed between all the stations. The IEEE 802.11 defines two layers, which are the MAC and PHY layers. These two layers are explained in the following two sections, respectively.

2.3 IEEE 802.11 MAC Protocol

The primary purpose of an IEEE 802.11 MAC protocol is to regulate the access of multiple user stations to the shared wireless

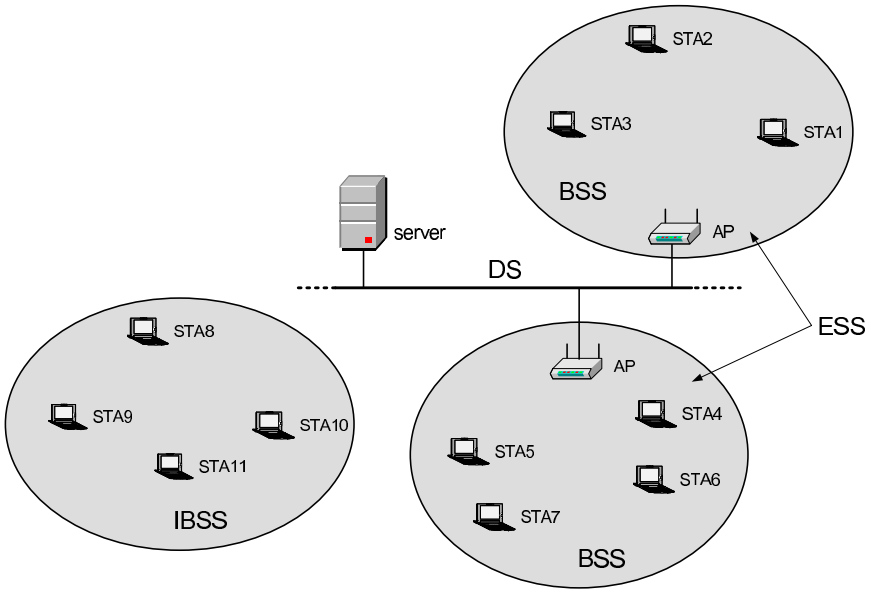

Figure 2.1: The IEEE 802.11 WLAN architecture (BSS, IBSS, DS).

channel/medium, thus achieving reliable data delivery and security (18). The IEEE 802.11 standards (1) allocate the same MAC layer to operate on top of one of several PHY layers [1]. As shown in Fig. 2.2, the lower sublayer of the MAC layer is Distributed Coordination Function (DCF), which provides a contention based service to access the shared medium. As an optional choice, the Point Coordination Function (PCF) is a centralised method exploiting the features in DCF sublayer to provide a contention-free medium access service for users.

2.3.1 Distributed Coordination Function

DCF is the fundamental medium access method of the IEEE 802.11 standards (1), used in both infrastructure and ad hoc modes. DCF is based on the Carrier Sense Multiple Access with Collision Avoidance (CSMA/CA) protocol, which works as follows.

[1]The IEEE 802.11n standard has a different MAC Layer.

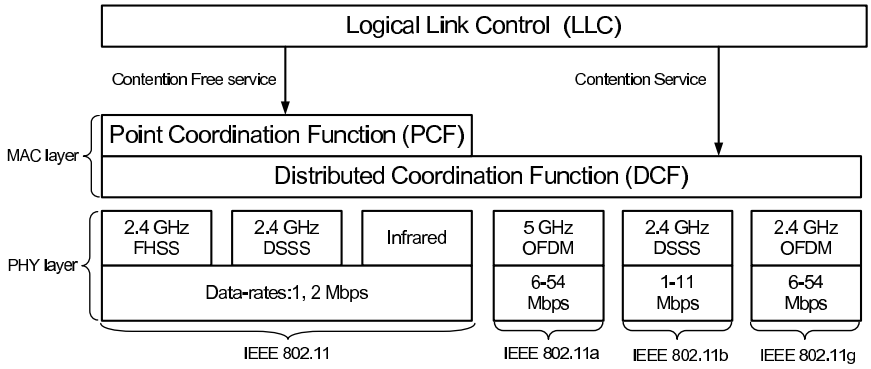

Figure 2.2: IEEE 802.11 standards.

- Before transmitting a packet, a source station, senses the medium by measuring the signal level at the carrier frequency.
- If the medium is found to be idle, the source waits a minimum specified duration called Distributed Interframe Space (DIFS).
- If the medium stays idle, the source station transmits its data packet to the receiving station.
- If the medium is sensed busy, the source defers its transmission after a random backoff delay.
- The source decrements the backoff interval counter while the medium is idle, and freezes the counter when the medium is sensed busy.
- The source will transmit its packet when its backoff counter reaches zero.

2.3.1.1 Carrier Sense Mechanism

The carrier sense mechanism is used to determine the state of the medium. There are two ways in which a carrier sense is performed: virtual

carrier sense and physical carrier sense functions. When either function indicates a busy medium, the MAC layer considers a busy medium; otherwise the medium is considered idle.

The physical carrier sense is provided by the IEEE 802.11 PHY layer in which a Clear Channel Assignment (CCA) is a logical function implemented. The CCA procedure employs a single fixed power carrier sense threshold. If a station detects a signal with Received Signal Strength Intensity (RSSI) less than the threshold value, the channel is then assumed to be idle. Otherwise, the medium is assumed to be busy and then unavailable for transmission.

The virtual carrier sense is provided the IEEE 802.11 MAC layer. It is referred to as the Network Allocation Vector (NAV). The NAV is a timer maintained by all stations to indicate the time interval during which the medium is reserved by other stations. The NAV timer decrements even though the station's CCA function indicates a busy medium. The NAV is set after receiving a frame from another station in the network. Each frame includes a duration field that indicates the required time period for the following frame exchange. When either the CCA indicates the channel is busy or the NAV is set, a station defers it transmissions.

2.3.1.2 Interframe Space

The Interframe Space (IFS) is the time duration between two MAC frames. There are four different IFSs durations defined to access the wireless medium at different priority levels. These IFSs are the Short Interframe Space (SIFS), the Point Coordination Function Interframe Space (PIFS), the Distributed Coordination Function Interframe Space (DIFS), and the Extended Interframe Space (EIFS). Fig. 2.3 shows some of these IFSs.

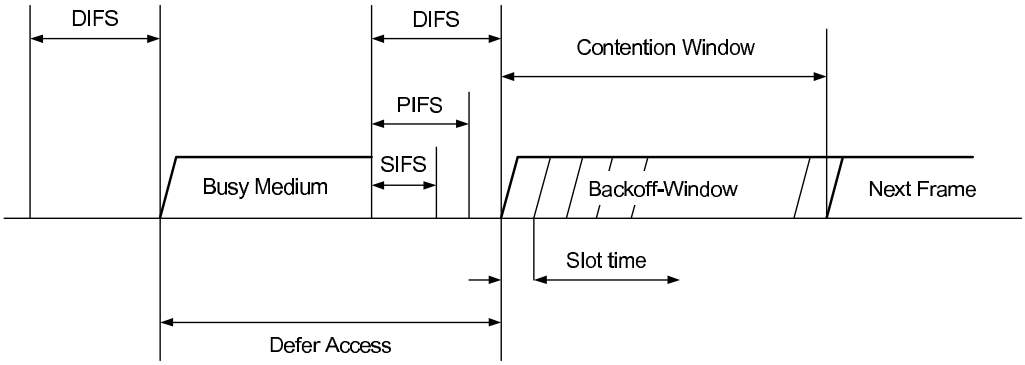

Figure 2.3: DCF timing relationships

- **SIFS Interval**

  It is the time interval between a response frame and the frame that requested the response, for example between a data frame and the Acknowledgment (ACK) frame. The SIFS is the shortest of the inter-frame spaces, but it is longer than the propagation delay and processing time at PHY and MAC layers. This delay includes demodulation and decoding the frame at the PHY layer, the MAC layer processing time for the received frame and constructing the response frame. The SIFS value for the 802.11b is $20\ \mu s$, and for the 802.11a, 802.11g, and 802.11n is $16\ \mu s$.

- **PIFS Interval**

  It is the next highest priority following the SIFS interval. The PIFS is employed by stations operating under the PCF mode to gain priority access to the wireless channel at the start of the Contention Free Period (CFP).

- **DIFS Interval**

  It is used by stations operating under the DCF mode. A station using the DCF sends its frame if its backoff counter reaches zero and the channel is sensed idle for the duration of the DIFS.

Parameter	Value
SIFS	aSIFSTime $= 20\ \mu s$ (802.11b) and $16\ \mu s$ (802.11a/g/n)
PIFS	aSIFSTime + aSlotTime
DIFS	aSIFSTime + $2 \times$ aSlotTime
EIFS	aSIFSTime + ACKTxTime + DIFS

Table 2.2: Interframe spaces values

- **EIFS Interval**

  It is used by a station operating under the DCF mode instead of the DIFS interval when the received frame is incorrect. This occurs due to imperfect channel conditions or when two or more stations transmit at the same time (collision). The EIFS begins following the PHY layer indication that the medium is sensed idle after detection of the erroneous frame. The EIFS is lowest access priority (longest IFS), which gives the sending station a higher priority to access the medium. Table 2.2 illustrates the values of the different interframe spaces; where aSlotTime is the duration of a slot time. In 802.11b, aSlotTime is $10\ \mu s.$, and in 802.11a/g/n is $9\ \mu s$. ACKTxTime is the duration of the ACK frame at the lowest data-rate.

2.3.1.3 Random Backoff Algorithm

When the medium is sensed idle, two or more stations may transmit at the same slot time. This is known as a collision. To minimise the collision probability, a station performs the so-called backoff procedure before starting transmission. If the medium is sensed busy, a station defers until the channel becomes idle without interruption for a DIFS (or EIFS) interval when the last frame is received correctly (or incorrectly). After this DIFS

(or EIFS) idle period, the station selects a random backoff period, which is a multiple of a slot time duration, and defers for that number of slot times. Each station selects the backoff count from a uniform distribution over the interval (0, CW-1), where CW is the Contention Window.

A station decreases its counter by one for every idle slot time. The transmission is then started when the backoff counter reaches zero. If the transmission is failed due to an erroneous transmission or a collision, the CW is doubled until it reaches the maximum value aCW_{max}, where CW takes the initial value of aCW_{min}. $aCW_{min} = 31$ and $aCW_{max} = 1023$ for the DSSS technique, as shown in Fig. 2.4. If the maximum retry limit is reached, which is six in Fig. 2.4, the frame should be dropped and the CW should be reset to the initial value aCWmin. If the channel is sensed busy by the CCA function, the station freezes its backoff counter until the medium becomes idle for a DIFS or EIFS once more a gain. The station then resumes its counter and does not select a new backoff value. Thus, the station takes a higher priority to access the channel in the following transmission. The procedure of doubling the CW is called the Binary Exponential Backoff (BEB) algorithm (1). This algorithm decreases the collision probability when there are multiple stations trying to access the channel at the same slot time.

After each successful or dropped frame transmission, there is always at least one backoff interval preceding (the initial attempt in Fig. 2.4) a packet transmission even there is no other frame to send. This is referred to as *post-backoff*. Alternatively, there is an exception to the essential rule that an a packet from the upper layer has to be transmitted after performing the backoff mechanism. The packet arriving from the upper layer may be transmitted immediately without waiting any time if the transmission queue is empty, the latest post-backoff is finished, and at the same time

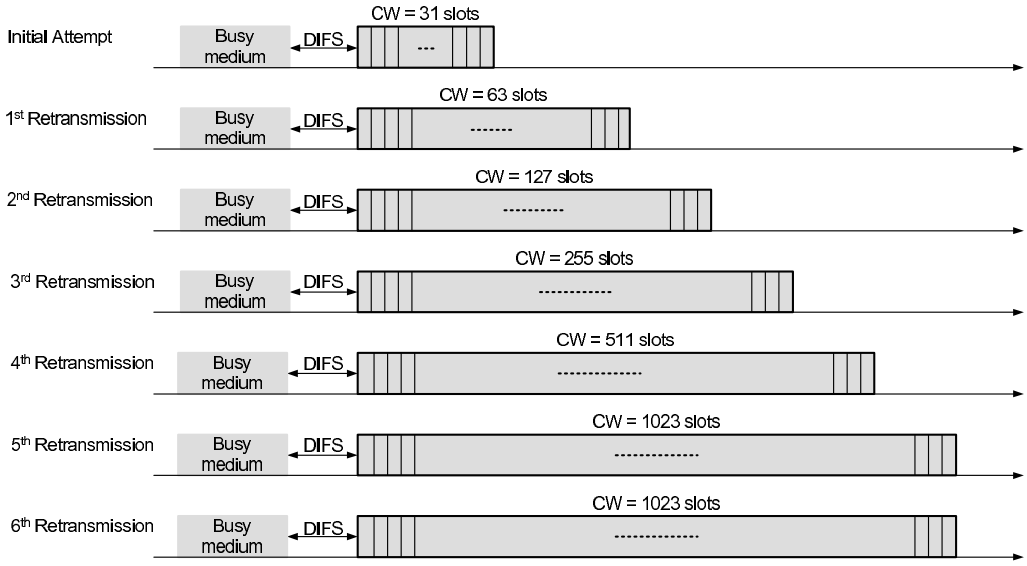

Figure 2.4: Exponential increase of CW

the channel has been idle for at least one DCF or EIFS interval.

2.3.1.4 DCF Access Procedure

The DCF protocol describes two modes for packet transmission. The mandatory scheme is referred to as a basic access or a two-way handshaking scheme. In addition to the basic access, the other scheme is the RTS/CTS (19,20) mechanism, and is referred to as a four-way handshaking mechanism and it is an optional mechanism.

Basic Access Mechanism

According to the CSMA/CA protocol, a station having a frame to transmit should listen until the wireless channel becomes idle for a DCF period when the last frame is received correctly, or an EIFS period when the last frame is received in error due to collision or imperfect channel conditions. After this DIFS or EIFS medium idle time, the station generates a

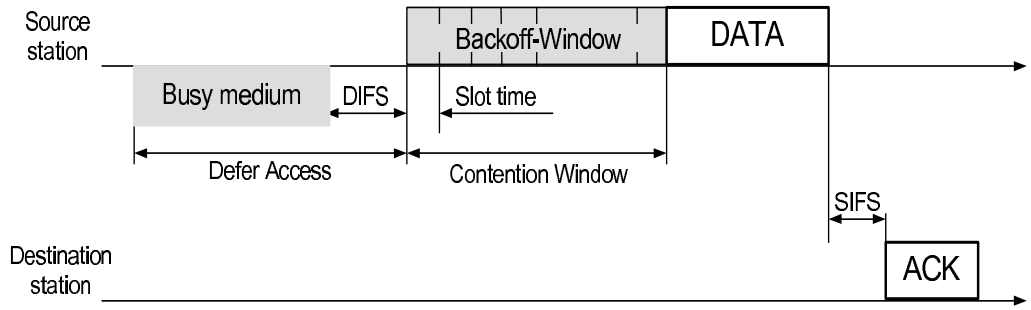

Figure 2.5: DCF basic access mechanism.

random backoff interval according to the rules of the BEB algorithm. A station transmits its data packet when the backoff timer reaches zero. If the data packet is correctly received, the destination station then sends an ACK frame immediately following a SIFS period. Otherwise, the destination station defers for an EIFS interval. If the transmitting station does not receive the ACK frame within a predefined ACKtimeout, it increases its Retry Count by one for each unsuccessful transmission, rescheduling the data frame retransmission according to the backoff rules. The CW should be reset to its minimum value aCWmin after every successful transmission or when retry count reaches the maximum value. The retry count is reset to zero whenever an ACK frame is received correctly. The Frame exchange sequence of the basic access mechanism is shown in Fig. 2.5.

Hidden Node And Exposed Node Problems

The basic access mechanism is inefficient in WLANs due to two unique problems: the hidden node problem (21) and exposed node problem. These two problems are illustrated in Fig. 2.6. A hidden node (node C in Fig. 2.6) is a node which is out of range of a sending node (node A in Fig. 2.6), but in the range of a receiving node (node B in Fig. 2.6). When the node A is transmitting to the node B, the node C senses the channel to be

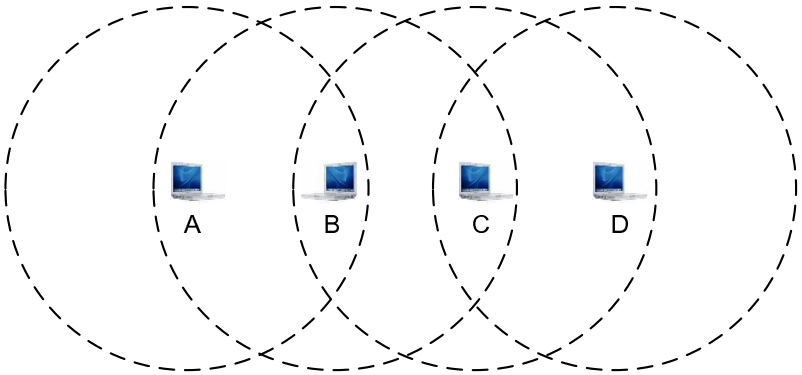

Figure 2.6: Hidden node and exposed node problems.

idle and also may start transmission to the node B. Consequently, a collision occurs at the node B. In the case the basic access fails to avoid the collision because node A and C are hidden to each other. The hidden node problem occurs in both infrastructure and ah hoc configurations. The hidden node problem is fixed by using the RTS/CTS handshaking mechanism as will be explained latter.

An exposed node (node C in Fig. 2.6) is a node that is in the range of a sending node (node B in Fig. 2.6), but out of range of receiving node (node A in Fig. 2.6). While node B is sending to node A, node C has a packet intended to node D. The node C senses busy channel because it is in the range of node B. The node C is then not allowed to transmit to the node D, despite a transmission from the node C is not interfering with the reception at the node A. The exposed node problem occurs only in the ad hoc mode, because in the infrastructure mode each node can not send directly to its destination. It first sends to the AP and the AP then sends to the receiving node. There is currently no solution for the exposed node problem within the IEEE 802.11 standards. The hidden node and exposed node problems cause degradation (20,22) in the WLANs performance.

RTS/CTS Mechanism

To reduce the collision probability caused by the hidden node, the IEEE 802.11 (1) standards employed a so-called Request-To-Send/ Clear-To-Send (RTS/CTS) mechanism. The RTS/CTS also is called the four-way handshake mechanism. It has been shown that the RTS/CTS is an effective mechanism to solve the hidden station problem (20, 23–25) and to improve the system performance when the packet size is large (26–28). The RTS/CTS mechanism is explained below.

- **Source Station**

  1. The source station sends out a RTS packet to the destination.
  2. If a CTS packet is not received within $CTS_{timeout}$, the source starts a new retransmission cycle after applying the BEB rules. The $CTS_{timeout}$ is set as follows:

$$CTS_{timeout} = T_{CTS} + 2 \times T_{SIFS}$$

  3. If the CTS packet is received, the source sends the data packet to the destination and set the $ACK_{timeout}$ as follows:

$$ACK_{timeout} = T_{data} + T_{ACK} + 2 \times T_{SIFS}$$

  4. If the ACK packet is not received within the $ACK_{timeout}$, the source starts a new retransmission cycle after performing a random backoff following the BEB algorithm. Otherwise, the source receives the ACK packet and start a new transmission cycle.

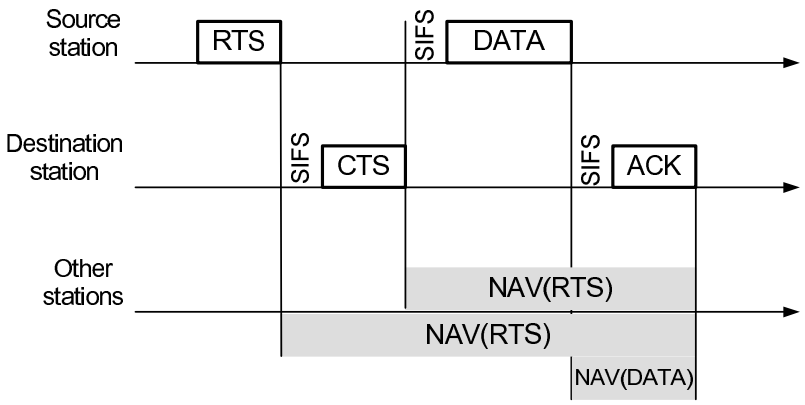

Figure 2.7: DCF RTS/CTS access mechanism.

where T_{CTS}, T_{data}, and T_{ACK} stand for the duration of a CTS, a data, and an ACK packet, respectively. T_{SIFS} is the duration of a SIFS interval. The reason that CTS packet may be unsuccessful is due to collision or imperfect channel conditions.

- **Destination Station**

  1. If the RTS packet is successfully received, the destination transmits a CTS packet back to the source following a SIFS interval. It sets a $DATA_{timout}$ as follows:

$$DATA_{timout} = T_{data} + 2 \times T_{SIFS}$$

  2. If the data packet is received from the source within the $DATA_{timout}$, the destination sends an ACK packet back to the source after a SIFS interval. Otherwise, it assumes that the transmission is terminated, and starts a new transmission cycle if there is a packet ready for transmission in its buffer.

Packet Type	The duration
RTS	$T_{CTS} + T_{data} + T_{ACK} + 3 \times T_{SIFS}$
CTS	$T_{data} + T_{ACK} + 2 \times T_{SIFS}$
DATA	$T_{ACK} + T_{SIFS}$

Table 2.3: The duration field of the RTS/CTS mechanism.

The neighbours of both source and destination stations set their NAV after receiving the RTS, CTS, data, and ACK packets. Each packet includes a *duration* field that indicates the required time period for the following frame exchange. The frame exchange and the corresponding NAV settings are given in Fig. 2.7. The duration field values are given in Table 2.3. The duration field of the ACK packet is set to zero as the end of the transmission.

The RTS/CTS access mechanism solves the hidden node problem and then minimise the collision probability. For example, node A in Fig. 2.6 sends a RTS packet to node B. After receiving the RTS packet, the node B replies a CTS back to the node A. The node C receives also the CTS packet from the node B and defers sets its NAV after extracting the duration field of the CTS packet. The node C can access the medium after receiving the ACK packet from the node B. Therefore, the node C is aware of the transmission between the node A and node B.

2.3.2 Frames Format

The format of the most common MAC frames is specified in this section. The information presented here does not provide a comprehensive list of all field components, but it is adequate to be a reference for the

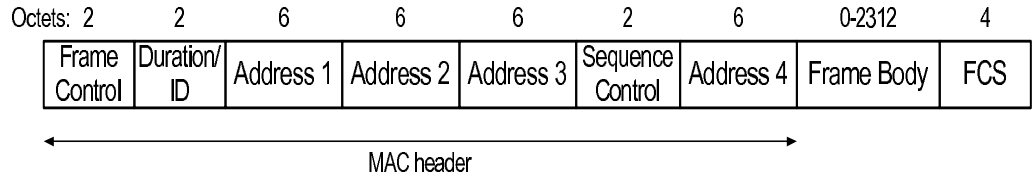

Figure 2.8: IEEE 802.11 general frame format.

subjects discussed in this research. For a detailed list of the MAC frame formats refer to the IEEE 802.11 (1,5,6,8,9,14). All stations is able to construct frames for transmission and decode frames up on reception. Each frame in the IEEE 802.11 standards (1) is composed by the following basic components: A MAC header, a variable length frame body, and a frame check sequence.

2.3.2.1 General MAC Frame Format

The IEEE 802.11 (1) standards specifies a general frame format as shown in Fig. 2.8. The general MAC frame format consists of a set of the fields that occur in a fixed order in all frames. The *Address 2*, *Address 3*, *Address 4*, *Sequence Control*, and *Frame body* fields are only exist in a certain frame types as will be explained latter. The following defines each of the general MAC frame fields.

- **Frame Control Field**

  It is two octets in length and is illustrated in Fig. 2.9. It consists of *Protocol Version, Type, Subtype, To DS, From DS, More Fragments, Retry, Power Management, More Data, Wired Equivalent Privacy (WEP),* and *Order* subfields.

  - **Protocol Version Field**

    It is two bits in length and represents the protocol version. The

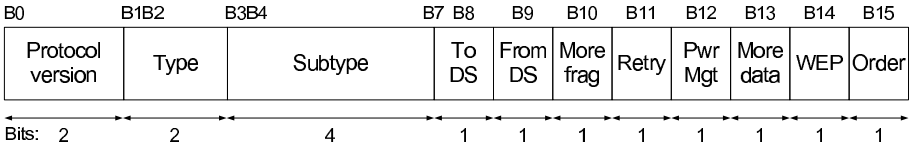

Figure 2.9: Frame control field.

b_2 b_3	Frame type
00	Management frame
01	Control frame
10	Data frame
11	Reserved

Table 2.4: Type field value.

value of the protocol version is zero for the current standards.

– **Type Field**

It is a two bits in length and defines whether the frame is a management, control, or data frame as indicated by Table 2.4.

– **Subtype Field**

It is four bits in length and it defines the function of the frame. Some *Subtype* field functions is shown in Table 2.5.

– **To DS Field**

It is a single bit in length and is set to 1 in any data frame destined for the DS; otherwise, it is set to 0 in all other frames.

– **From DS Field**

It is a single bit in length and it is set to 1 in any data frame leaving the DS; otherwise it is set to 0 in all other frames. The bit combinations and their meanings of both To DS and From DS fields are illustrated in Table 2.6.

Type $(b_2\ b_3)$	Subtype $(b_4\ b_5\ b_6\ b_7)$	Frame function
01	1011	RTS
	1100	CTS
	1101	ACK
10	000	DATA

Table 2.5: Subtype field value.

To DS	From DS	Meaning
0	0	A data frame from one STA to another in the same IBBS
0	1	A data frame leaving the DS
1	0	A data frame destined for the DS
1	1	A data frame from one AP through the DS to another AP

Table 2.6: To/From DS Combinations.

- **More Fragment Field**

  It is a single bit in length and is set to 1 if another fragment of the current data frame follows in a subsequent frame; otherwise it is set to 0 in all other frames.

- **Retry Field**

  It is a single bit in length and is set to 1 if the current data frame is a retransmission of the earlier frame; otherwise it is set to 0 in all other frames.

- **Power Management Field**

  It is a single bit in length and is set to 1 if the station will be in the power-save mode. It is set to 0 to indicate the station will be the active mode. It is also set to 0 in frames transmitted by the AP.

- **More Data Field**

  It is a single bit in length and is set to 1 if the AP has at least one additional data frame for a station in the power-save mode; otherwise it is set to 0 in the all other frames.

- **Wired Equivalent Privacy (WEP) Field**

  It is a single bit in length and is set to 1 if the *Frame Body* field of a data frame has been processed by the WEP algorithm (encrypted); otherwise it is set to 0 in all other frames.

- **Order Field**

  It is a single bit in length and is set to 1 in any data frame that is being sent using the StrictlyOrder service class. The StrictlyOrder service class is used to tell the receiving station that the data frames must be processed in order. The Order field is set to 0 in all other frames.

- **Duration/ID Field**

  It is a two octets in length and is used by a receiving station to set or update its NAV when the frame is not addressed to that station. The duration value represents the expected time duration during which the medium is expected to be busy before another station can contend for the medium.

- **Address Fields**

  The IEEE 802.11 (1) standards defines the following address types which are the Destination Address (DA), Receiver Address (RA), Source Address (SA), Transmitter Address (TA), and Basic Service Set Identifier (BSSID). The DA is the MAC address of the ultimate receiving station that will handle the frame to the upper layers for processing.

To DS	From DS	Address 1	Address 2	Address 3	Address 4
0	0	DA	SA	BSSID	N/A
0	1	DA	BSSID	SA	N/A
1	0	BSSID	SA	DA	N/A
1	1	RA	TA	DA	SA

Table 2.7: Address field contents.

The RA is the MAC address of a station (e.g. the AP) that should process the frame. The SA is the MAC address of the original source of the frame. The TA is the MAC address of a station that transmitted the frame onto the medium. The content of *Address* fields of the MAC frame is dependent upon the value of *To DS* and *From DS* fields and given in Table 2.7.

- **Sequence Control Field**

  It a two octet in length and consists of two subfields which are the *Fragment Number* (the leftmost four bits) and *Sequence Number* (the next 12 bits). The *Fragment Number* indicates the number of each fragment of a data frame. It is set to zero and incremented by one for each succeeding transmission. The *Fragment Number* is having the same number in all retransmissions of the fragment. *Sequence Number* specifies the sequence number of a data frame. Each data frame is assigned a sequence number starting at zero and incrementing by one for data frame. The *Sequence Number* subfield remains constant in each fragment or all retransmissions of the data frame.

- **Frame Body Field**

  The *Body Frame* field has a variable length payload and contains information that relates to the specific frame being sent.

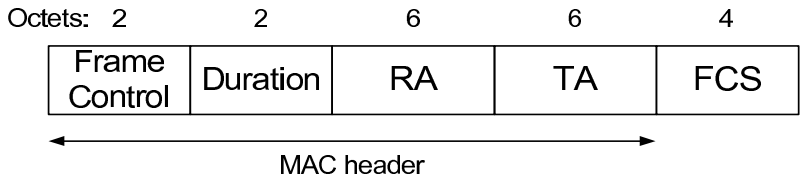

Figure 2.10: RTS frame.

- **Frame Check Sequence (FCS) Field**

  The FCS is eight octets in length containing a 32-bit Cyclic Redundancy Code (CRC). The CRC is used by a sending station to calculate a checksum of all fields of the MAC frame. The receiving station also calculates the CRC of the received frame and compares it with the attached CRC. If the two CRCs are the same, the receiver verifies that the frame has been received correctly; otherwise the frame has been corrupted while in transmission due to collision or imperfect channel conditions.

2.3.2.2 Common Frames Format

- **Request To Send (RTS) Frame**

  The RTS frame format is illustrated in Fig. 2.10. The *TA* field of the RTS frame is the address of the transmitting station and RA is the address of the intended recipient of the frame (e.g. the AP in the infrastructure mode). The Duration field, in microseconds, is the time that the sending station needs to transmit the data frame, plus one CTS frame, plus one ACK frame, plus three SIFS intervals.

- **Clear To Send (CTS) Frame**

  The CTS frame format is given in Fig. 2.11. The *Duration* field value, in microseconds, is the *Duration* field value of the immediately pre-

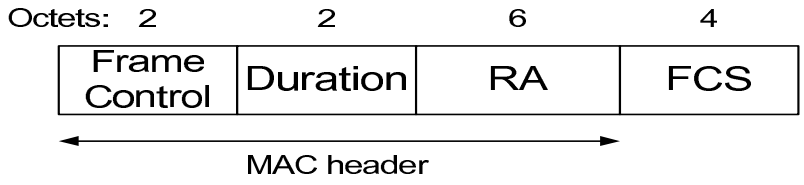

Figure 2.11: CTS frame.

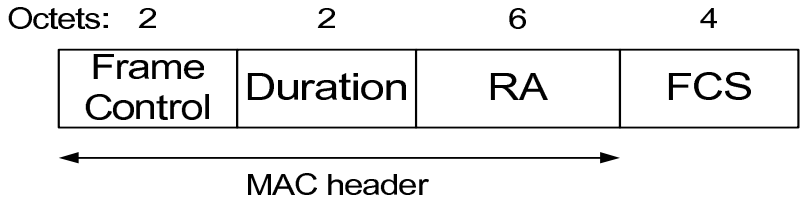

Figure 2.12: ACK frame.

ceding RTS frame minus the time of one CTS frame, minus one SIFS interval. The *RA* field of the CTS frame is the *TA* field of the immediately preceding RTS frame.

- **Acknowledgment (ACK) Frame**

  The ACK frame format is shown in Fig. 2.12. The *Duration* field value, in microseconds, is equal to zero if the *More Fragment* field of the immediately preceding data frame was set to zero. Otherwise, if the *More Fragment* field of the immediately preceding data frame was set to one, the *Duration* field value of the ACK is the Duration value of the immediately preceding data frame minus the time of one ACK frame, minus one SIFS interval. The *RA* field is the ACK frame is the *Address 2* field of the immediately preceding data frame.

- **DATA Frame**

  The Logical Link Control (LLC) sublayer generates a DATA frame which is called the MAC service Data Unit (MSDU). The MAC sublayer may fragment the MSDU into smaller MAC frames called MAC Protocol

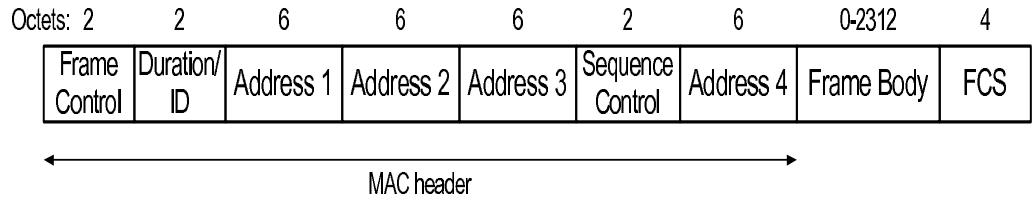

Figure 2.13: MPDU frame.

Data Units (MPDUs), as indicated in the IEEE 802.11 (1) standard. The frame format of the MPDU is shown in Fig. 2.13. The *Frame Body* field has a variable length from zero to 2312 octets, and the contents of *Address* fields are specified in Table 2.7.

2.3.3 Point Coordination Function (PCF)

The PCF is an optional priority-based providing a contention-free frame transfer. The PCF access method is only employable on infrastructure network configurations. The PCF uses a Point Coordinator (PC) which exists in the AP to control the transmission of the stations. All stations follow the PC by setting their NAV value at the beginning of each Contention-Free Period (CFP). The PC senses the medium at the beginning of a CFP. If the medium becomes free for the PIFS interval, the PC transmits a beacon frame. All stations receiving the beacon frame set their NAV to the maximum duration of the CFP to lock out DCF-based access to the medium until the end of the CFP. The difference between the DCF and PCF is that the stations should contend to access the wireless medium in the DCF mode while in the PCF mode, the PC controls the stations access to the medium. The PCF has not been widely employed. The details of PCF access method and frame formats are beyond the scope of this research. More detailed information for the PCF access method can be found in (1, 15, 29).

2.4 IEEE 802.11 Physical Layer (PHY)

The PHY layer is the second layer in the IEEE 802.11 WLAN architecture shown in Fig. 2.2. The general operation of the PHYs is very similar. The PHYs provides the following functions: carrier sense, transmission, and reception on the wireless medium. The original IEEE 802.11 (1) standard defines three different PHYs specifications. These three PHYs are 2.4 GHz FHSS, 2.4 GHz DSSS, and Infrared (IR). There are additional three PHYs defined in the 802.11a, 802.11b, 802.11g, and 802.11n standards. Except the 802.11b which is based on the DSSS and Complementary Code Keying (CCK) (5) techniques, all the other PHYs are based on the OFDM scheme. IEEE 802.11a (6) operates in the 5 GHz ISM band at data-rate up to 54 MHz. The IEEE 802.11g (9) operates in the 2.4 GHz ISM band at data-rate up to 54 Mbps. The IEEE 802.11b (5) also operates in the 2.4 GHz ISM band at data rat up to 11 Mbps. Finally, the IEEE 802.11n operates in either 2.4 GHz or 5 GHz ISM band at data rate up to 248 Mbps. More details of these IEEE 802.11 PHY layers can be found in (18,29).

2.4.1 PHY Architecture

The architecture of PHY is shown in Fig. 2.14, and consists of two sublayers which are Physical Layer Convergence Procedure (PLCP) and Physical Medium Dependent (PMD). The PLCP sublayer maps the MPDUs packet into a PLCP Service Data Units (PSDUs) that is suitable for the transmission and reception on the wireless medium. The PMD sublayer is responsible for the frame transmission and reception on the wireless medium. These responsibilities include modulation, demodulation, signal encoding, and interacting with the wireless medium. The PLCP communicates with

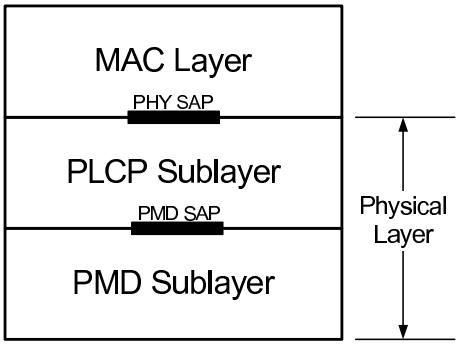

Figure 2.14: Anomaly performance.

MAC layer through a Service Access Point (SAP) called PHY SAP, and the PLCP communicates with the PMD sublayer through the PMD SAP.

2.4.2 PHY Frame Format

The IEEE 802.11b (5) is employed here to explain the IEEE 802.11 PHY frame. The other PHYs employ a similar frame format with slight changes that beyond the scope of this work. The transmitted frame on the wireless channel is called PLCP Protocol Data Unit (PPDU) shown in Fig. 2.15. It consist of *PLCP preamble*, *PLCP header*, and *PSDU* fields.

- **PLCP Preamble Field**

  The IEEE 802.11b defines two PPDU frames that differ only in the length of the preamble. The long preamble, shown in Fig. 2.15(a), is a 144-bit field including a 128-bit *Sync* field that enables the receiver to synchronise with the transmitter and a 16-bit Start of Frame Delimiter (SFD) field. The long preamble is the same as employed in the original IEEE 802.11 (1). The short preamble, illustrated in Fig. 2.15(b), is a 72-bit field consists of a 56-bit *Sync* field and 16-bit *SFD* field. The short preamble improves the performance efficiency. Both short and long PLCP preambles are sent at data-rate of 1 Mbps using the Differential

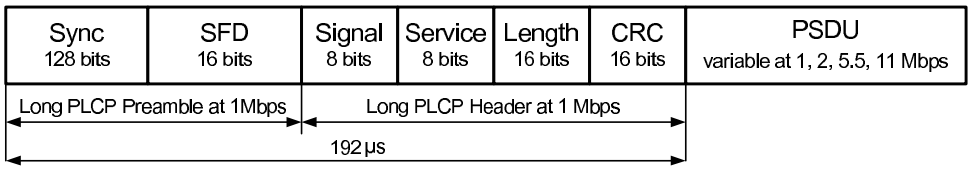

(a) Long Preamble PLCP PPDU format.

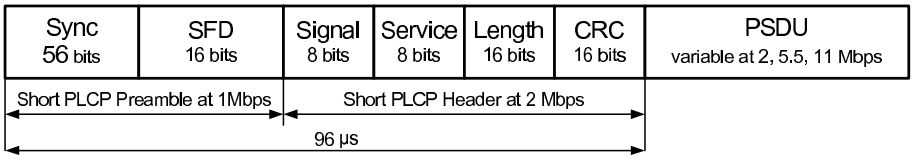

(b) Short Preamble PLCP PPDU format.

Figure 2.15: PLCP PPDU format.

Binary Phase Shift Keying (DBPSK) modulation technique.

- **PLCP Header Field**

  It is a 48-bit field, and consists of *Signal, Service, Length,* and *CRC* fields. It is sent at 1 Mbps with DBPSK modulation under long PLCP preamble (Fig. 2.15(a)), and is sent at 2 Mbps with Differential Quadrature Phase Shift Keying (DQPSK) modulation under the short PLCP preamble (Fig. 2.15(b)).

  - **Signal Field**

    It describes the type of modulation that the receiving station must employ to demodulate the received signal. The value of the *Signal* field is equal to the data-rate divided by 100 Kbps. The data-rates supported by the IEEE 802.11b (5) are 1, 2, 5.5, and 11 Mbps. The corresponding *Signal* field value is given in Table 2.8.

  - **Service Field**

    It is one octet in length, and is reserved for future use except

Data-rate	Signal field value
1	00001010
2	00010100
5.5	00110111
11	01101110

Table 2.8: Signal field contents.

b_1	b_2	b_3	b_4	b_5	b_6	b_7
Reserved	Reserved	Locked clocks bit 1=locked 0=not	Mod. selection bit 1=PBCC 0=CCK	Reserved	Reserved	Length extension bit

Table 2.9: Service field contents.

three bits that are used in the IEEE 802.11b, as shown in Table 2.9. Bit 2 is employed to show that the transmit frequency and symbol clocks are generated from the same oscillator. Bit 3 is used to specify either the modulation method is CCK or Packet Binary Convolutional Code (PBCC). The PBCC is pioneered by Texas Instruments (TI) at a data-rate 5.5, 11, 22 Mbps. The PBCC is another option for compatibility with IEEE 802.11b and is called IEEE 802.11b+ (30). Bit 7 is used an extension for the *Length* field.

– **Length Field**

It is an unsigned two octets integer specifying the number of microseconds required to transmit the MPDU. Given the data-rate, the length of the MPDU can be calculated at the receiver.

- **Cyclic Redundancy Code (CRC) Field**

  It is two octets in length, and is used for error detection of *Signal, Service,* and *Length* fields.

- **PSDU Field**

  The PSDU is actually the MPDU sent by the MAC layer. It has a variable length, and is transmitted at the data-rate indicated in the *Signal* field. For the long PLCP preamble PPDU frame (Fig. 2.15(a)), the PSDU can be sent at 1Mbps with DBPSK, 2 Mbps with DQPSK, 5.5 Mbps with CCK (or PBCC), or 11 Mbps with CCK (or PBCC). For the short PLCP preamble PPDU frame (Fig. 2.15(b)), the PSDU is sent at 2 Mbps, 5.5 Mbps, or 11 Mbps.

2.5 IEEE 802.11 Performance Metrics

The IEEE 802.11 study group set out, according to the application desires, some performance requirements for an efficient MAC protocol. For instant, applications such as email and file transfer are delay insensitive services, while other applications such as multimedia services require low delay. Throughput, average packet delay, and energy consumption can be counted as the most critical performance metrics to design an appropriate MAC protocol (31–35). Many analytical models and evaluation methods have been proposed in literature to study the performance of IEEE 802.11 MAC protocols, thanks to its popularity. The following section reviews some related work on cooperative communications and performance evaluation of IEEE 802.11 WLANs.

2.6 Related Work

Heusse et al (4) showed that the IEEE 802.11 causes a performance anomaly when in the same BSS exist stations with different data-rates due to the channel conditions. In this case, the low data rate station reduces the overall performance of the network below the level of the lower rate. This is because, comparing to a high data rate stations, the low data-rate stations will occupy the shared communication channel for a longer period for transmitting a fixed-size packet to the AP, thus reducing the channel efficiency and overall system performance.

This adverse performance can be mitigated by allowing both the low and high data-rate stations to occupy the shared wireless medium for the same time interval. Several research works have been proposed to tackle this issue in different ways, with solutions at different levels of the protocols stack. Consequently, we review the most related researches, that try to solve the performance anomaly by introducing minimum modifications in the MAC layer of the IEEE 802.11 standards.

The concept of cooperative communication has been proposed to improve link capacity, transmission reliability and network coverage in multiuser wireless communication networks. Different from conventional point-to-point and point-to-multipoint communications, cooperative communication allows multiple users or stations in a wireless network to coordinate their packet transmissions and share each other's resources, thus achieving *cooperative diversity* or *user cooperative diversity* (36–43). Despite of the extensive research is proposed for the physical layer of cooperative communications (44), a small number of papers (45–52) considers the MAC layer.

Wong et al (45) proposed a Relay-based Adaptive Auto Rate

(RAAR) protocol using central control at the AP to select relay nodes. The RAAR also employs a two-hop transmission through a suitable relay node. The transmission rate is dynamically adjusted according to the channel quality. The RAAR allows for transmission of multiple back to back (i.e. fragmentation) from the sender to the AP through the selected relay node and hence affects the long term channel access fairness of the MAC.

Zhu et al (46) presented the relay-enabled Point Coordination Function (rPCF) MAC protocol. The rPCF exploits the physical multi-rate capability allowing a low data-rate station to employ a neighbouring station as a relay to forward its information to the AP. In rPCF, each mobile node reports the sensed channel condition to the AP. Based on the collected information, the AP decides and notifies the node at which rates to apply relay through the polling packet. When the link from the sender and the AP supports a low data-rate, whereas the sender-relay link and the relay-AP link can support a high transmission data-rate, the sender sends to the relay instead of sending to the AP. The AP estimates the channel conditions between itself and each station, and notifies the stations which data-rate to employ and whether to employ a relay station. This relay-type cooperative communication can effectively improve network coverage, transmission data rate and reliability, and system throughput in WLANs. The rPCF is centralised where the AP is responsible to establish the two-hop transmission. In addition, the rPCF is designed to work in the PCF mode which is rarely used due to implementation complexity.

Zhu et al (47,48) and Panwar (49,50) proposed independently two similar protocols called relay-enabled Distributed Coordination Function (rDCF) and Cooperative MAC (CoopMAC) protocols, respectively. These two protocols are based on the IEEE 802.11 DCF mode which is the funda-

mental transmission mode instead of the PCF mode in the rPCF protocol. The rDCF and CoopMAC work in a distributed manner, since each station contains a table of the potential relay nodes that can be used to forward its information to the AP through a two-hop transmission. The rDCF enables packet relaying in the ad hoc mode of 802.11 systems by requesting each station to broadcast the rate information between stations explicitly. The CoopMAC is applied in the infrastructure mode, and chooses the best relay station to realize high rate two-hop transmissions, and then the overall system throughput can be improved. Later, the CoopMAC protocol is implemented in a testbed and evaluated through experiments (53, 54). CoopMAC and rDCF change is not fully compatible with the standard IEEE 802.11 protocols by introducing many changes in the IEEE 802.11 protocol. In addition, CoopMAC and rDCF only achieve cooperative diversity gain through two-hop transmission.

Chou et al (51) presented another MAC protocol to provide cooperative communication in distributed manner. In order to select the relay node among its neighbors, The proposed protocol employs a relay selection with relay collision avoidance and three way handshaking mechanism. The MAC performance metrics such as throughput, energy efficiency, and service delay are not considered in the analysis.

Wang et al (52) presented a distributed cooperative MAC protocol for multi-hop wireless networks based on the IEEE 802.11 DCF mode. The relay selection criteria of this protocol is different from the rDCF and CoopMAC protocols. The relay selection in both rDCF and CoopMAC is selected by the sender via a table of the potential relay stations, while the protocol in (52) employs a similar selection criteria as in (55). The neighbouring stations of the sender and destination monitor the channel conditions to-

ward them through the received RTS and CTS packets. If the two-hop transmission is better than the direct transmission, every willing station sends out a busy tone followed by a random backoff period before sending a Ready-To-Help (RTH) packet. If there is no collision between the competing relay stations, the sender transmits its information to the destination through the relay station. Therefore, the two-hop transmission is initiated by the relay node itself no by the sender or the destination, and then there is no relay table as in the rDCF and CoopMAC protocols. The collision between relay station can cause a severe performance degradation. Consequently, minimising the collision relay probability is still an open research point.

Since bandwidth is a scarce resource in wireless networks, throughput is then considered the most critical metric in the design of an appropriate MAC protocol. In order to enhance the bandwidth utilisation, it is important to study the IEEE 802.11 throughput. There have been many performance studies for the IEEE 802.11 standards. Binachi in his seminal work (26–28) presents a Markov channel model to calculate the saturation throughput of the IEEE 802.11 protocol assuming ideal channel conditions and infinite number of retransmissions.

Ziouva et al (56), Xiao (57), and Ergen et al (58) extend the Bianchi's model taking into account the backoff counter suspension during a busy wireless medium. However, it is assumed in (56) that there is no post-backoff stage; this assumption is not compatible with the IEEE 802.11 standard. Wu et al (59) modifies Bianchi's model through incorporating the maximum number of retransmissions. The above mentioned analysis assume ideal channel condition. Saturated throughput analysis in presence of imperfect channel conditions is investigated in (56,60–66).

The throughput analysis, in (67–77), has been shifted to the IEEE 802.11 WLANs under finite traffic conditions by extending the Markov chain model proposed by Bianchi (27). The performance analysis of the IEEE 802.11 taking into considerations the effect of the backoff window size is investigated in (78–84). This analysis only considers a single-hop transmission and do not consider the multi-rate capability supported by the IEEE 802.11 standards.

Delay is an important performance metric in the design an efficient MAC protocol given that the IEEE 802.11 standards are applied not only for asynchronous data service (i.e. best effort service), but also applied for time-bounded multimedia applications such as voice and video. Concerning the delay analysis of the IEEE 802.11, there is a lot of research in modeling and studying delay performance (56, 85–98). The delay analysis mention above only considers a single-hop transmission, ideal channel conditions, and do not consider the multi-rate capability supported by the IEEE 802.11 standards.

The wireless clients are designed to be portable and/or mobile and have limited battery power. The wireless clients must be designed to be energy efficient. Therefore, energy efficiency is one of the important IEEE 802.11 parameters. Modeling the energy efficiency, in (99–110), can provide insights into the metrics that can improve the energy efficiency of the IEEE 802.11-based networks. The energy efficeincy analysis mention above only considers a single-hop transmission and do not consider the multi-rate capability supported by the IEEE 802.11 standards.

The support of differentiated QoS has become one of the critical requirements of the WLANs. The IEEE 802.11e (8) is then the solution of the IEEE 802.11 study group to provide the required QoS for some applica-

tions such as voice and video. There have been several theoretical studies developed to address the problem of modeling and optimising the performance of the IEEE 802.11e standards.

In (111–114), Bianchi's model (28) is modified to analyse the Enhanced Distributed Coordination Function (EDCF). The EDCF is the fundamental access method in the IEEE 802.11e (8). In (115–117), the performance of the IEEE 802.11e (8) is provided via simulations. The EDCF is classified into three different kinds (118): backoff, IFS, and hybrid priority schemes. Readers may refer to (119–129) for the EDCF priority models. The analysis of the IEEE 802.11e is applied for single-hop transmission and single data rate. This assumption is not valid for the IEEE 802.11e standards.

IEEE 802.11 standards such as the IEEE 802.11a/b/g/n provide multi-rate transmission capabilities. Consequently, design of a new MAC protocols taking into account this feature is required to achieve high performance. There is a lot of research to design a MAC protocol, in (130–136), considering the multi-rate capability provided by the IEEE 802.11 standards.

Kamerman et al (130) proposed the Auto Rate Fallback (ARF) protocol, in which the sending station increases the transmission rate after consecutive transmission successes and decreases its rate after transmission failure. ARF does not work well when the channel condition becomes unstable.

Holland et al (131), designed the Receiver Based Auto Rate (RBAR) protocol. The RBAR is different from the ARF protocol, since the receiver measures the channel quality and feedbacks its to the sender. The RBAR is then more accurate than the ARF protocol. Qiao et al (132, 133) investigated that the link adaptation based on dynamic packet fragmentation

is efficient to enhance the performance of the IEEE 802.11a (6) WLANs.

Lung at el in (134), designed a protocol in which the transmission rate of each packet is selected dynamically based on the estimated Signal to Noise Ratio (SNR) of the pervious either received or transmitted frame. Later, Sadeghi et al (135,136) proposed the Opportunistic Auto Rate (OAR) protocol. In the OAR, the sending stations transmit multiple back-to-back packets (i.e. packet fragmentation) to the receiving station whenever access the medium. The OAR is better than the RBAR when the channel quality is good between the sender and receiver. Other research studies that consider the multi-rate capability to design of an efficient MAC protocol can be found in (137–141).

2.7 Summary

The IEEE 802.11 WLANs standards have been globally accepted and adopted to provide wireless broadband access services in university campus, office, home and city hotspot areas. In this chapter, the concepts behind the IEEE 802.11 standards that are used in WLANs are introduced. The aim of these standards is to provide better performance and to extend the coverage area of the WLANs. The most well known IEEE 802.11 standards are 802.11b, 802.11a, IEEE 802.11g, IEEE 802.11e, and IEEE 802.11n. The IEEE 802.11a/.11g/.11b standards provide a best effort service, while the IEEE 802.11e/.11n standards provide mechanisms to guarantee QoS transmission. The IEEE 802.11 consists of two layers which are the MAC and PHY layers. Except the IEEE 802.11n, the other IEEE 802.11 standards have the same MAC layer with a different PHY layer. There are two MAC transmission schemes in the IEEE 802.11 networks called the DCF and PCF.

The DCF is the fundamental access method, and provides a contention-based service for delay insensitive traffic. The DCF employs the CSMA/CA algorithm that requires each station listen to the channel before transmission, and uses the BEB algorithm that can decrease the collision probability. The DCF defines two modes for frame transmission over the wireless medium. These modes are the basic access and RTS/CTS access which is an optional scheme.

There are two unique problems in the WLANs called the hidden node and exposed node problems. The hidden node is the node which is out of sending node range, but in the receiving node range. The RTS/CTS scheme is used to solve the hidden node problem that can occur in the network and hence decreases the collision probability. On the other hand, the exposed node is the node that is in the sending node range, but out of the receiving node range. The exposed node problem occurs only in the ad hoc network structure, and there is currently no solution to this problem. The hidden and exposed node problems cause a reduction in the network performance.

The PCF is an optional scheme that provides a contention free service for delay sensitive traffic. The PCF is used only in the infrastructure network configuration. The PCF uses a Point Coordinator (PC) existing in the AP to control the transmission of the stations. The PCF is not widely employed due to implementation complexity.

The function of the IEEE 802.11 PHY is to provide carrier sense, transmission, and reception on the wireless medium. The IEEE 802.11 standards support different PHYs. The original IEEE 802.11 standard provide three PHYs which are 2.4 GHz band with DSSS technique, 2.4 GHz band with FHSS, and IR. The IEEE 802.11b is based on the DSSS and 2.4 GHz band.

The IEEE 802.11a/g/n are based on the OFDM scheme. The IEEE 802.11g operates in the 2.4 GHz band, the IEEE 802.11a operates in 5 GHz band, and the IEEE 802.11n operates in either 2.4 GHz or 5 GHz band.

Throughput, Delay, and energy efficiency are counted as the most critical requirements to design an efficient MAC protocol in the IEEE 802.11 standards. This is due to the bandwidth limitations in wireless networks, the increasing demand to support multimedia applications with guaranteed QoS, and the fact that wireless devices are typically portable and have limited battery power. Therefore, modeling and analysing of these requirements can provide insights into the metrics that can improve the energy efficiency of the IEEE 802.11-based networks.

According to the IEEE 802.11 standards, WLANs can support multiple transmission data rates depending on the instantaneous channel condition between the sender and the receiver. To achieve the target Packet Error Rate (PER) in data transmission, the sender transmits its packets to the receiver at a low date rate when the channel quality is poor. In this case, the low data rate station reduces the overall performance of the network below the level of the lower rate.

This adverse performance can be mitigated by using the concept of cooperative communications at the MAC layer. The sender node can use a neighboring node, called a relay, which has high-quality communication channels to both the sender and the receiver, to transmit its packets to the latter at much higher data rate. This relay-type cooperative communication can effectively improve network coverage, transmission data rate and reliability, and system throughput in WLANs.

Chapter 3

BTAC: A Busy Tone Based Cooperative MAC Protocol

Cooperative communications is the concept of engaging multiple stations/nodes in a wireless network to share their resources and achieve multi-user/spatial diversity gain. This gain is achieved through distributed but cooperative transmissions, thus improving overall system performance under dynamic wireless channel conditions. Many novel cooperative algorithms and analytical models have been introduced in the literature for the physical layer (36–43), Medium Access Control (MAC) layer (45–52), or across multiple layers (142, 143). Based on the cooperative communications concept, this chapter proposes and analyses a Busy Tone based cooperative MAC protocol, namely BTAC, for multi-rate Wireless Local Area Networks (WLANs). A cross-layer Markov chain model is then developed to evaluate the performance of BTAC under dynamic wireless channel conditions. Analytical and simulation results show that the BTAC protocol is simple, robust, and fully compatible with the IEEE 802.11b standard (5).

Along with improvements in system throughput, BTAC can also achieve better energy efficiency and media access delay than the standard Distributed Coordination Function (DCF) protocol and the recently proposed CoopMAC protocol (50).

The remainder of the chapter is organised as follows. In Section 3.1, the proposed BTAC protocol is described in detail and compared with the IEEE 802.11b standard to show its compatibility with the latter. A cross-layer analytical approach is developed in Section 3.3 to evaluate the performance of BTAC in terms of throughput, energy efficiency, and service delay. Section 3.4 presents and discusses the analytical and simulation results for BTAC under different wireless channel conditions. Finally, conclusions are presented in Section 3.5.

3.1 The BTAC Protocol

3.1.1 System Model

This research considers a typical IEEE 802.11b WLAN as can be seen in Fig. 3.1, consisting of an Access Point (AP) at the center of the network and N contending stations/nodes that are uniformly distributed in four data-rate zones. It is assumed that a single physical channel is available for transmissions, and the channel is symmetric between the transmitter and the receiver. Each node supports four different data-rates $R_1 = 11\ Mbps,\ R_2 = 5.5\ Mbps,\ R_3 = 2\ Mbps$, and $R_4 = 1\ Mbps$, and maximum transmission ranges $r_1 < r_2 < r_3 < r_4$, respectively. The nodes in zone I ($0 \leq r < r_1$) and zone II ($r_1 \leq r < r_2$) are defined as the high data-rate nodes, e.g. nodes A and B in Fig. 3.1, which can act as source and relay

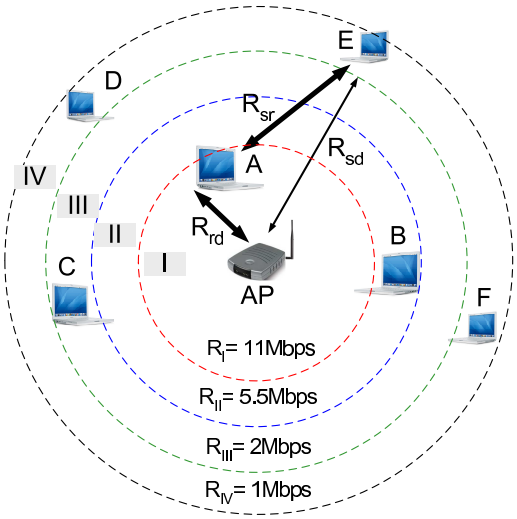

Figure 3.1: Multi-rate IEEE 802.11b WLAN.

nodes and always communicate directly with the AP; while those in zone III ($r_2 \leq r < r_3$) and zone IV ($r_3 \leq r < r_4$) are low data-rate nodes, e.g. nodes C-F, which can only act as source nodes and each of them needs a high data-rate relay station to improve its communication performance with the AP. As described later, the low data-rate nodes continuously re-evaluate their high data-rate neighbouring nodes in a distributed manner, so as to select the best (in terms of effective throughput) potential relay node.

3.1.2 Relay Selection Algorithm

The task of a relay selection algorithm is to find a relay node that provides the *best* end-to-end communication path between a source node and its destination (the AP[1]). However, the selection criteria that operate in a distributed manner and introduce a minimum overhead in terms of complexity and delay are preferable. To achieve these requirements, in

[1]we consider only the infrastructure mode in this work.

the same way to existing work (47, 48, 50), each node maintains an up-to-date list, named *a Relay list* of the high data-rate neighbouring (relay) nodes. Each row in the list consists of five fields which are MAC identifier (ID), i.e. MAC address, R_{sr}, R_{rd}, G_R, and *success rate* of one potential relay node. The two fields R_{sr} and R_{rd} stand for the data-rate between source and relay, and data-rate between relay and AP, respectively. G_R in equation (3.1) stands for the rate gain and is defined as the ratio between the composite data-rate of a two-hop transmission to the data-rate of a direct transmission rate, which is R_{sd}. The composite data-rate R_C is calculated by $R_C = \frac{1}{\frac{1}{R_{sr}} + \frac{1}{R_{rd}}}$. A relay node is added to the *Relay list* when the two-hop data transmission (via the relay) is more efficient than the direct data transmission between the source node and the AP.

$$G_R = \frac{R_C}{R_{sd}}\% \; = \; \frac{R_{sr}R_{rd}}{R_{sd}(R_{sr} + R_{rd})}\% \tag{3.1}$$

Each node creates and updates the Relay list by passively listening to all ongoing transmissions, e.g. Request-To-Send (RTS), Clear-To-Send (CTS), acknowledgement (ACK), and data packets. Each node then decodes the control packets (i.e., RTS, CTS, and ACK), and the header of the data packets to acquire the channel reservation information and receive the packets intended for itself. These packets are sent at the maximum power and at the base rate (e.g. 1 Mbps for 802.11b and 6Mbps for 802.11a/g). Considering a symmetric wireless channel condition in this research, R_{sd} and R_{sr} can be estimated from the signal strengths of CTS/ACK and RTS packets, respectively. R_{rd} can be extracted from the Physical Layer Convergence Procedure (PLCP) header in a potential relay node's transmitted data packets. For example, node-E in Fig. 3.1 overhears a RTS

packet from node-A (which will be the potential relay node) to the AP. It can calculate the achievable data rate R_{sr} between itself and node-A by evaluating the channel quality between them. Upon receiving a CTS packet from the AP, node-E can derive its feasible transmission data-rate R_{sd} to the AP. It also calculates the data-rate R_{rd} between node-A and the AP by extracting the piggy-backed transmission rate from the PLCP header.

The *success rate* field in the Relay list is calculated as follows:

- Its value for a new added relay node is set to $\alpha_1\%$.
- For an existing relay node, the success rate is increased by $\alpha_2\%$ for each successful transmission via the selected relay, and decreased by $\alpha_2\%$ when the transmission fails.
- The relay node is removed from the *Relay list* when its *success rate* is less than $\alpha_1\%$.
- If the G_R value of a relay node is changed, the *success rate* of that relay is reset to $\alpha_1\%$ as a new added relay.
- Each time a source node overhears the transmission from the relay node to the AP, its *success rate* is increased (or decreased) by $\alpha_3\%$ for each successful (or failed) transmission between them.
- A source node selects a relay which has a maximum G_R value. When multiple relay nodes have the same G_R value, the one with a high success rate will be selected to serve the user as a relay.

These percentage α_1, α_2, and α_3 are design parameters optimized based on the channel conditions and the data packet length. The source node updates its *Relay list* for each successful transmission between any

neighbouring node and the AP. In order to reduce the control overhead, the length of the *Relay list* can be limited for example to five entries. In this way, each low data-rate node maintains an up-to-date list of high data-rate neighbouring nodes with their IDs, rates (R_{sr} and R_{rd}), G_R's , and success rates. Taking into account the IEEE 802.11b data-rates and the rate gain in equation 3.1, only the nodes in zones III and IV at the data-rates $2,\ 1\ Mbps$, respectively can benefit form the two-hop transmission (i.e. $G_R > 1$) when there is a relay node available. However, the nodes in zone-II at data-rate $R_{sd} = 5.5Mbps$ or nodes in zone-I at data-rate $R_{sd} = 11Mbps$ use the standard DCF protocol for the IEEE 802.11b WLANs between a source node and the AP. Considering backward compatibility with the standard DCF and the principles given above, the next section describes the principles of the BTAC protocol.

3.1.3 BTAC Transmission Algorithm

1. The source node sends a Modified RTS (MRTS) packet to the AP and potential relay node at the base data rate, i.e. 1 Mbps for 802.11b.

2. Upon receiving the MRTS packet, the AP sends a CTS packet to the source node at rate 1 Mbps. The selected relay node overhears the CTS packet.

3. IF the selected relay is ready, THEN do the following:

   (a) The relay sends a Busy-Tone-Signal (BTS) to both the source and the AP.

   (b) Upon receiving the BTS, the source sends its data packet "DATA-S" to the relay at a high data-rate R_{sr}.

(c) Upon receiving "DATA-S" from the source, the relay forwards "DATA-S" to the AP at a high data rate R_{rd}.

4. ELSE (no relay for the source): The source sends its data packet "DATA-S" to the AP at a low data rate R_{sd}.

5. Upon successfully receiving "DATA-S", the AP sends an "ACK" to the source at rate 1 Mbps.

As shown in Fig. 3.2(b), the proposed Modified MRTS packet has the same size as the standard RTS packet which in turn is shown in Fig. 3.2(a). However, the six-byte Transmitter Address (*TA*) and Receiver Address (*RA*) fields in a standard RTS packet are now replaced with $TA \oplus RA$ [2] and Helper Address (*HA*), respectively. IEEE 802.11 (1) defines two fields: *type* and *subtype* fields in the frame control of the MAC header as shown in Fig. 3.2(c). The *type* and *subtype* fields together identify the function of the frame. There are three frame types: control, data, and management. The *type* field value 01 is used for control frames (e.g., RTS, CTS, and ACK) and values from 0000 to 1001 of the subtype field are reserved. For example, in a regular RTS, the type field value is 01 and the subtype field value is 1011. To enable the AP and all the nodes in the network to recognise the new MRTS packet, the same value of the *type* field of RTS packet is used but the value 1001 is set in the *subtype* field. Thereby, each node in a Basic Service Set (BSS) will be able to identify the MRTS packet in which the TA field is bitwise XOR between the address of the source node and the address of the AP. The *duration* field in both the MRTS and the RTS packet provides the neighbours of the source node with the information required to update their Network Allocation Vector (NAV) as explained later.

[2] The sign $\oplus$ represents bitwise XOR operation.

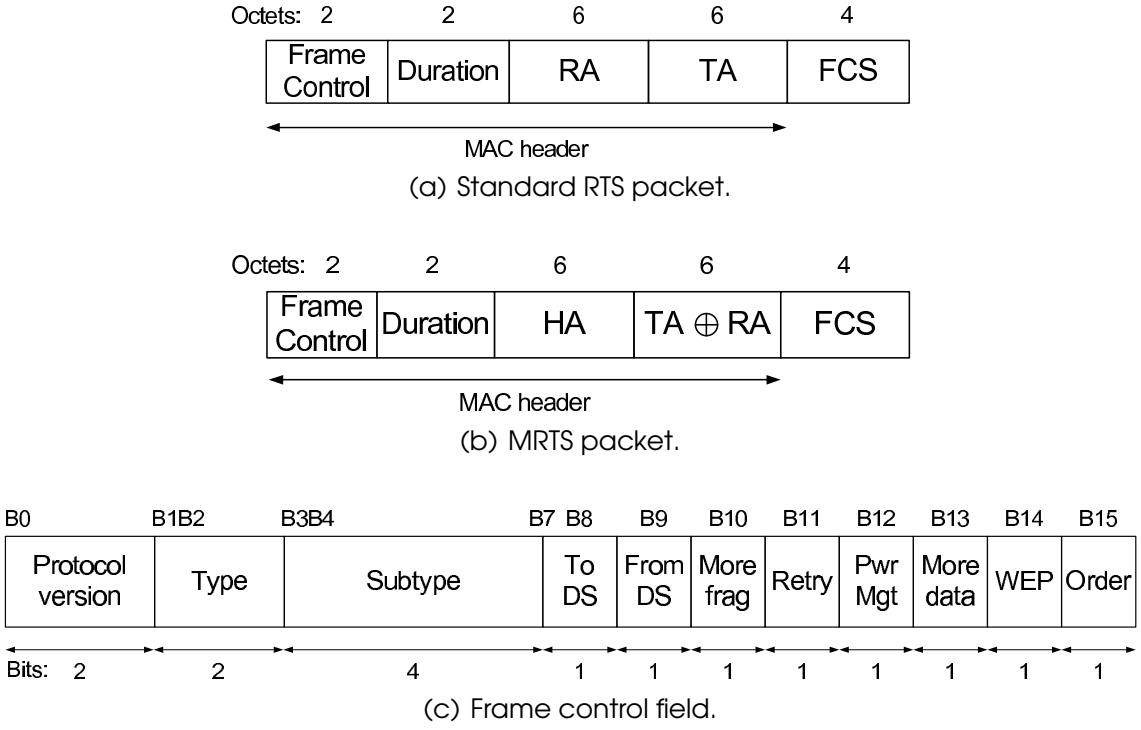

Figure 3.2: Frame formats.

After receiving the MRTS packet, each node including the potential relay, checks the *RA* field to determine whether the packet is intended for itself, and if so stores it. Each node also checks both *type* and *subtype* fields to identify the packet. If it is a MRTS packet and *HA* is its address, the node concludes that it is the potential relay and stores the packet until receiving a CTS packet from the AP. Since the CTS packet has the MAC address of the source node obtained from the received MRTS packet, the relay node then extracts the AP address by using bitwise XOR between the *RA* field of the CTS (source address) and the $TA \oplus RA$ field of the MRTS packet. Therefore, the relay node obtains the MAC addresses of both the source node and the AP. The relay then sends a BTS to make the source node and the AP aware of its willingness for cooperation, i.e. the two-hop transmission. A BTS is a single-frequency sinusoidal signal sent by the relay

node to both the AP and the source node at the same time. The duration of a BTS is one or two slot times (e.g. $20\ \mu s$ for 802.11b).

The AP also checks the *type* and *subtype* fields of the MRTS packet. It uses its own address to execute the XOR operation with the "$TA \oplus RA$" field to obtain the *TA*, and sends a CTS packet back to the source node. In this case, the AP can identify both the *TA* of the sender (source node) and *RA* of its selected relay. Upon receiving a CTS packet, the neighbours of the AP update their NAV by extracting the *duration* field information available in a CTS packet.

After receiving both the CTS and the BTS from the AP and the relay node, respectively, the source node updates its *Relay list*. The source node calculates the data-rate R_{sd} and R_{sr} by estimating the Signal to Noise Ration (SNR) of both the CTS packet and the BTS, respectively. It then sends its data packet (DATA-S) to the relay node at data-rate R_{sr}. If DATA-S is received correctly, the relay node forwards DATA-S to the AP at data-rate R_{sr}. The AP sends an ACK packet to the source node after receiving DATA-S from the relay node to the AP.

The basic operation of BTAC protocol is illustrated in Fig. 3.3. This handshake procedure of control packets, MRTS, CTS and BTS, is shown in Fig. 3.3(a) and the data packets transmission from the source and relay nodes to the AP is shown in Fig. 3.3(b).

3.1.4 Network Allocation Vector Setting

Fig. 3.4(a) shows the NAV setting of successfully transmitting a data packet "DATA-S" via a selected relay node under the BTAC protocol. Similarly to the standard IEEE 802.11b WLAN, two control packets, MRTS and CTS, are used in BTAC to set the Network Allocation Vector (NAV), which

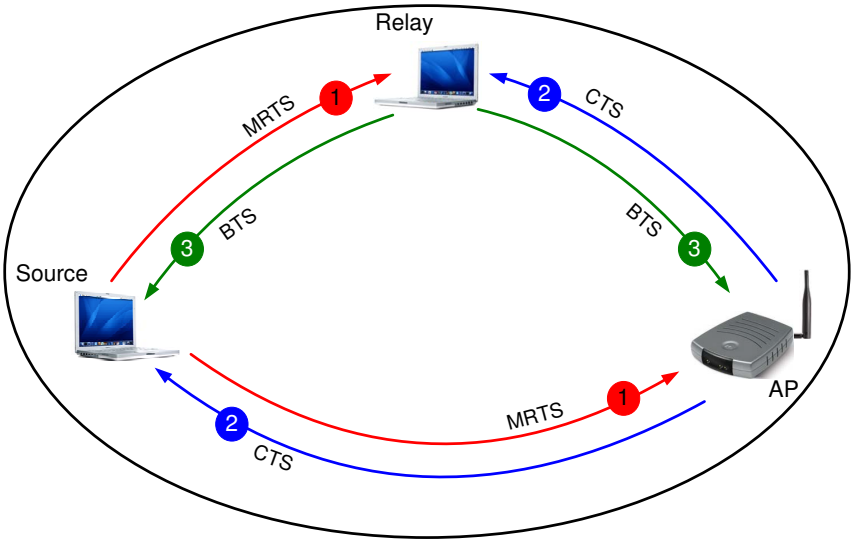

(a) Control packets handshake.

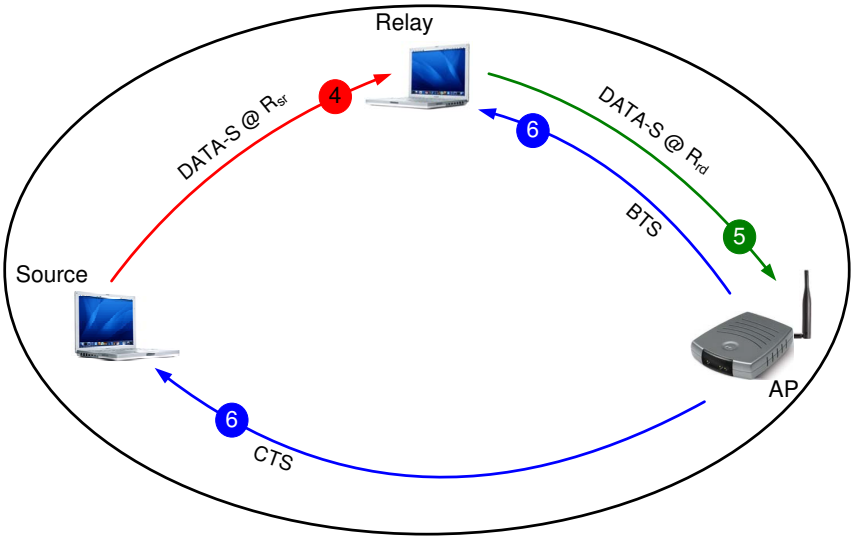

(b) Data packets transmission.

Figure 3.3: Access mechanism of BTAC protocol.

stores the channel reservation information. This method can effectively avoid the "hidden relay node" problem which is explained later. The *duration* field in a MRTS packet shown in Fig. 3.2(b), denoted by D_{MRTS}, is computed as follows:

$$D_{MRTS} = T_{CTS} + \frac{8L_s}{R_{sd}} + \frac{8L_{PLCP}}{R_b} + T_{ACK} + 5T_{SIFS} + 6\delta \tag{3.2}$$

where T_{CTS}, T_{ACK}, and T_{SIFS} stand for the time duration for the CTS packet, ACK packet, and the Short Inter-Frame Space (SIFS), respectively. The data packet size is L_s octets and the PLCP header length, explained in (Chapter 2, Section 2.4.2), is L_{PLCP} octets. R_b and δ are the basic data-rate and channel propagation delay, respectively. After receiving a MRTS, the AP sends a CTS back to the source node after SIFS interval. The *duration* field D_{CTS} of a CTS packet is expressed as follows:

$$D_{CTS} = D_{MRTS} - (T_{CTS} + T_{SIFS} + \delta) \tag{3.3}$$

After exchanging both the MRTS and the CTS packets between a source node and the AP, the communication channel is successfully reserved. The selected relay node, which has overheard both the MRTS and the CTS packets, transmits a one-time slot BTS signal to indicate its readiness for relaying data packets. The source node then sends its data packet "DATA-S" to the relay at a high data-rate R_{sr}. The *duration* field D_{data1} of DATA-S (source-relay) is computed as follows:

$$D_{data1} = \frac{8L_s}{R_{rd}} + \frac{8L_{PLCP}}{R_b} + T_{ACK} + 2T_{SIFS} + 2\delta \tag{3.4}$$

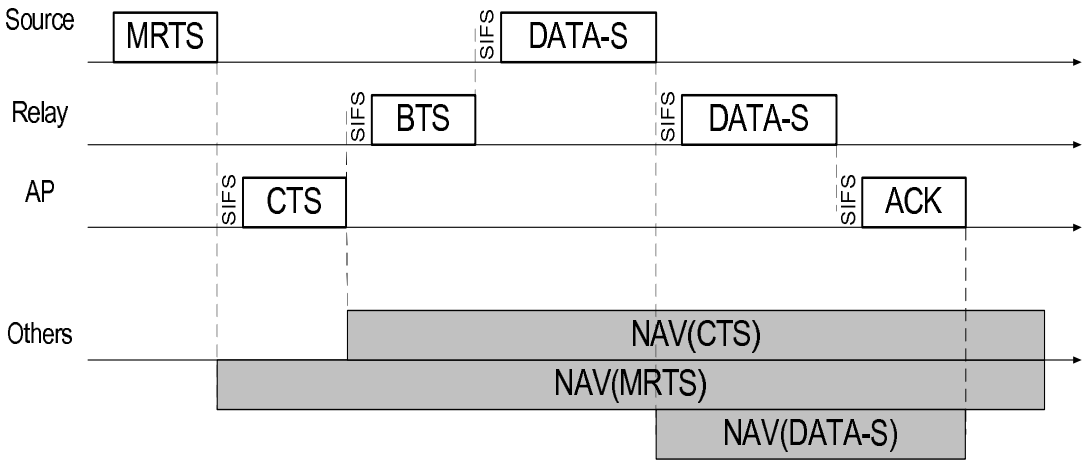

(a) NAV for BTAC-Relay available.

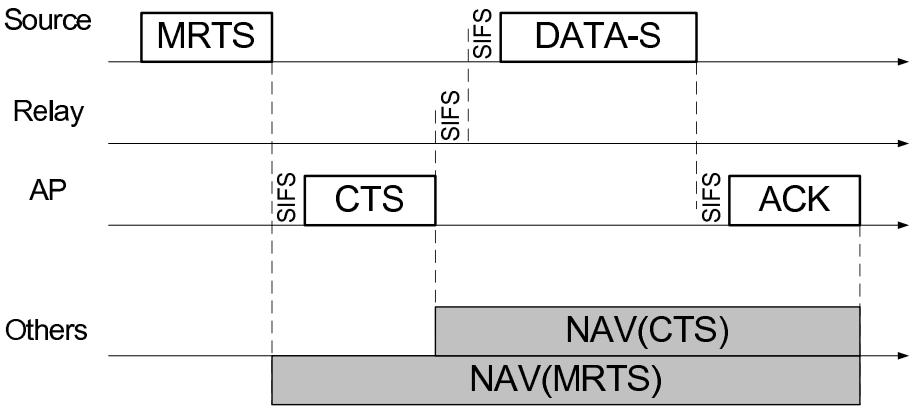

(b) NAV for BTAC-Relay not available.

Figure 3.4: NAV setting in BTAC.

The relay node forwards the DATA-S packet to the AP at a data-rate R_{rd}. The *duration* field D_{data2} of the DATA-S (relay-AP) is the sum of the time required to transmit the ACK packet plus one SIFS interval and the propagation delay δ. The AP replies with an ACK packet when "DATA-S" from the relay is correctly received. The *duration* field of the ACK is set to zero. If the source node does not receive the BTS, it sends its "DATA-S" directly to the AP at a low data rate R_{sd} as shown in Fig. 3.4(b). The *duration* field of the DATA-S (source-AP) is the duration field of the immediately preceding CTS packet given in equation (3.3) minus the time required to transmit the DATA-S packet and one SIFS interval and propagation delay δ. If the source node does not receive the CTS packet or the ACK packet from the AP, it starts a new cycle of transmission after applying a Binary Exponential Backoff algorithm (BEB) as in IEEE 802.11b (5).

3.1.5 The Hidden Relay Node Problem

In the CoopMAC protocol (50), the source node first sends a RTS packet, a neighbouring relay node responds with a Helper- ready To Send (HTS) packet, and then the AP sends a CTS packet to reserve the channel for the upcoming data transmission. As some nodes cannot hear the ongoing packet transmission from the source and relay nodes, they may send a RTS packet to the AP at the same time and cause a collision with the HTS packet. This is defined as the "Hidden Relay Node Problem". A packet collision directly affects the channel reservation procedure and leads to the failure of establishing a two-hop communication path with the relay node, thus causing serious delays in the channel access and packet transmission.

As described in Section 3.1, in the BTAC protocol, the potential relay responds with a BTS signal after receiving a MRTS packet from the source

node and a CTS packet from the AP, i.e. after the channel reservation procedure is completed. All the nodes in the network can hear the AP's CTS packet and will then defer their packet transmission requests, if any. As a result, the BTS from the relay is guaranteed no collision and the two-hop communication path will be successfully established after the BTS is received by the source node and the AP. Therefore, the BTAC protocol completely solves the "Hidden Relay Node Problem" and effectively enables cooperative relay communication in WLANs.

3.2 Enhanced BTAC (EBTAC) Protocol

The dynamic channel condition may have significant impacts on the performance of BTAC. In order to mitigate the impacts of dynamic channel conditions, it is desirable to adaptively decide when to use two-hop transmission according to the channel conditions. We design a heuristically algorithm named Enhanced BTAC (EBTAC) which considers the dynamic nature of the wireless channel and bandwidth utilization.

EBTAC is intended to further improve the performance of the BTAC protocol described in Section 3.1. However, performance of EBTAC is not considered in this work. It is required to test EBTAC experimentally taking into account the physical channel condition, and this beyond the scope of this research.

In EBTAC, a new carrier sense mechanism is employed as shown in Fig. 3.5. The source node sends a MRTS packet in which the *duration* field carries the duration of the CTS packet and the BTS signal. After receiving both the CTS and BTS, the source node calculates the data rates R_{sr} and R_{rd}. The source node then sends its data packet (DATA-S) to the relay node

with the actual transmission time in the *duration* field of the data packet. In this way, the nodes within the transmission range of the source node defer medium access for the exact transmission time. The source node drops the data packet from its buffer after receiving DATA-S from the relay to the AP. The DATA-S then works as an indirect ACK from the relay node to the source node of receiving the data packet correctly. In this case, the source node does not require to wait for receiving an ACK from the AP.

Similarly to the Receiver-Based Auto Rate (RBAR) scheme (131), the AP after receiving the MRTS packet from the source node, estimates the channel quality between itself and the source node and then calculates the appropriate direct transmission data-rate R_{sd}. Following this the AP sends a CTS packet, shown in Fig. 3.6(b), with a new field R_{sd} added, which contains the data-rate between the source node and the AP. The R_{sd} is a two bit field and uses encoding similar to the *rate* field in the PLCP header in the IEEE 802.11a (6). This method measures the Signal to Noise Ratio (SNR) at the receiver at the time instant just before the data packet transmission. Therefore, it is more accurate than adapting the transmission rate based on the history of preceding transmission.

The neighbours of the AP extract the *duration* field information from the received CTS packet to update their NAV. The AP uses the maximum data packet length L_{max} (e.g. 2312 octets for 802.11b) because the AP has no sufficient information about the actual data packet length. These settings will be cancelled after receiving the ACK packet with a zero *duration* field. After receiving DATA-S (relay-AP), the AP sends an ACK packet back to the relay node to confirm correct receipt of the data packet. All the nodes in the network start a new transmission cycle after receiving the ACK from the AP.

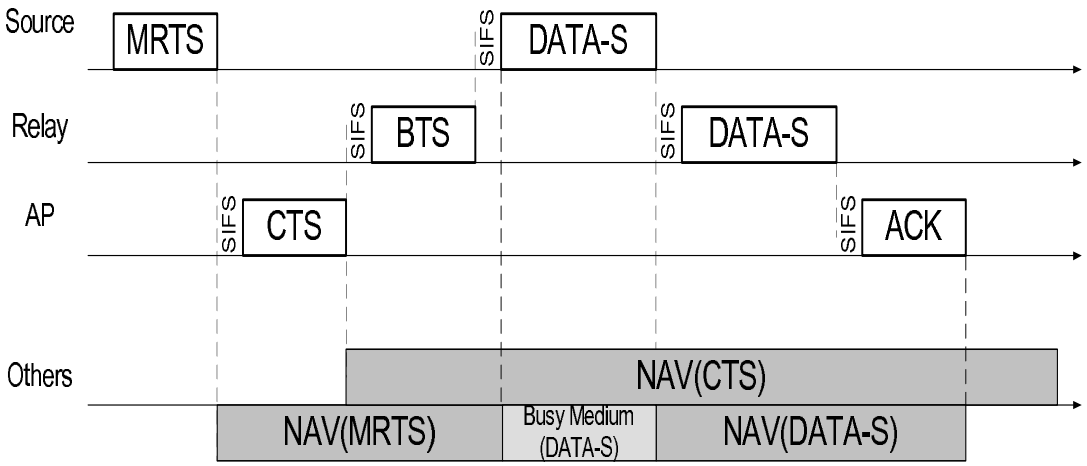

(a) NAV for EBTAC-Relay available.

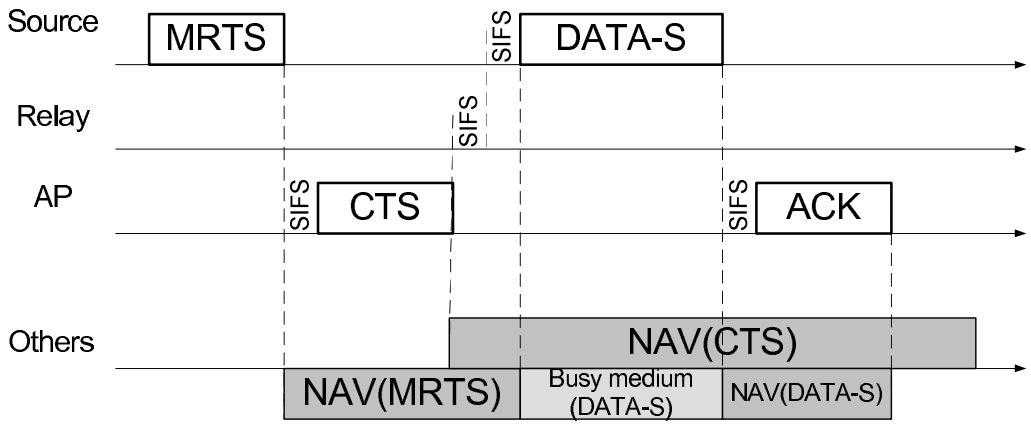

(b) NAV for EBTAC-Relay not available.

Figure 3.5: NAV setting in EBTAC.

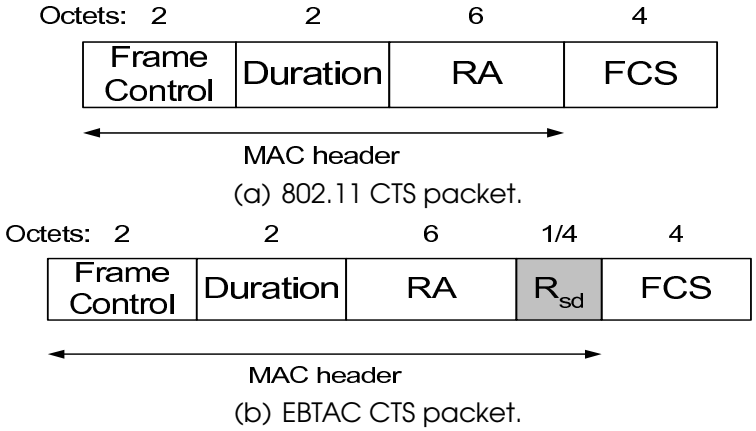

Figure 3.6: Frame formats.

After receiving both the MRTS and CTS packets, the relay node estimates the channel quality and calculates the data-rate R_{sr} and R_{rd} between itself and both the source node and the AP, respectively. The relay node also extracts data-rate R_{sd} (between the source and the AP) from the received CTS packet. The relay node then sends a BTS if the two-hop transmission is faster than the single-hop transmission. Otherwise, the relay node updates its NAV by the reservation information available within the *duration* field of the CTS packet. Therefore, this method can mitigate frequent changes in the channel conditions and hence improve the performance of the EBTAC protocol.

The relay node manages an additional queue containing the packets to be forwarded. This option is available in the IEEE 802.11 (8) standard. When the relay receives "DATA-S" from the source node, it stores the packet in this queue. The relay node forwards the received data packet to the AP after updating the *duration* field within "DATA-S" with the remaining transmission time. The duration field for each packet used in EBTAC is given in Table. 3.1, where other unlisted packets have zero durations.

On the other hand, if the CTS packet is corrupted at both the source

Packet type	The Duration
MRTS	$T_{CTS} + T_{BTS} + 3T_{SIFS} + 3\delta$
CTS	$\frac{8L_{max}}{R_{sd}} + \frac{8L_{PLCP}}{R_b} + T_{ACK} + 2T_{SIFS} + 2\delta$
DATA-S (source-relay)	$\frac{8L_s}{R_{rd}} + \frac{8L_{PLCP}}{R_b} + T_{ACK} + 2T_{SIFS} + 2\delta$
DATA-S (relay-AP)	$T_{ACK} + T_{SIFS} + \delta$
DATA-S (source-AP)	$\frac{8L_s}{R_{sd}} + \frac{8L_{PLCP}}{R_b} + T_{ACK} + 2T_{SIFS} + 2\delta$

Table 3.1: EBTAC Duration field contents

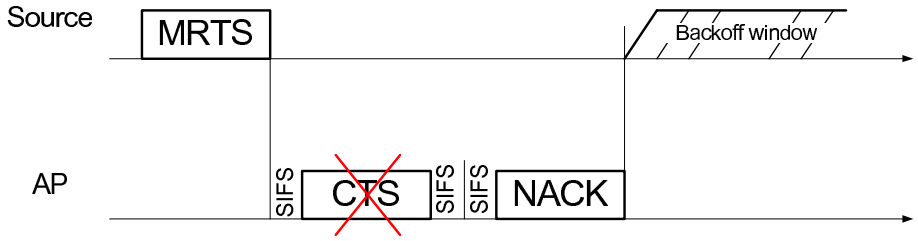

Figure 3.7: CTS corruption in EBTAC.

and relay nodes due to imperfect channel condition, the Relay node does not send a BTS signal. As a result, the source node stops its transmission. The AP waits a two SIFS interval after sending the CTS packet. As shown in Fig. 3.7, when there is no activity on the channel during this interval, it broadcasts a Negative Acknowledgment (NACK) packet with zero *duration* field. The frame format of the NACK is similar to the frame format of the ACK packet with no receiver address. All the nodes then reset their NAV and start a new transmission cycle after receiving the NACK. Therefore, the EBTAC protocol improves the bandwidth utilization under imperfect channel conditions.

If the CTS packet is corrupted at the source node only, the relay node sends a BTS to the source node and the AP. The source concludes

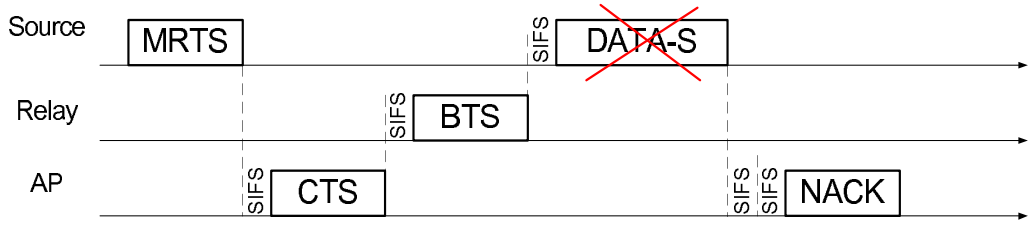

Figure 3.8: DATA source to relay corruption in EBTAC.

that the CTS packet is received correctly at the relay node which is ready to receive the data packet from the source node. As discussed before the relay node sends the BTS only when the two-hop transmission is faster than the single-hop transmission. Consequently, the source node sends the DATA-S packet to the relay node. The relay node forwards the DATA-S to the AP and waits to receive either an ACK for successful transmission or NACK for unsuccessful transmission.

If the DATA-S from the source to the relay is corrupted, as shown in Fig. 3.8, the relay node does not forward this packet to the AP. The AP waits for a two SIFS interval after receiving the DATA-S (source-relay). If the AP does not receive the DATA-S packet from the relay node, it immediately sends NACK to all of the node to start a new transmission cycle. Finally, if the DATA-S (source-relay) is received correctly, the relay node forwards this packet after a SIFS interval to the AP which in turn send an ACK packet for successful transmission or a NACK for unsuccessful transmission.

In the standard IEEE 802.11 and the BTAC protocols, the data packet header is sent at the base data-rate to allow all nodes in the transmission range of the sender to decode the header upon reception. The frame format of data packet under the IEEE 802.11 and BTAC is shown in Fig. 3.9(a). By contrast, the EBTAC follows modifies the data packet header as

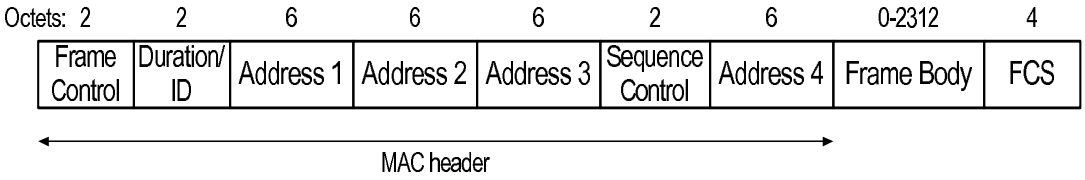

(a) MAC frame format in BTAC and 802.11 (5).

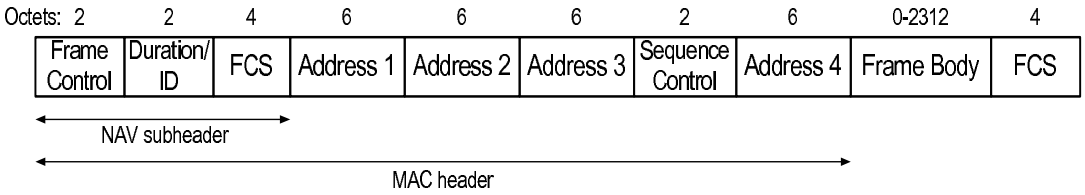

(b) MAC frame format in rDCF (48) and EBTAC.

Figure 3.9: MAC frame format.

in (47,48) by sending only frame control, duration, and Frame Check Sequence (FCS) fields at the base rate. All neighbours of the sender extract the duration field and update their NAV values accordingly. The frame format of a data packet in the EBTAC protocol is shown in Fig. 3.9. Since the remainder of the header is sent at the same data rate as the frame body, the data packet header overhead is smaller for the EBTAC than for the BTAC. Therefore, taking into account the impact of multi-rate transmissions, bandwidth utilization, and the imperfect channel conditions due to a fading, interference and noise, the EBTAC protocol compared to the BTAC protocol improves the system performance.

3.3 Performance Analysis

In this section an analytical model is presented to study the performance of the BTAC protocol under imperfect channel conditions. The per-

formance metrics considered in this chapter are the saturated throughput, energy efficiency, and delay.

3.3.1 Markov Chain Model

The analysis presented in this section is an extension of Bianchi's work (27), where $b(t)$ is defined as a random process representing the value of the backoff counter for a given node at slot time t; while $s(t)$ is a random process representing the backoff stage $j(j = 0, 1, ..., m)$ for the same node at time t. Let $P_{u,i}$ be the probability that a transmitted packet of a given node i has failed. The probability $P_{u,i}$ consists of two parts: the collision probability $P_{c,i}$ caused by collisions with transmissions from other nodes, and the packet error rate probability (PER) $P_{e,i}$ caused by imperfect channel conditions. The probability $P_{b,i}$ is the probability that the channel is busy, as sensed by a given node i during the backoff stages. As in (56, 57), it is assumed that both $P_{b,i}$ and $P_{u,i}$ are independent of the backoff algorithm. The state of a node can be described by $\{j, k\}$, where j is the backoff stage taking values $(0, 1, ..., m)$, and k is the backoff delay taking values $(0, 1, ..., W_j - 1)$ in time slots. W_j is the current Contention Window (CW) size, where $W_j = 2^j W_0$, $CW_{max} = 2^m W_0$, and m is the maximum backoff stage.

In contrast to Bianchi's model (27), Fig. 3.10 illustrates the following differences:

1. The proposed model considers that the backoff counter is stopped when the channel becomes busy, as in (56).

2. Fig. 3.10 takes into account the dynamic channel conditions, as in (63), whereas Bianchi's model assumes ideal channel conditions.

3. The proposed model considers the multi-rate capabilities, as in (144). Bianchi's model is applied for a single data-rate channel.

4. A finite retry limit is modeled, as in (59). Bianchi's model assumes an infinite retry limit.

5. In the proposed model, the probability $P_{b,i}$, that the channel is sensed busy and the probability $P_{u,i}$, that the packet is unsuccessful because of collision or corruption are modeled, as in (56,57).

The probabilities $P_{c,i}$ and $P_{e,i}$ are assumed to be statistically independent (63). Therefore, the probability $P_{u,i}$, that a packet from a given node i is unsuccessfully transmitted, is calculated as follows:

$$P_{u,i} = 1 - (1 - P_{c,i})(1 - P_{e,i}) = P_{c,i} + (1 - P_{c,i})P_{e,i} \tag{3.5}$$

To analyse this Markov model, the steady state probability for a node to be in state $\{j, k\}$ is calculated. Let $\pi_{j,k} = lim_{t\to\infty} Pr\{s(t) = j, b(t) = k\}$ be the stationary probability of the Markov model, and $0 \leq j \leq m, 0 \leq k \leq W_j - 1$. In this Markov chain, the only non-null one step transition probabilities are

$$\begin{cases} P\{j,k|j,k+1\} = 1 - P_{b,i} & 0 \leq k \leq W_j - 2 \;\; 0 \leq j \leq m \\ P\{j,k|j,k\} = P_{b,i} & 1 \leq k \leq W_j - 1 \;\; 0 \leq j \leq m \\ P\{0,k|j,0\} = \frac{1-P_{u,i}}{W_0} & 0 \leq k \leq W_0 - 1 \;\; 0 \leq j \leq m-1 \\ P\{j,k|j-1,0\} = \frac{P_{u,i}}{W_j} & 0 \leq k \leq W_j - 1 \;\; 1 \leq j \leq m \\ P\{0,k|m,0\} = \frac{1}{W_0} & 0 \leq k \leq W_0 - 1 \end{cases} \tag{3.6}$$

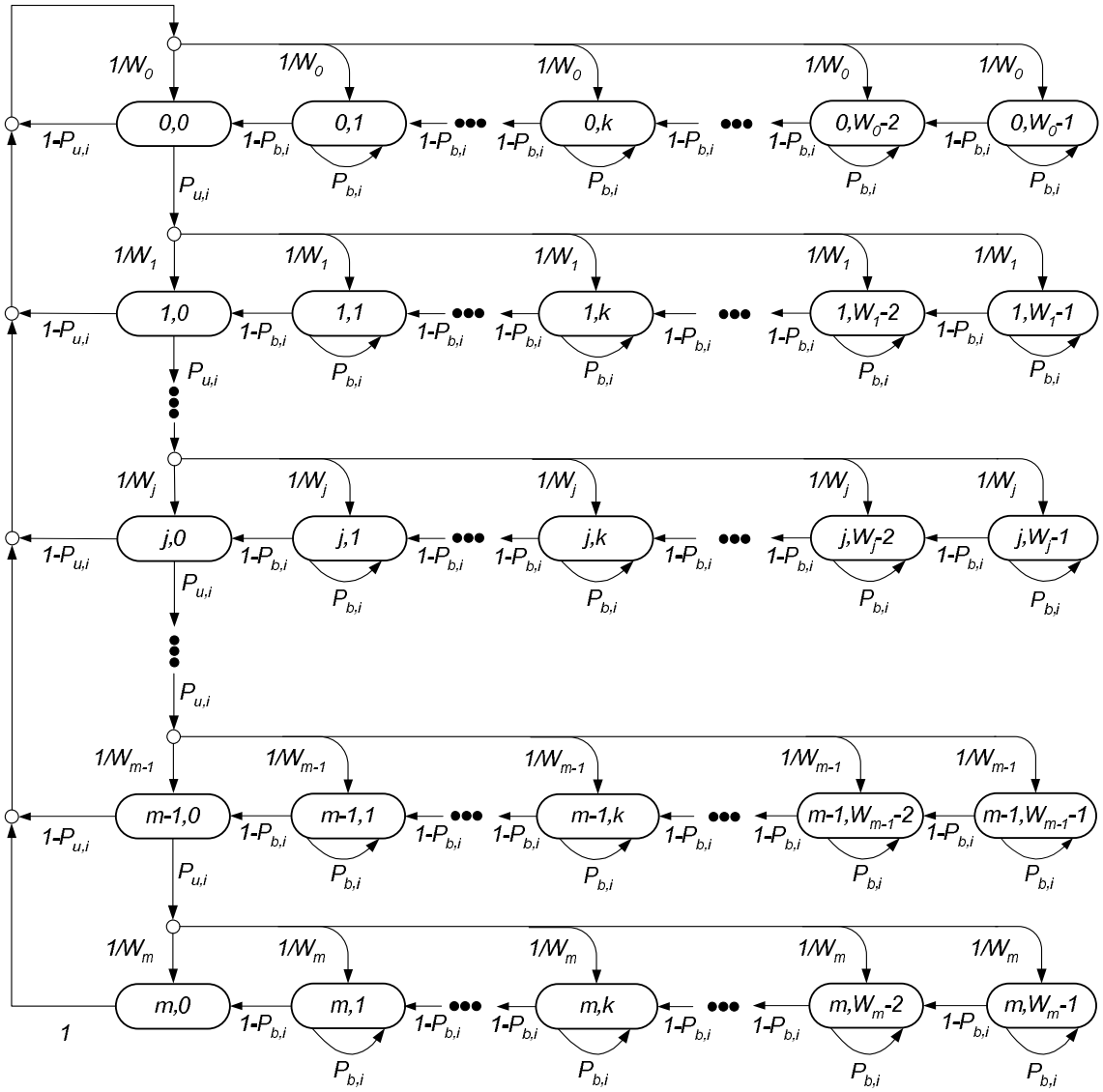

Figure 3.10: BTAC cross layer Markov chain model.

The first equation in (3.6) is the probability that the backoff counter reduces by one when the channel becomes idle during a slot time. The second equation is the probability that at the beginning of each slot time the backoff counter freezes when the channel is sensed busy. A new backoff delay of stage $j = 0$ is selected if the current packet is successfully transmitted and is given by the third equation in (3.6). The other cases model the system after unsuccessful transmission. As considered in the fourth equation in (3.6), if an unsuccessful transmission occurs, the backoff stage increases. Finally, the fifth equation in (3.6) models the fact that at the last backoff stage, the CW will be reset when the transmission is unsuccessful or restart the backoff stage for a new packet when the transmission is successful.

In the steady state, the following equations hold for the Markov chain illustrated in Fig. 3.10.

$$\pi_{j-1,0} \cdot P_{u,i} \;=\; \pi_{j,0}, \qquad \text{then} \qquad \pi_{j,0} = P_{u,i}^{j} \cdot \pi_{0,0} \qquad 0 \le j \le m \tag{3.7}$$

Due to the regularities of the Markov chain, for each $1 \le k \le W_j - 1$, the probability $\pi_{j,k}$ is calculated as follows:

$$\pi_{j,k} = \frac{W_j - k}{W_j(1 - P_{b,i})} \begin{cases} (1 - P_{u,i}) \sum_{x=0}^{m-1} \pi_{x,0} + \pi_{m,0} & j = 0 \\ P_{u,i}\pi_{i-1} & 0 < j \le m \end{cases} \tag{3.8}$$

By using (3.7) and using $\sum_{x=0}^{m-1} \pi_{x,0} = \frac{\pi_{0,0}(1-P_{u,i}^{m})}{1-P_{u,i}}$, equation (3.8) can be rewritten as follows:

$$\pi_{j,k} = \frac{W_j - k}{W_j(1 - P_{b,i})}\pi_{j,0} \qquad 0 \le j \le m, \quad 1 \le k \le W_j - 1 \tag{3.9}$$

By using equations (3.7) and (3.9), the following equation is solved by imposing the normalization condition for a stationary distribution. It is calculated as follows.

$$\begin{aligned} 1 &= \sum_{j=0}^{m} \sum_{k=0}^{W_j-1} \pi_{j,k} \\ &= \sum_{j=0}^{m} \pi_{j,0} \sum_{k=1}^{W_j-1} \frac{W_j - k}{W_j(1-P_{b,i})} + \sum_{j=0}^{m} \pi_{j,0} \\ &= \sum_{j=0}^{m} \pi_{0,0} P_{u,i}^{j} \frac{W_j - 1}{2(1-P_{b,i})} + \frac{1-P_{u,i}^{m+1}}{1-P_{u,i}} \pi_{0,0} \\ &= \frac{\pi_{0,0}}{(1-P_{b,i})} \left[\sum_{j=0}^{m} P_{u,i}^{j} \frac{2^j W_0 - 1}{2} + \frac{(1-P_{b,i})(1-P_{u,i}^{m+1})}{1-P_{u,i}} \right] \end{aligned} \tag{3.10}$$

The second term between square practice on the R.H.S. is calculated as follows.

When $m \leq m'$

$$\sum_{j=0}^{m} P_{u,i}^{j} \frac{2^j W_0 - 1}{2} = \frac{W_0(1-(2P_{u,i})^{m+1})}{2(1-2P_{u,i})} - \frac{1-P_{u,i}^{m+1}}{2(1-P_{u,i})} \tag{3.11}$$

When $m > m'$

$$\begin{aligned} \sum_{j=0}^{m} P_{u,i}^{j} \frac{2^j W_0 - 1}{2} &= \sum_{j=0}^{m'} P_{u,i}^{j} \frac{2^j W_0 - 1}{2} + \sum_{j=m'+1}^{m} P_{u,i}^{j} \frac{2^{m'} W_0 - 1}{2} \\ &= \frac{W_0(1-(2P_{u,i})^{m'+1})}{2(1-2P_{u,i})} - \frac{1-P_{u,i}^{m'+1}}{2(1-P_{u,i})} \\ &\quad + \frac{(2^{m'} W_0 - 1)(P_{u,i}^{m'+1} - P_{u,i}^{m+1})}{2(1-P_{u,i})} \end{aligned} \tag{3.12}$$

By substituting equation (3.11) into equation (3.10) for $m \leq m'$, we

have:

$$\pi_{0,0} = \frac{\mathcal{A}}{\mathcal{B} + W_0(1 - P_{u,i})(1 - (2P_{u,i})^{m+1})} \tag{3.13}$$

And by substituting equation (3.12) into equation (3.10) for $m > m'$, we have:

$$\pi_{o,o} = \frac{\mathcal{A}}{\mathcal{B} + W_0(1 - P_{u,i})(1 - (2P_{u,i})^{m'+1}) + 2^{m'}W_0(1 - 2P_{u,i})(P_{u,i}^{m'+1} - P_{u,i}^{m+1})} \tag{3.14}$$

where

$$\begin{aligned} \mathcal{A} &= 2(1 - P_{b,i})(1 - P_{u,i})(1 - 2P_{u,i}) \\ \mathcal{B} &= (1 - 2P_{b,i})(1 - 2P_{u,i})(1 - P_{u,i}^{m+1}) \end{aligned}$$

As any transmission occurs when the backoff counter reaches zero regardless of the backoff stage, the probability τ_i that a node i transmits its packet in a randomly chosen slot time is calculated as follows.

$$\begin{aligned} \tau_i &= \sum_{j=0}^{m} \pi_{j,0} = \sum_{j=0}^{m} P_{u,i}^{j} \pi_{0,0} \\ &= \frac{1 - P_{u,i}^{m+1}}{1 - P_{u,i}} \cdot \pi_{0,0} \end{aligned} \tag{3.15}$$

Therefore, the probability τ_i is calculated by substituting equation (3.13) for $m \leq m'$ and equation (3.14) for $m > m'$ into equation (3.15).

The collision probability $P_{c,i}$ that at least one of the $N - 1$ remaining nodes other than the current transmitting node i transmits simultaneously

in a chosen slot time can be expressed as follows.

$$P_{c,i} = 1 - \prod_{\substack{j=1 \\ j \neq i}}^{N} (1 - \tau_j) \tag{3.16}$$

The probability $P_{b,i}$, that the channel is sensed busy by the given node i due to the transmissions of the $N-1$ remaining nodes, is calculated as follows.

$$P_{b,i} = 1 - \prod_{\substack{j=1 \\ j \neq i}}^{N-1} (1 - \tau_j) \tag{3.17}$$

3.3.2 Cross Layer MAC-Channel Model

To calculate the packet error rate probability $P_{e,i}$ (at node i), a simple and widely used model called "Gilbert-Elliot model" (145, 146) is used to capture the burst behavior of the wireless channel caused by fading. Albeit this simplified model does not capture all the fading aspects, however it gives some indications of burst errors caused by deep fading. The model is shown in Fig. 3.11 and it consists of two states, where one state represents a good (G) channel condition and the other one represents a bad (B) channel condition. In the simplest Gilbert model the probability of packet loss in a good state is assumed to be zero, whereas in a bad state the packet loss is assumed to be one.

In this model the state sojourn time (duration to be in a state) is a random variable having a geometric distribution. For a high probability of staying in one state, the sojourn time of the channel in state G (or B) is modeled by an exponential distribution with probability density function (pdf) $\lambda_g e^{-\lambda_g t}$ (or $\lambda_b e^{-\lambda_b t}$); where λ_g and λ_b are the transition rate constants

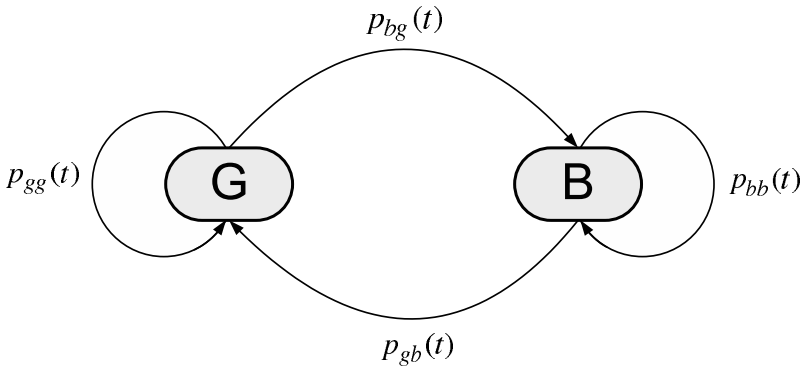

Figure 3.11: Gilbert-Elliot channel model.

from state G to state B and from state B to state G, respectively. Hence the average sojourn times T_G and T_B in a good state and in a bad state, respectively are given by:

$$T_G = \frac{1}{\lambda_g} \quad \text{and} \quad T_B = \frac{1}{\lambda_b} \tag{3.18}$$

From which the steady state probability, π_G, of being in a state G is calculated as follows:

$$\pi_G = \frac{T_G}{T_G + T_B} \tag{3.19}$$

Similarly, the steady state probability, π_B, for being in a state B is obtained as follows:

$$\pi_B = \frac{T_B}{T_G + T_B} \tag{3.20}$$

Substituting equation (3.18) into equations (3.19) and (3.20), we

have:

$$\pi_G = \frac{\lambda_b}{\lambda_g + \lambda_b} \quad \text{and} \quad \pi_B = \frac{\lambda_g}{\lambda_g + \lambda_b} \tag{3.21}$$

Theorem 2.1.1 (147) is used to obtain the stochastic transition matrix $P(t) = (p_{ij}(t), i, j \in S)$, where S is the state set. This theorem shows that P(t) satisfies the set of equations:

$$P'(t) = QP(t) \quad \text{and} \quad P(0) = I \tag{3.22}$$

And their solution is:

$$P(t) = P(0)e^{Qt} = e^{Qt} = \sum_{k=0}^{\infty} \frac{(Qt)^k}{k!} \tag{3.23}$$

where I is the identity matrix and the matrix Q is called *infinitesimal generator,* or *transition rate matrix* of the process and is given by:

$$Q = \begin{pmatrix} -\lambda_g & \lambda_g \\ \\ \lambda_b & -\lambda_b \end{pmatrix}$$

If $\{X(t) : t \geq 0\}$ represents the channel state at time t, the transition probabilities for all $t, t_0 \geq 0$ are given by:

$$\begin{aligned} p_{i,j}(t_0) &= Pr(X(t+t_0) = j \mid X(t) = i) \quad \text{for all } i, j \in S \\ &= U_I^T P(t_0) U_F = U_I^T e^{Qt_0} U_F \end{aligned} \tag{3.24}$$

where U_I is the initial probability vector representing the initial distri-

bution, and U_F is the final probability vector. The U_I (or U_F) vector is simply chosen with ith (or jth) entry equal to 1 and all other entries equal to 0.

When a source node i transmits a MRTS without collision, there are still five events where the transmission could fail due to corruption. These events include corruption of the MRTS, CTS, DATA-S from source to relay, DATA-S from relay to AP, and ACK packets. It is assumed that there is no BTS corruption, since it is a sinusoidal signal with no information to be corrupted.

The probability v_1, that a MRTS is corrupted given that only one MRTS is transmitted (no collision), is calculated as follows:

$$\begin{aligned} v_1 &= P_r(\text{MRTS corrupted}|\text{1 MRTS sent}) \\ &= 1 - P_r(G \text{ state at MRTS start}) P_r(G \text{ state duration} > T_{MRTS} + \delta) \\ &= 1 - \frac{\lambda_b}{\lambda_g + \lambda_b} e^{-\lambda_g (T_{MRTS} + \delta)} \end{aligned} \tag{3.25}$$

where $T_{MRTS} = \frac{L_{MRTS}}{R_b}$ is the duration of a MRTS packet, L_{MRTS} is a MRTS packet length, R_b is the base data-rate (e.g. 1Mbps in 802.11b), and δ is the channel propagation delay.

The probability v_2, that a CTS packet is corrupted given that a single MRTS packet is successfully received, is expressed as follows:

$$\begin{aligned} v_2 &= P_r(\text{CTS corrupted} \mid \text{MRTS is correct}) \\ &= P_r(B \text{ state at CTS start} \mid G \text{ state at MRTS end}) \\ &\quad + P_r(G \text{ state at CTS start and } B \text{ state before CTS end} \mid G \text{ state at MRTS end}) \end{aligned} \tag{3.26}$$

The second term on the R.H.S of equation (3.26) is expressed as fol-

lows:

$$\begin{aligned}
&P_r(G \text{ state at CTS start and } B \text{ state before CTS end} \mid G \text{ state at MRTS end}) \\
&= P_r(G \text{ state at CTS start} \mid G \text{ state at MRTS end}) P_r(G \text{ state duration} < T_{CTS} + \delta) \\
&= P_r(G \text{ state at CTS start} \mid G \text{ state at MRTS end}) \Big(1 - e^{\lambda_g (T_{CTS} + \delta)}\Big)
\end{aligned} \tag{3.27}$$

where $T_{CTS} = \frac{L_{CTS}}{R_b}$ is the duration of a CTS packet, and L_{CTS} is a CTS packet length. From equations (3.27) and (3.24), we have:

$$\begin{aligned}
P_r(G \text{ state at CTS start} \mid G \text{ state at MRTS end}) &= P_r(X(t + T_{SIFS}) = G \mid X(t) = G) \\
&= p_{gg}(T_{SIFS}) = U_I^T e^{Q T_{SIFS}} U_F
\end{aligned} \tag{3.28}$$

where T_{SIFS} is the duration of a SIFS interval, and

$$U_I = U_F = \begin{pmatrix} 1 \\ \\ 0 \end{pmatrix}$$

Substituting equation (3.28) into equation (3.27), we have:

$$\begin{aligned}
&P_r(G \text{ state at CTS start and } B \text{ state before CTS end} \mid G \text{ state at MRTS end}) \\
&= U_I^T e^{Q T_{SIFS}} U_F \Big(1 - e^{\lambda_g (T_{CTS} + \delta)}\Big)
\end{aligned} \tag{3.29}$$

Recalling the first term on the R.H.S of equation (3.26), hence we

have:

$$\begin{aligned} P_r(B \text{ state at CTS start} \mid G \text{ state at MRTS end}) &= p_{bg}(T_{SIFS}) = 1 - p_{gg}(T_{SIFS}) \\ &= 1 - U_I^T e^{QT_{SIFS}} U_F \end{aligned} \quad (3.30)$$

Substituting equations (3.29) and (3.30) into equation (3.26), we have:

$$v_2 = \left(1 - U_I^T e^{QT_{SIFS}} U_F\right) + U_I^T e^{QT_{SIFS}} U_F \left(1 - e^{-\lambda_g (T_{CTS} + \delta)}\right) \quad (3.31)$$

The probability, v_3, that a DATA-S packet from the source node to the relay node is corrupted given that the CTS packet is received correctly, is calculated as follows:

$$\begin{aligned} v_3 = {} & P_r(\text{DATA-S corrupted} | \text{correct CTS}) = P_r(B \text{ state at DATA-S start} | G \text{ state at CTS end}) \\ & + P_r(G \text{ state at DATA-S start and } B \text{ state before DATA-S end} \mid G \text{ state at CTS end}) \end{aligned} \quad (3.32)$$

where the second term on the R.H.S. of equation (3.32) can be calculated as follows:

$$\begin{aligned} & P_r(G \text{ state at DATA-S start and } B \text{ state before DATA-S end} \mid G \text{ state at CTS end}) \\ & = P_r(G \text{ state at DATA-S start} \mid G \text{ state at CTS end}) \cdot P_r(G \text{ state duration} < T_{DATA-S} + \delta) \\ & = Pr(G \text{ state at DATA-S start} \mid G \text{ state at CTS end}) \left(1 - e^{\lambda_g (T_{sr} + \delta)}\right) \end{aligned} \quad (3.33)$$

where $T_{sr} = \frac{L_s}{R_{sr}} + \frac{L_{PLCP}}{R_b}$ is the duration of a DATA-S packet from the source node to the relay node, L_s is the data packet length, L_{PLCP} is the

PLCP header size, and R_b is the base data rate. Recalling equation (3.24) and assuming no BTS corruption, we have:

$$\begin{aligned} P_r(G \text{ state at DATA-S start} \mid G \text{ state at CTS end}) &= P_r(X(t+T_0) = G \mid X(t) = G) \\ &= p_{gg}(T_0) = U_I^T e^{QT_0} U_F \end{aligned} \tag{3.34}$$

where $T_0 = T_{BTS} + 2T_{SIFS}$, and T_{BTS} is the BTS duration. Then substituting equation (3.34) into (3.33), we have:

$$\begin{aligned} &P_r(G \text{ state at DATA-S start and } B \text{ state before DATA-S end} \mid G \text{ state at CTS end}) \\ &= U_I^T e^{QT_0} U_F \Big(1 - e^{\lambda_g (T_{sr}+\delta)}\Big) \end{aligned} \tag{3.35}$$

Recalling the first term on the R.H.S. of equation (3.32), we have:

$$\begin{aligned} P_r(B \text{ state at DATA-S start} \mid G \text{ state at CTS end}) &= p_{bg}(T_0) = 1 - p_{gg}(T_0) \\ &= 1 - U_I^T e^{QT_0} U_F \end{aligned} \tag{3.36}$$

Substituting equations (3.35) and (3.36) into equation (3.32), we have:

$$v_3 = \Big(1 - U_I^T e^{QT_0} U_F\Big) + U_I^T e^{QT_0} U_F \Big(1 - e^{-\lambda_g (T_{sr}+\delta)}\Big) \tag{3.37}$$

Similarly, the probability v_4, that the DATA-S packet from the relay node to the AP is corrupted given that the DATA-S from the source to the

relay is correctly received, is expressed as follows:

$$\begin{aligned} v_4 &= Pr(\text{DATA-S (R to AP) corrupted} \mid \text{DATA-S (S to R) is correct}) \\ &= \left(1 - U_I^T e^{QT_{SIFS}} U_F\right) + U_I^T e^{QT_{SIFS}} U_F \left(1 - e^{-\lambda_g (T_{rd}+\delta)}\right) \end{aligned} \quad (3.38)$$

where $T_{rd} = \frac{L_s}{R_{rd}} + \frac{L_{PLCP}}{R_b}$ is the duration of the DATA-S packet from the relay node to the AP.

The probability v_5, that the ACK packet is corrupted given that the DATA-S from the relay to the AP, is calculated as follows:

$$v_5 = \left(1 - U_I^T e^{QT_{SIFS}} U_F\right) + U_I^T e^{QT_{SIFS}} U_F \left(1 - e^{-\lambda_g (T_{ACK}+\delta)}\right) \quad (3.39)$$

Let p_{e1}^c be the probability of a MRTS corruption, p_{e2}^c be the probability of a CTS corruption, p_{e3}^c be the probability of a DATA-S (from the source to the relay) corruption, p_{e4}^c be the probability of a DATA-S (from the relay to the AP) corruption, and p_{e5}^c be the probability of an ACK corruption. These probabilities are calculated as follows:

$$\begin{aligned} p_{e1}^c &= v_1 \\ p_{e2}^c &= (1 - v_1) v_2 \\ p_{e3}^c &= (1 - v_1)(1 - v_2) v_3 \\ p_{e4}^c &= (1 - v_1)(1 - v_2)(1 - v_3) v_4 \\ p_{e5}^c &= (1 - v_1)(1 - v_2)(1 - v_3)(1 - v_4) v_5 \end{aligned} \quad (3.40)$$

Therefore, the probability of packet error rate, $P_{e,i}$, of using cooper-

ative (two-hop) transmission can be expressed as follows:

$$P_{e,i} = p_{e1}^c + p_{e2}^c + p_{e3}^c + p_{e4}^c + p_{e5}^c \tag{3.41}$$

The time duration of these five different scenarios are denoted by T_{e1}^c, T_{e2}^c, T_{e3}^c, T_{e4}^c, and T_{e5}^c, respectively, which can be expressed as follows:

$$\begin{aligned}
T_{e1}^c &= T_{MRTS} + T_{CTS} + T_{SIFS} + T_{DIFS} + 2\delta \\
T_{e2}^c &= T_{MRTS} + T_{CTS} + T_{SIFS} + T_{DIFS} + 2\delta \\
T_{e3}^c &= T_{MRTS} + T_{CTS} + T_{BTS} + T_{sr} + 4T_{SIFS} + 4\delta \\
T_{e4}^c &= T_{MRTS} + T_{CTS} + T_{BTS} + T_{sr} + T_{rd} + T_{ACK} + 3T_{SIFS} + T_{DIFS} + 6\delta \\
T_{e5}^c &= T_{MRTS} + T_{CTS} + T_{BTS} + T_{sr} + T_{rd} + T_{ACK} + 3T_{SIFS} + T_{DIFS} + 6\delta
\end{aligned} \tag{3.42}$$

where T_{DIFS} is the duration of the Distributed Inter-Frame Space (DIFS). In the same manner, $P_{e,i}$ can be calculated for a node which uses a direct transmission scheme. Let u_1^d be the probability of a RTS corruption given that a single RTS is sent, u_2^d be the probability of a CTS corruption given that a RTS is correct, u_3^d be the probability of a DATA-S (source-AP) corruption given that a CTS is correct, and u_4^d be the probability of an ACK corruption given that a DATA-S is correct. These probabilities are calcu-

lated as follows:

$$\begin{aligned} u_1^d &= 1 - \frac{\lambda_g}{\lambda_g + \lambda_b} e^{T_{RTS}+\delta} \\ u_2^d &= \left(1 - U_I^T e^{QT_{SIFS}} U_F\right) + U_I^T e^{QT_{SIFS}} U_F \left(1 - e^{-\lambda_g (T_{CTS}+\delta)}\right) \\ u_3^d &= \left(1 - U_I^T e^{QT_{SIFS}} U_F\right) + U_I^T e^{QT_{SIFS}} U_F \left(1 - e^{-\lambda_g (T_{sd}+\delta)}\right) \\ u_4^d &= \left(1 - U_I^T e^{QT_{SIFS}} U_F\right) + U_I^T e^{QT_{SIFS}} U_F \left(1 - e^{-\lambda_g (T_{ACK}+\delta)}\right) \end{aligned} \quad (3.43)$$

where T_{RTS} is the duration of a RTS packet, and $T_{sd} = \frac{L_s}{R_{sd}} + \frac{L_{PLCP}}{R_b}$ is the duration of the DATA-S packet from the source node to the AP. We define that p_{e1}^d is the probability of a RTS corruption, p_{e2}^d is the probability of a CTS corruption, p_{e3}^d be the probability of a DATA-S (source-AP) corruption, and p_{e4}^d be the probability of an ACK corruption given that exactly one RTS is sent. These probabilities are then expressed as follows:

$$\begin{aligned} p_{e1}^d &= u_1^d \\ p_{e2}^d &= (1 - u_1^d) u_2^d \\ p_{e3}^d &= (1 - u_1^d)(1 - u_2^d) u_3^d \\ p_{e4}^d &= (1 - u_1^d)(1 - u_2^d)(1 - u_3^d) u_4^d \end{aligned} \quad (3.44)$$

Therefore, the probability $P_{e,i}$ of the node i, that uses a direct transmission, is calculated as follows:

$$P_{e,i} = p_{e1}^d + p_{e2}^d + p_{e3}^d + p_{e4}^d \quad (3.45)$$

The corresponding time durations of the events identified in equa-

tion (3.43) are expressed as follows:

$$\begin{aligned} T_{e1}^{d} &= T_{RTS} + T_{CTS} + T_{SIFS} + T_{DIFS} + 2\delta \\ T_{e2}^{d} &= T_{RTS} + T_{CTS} + T_{SIFS} + T_{DIFS} + 2\delta \\ T_{e3}^{d} &= T_{RTS} + T_{CTS} + T_{sd} + T_{ACK} + 3T_{SIFS} + T_{DIFS} + 4\delta \\ T_{e4}^{d} &= T_{RTS} + T_{CTS} + T_{sd} + T_{ACK} + 3T_{SIFS} + T_{DIFS} + 4\delta \end{aligned} \tag{3.46}$$

Therefore, given the set of equations (3.5) - (3.16), (3.25) - (3.41), and (3.43) - (3.45), a non-linear system can be solved to determine the values of $P_{u,i}$ and τ_i for any node $i \in S$. Since S is the set of nodes in zones I, II, III, and IV. S includes the nodes operating at a direct transmission rate and at a cooperative transmission rate. The calculation of S is given in Appendix A.

The next section investigates the system performance in terms of throughput, energy efficiency, and delay.

3.3.3 Throughput Analysis

In this section, an expression for the saturated throughput of the BTAC protocol in presence of transmission errors is derived. The saturated throughput $\mathbf{S}$ is defined as a ratio of successfully transmitted payload size to the slot time between two consecutive transmissions. A slot time may be idle or busy due to collision, successful transmission, and erroneous transmission due to imperfect channel conditions. According to this definition, the throughput S is expressed as follows:

$$\mathbf{S} = \frac{E[PL]}{E[T_I] + E[T_C] + E[T_S] + E[T_E]} \tag{3.47}$$

where E(PL) is the average payload size, $E[T_I]$ is the average duration of an empty slot time, $E[T_C]$ is the average time that the channel is sensed busy due to a collision, $E[T_S]$ is the average time the channel is sensed busy due to a successful transmission, and $E[T_E]$ is the average time that the channel is sensed busy due to an erroneous transmission. Mathematical relations defining the average slot durations are expressed in the following analysis.

Let P_{tr} be the probability at least one transmission occurs in the considered slot time. Since N nodes contend the channel with probability τ_i, where $i = 1, 2, ..., N$, P_{tr} is then calculated as follows:

$$P_{tr} = 1 - \prod_{i=1}^{N}(1 - \tau_i) \tag{3.48}$$

Given a transmission on the channel from any node i, let $P_{s,i}$ be the probability that a successful transmission occurs in a slot time. $P_{s,i}$ is then expressed as follows:

$$P_{s,i} = \tau_i \prod_{\substack{j=1 \\ j \neq i}}^{N}(1 - \tau_j), \quad i = 1,\ 2,\ ...,\ N \tag{3.49}$$

The total successful probability P_s that there is a successful transmission on

the channel, is calculated as follows:

$$P_s = \sum_{i=1}^{N} P_{s,i} \tag{3.50}$$

The average idle slot duration before a transmission takes place is calculated as follows:

$$E[T_I] = (1 - P_{tr})\sigma \tag{3.51}$$

where $1 - P_{tr}$ is the probability that the chosen slot time is empty, and σ is the duration of an empty slot time (e.g. 20 μs in 802.11b). The probability that the channel is neither idle nor busy due to a successful transmission in the considered slot time is defined as the collision probability which is $[1 - (1 - P_{tr}) - P_s] = P_{tr} - P_s$. The average collision duration $E[T_C]$ can then be calculated as follows:

$$E[T_C] = (P_{tr} - P_s) \cdot T_c \tag{3.52}$$

where T_c stands for the collision time duration between either at least two RTS packet, two MRTS, or RTS and MRTS packets. T_c is the same for all cases because both RTS and MRTS have the same packet length. The T_c is then expressed as follows:

$$T_c = T_{RTS}/T_{MRTS} + T_{CTS} + T_{SIFS} + T_{DIFS} + \delta \tag{3.53}$$

The average slot duration of a successful transmission of a node, that uses either a single-hop transmission or a two-hop transmission is calcu-

lated as follows:

$$E[T_S] = \sum_{i=1}^{N} P_{s,i}(1 - P_{e,i}) \Big[I(i \in S^d) T_{s,i}^d + I(i \in S^c) T_{s,i}^c \Big] \tag{3.54}$$

where $S^c = \{S_1^c \cup S_2^c\}$ is the set of nodes operating at two-hop transmission. S_1^c and S_2^c are the set of nodes in zone IV (at data-rate 1 Mbps) and zone III (at data-rate 2Mbps), respectively using a two-hop transmission. The set S^d is the set of nodes in zones IV, III, II, and I operating at a direct transmission rate 1, 2, 5.5, and 11 Mbps, respectively. The sets S^d, S_1^c, and S_2^c are given in Appendix A. The probability $P_{s,i}(1 - P_{e,i})$ is the probability that the transmitted packet is received correctly by the receiving node. $I(x)$ is 1 if x is true, and is 0 otherwise. $T_{s,i}^d$ and $T_{s,i}^c$ stand for the average time the channel is sensed busy because of successful transmission under single-hop and two-hop transmission, respectively. It is calculated as follows:

$$T_{s,i}^d = T_{RTS} + T_{CTS} + T_{sd}^{(i)} + T_{ACK} + 3T_{SIFS} + T_{DIFS} + 4\delta \tag{3.55}$$

$$T_{s,i}^c = T_{MRTS} + T_{CTS} + T_{BTS} + T_{sr}^{(i)} + T_{rd}^{(i)} + T_{ACK} + 3T_{SIFS} + T_{DIFS} + 6\delta \tag{3.56}$$

The transmitted packet may be corrupted due to imperfect channel conditions. Consequently, the average time $E[T_E]$ that the channel becomes busy due to an erroneous transmission is expressed as follows:

$$E[T_E] = \sum_{i=1}^{N} P_{s,i} \Big[I(i \in S^d) \sum_{j=1}^{4} p_{ej}^d T_{ej}^d + I(i \in S^c) \sum_{j=1}^{5} p_{ej}^c T_{ej}^c \Big] \tag{3.57}$$

where p_{ej}^c, T_{ej}^c, p_{ej}^d, and T_{ej}^d are given in equations (3.40), (3.42), (3.44), and (3.46), respectively.

The average payload size $E[PL]$ is calculated as follows:

$$E[PL] = 8L \sum_{i=1}^{N} P_{s,i}(1 - P_{e,i}) \tag{3.58}$$

Finally, given the average slot durations and the payload size, the saturated throughput can be calculated from equation (3.47).

3.3.4 Energy Efficiency Analysis

The energy efficiency, denoted by η, is defined as the ratio of the successfully transmitted data bits to the total energy consumed (99, 100); the unit of energy efficiency is bits/joule. In the IEEE 802.11 DCF, two management mechanisms are supported: active and Power Saving Mechanism (PSM). In this research, only the active mechanism is considered, in which a node may be in transmit, receive, and sense/idle modes. Under a wireless fading channel, an unsuccessful transmission occurs not only due to collision, but also due to channel errors. Thus, there is extra energy consumption due to transmission errors. Let any node $i = 1, 2, ...N$ act as a generic node. The total energy consumed by this node i in the network can be classified into five parts: the energy consumption during the backoff period, denoted by $E_B^{(i)}$, the energy consumption during the collision period, denoted by $E_C^{(i)}$, the energy consumption during the overhearing transmissions, denoted by $E_O^{(i)}$, the energy consumption when there is no packet collision but there are transmission errors, denoted by $E_E^{(i)}$, and the energy consumption during the successful transmission (neither collision

nor errors), denoted by $E_S^{(i)}$. It is assumed that a node consumes power P_{TX} for transmitting, P_{RX} for receiving, and P_{IX} for sensing or being idle, respectively. Consequently, for an average packet length $E[L]$, the energy efficiency, η, can be written as follows:

$$\eta = \frac{E[L]}{\sum_{i=1}^{N}\left(E_B^{(i)} + E_C^{(i)} + E_O^{(i)} + E_E^{(i)} + E_S^{(i)}\right)} \tag{3.59}$$

Let $\overline{N_{b,i}}$ represent the average total number of backoff slots, which the node i encounters without considering the case when the counter freezes. $\overline{N_{b,i}}$ is calculated as follows:

$$\overline{N_{b,i}} = \sum_{j=0}^{m} \frac{P_{u,i}^{j}(1-P_{u,i})}{1-P_{u,i}^{m+1}} \sum_{k=0}^{j} \frac{W_k - 1}{2}, \quad i = 1, 2, ..., N \tag{3.60}$$

where $\sum_{k=0}^{j} \frac{W_k-1}{2}$ is the average number of backoff slots required by the node i in order to transmit its packet successfully after j retries. $1-P_u^{m+1}$ is the probability that the packet is not dropped. $\frac{P_{u,i}^{j}(1-P_{u,i})}{1-P_{u,i}^{m+1}}$ is the successful transmission probability after the jth backoff stage conditioned that the packet is not dropped.

Hence, given the duration of empty slot σ and the idle power consumption P_{IX}, the energy that the node i spends during the backoff stage can be calculated as follows:

$$E_B^{(i)} = \sigma \cdot P_{IX} \cdot \overline{N_{b,i}}, \quad i = 1, 2, ..., N \tag{3.61}$$

Let $\overline{N}_{idle,i}$ be the average number of consecutive idle slots between two consecutive busy slots of the $N-1$ remaining nodes. $\overline{N}_{idle,i}$ is then

calculated as follows:

$$\overline{N}_{idle,i} = \sum_{j=0}^{\infty} j(1-P_{b,i})^j P_{b,i} = \frac{1}{P_{b,i}} - 1 \tag{3.62}$$

The average number of transmissions $\overline{N_{o,i}}$ overheard by the node i from the other $N-1$ nodes during the backoff process is calculated as follows:

$$\overline{N_{o,i}} = \frac{\overline{N_{b,i}}}{\overline{N}_{idle,i}} = \frac{\overline{N_{b,i}}}{1-P_{b,i}} P_{b,i} \tag{3.63}$$

Both $\overline{N_{b,i}}$ and $\overline{N_{o,i}}$ can be treated as the total number of idle and busy slots that a packet encounters during the backoff stages, respectively. The generic node i overhears collisions, successful transmissions, and erroneous transmissions.

The energy $E_O^{(i)}$, that the node i consumes in overhearing transmissions of other nodes during the backoff stages is calculated as follows:

$$E_O^{(i)} = \overline{N_{o,i}} P_{RX} \Big[E[T_{C_i}] + E[T_{S_i}] + E[T_{E_i}] \Big] \tag{3.64}$$

where $E[T_{C_i}]$, $E[T_{S_i}]$, and $E[T_{E_i}]$ stand for average collision duration, average successful transmission duration, and average erroneous transmission duration given that at least one of the $N-1$ nodes transmits during the backoff process of the node i. Thus, we have:

$$E[T_{C,i}] = \Big[1 - \sum_{\substack{j=1 \\ j \neq i}}^{N-1} P'_{s,j} \Big] T_c \tag{3.65}$$

where $P'_{s,k}$ is the successful transmission probability of node k of the

$N-1$ remaining nodes given that the channel is sensed busy by the generic node i. $P'_{s,k}$ is expressed as follows:

$$P'_{s,k} = \frac{\tau_k \prod_{j=1, j\neq k}^{N-1} (1-\tau_j)}{P_{b,i}} \tag{3.66}$$

The average successful transmission duration $E[T_{S,i}]$ is computed as follows:

$$E[T_{S,i}] = \sum_{\substack{j=1 \\ j\neq i}}^{N-1} P'_{s,j}(1-P_{e,j}) \Big[I(j \in S^d) T^d_{s,j} + I(j \in S^c) T^c_{s,j} \Big] \tag{3.67}$$

where $T^d_{s,j}$ and $T^c_{s,j}$ are given in equations (3.55) and (3.56), respectively. The average erroneous transmission duration, $E[T_{E,i}]$, is expressed as follows:

$$E[T_{E,i}] = \sum_{\substack{j=1 \\ j\neq i}}^{N-1} P'_{s,j} \Big[I(j \in S^d) \sum_{j=1}^{4} p^d_{ej} T^d_{ej} + I(j \in S^c) \sum_{j=1}^{5} p^c_{ej} T^c_{ej} \Big] \tag{3.68}$$

The average number of retries $\overline{N_{r,i}}$ that the generic node i encounters before delivering its packet correctly to the AP, is calculated as follows:

$$\overline{N_{r,i}} = \sum_{k=0}^{m} \frac{k P^k_{u,i}(1-P_{u,i})}{1-P^{m+1}_{u,i}} = \frac{1-P_{u,i}}{1-P^{m+1}_{u,i}} \left[\frac{P_{u,i}}{(1-P_{u,i})^2}(1-P^m_{u,i}) - \frac{m P^{m+1}_{u,i}}{1-P_{u,i}} \right] \tag{3.69}$$

The $\overline{N_{r,i}}$ is the sum of retries due to both collision and erroneous transmission. From equation (3.5), $\frac{P_{c,i}}{P_{u,i}}$ is the fraction of the total retries due to collisions. Hence the average number of retries $\overline{N_{c,i}}$ due to collisions in the

total retries is expressed as follows:

$$\overline{N_{c,i}} = \overline{N_{r,i}} \frac{P_{c,i}}{P_{u,i}} \tag{3.70}$$

Consequently, the energy consumption due to collisions is calculated as follows:

$$E_C^{(i)} = \overline{N_{c,i}} \Big[P_{TX} T_{RTS/MRTS} + P_{RX} T_{CTS} + P_{IX} (T_{DIFS} + T_{SIFS} + \delta) \Big] \tag{3.71}$$

The fraction of the total retries due to packet corruption is $\frac{(1-P_{c,i})p_{ek}^c}{P_{u,i}}$, where $k \in (1,5)$ in a two-hop transmission. Let $\overline{N_{ek}^c}$, where $k = 1, 2, ...5$ be the average number of retries due to corruption of MRTS, CTS, DATA-S (source to relay), DATA-S (relay to AP), and ACK , respectively. $\overline{N_{ek}^c}$ is calculated as follows:

$$\overline{N_{ek}^c} = \overline{N_{r,i}} \frac{(1-P_{c,i})p_{ek}^c}{P_{u,i}}, \qquad k = 1, 2, ...5 \tag{3.72}$$

The calculations are similar in the case of a direct transmission. Let $\overline{N_{ek}^d}$, $k \in (1,4)$ be the average number of retries due to corruption of the RTS, CTS, DATA-S (source to AP), and ACK packets given successful RTS contention, respectively. we have:

$$\overline{N_{ek}^d} = \overline{N_{r,i}} \frac{(1-P_{c,i})p_{ek}}{P_{u,i}}, \qquad k = 1, 2, ...4 \tag{3.73}$$

Let E_{e1}^c, E_{e2}^c, ..., and E_{e5}^c be the energy consumption during the time durations T_{e1}^c, T_{e2}^c, ..., and T_{e5}^c in equation (3.42), respectively. These energy

values are calculated as follows:

$$\begin{aligned}
E^c_{e1} &= P_{TX}T_{MRTS} + P_{IX}(T_{CTS} + T_{SIFS} + T_{DIFS} + 2\delta) \\
E^c_{e2} &= P_{TX}T_{MRTS} + P_{RX}T_{CTS} + P_{IX}(T_{SIFS} + T_{DIFS} + 2\delta) \\
E^c_{e3} &= P_{TX}(T_{MRTS} + T_{sr}) + P_{RX}(T_{CTS} + T_{BTS}) + P_{IX}(4T_{SIFS} + T_{DIFS} + 5\delta) \\
E^c_{e4} &= P_{TX}(T_{MRTS} + T_{sr}) + P_{RX}(T_{CTS} + T_{BTS} + T_{rd}) + P_{IX}(T_{ACK} + 5T_{SIFS} + T_{DIFS} + 6\delta) \\
E^c_{e5} &= P_{TX}(T_{MRTS} + T_{sr}) + P_{RX}(T_{CTS} + T_{BTS} + T_{rd} + T_{ACK}) + P_{IX}(5T_{SIFS} + T_{DIFS} + 6\delta)
\end{aligned} \tag{3.74}$$

For direct transmission, E^d_{ek}, where $k \in (1, 4)$ stand for the RTS, CTS, DATA-S (source-AP), and ACK packets corruption, respectively. These values is computed as follows:

$$\begin{aligned}
E^d_{e1} &= P_{TX}T_{RTS} + P_{IX}(T_{CTS} + T_{SIFS} + T_{DIFS} + 2\delta) \\
E^d_{e2} &= P_{TX}T_{RTS} + P_{RX}T_{CTS} + P_{IX}(T_{SIFS} + T_{DIFS} + 2\delta) \\
E^d_{e3} &= P_{TX}(T_{RTS} + T_{sd}) + P_{RX}T_{CTS} + P_{IX}(4T_{SIFS} + T_{DIFS} + T_{ACK} + 5\delta) \\
E^d_{e4} &= P_{TX}(T_{RTS} + T_{sd}) + P_{RX}(T_{CTS} + T_{ACK}) + P_{IX}(4T_{SIFS} + T_{DIFS} + 5\delta)
\end{aligned} \tag{3.75}$$

Therefore, the energy consumption due to erroneous transmission is expressed as follows:

$$E^{(i)}_E = I(i \in S^d) \sum_{k=1}^{4} \overline{N^d_{ek}} E^d_{ek} + I(i \in S^c) \sum_{k=1}^{5} \overline{N^c_{ek}} E^c_{ek} \tag{3.76}$$

The energy consumed by the generic node i under a successful two-

hop transmission is calculated as follows:

$$\begin{aligned} E_S^c &= P_{TX}(T_{MRTS} + T_{sr}) + P_{RX}(T_{CTS} + T_{BTS} + T_{rd} + T_{ACK}) \\ &\quad + P_{IX}(5T_{SIFS} + T_{DIFS} + 6\delta) \end{aligned} \tag{3.77}$$

E_S^d in a single-hop transmission is computed as follows:

$$E_S^d = P_{TX}(T_{RTS} + T_{sd}) + P_{RX}(T_{CTS} + T_{ACK}) + P_{IX}(4T_{SIFS} + T_{DIFS} + 5\delta) \tag{3.78}$$

Hence the energy consumption during a successful transmission is expressed as follows:

$$E_S^{(i)} = I(i \in S^d)E_S^d + I(i \in S^c)E_S^c \tag{3.79}$$

Finally, the average packet length $E[L] = \sum_{i=1}^{N} 8L$ assuming a fixed packet length. Therefore, the energy efficiency η can be calculated from (3.59).

3.3.5 Delay

The average packet delay is defined as the duration of time from the time instant the packet is at the Head-Of-Line (HOL), i.e. it becomes head of its MAC queue ready for transmission, to the time instant when the packet is acknowledged for a successful transmission. Average packet delay includes the backoff delay, the transmission delay, and the inter-frame spaces. The backoff delay depends on the value of a node's back-

off counter and the duration when the counter freezes due to a busy channel.

Let D_i $(i = 1, 2, ..., N)$ denote a random variable representing a packet delay of a generic node i. The average packet delay $E[D_i]$ can be expressed as follows:

$$E[D_i] = E[D_{b,i}] + E[D_{c,i}] + E[D_{o,i}] + E[D_{e,i}] + E[D_{s,i}] \tag{3.80}$$

where $E[D_{b,i}]$, $E[D_{c,i}]$, $E[D_{o,i}]$, $E[D_{e,i}]$, and $E[D_{s,i}]$ stand for the average delay in backoff stages, the average delay due to collisions, the average delay of overhearing during the backoff process, the average delay due to an erroneous transmission, and the average delay of a successful transmission, respectively. It is calculated as follows:

$$\begin{aligned}
E[D_{b,i}] &= \sigma\overline{N_{b,i}} \\
E[D_{c,i}] &= \overline{N_{c,i}}T_c \\
E[D_{o,i}] &= \overline{N_{o,i}}\Big[E[T_{C_i}] + E[T_{S_i}] + E[T_{E_i}]\Big] \\
E[D_{e,i}] &= P'_{s,i}\Big[I(i \in S^d)\sum_{k=1}^{4}\overline{N_{ek}^d}p_{ek}^d T_{ek}^d + I(i \in S^c\})\sum_{k=1}^{5}\overline{N_{ek}^c}p_{ek}^c T_{ek}^c\Big] \\
E[D_{s,i}] &= I(i \in S^d)T_{s,i}^d + I(i \in S^c)T_{s,i}^c
\end{aligned} \tag{3.81}$$

where $\overline{N_{b,i}}$ and $\overline{N_{c,i}}$ are given in equations (3.60) and (3.63), respectively. $E[T_{C_i}]$, $E[T_{S_i}]$, and $E[T_{E_i}]$ are given in equations (3.65), (3.67), and (3.68), respectively. T_c, $T_{s,i}^d$, and $T_{s,i}^c$ are given in (3.53), (3.55), and (3.56), respectively. T_{ek}^c and T_{ek}^d are given in (3.42) and (3.46), respectively. $\overline{N_{ek}^c}$ and $\overline{N_{ek}^d}$ are given in (3.72) and (3.73), respectively. Therefore, the total

average delay of the network is computed as follows:

$$E[D_T] = \frac{1}{N} \sum_{i=1}^{N} E[D_i] \tag{3.82}$$

3.4 Analytical and Simulation Results

To validate the above analysis, a custom event driven simulator developed by using the Mobile Framework (MF) of the OMNET++ (148) package written in C++ programming language. The parameters used in simulation and analysis are set to the default values specified in IEEE 802.11b standard which are summarized in Table 3.2. The performance of the proposed protocols is evaluated assuming static network topologies. The curves presented hereafter were averaged over 50 runs, each of which had a different topology and ran for a period of time that was long enough to get stabilised results. Packets are transmitted at different rates, depending on the location of the nodes with respect to the AP. Specifically, the distance thresholds for 11Mbps, 5.5Mbps, 2Mbps and 1Mbps are set to 50m, 65m, 75m and 100m, respectively. Whereas the data rates versus distances are used for demonstration purposes, which can be varied in reality. The traffic is uniformly distributed across all the nodes in the network, and the packets arrive in the network according to the Poisson distribution.

In the following figures, solid lines are fro the analytical model results through Matlab software package. Whereas dot-dashed lines are for the simulation results through OMNET++ software package.

Parameter	Value	Parameter	Value
MAC header	272 bits	Slot time, δ	20, 1 μs
PHY header	192 bits	SIFS	10 μs
RTS	352 bits	DIFS	50 μs
CTS	304 bits	BTS	20 μs
ACK	304 bits	CW_{min}	31 slots
PLCP data-rate	1 Mbps	CW_{max}	1023 slots
P_{TX}, P_{RX}, P_{IX}	1.0,0.8,0.8 W	m', m	5,7

Table 3.2: Parameters used for both analytical results and simulation runs.

3.4.1 Throughput Results

Fig. 3.12 shows the simulation and analytical results of the saturated throughput of the BTAC, CoopMAC and IEEE 802.11b protocols against the number of nodes under ideal channel conditions. It is assumed that the data packet length is fixed and is set to be 1024 bytes. As illustrated in Fig. 3.12, there is a good agreement between the analytical model and simulation results. As the network size increases, the throughput of the IEEE 802.11b decreases while the throughput of both the BTAC and CoopMAC protocols increases. However, the BTAC protocol achieves a higher throughput than the CoopMAC protocol. Since the throughput of the BTAC increases from 2.0 Mbps to 2.41 Mbps, and the throughput of the CoopMAC increases from 1.84 Mbps to 2.06 Mbps as the network size increases. The reason is that the overhead control in the BTAC is less that the overhead control in the CoopMAC protocol.

From Fig. 3.13, it can be seen that the collision probability increases as the network size increases. For this reason the throughput of the 802.11 decreases as the number of node increases. On the other hand, as the network size increases, the probability of a low data-rate node finding a relay node increases, as illustrated in Fig. 3.13. Consequently, the low

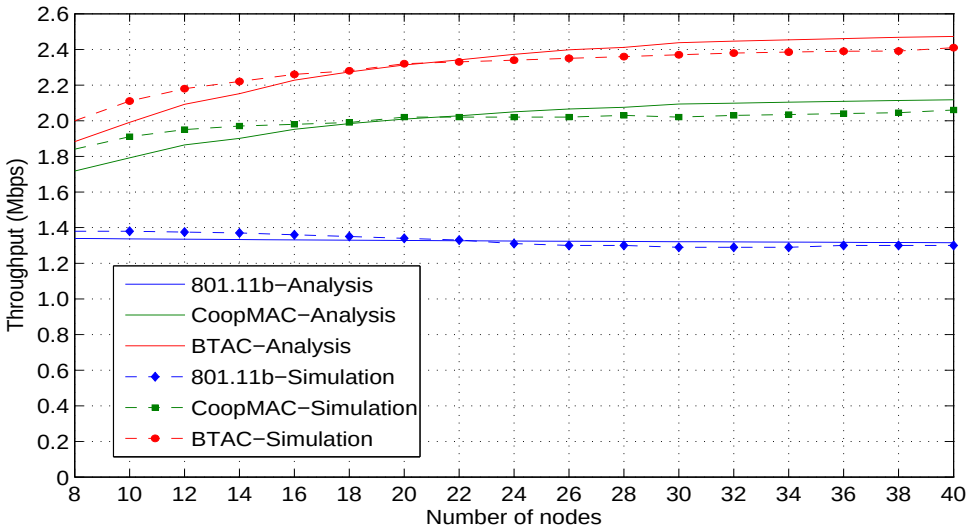

Figure 3.12: Throughput of IEEE802.11b, CoopMAC, and BTAC, L=1024 byte.

data-rate node can send its data packet to the AP in a two-hop transmission, and hence the transmission time decreases. The reduction in the transmission time not only compensates the increasing in the collision time, but also increases the overall throughput of the network.

The effect of the imperfect channel conditions on the throughput performance is investigated in Fig. 3.14. Fig. 3.14 shows the relationship between the throughput gain of both BTAC and CoopMAC protocols and number of nodes under imperfect channel conditions and fixed data packet length. The throughput gain is defined as the throughput of the BTAC and CoopMAC protocols related to the throughput of the IEEE 802.11b protocol. The Good and Bad durations (T_G and T_B, respectively) are assumed to be $50ms$ and $5ms$, and $10ms$ and $1ms$, respectively. As expected, the lower the Good duration, the lower the throughput gain. The reason is that as the Good duration decreases, the probability of the packet error increases and so on the throughput decreases. The BTAC protocol outperforms the CoopMAC protocols even under the imperfect

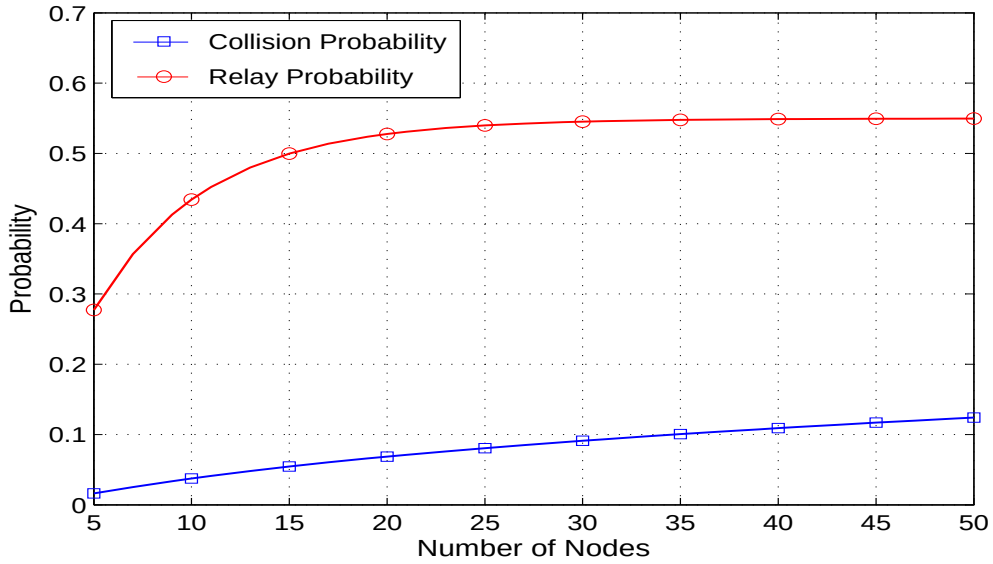

Figure 3.13: Collision and Relay probabilities versus number of nodes, L=1024 byte.

channel conditions.

As shown in Fig. 3.14 the throughput gain of the BTAC protocol under the case of $T_G = 10ms$ is higher than the throughput gain of the CoopMAC protocol under the case of $T_G = 100ms$. In addition to the reduction in the overhead of the BTAC protocol, the busy tone signal used in the BTAC is better than the helper ready to send packet used in the CoopMAC protocol. Therefore, the BTAC is more reliable than the CoopMAC protocol under both ideal and imperfect channel conditions.

It is well known that the packet length has a major effect on the performance of WLANs. The relationship between the throughput and the packet length under error free wireless medium and at a fixed number of nodes which is chosen to be 30 nodes is illustrated in Fig. 3.15. The packet size is changed from 400 bytes, which the threshold to use RTS/CTS transmission in the standard IEEE 802.11, to 2000 byte, which is approximately the maximum packet length supported by the IEEE 802.11b. It can be seen that the analytical results match well the simulation results. As the packet

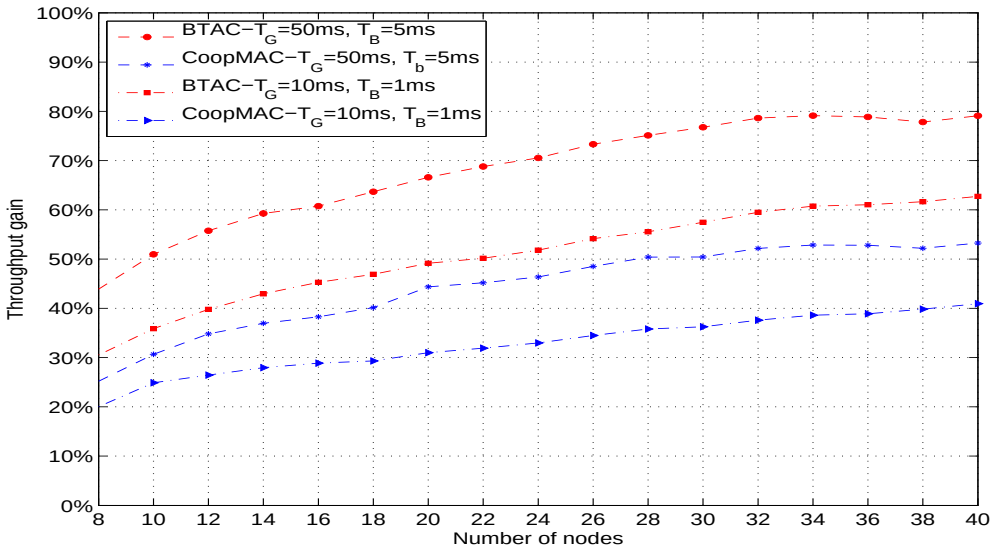

Figure 3.14: Throughput gain, L=1024 byte.

length increases, the throughput of the 802.11b, CoopMAC, and BTAC protocols increases as well. The reason is that the effect of overhead control decreases as the packet length increases, and hence the transmission time required to send a data packet decreases and the throughput increases. From Fig. 3.15, the BTAC protocol outperforms the CoopMAC protocol under a different packet length. This is because the overhead control of the BTAC protocol is less than that of the CoopMAC protocol.

Fig. 3.16 shows the throughput gain of both BTAC and CoopMAC protocols versus the packet length at a fixed network size which is 30 nodes and under imperfect channel conditions. The throughput gain decreases as the channel becomes poor. This is because the number of retries to send a data packet increases and hence the transmission time for that packet also increases. Consequently the throughput gain is degraded as the channel conditions become poor. The throughput gain increases as the packet length increases under the same channel conditions, because the effect of overhead control of the two-hop transmission becomes neg-

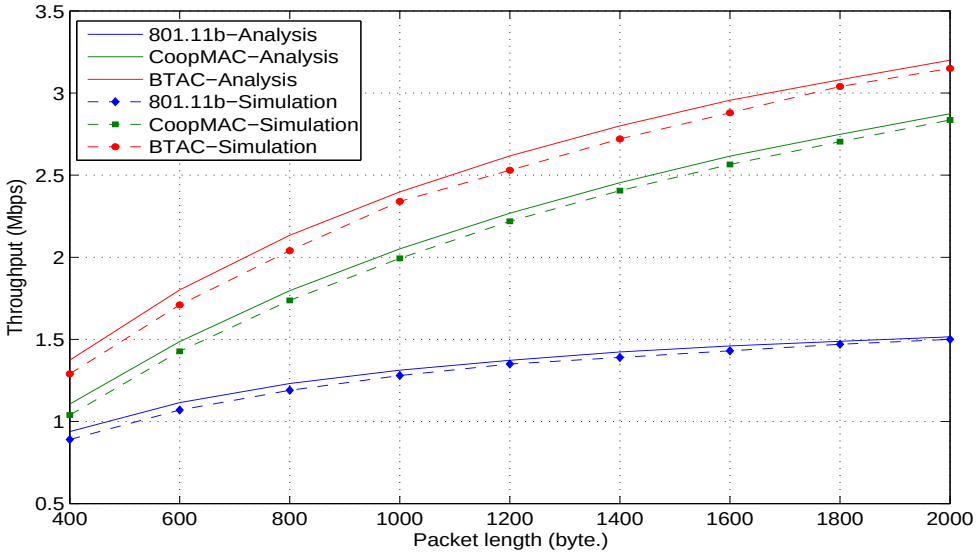

Figure 3.15: Throughput vs. packet length under ideal medium, L=1024 byte.

ligible. When the packet length increases, the throughput that can be achieved by the BTAC protocol is higher than that can be achieved by CoopMAC protocol. The reason is that the error probability of the BTAC is less than the CoopMAC due to replacing the helper reday to send packet by thee busy tone signal. Consequently, when the channel becomes poor, the BTAC protocol becomes more reliable than the CoopMAC protocol. Another point is that as the packet length increases, the effect of the channel conditions becomes effective. This is because as the packet length increases, the probability of the packet error increases and hence the number of retries to send a data packet increases. Hence, the throughput performance of both the BTAC and the CoopMAC protocols decreases.

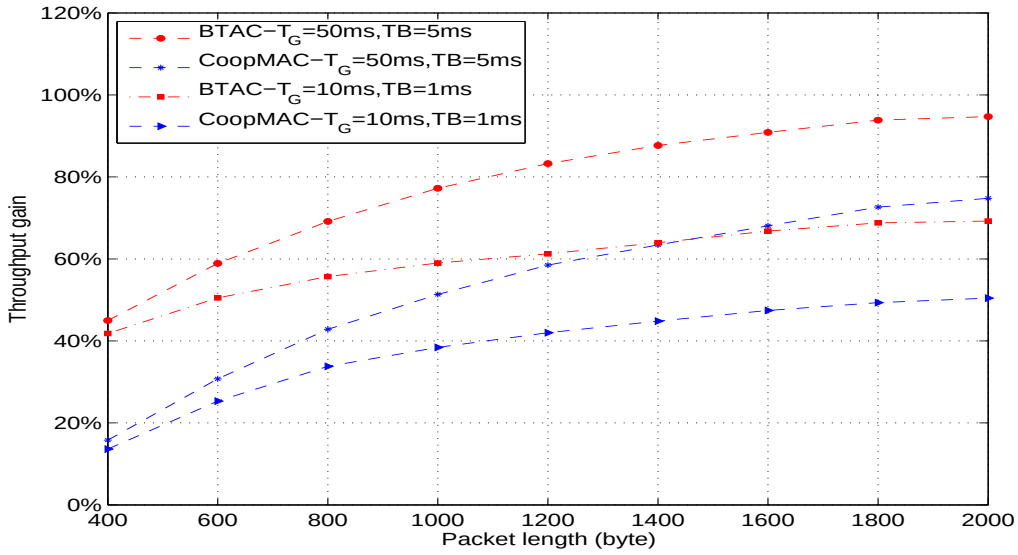

Figure 3.16: Throughput gain versus packet length, N=30.

3.4.2 Energy Efficiency Results

The energy efficiency is counted as one of the most important requirements to design an efficient MAC protocol. The energy efficiency of the 802.11b, CoopMAC, and BTAC protocols versus the number of nodes under ideal channel conditions and fixed packet length is shown in Fig. 3.17. The energy efficiency of both the BTAC and CoopMAC protocols is better than the energy efficiency of the 802.11b protocol due to the advantage of using the two-hop transmission. The energy efficiency decreases as the number of nodes increases due to two different reasons. The first reason is that as the number of nodes increases, the collision probability increases as shown in Fig. 3.13. As the collision probability increases, the retransmission probability increases. Therefore, the node consumes more energy on the retransmissions, receiving and sensing the medium. The second reason is that the overhearing energy consumption increases as the number of nodes increases. Consequently, the energy efficiency

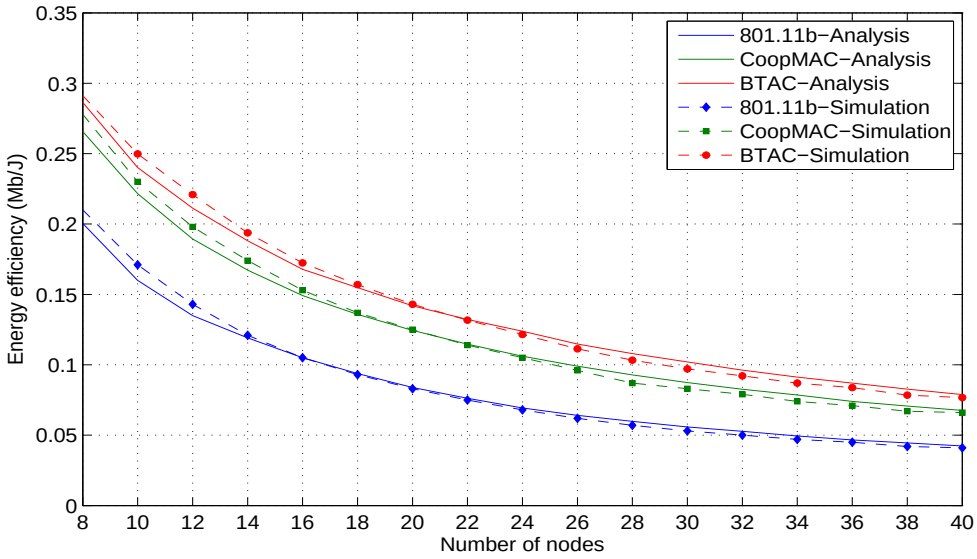

Figure 3.17: Energy efficiency versus number of nodes, L=1024 byte.

decreases as the number of nodes increases. The BTAC protocol achieves higher energy efficiency than the CoopMAC protocol due to the lower overhead control of the BTAC protocol.

The effect of the channel conditions on the energy efficiency versus the number of nodes is shown in Fig. 3.18. In Fig. 3.18(a), the good and bad durations are assumed to be $T_G = 50ms$ and $T_B = 5ms$, respectively, where in Fig. 3.18(b), it is assumed that $T_G = 10ms$ and $T_B = 1ms$. When the channel quality becomes poor, the energy efficiency decreases for the same number of nodes. The reason is that under the imperfect channel conditions, the number of retransmission retries increases causing increasing in the energy consumption of sending, receiving, overhearing, and sensing. The energy efficiency of the BTAC protocol is better than the 802.11b and CoopMAC protocols under different channel conditions. This is because of using a two-hop transmission with lower control overhead than the CoopMAC protocol.

The effect of packet length on the energy efficiency at a fixed num-

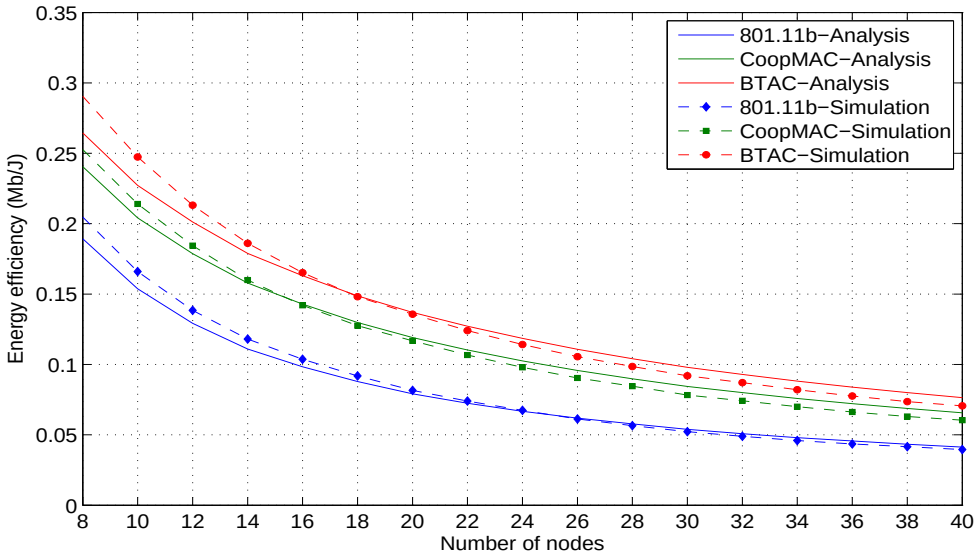

(a) Energy efficiency vs. number of nodes at $T_G = 50ms$ and $T_B = 5ms$.

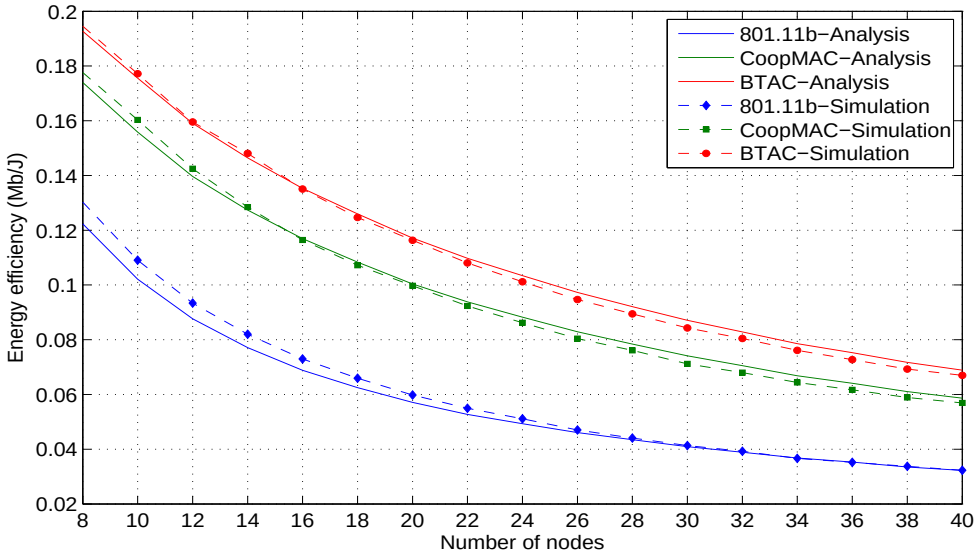

(b) Energy efficiency vs. number of nodes at $T_G = 10ms$ and $T_B = 1ms$.

Figure 3.18: Energy efficiency performance versus number of nodes under imperfect medium conditions, L=1024byte.

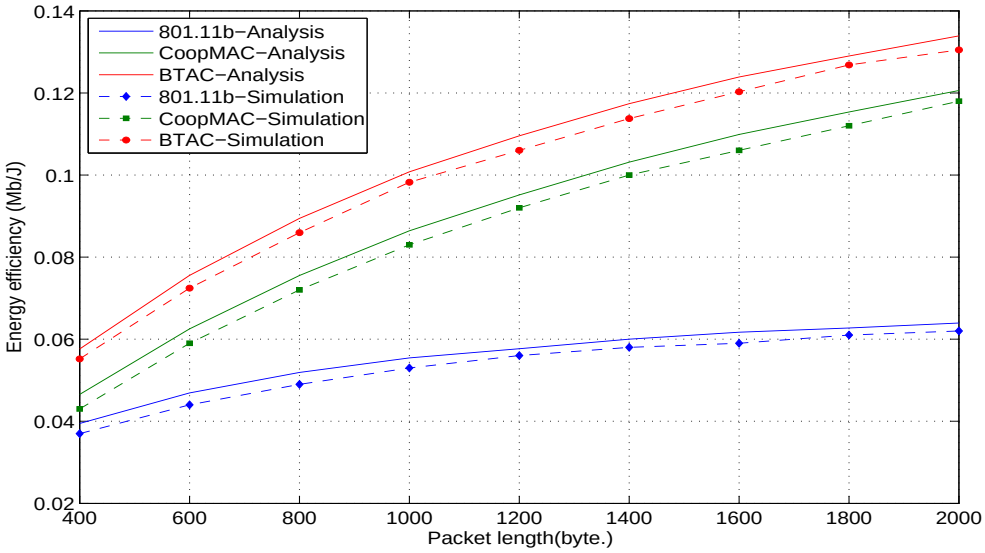

Figure 3.19: Energy efficiency versus packet length, N=30.

ber of nodes (30 nodes) is studied in Fig. 3.19 and Fig. 3.20 under ideal and imperfect channel conditions, respectively. As the packet size increases, the energy efficiency of the 802.11, CoopMAC, and BTAC protocols increases. The reason is that the overhead including the PLCP header and control frames (e.g. RTS and CTS packets) is reduced when the packet length increases. Therefore, more energy is saved, and the energy efficiency is then increased. The energy efficiency decreases as the channel becomes poor. This is because the retransmissions increase and the nodes consume more energy to deliver their packets to the AP. Consequently, the energy efficiency decreases. The BTAC protocol outperforms both the 802.11b and CoopMAC protocols under the ideal and the imperfect channel conditions.

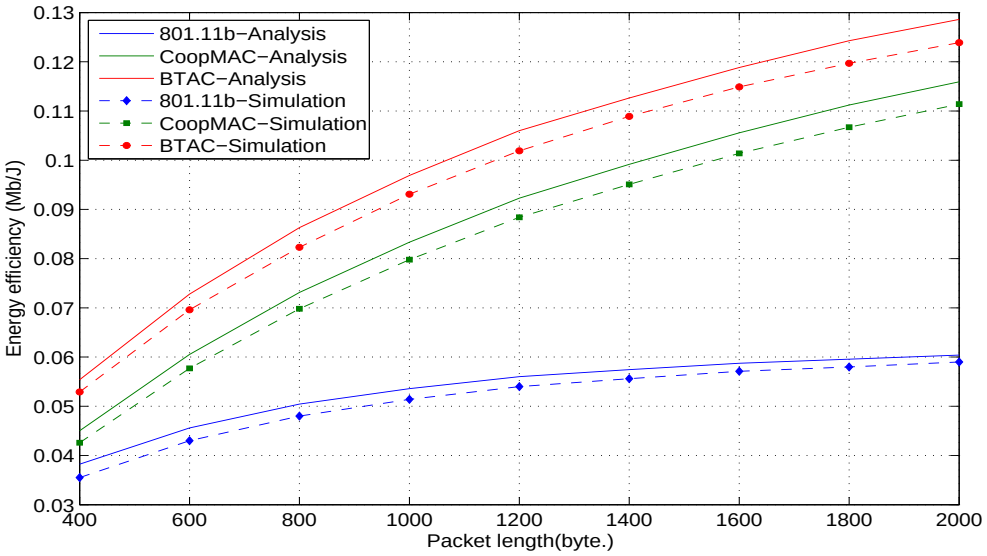

(a) Energy efficiency vs. packet length at $T_G = 50ms$ and $T_B = 5ms$.

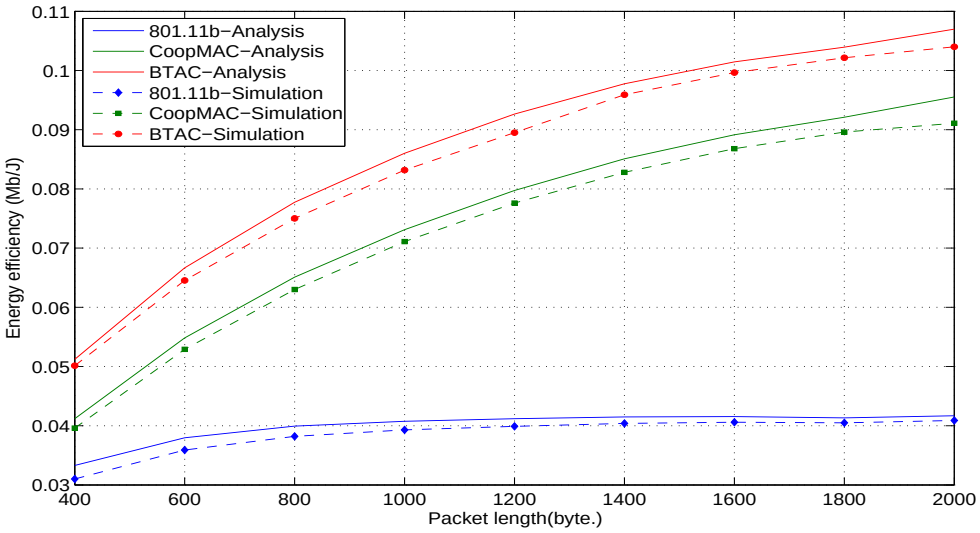

(b) Energy efficiency vs. packet length at $T_G = 10ms$ and $T_B = 1ms$.

Figure 3.20: Energy efficiency performance vs. packet length under imperfect channel conditions, N=30.

3.4.3 Delay Results

The improvement in the system throughput also transforms into a better delay performance. The relation between the service delay and the network size under ideal channel conditions and a fixed packet size which is 1024 bytes is shown in Fig. 3.21. The delay increases as the number of nodes increases. This due to collision probability increases as the number of nodes increases as illustrated in Fig. 3.13. Subsequently, the number of retries to send a data packet from a source node to the AP increases which causes increasing the service delay. On the other hand, both BTAC and CoopMAC protocols outperform the 802.11b protocol as the number of nodes increases. This because the probability of finding a relay node increases (Fig. 3.13) as the number of nodes increases. As explained, the transmission time of the two hop transmission is less that that of a single hop transmission, Therefore, the service delay of both the BTAC and CoopMAC protocols is less that that of the 802.11b. The delay of the BTAC is less than the delay of the CoopMAC protocol. The reason is that the overhead of the BTAC protocol is less than that of the CoopMAC protocol.

The effect of the channel conditions on the delay performance is shown in Fig. 3.22. The delay performance under $T_G = 50ms$ and $T_B = 5ms$, and under $T_G = 10ms$ and $T_B = 1ms$ is illustrated in Fig. 3.22(a) and Fig. 3.22(b), respectively. As the channel conditions becomes poor, the service delay increases due to increasing number of retries to deliver a data packet from the sender to AP. On the other hand, the degradation in the delay performance of both the BTAC and the CoopMAC protocols is less than that of the 802.11b. This is due to the advantage of the two-hop transmission under which the transmission time decreases and then the service delay decreases.

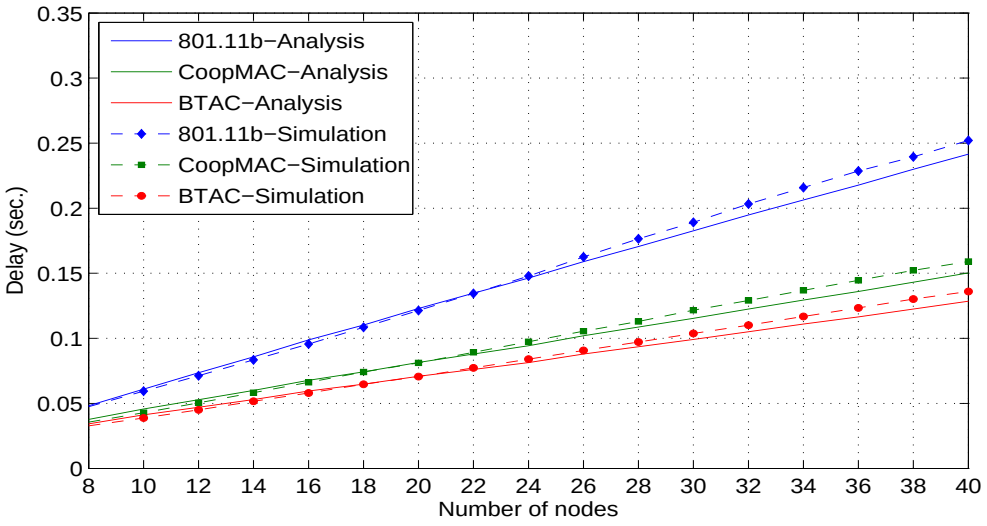

Figure 3.21: Delay performance versus number of nodes under ideal medium, L=1024 byte.

The effect of the packet length on the service delay under ideal channel conditions is shown in Fig. 3.23. As the packet length increases, the service delay of the 802.11b, the CoopMAC, and the BTAC protocols also increases. The delay is defined as the time from the packet ready for transmission until receiving acknowledge packet from the AP, where the transmission time of a data packet is included in the calculations of the delay. Hence, as the packet length increases, the transmission time increases and the delay increases. Both the CoopMAC and the BTAC protocols achieve lower delay performance than the 802.11b protocol. This due the fact that under the two-hop transmission, the transmission rate increases and then the transmission time decreases. On the other hand, the BTAC has lower delay than the CoopMAC protocol due to the reduction in the control overhead of the BTAC protocol.

The effect of the channel conditions on the delay performance versus the packet length is shown in Fig. 3.24. As the channel becomes poor,

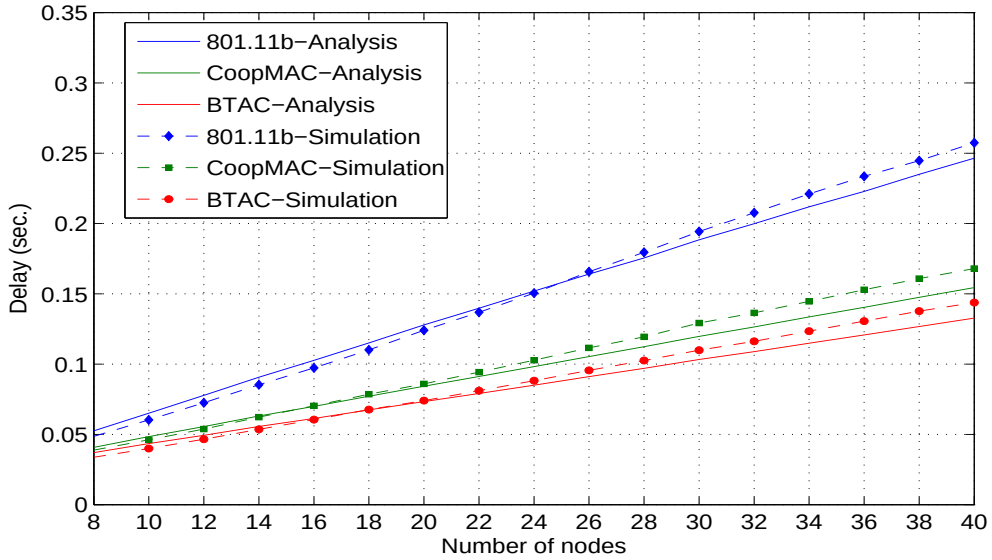

(a) Delay vs. number of nodes at $T_G = 50ms$ and $T_B = 5ms$.

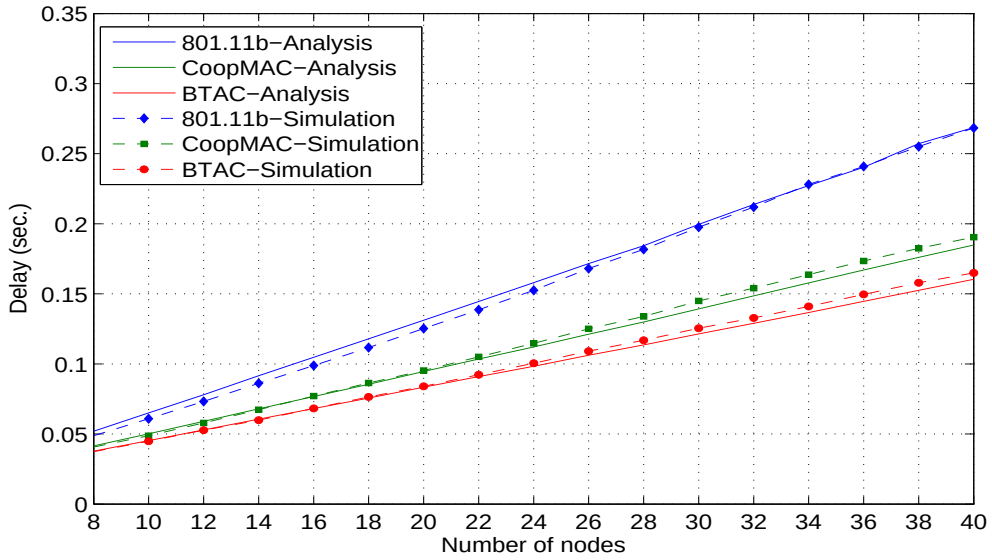

(b) Delay vs. number of nodes at $T_G = 10ms$ and $T_B = 1ms$.

Figure 3.22: Delay performance versus number of nodes under imperfect medium, L=1024byte.

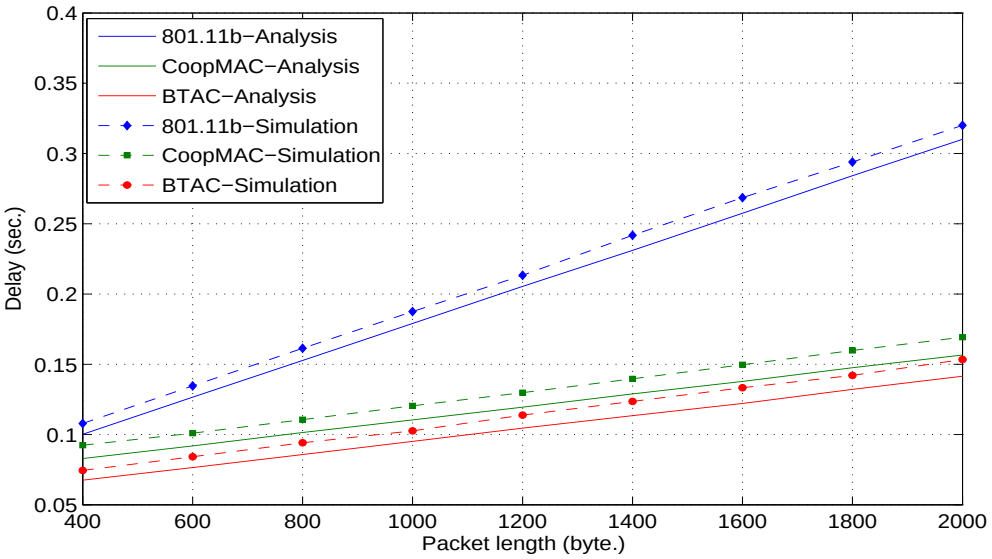

Figure 3.23: Delay performance versus packet length, N=30.

the transmission error increases, and the number of retransmission retries increases which means that the service delay increases.

3.5 Conclusions

In this chapter, a Busy Tone based cooperative Medium Access Control, namely BTAC, protocol is proposed and analysed for multi-rate WLANs. In a multi-rate WLAN, the system throughput, energy efficiency, and delay performance are significantly degraded when the number of low data rate nodes increases. BTAC applies the concept of cooperative communications to effectively improve the equivalent transmission data rate of those low data rate nodes and, therefore, can achieve better system performance. Compared with the IEEE 802.11b standard, the signalling changes and overheads in BTAC are minimal, thus making BTAC fully compatible with the IEEE 802.11b standard and suitable for coexisting with the

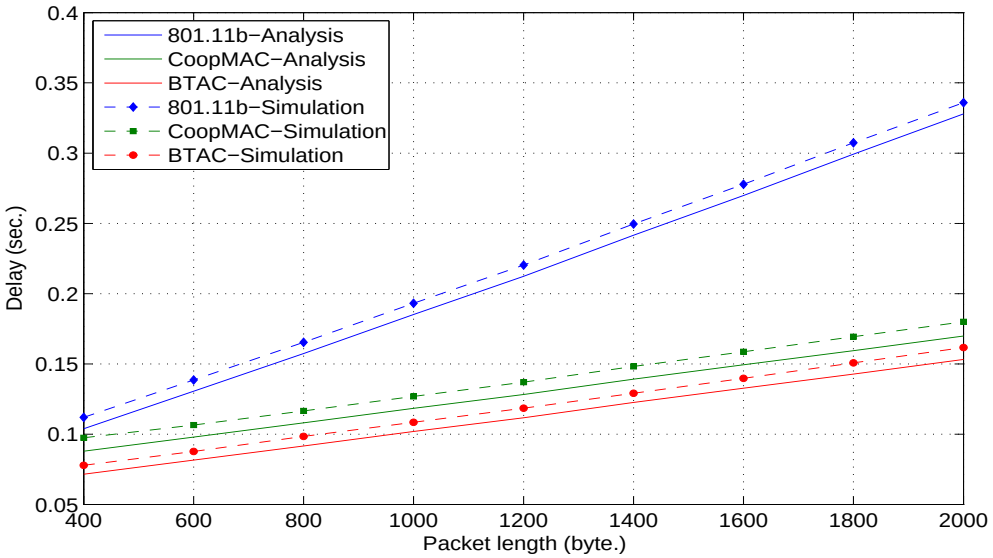

(a) Delay vs. packet length at $T_G = 50ms$ and $T_B = 5ms$.

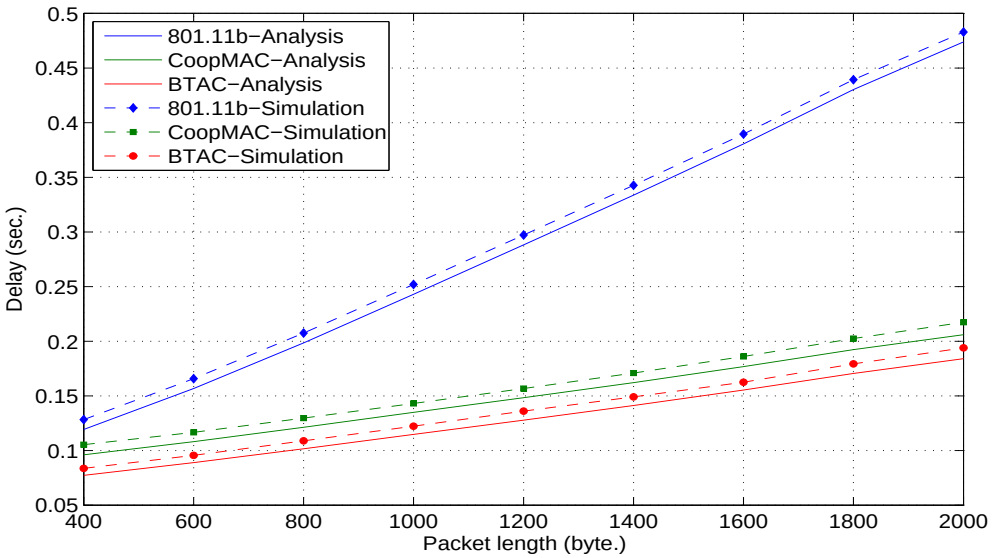

(b) Delay vs. packet length at $T_G = 10ms$ and $T_B = 1ms$.

Figure 3.24: Delay performance vs. packet length under imperfect medium, N=30.

standard DCF protocols. In addition, the BTAC is simple and robust, since the Busy Tone Signal is easy to generate and detect, thus minimizing the overhead of exchanging control messages between the relay and the source node. The BTAC protocol completely avoids the hidden relay problem that may occur in the CoopMAC protocol.

To select the appropriate relay node by the source node, a distributed relay selection algorithm is proposed. This algorithm operates in a distributed manner and introduces a minimum overhead in terms of complexity and delay. On the other hand, taking into account the impact of multi-rate transmissions, bandwidth utilization, and the imperfect channel conditions due to the fading, interference, and noise, an enhanced version of BTAC, named EBTAC, is proposed. The EBTAC protocol compared to the BTAC protocol improves the system performance.

A cross-layer analytical approach is developed to evaluate the performance of BTAC under dynamic wireless channel conditions. A simple and widely used model, called "Gilbert-Elliot model", is used to capture the burst behavior of the wireless channel caused by fading. Analytical and simulation results show that, compared with other cooperative MAC protocols, our BTAC protocol can achieve better throughput gain, and acceptable energy efficiency and service delay performance.

Chapter 4

CARD: Cooperative Access with Relay's Data

In this chapter, a new Medium Access Control (MAC) protocol, called Cooperative Access with Relay's Data (CARD) for multi-rate wireless local area networks (WLANs) is proposed. The CARD protocol allows remote nodes to transmit their information at a higher data rate to Access Point (AP) by using intermediate nodes as relays. Particularly, under the CARD protocol, a relay node sends its own data packet after forwarding a packet from the original source node, thus to improve system performance. A Markov chain model is proposed taking into account the multi-rate transmissions and the wireless channel conditions. The analytical and simulation results show that the CARD protocol can significantly improve the system quality of service (QoS) in terms of throughput, service delay and energy efficiency under different channel conditions. As a result the CARD protocol can achieve: (1) potential benefits for the relay node in cooperative communications; (2) both cooperative diversity gain and

multiplexing gain in MAC layer; (3) further increasing in system throughput and substantial service delay improvement; (4) energy efficiency improvement

The remainder of the chapter is organised as follows. The proposed CARD protocol with three algorithms for source nodes, relay nodes and the AP is described in detail in Section 4.1. An analytical model is then derived to analyse the throughput, delay, and energy efficiency performance of the CARD protocol in Section 4.2. The analytical and simulation results are presented and discussed in Section 4.3. Section 4.4 concludes the chapter.

4.1 The CARD Protocol

This section describes the proposed CARD protocol based on physical specifications of IEEE 802.11b standard (5). As described in (Sec. 3.1.1, pp. 49) each node supports transmission data-rates of 1, 2, 5.5, 11 Mbps, and the maximum transmission ranges $r_4 > r_3 > r_2 > r_1$, respectively. Without loss of compatibility with standard WLAN protocols, the standard Request-To-Send (RTS), Clear-To-Send (CTS) and Acknowledgment (ACK) packets are slightly modified to create a Cooperative RTS (CRTS), a Relay-Ready-To-Send (RRTS), a Cooperative CTS (CCTS) and a Cooperative ACK (CACK) packets for the proposed CARD protocol. The frame formats of these standard and cooperative control packets are shown in Fig. 4.1. In particular, the *Relay ID* field in a CRTS packet specifies the MAC address of the most appropriate neighbouring station selected by a low data-rate source node. Hence, the source node uses the CRTS packet to reserve the shared communication channel for its upcoming data packet transmission

and, more importantly, to request the selected high data-rate neighbouring node to serve as its relay node. The RRTS packet has the same format as the CTS packet in the IEEE 802.11b standard (5). The 2-bit *flag* field in a CACK packet indicates if the two data packets from the source and relay stations have been successfully received by the AP. If not, the corresponding source or relay station requires to retransmit one or both packets accordingly to the AP. The details are given in Section 4.1.3. With these new control packets, the proposed CARD protocol consists of three algorithms for the source nodes, the relay nodes and the AP. The following three subsections describe the principles of these algorithms.

4.1.1 Source Node Algorithm

1. As soon as a data packet "DATA-S" is ready to transmit, the source node senses the shared communication channel to the AP.

2. IF the channel is busy, THEN the source node waits until it becomes idle.

3. IF the source node is located in zones III or IV, i.e. low data-rate zones, THEN it checks the *rate-gain* G_R of neighbouring high data-rate nodes and identifies the most appropriate one as its relay node.

4. IF the source node is located in zones I or II, i.e. high data-rate zones, or IF no relay node is identified in Step (3), THEN the source node uses the standard RTS/CTS protocol to directly transmit its data packet to the AP. Go to Step (7).

5. The source node sends a CRTS packet to the selected relay node and the AP.

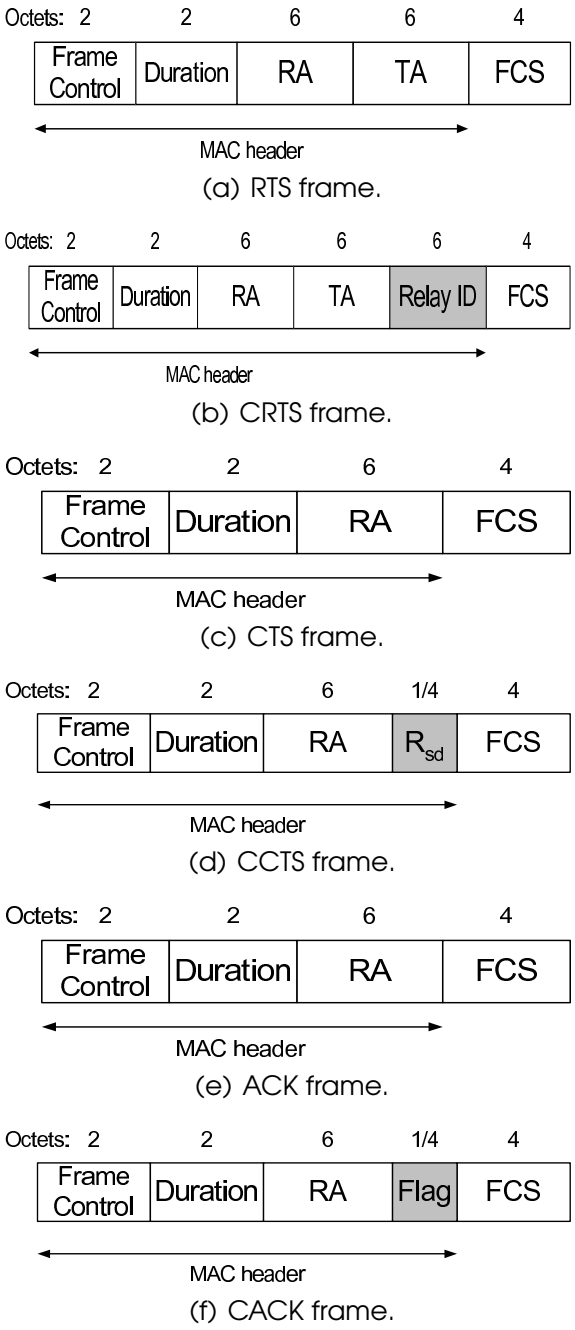

Figure 4.1: Frame format.

6. IF a CCTS packet (from the AP) and a RRTS packet (from the relay node) are both successfully received at the right time instances, THEN the source node sends its data packet "DATA-S" to the relay node at the data-rate R_{sr} after a delay of SIFS slots.
   ELSEIF only a CCTS packet (from the AP) is successfully received, i.e. the AP is ready but the selected relay node is not ready, THEN the source nodes sends its data packet "DATA-S" to the AP at the data-rate R_{sd} after a delay of SIFS slots.
   ELSE (i.e. the AP is not ready), THEN go to Step (8).

7. IF a CACK/ACK packet is received from the AP, THEN return "Data Transmission Successfully Completed". The source node waits for the next data packet. Go to Step (1).

8. Return "Data Transmission Failed". Go to Step (1) to retransmit the data packet "DATA-S" after a standard random backoff delay.

This "Source Node Algorithm" exists in all relay-capable nodes and is triggered when a node wants to transmit a new packet or retransmit a backoff packet. It supports a relay-type cooperative communication when the node is located in a low data-rate zones and the selected relay node is available. Otherwise, it becomes a normal RTS/CTS protocol, as seen in Steps (4) and (6), and is therefore fully compatible with the popular IEEE 802.11b standard. In Step (3), the G_R the rate gain and is given in equation (3.1) chapter 3. The source node selects the node from the *Relay list* with the maximum G_R as the potential relay node for its transmission. The details of the relay selection algorithm is given in (Sec. 3.1.2, pp. 50).

4.1.2 Relay Node Algorithm

1. After receiving a CRTS packet, the relay node checks the "Relay ID" field.

2. IF it is the selected relay node, THEN it waits for the next CCTS packet after a delay of SIFS slots.
   ELSE it waits for the next CRTS packet. Go to Step (1).

3. After receiving a CCTS packet, the relay node sends a RRTS packet to the source node and the AP after a delay of SIFS slots.

4. IF the data packet "DATA-S" is received from the source node after a delay of SIFS slots, THEN the relay node waits for a delay of SIFS slots and sends "DATA-S" and its own data packet "DATA-R" to the AP at the data-rate R_{rd}.
   ELSE the relay node waits for the next CRTS packet. Go to Step (1).

5. IF no CACK packet is received from the AP after a delay of SIFS slots, or IF the CACK packet indicates only one data packet has been successfully received by the AP, THEN the relay node retransmits "DATA-S", "DATA-R", or both accordingly to the AP.

6. The relay node waits for the next CRTS packet. Go to Step (1).

This "Relay Node Algorithm" is activated only in those high data-rate nodes in zones I and II. Different from previous work, a relay node in the CARD protocol transmits its own data packet "DATA-R" to the AP immediately after forwarding the source node's data packet "DATA-S" to the AP, as shown in Step (4). In doing this, the CARD protocol enables the relay node to utilise the successful handshake procedure between the source node and the AP for its own data transmission, thus achieving *cooperative*

multiplexing gain and benefiting the relay node and the whole system in terms of throughput and energy efficiency, as demonstrated by the analytical and simulation results in Section 4.3. In Step (3), a RRTS packet is transmitted for two purposes: (i) it serves as an acknowledgement message for the source node to know that the relay node is ready to receive the data packet "DATA-S", and (ii) it serves as a request-to-send message for the AP to know that the relay node is transmitting its own data packet "DATA-R".[1] The RRTS packet is sent after sending the CCTS packet, i.e. after the channel reservation procedure is completed, for two reasons. First, to solve the " *Hidden Relay Node Problem*" that is discussed in (ch. 3 pp. 60). As some nodes cannot hear the ongoing packet transmission from the relay node, they may send a RTS packet to the AP at the same time and cause a collision with the RRTS packet. All the nodes in the network can hear the AP's CCTS packet and will then defer their packet transmission requests, if any. As a result, the RRTS packet from the relay node is guaranteed no collision and the two-hop communication path will be successfully established after the RRTS packet is received by the source node and the AP.

Therefore, the CARD protocol completely solves the "Hidden Relay Node Problem" and effectively enables cooperative relay communication in WLANs. The second reason is that after receiving the CCTS packet, the relay node extracts R_{sd} (the data rate between the source and the AP) and estimates R_{rd} (the data rate between the relay and the AP). The relay node also estimates R_{sr} (the data rate between the source and the relay) of the received CRTS packet from the source node. In this case, it

[1] If the relay node does not have a data packet to transmit, CARD becomes a normal relay protocol and, after a RRTS packet, only the packet "DATA-S" will be forwarded from the relay node to the AP.

sends a RRTS packet only when a two-transmission is faster than a single-hop transmission. This method improves bandwidth utilization under dynamic channel conditions.

To support packet retransmissions in Step (5), the relay node needs to maintain two buffers (as in IEEE 802.11e (8)) for its own data packet and the source node's relayed packet, respectively. They are updated/empted in parallel according to the *flag* field in the CACK packet for each (re)transmission.

4.1.3 Access Point Algorithm

1. After receiving a CRTS packet (from a low data-rate node that requests a relay node) or a standard RTS packet (from a node that does not request a relay node), the AP checks the "Transmitter Address" (TA) field and sends a CCTS packet or a standard CTS packet, accordingly, to the source node after a delay of SIFS slots.

2. IF a CRTS packet is received in Step (1), THEN the AP waits for a RRTS packet after a delay of SIFS slots.
   ELSE (a standard RTS packet is received in Step (1)) the AP waits for the data packet "DATA-S" from the source node after a delay of SIFS slots. Go to Step (6).

3. IF a RRTS packet is received, THEN the AP waits for two data packets, i.e. "DATA-S" and "DATA-R", from the relay node after a delay of SIFS slots.
   ELSE the AP waits for the data packet "DATA-S" from the source node after a delay of SIFS slots. Go to Step (6).

4. IF both "DATA-S" and "DATA-R" are successfully received, THEN the

AP sets the *flag* field to "11" and sends a CACK packet to the source and relay nodes after a delay of SIFS slots.
ELSEIF only "DATA-S" is successfully received, THEN the AP sets the *flag* field to "10" and sends a CACK packet to the source and relay nodes after a delay of SIFS slots.
ELSEIF only "DATA-R" is successfully received, THEN the AP sets the *flag* field to "01" and sends a CACK packet to the source and relay nodes after a delay of SIFS slots.
ELSE (neither "DATA-S" nor "DATA-R" is received) the AP does not send a CACK packet.

5. IF "DATA-S", "DATA-R" or both are received after a delay of DIFS slots (packet retransmission), THEN the AP updates the *flag* field and sends a new CACK packet to the source and relay nodes after a delay of SIFS slots. Go to Step (5). ELSE go to Step (7).

6. IF "DATA-S" is successfully received, THEN the AP sends an ACK packet to the source nodes after a delay of SIFS slots.
   ELSE the AP does not send an ACK packet.

7. A new contention-based random access period starts. The AP waits for the next CRTS/RTS packet. Go to Step (1).

In Step (1), the AP may receive a standard RTS packet (without a relay node request) from a high data-rate node that does not need a relay node, a low data-rate node that does not have any high data-rate neighbouring nodes as its potential relay nodes, or a legacy node that does not support a relay-type cooperative communication. In this case, as well the case when no RRTS packet is received in Step (3), the source node

directly sends its data packet "DATA-S" to the AP at the data-rate R_{sd}. In this way, the CARD protocol can accommodate both new relay-capable nodes and legacy nodes in the same network and, hence, is compatible with the IEEE 802.11b standard. Connecting Step (5) in this algorithm, Step (5) in the "Relay Node Algorithm" and Step (8) in the "Source Node Algorithm", packet retransmissions are conducted by the relay node when the received CACK packet has an incomplete *flag* field (i.e. $flag \neq 11$), or when no CACK packet is correctly received (i.e. no CACK packet is transmitted at all, or the transmitted CACK packet is destroyed under unreliable radio channel condition).

The basic operation of CARD protocol is illustrated in Fig. 4.2. This handshake procedure of control packets, CRTS, CCTS and RRTS, is shown in Fig. 4.2(a) and the data packets transmission from the source and relay nodes to the AP is shown in Fig. 4.2(b).

4.1.4 Channel Access Procedure and NAV

As an example, the combined channel access procedure with the control and data packets in the CARD protocol is shown in Fig. 4.3(a), where a low data-rate source node successfully establishes a two-hop communication path through a high data-rate relay node for effectively transmitting two data packets, "DATA-S" (from the source node) and "DATA-R" (from the relay node), to the AP. If the source node does not receive a RRTS packet, i.e. the selected relay node is not available, it directly sends the data packet "DATA-S" to the AP at the low data-rate R_{sd} and then waits for an ACK packet, as shown in Fig. 4.3(b). For a legacy source node that does not support relay communication in the CARD protocol, its channel access procedure will be the same as the standard RTS/CTS

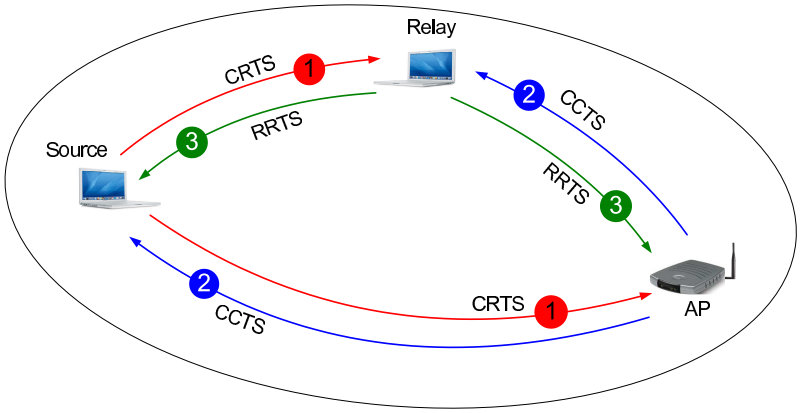

(a) Control packets handshake.

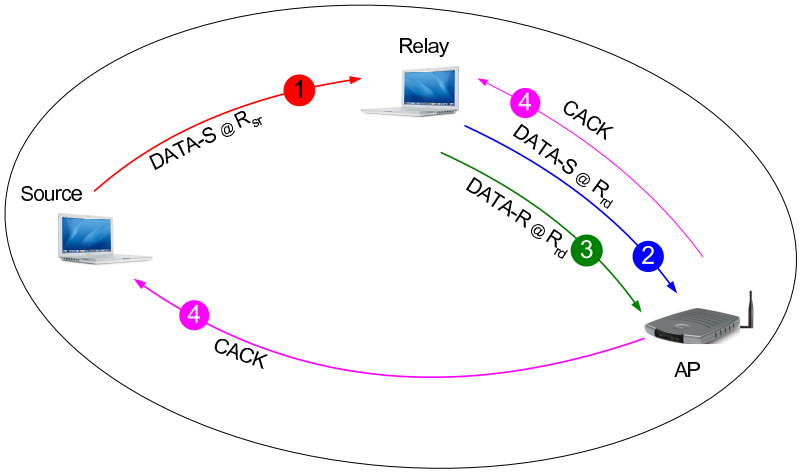

(b) Data packets transmission.

Figure 4.2: Access mechanism of CARD protocol.

Packet type	The Duration
CRTS	$T_{CCTS} + T_{RRTS} + 3T_{SIFS} + \delta$
CCTS	$\frac{8L_s}{R_{sd}} + T_{PLCP} + 2T_{SIFS} + T_{ACK} + 2\delta$
RRTS	$\frac{8L_s}{R_{sr}} + \frac{8L_s+8L_r}{R_{rd}} + 3T_{PLCP} + 4T_{SIFS} + T_{CACK} + 4\delta$
DATA-S (source-relay)	$\frac{16L}{R_{rd}} + 2T_{PLCP} + 3T_{SIFS} + T_{CACK} + 3\delta$
DATA-S (relay-AP)	$\frac{8L}{R_{rd}} + T_{PLCP} + 2T_{SIFS} + T_{CACK} + 2\delta$
DATA-R	$T_{CACK} + T_{SIFS} + \delta$
RTS	$T_{CTS} + 2T_{SIFS} + \delta$
CTS	$\frac{8L}{R_{sd}} + T_{PLCP} + 2T_{SIFS} + T_{ACK} + 2\delta$
DATA-S (source-AP)	$T_{ACK} + T_{SIFS} + \delta$

Table 4.1: CARD Duration field contents

protocol in IEEE 802.11b WLANs. Therefore, the proposed CARD protocol can flexibly support both relay-capable nodes and legacy nodes, and is fully compatible with the IEEE 802.11b standard.

As described in Section 4.1.1, the transmission data rates between a source node, a relay node and the AP, i.e. R_{sd}, R_{sr}, and R_{rd}, can be estimated at the source node by overhearing a few recent packet transmissions. As all control packets are transmitted at the basic data-rate, the source node can easily calculate the transmission time of RTS/CRTS, RRTS, CTS/CCTS and ACK/CACK packets. Furthermore, the corresponding Network Allocation Vectors (NAVs) can be estimated, as seen in Fig. 4.3, for the CARD protocol.

The *Duration* field value is expressed in Table 4.1. where L_s and L_r are the data packet length in octets of the source and the relay, respectively. δ is the channel propagation delay, and T_{PLCP} is the time duration of the PLCP header. T_{RTS}, T_{CTS}, T_{ACK}, T_{CRTS}, T_{CCTS}, T_{RRTS}, and T_{CACK} stand for

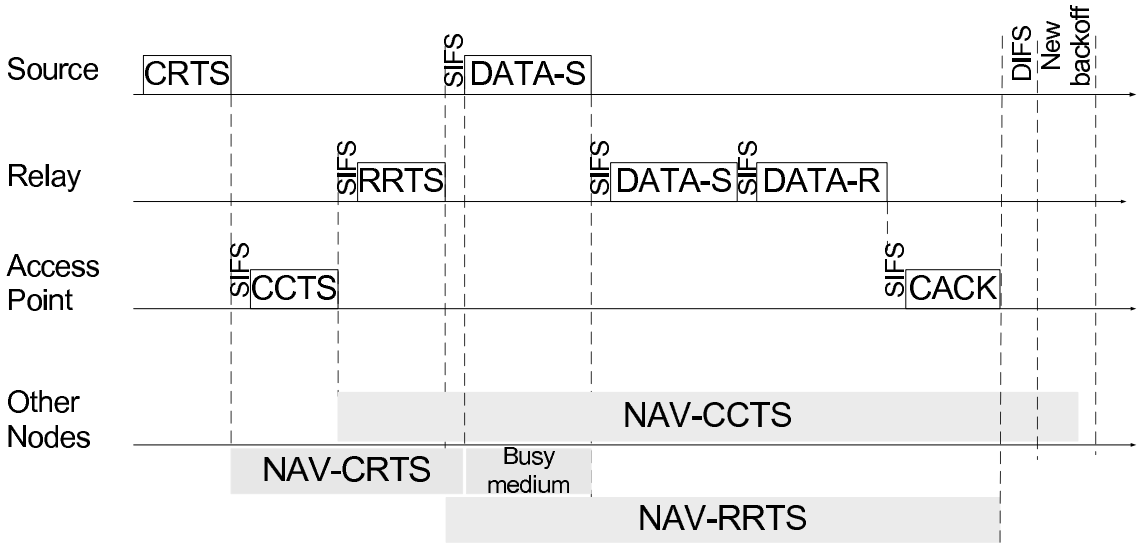

(a) Relay node is available.

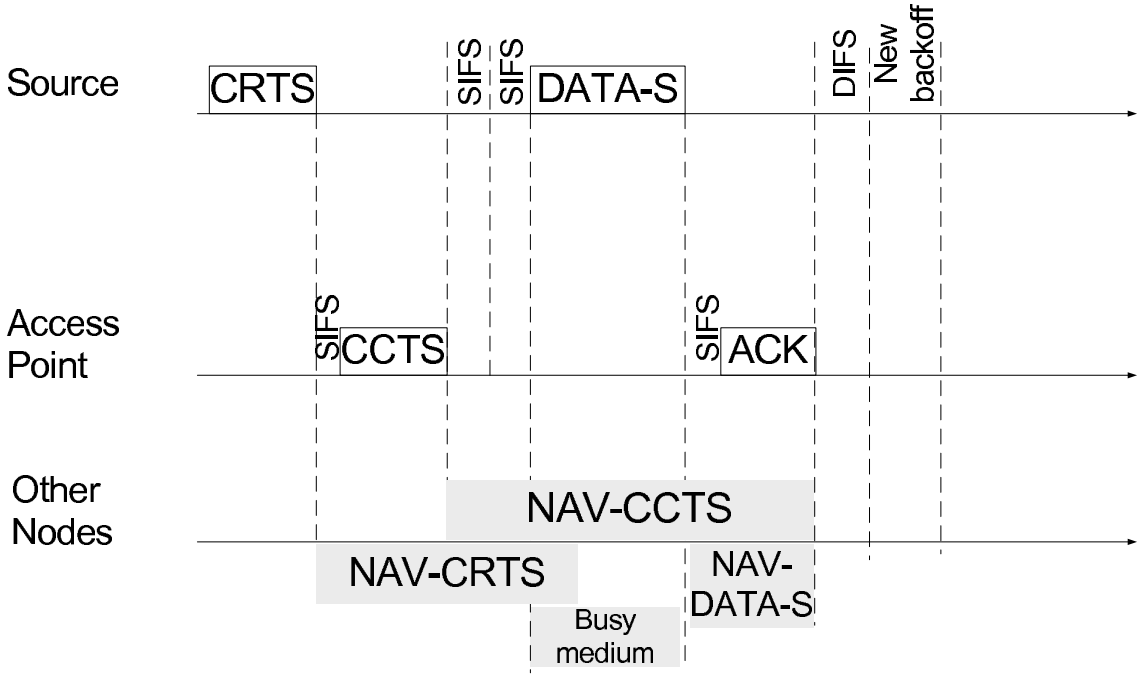

(b) No relay node is available.

Figure 4.3: Network allocation vector (NAV).

the duration of the RTS, CTS, ACK, CRTS, CCTS, RRTS, and CACK packets, respectively.

4.2 Performance Analysis

4.2.1 Channel Packet Error Rate

Over the wireless channel, the multipath fading, interference, and noise produce high error rates depending on the channel conditions and transmission data rate. For a generic node i, let $P_{e,i}$ be the probability of packet error rate (PER) due to imperfect channel conditions. Under the CARD protocol a source node can use a single-hop transmission when it is located either in zone I or zone II. When a source node is located either in zone III or zone IV and there is no relay available, the source node uses also a single-hop transmission to send its packet to the AP. Otherwise, when a source node is located either in zone III or zone IV and there is a relay node available, it uses a two-hop transmission. In the following $P_{e,i}$ is derived for single-hop and two-hop transmission.

4.2.1.1 Direct Transmission

In this case, ageneric node i is located either in zone I, zone II, or in zone III or zone IV where there is no relay available. It then sends its packet directly to the AP at a data-rate $R_{sd} = \{1, 2, 5.5, 11\}\ Mbps$ depending on the channel conditions. After sending a RTS packet with no collision to the AP, the wireless channel undergoes one of the following four events causing transmission failure. These events are RTS corruption, CTS corruption, DATA-S (source-AP) corruption, and ACK corruption. Consequently,

the probability that the RTS packet is corrupted given that there is no RTS collision is calculated as follows:

$$\begin{aligned} u_1 &= Pr(\text{RTS is corrupted} \mid \text{no RTS collision}) \\ &= 1-(1-BER_b)^{8L_{RTS}} \end{aligned} \tag{4.1}$$

where BER_b is the Bit Error Rate (BER) at the base data-rate (e.g. 1Mbps in 802.11b). The control packet, e.g. RTS, CTS, ACK, etc., are sent also at the base data-rate . L_{RTS} is the RTS packet length in octets. The probability u_2 that the CTS packet is corrupted given that the RTS packet is successfully transmitted and there is no RTS collision is calculated as follows:

$$\begin{aligned} u_2 &= Pr(\text{CTS is corrupted} \mid \text{no RTS corruption, no RTS collision}) \\ &= 1-(1-BER_b)^{8L_{CTS}} \end{aligned} \tag{4.2}$$

where L_{CTS} is the CTS packet length in octets. Similarly, the probability u_3 that the DATA-S packet from a source to the AP is corrupted given that both the RTS and CTS are successful, and exactly one RTS is transmitted is expressed as follows:

$$u_3 = 1-(1-BER_{sd})^{8L_s}(1-BER_b)^{8L_{PLCP}} \tag{4.3}$$

where L_s is the data packet length of the source node in octets. L_{PLCP} is the PLCP header size in octets. BER_{sd} is bit error rate of the DATA-S from a source node to the AP at the data-rate R_{sd}. The ACK corruption

probability u_4 is computed as follows:

$$u_4 = 1 - (1 - BER_b)^{8L_{ACK}} \tag{4.4}$$

where L_{ACK} is the ACK packet length in octets. Let p_{e1}^d be the portability of the RTS corruption, p_{e2}^d be the portability of the CTS corruption, p_{e3}^d be the portability of the DATA-S corruption, and p_{e4}^d be the portability of the ACK corruption under direct transmission. These probabilities are computed as follows:

$$\begin{aligned} p_{e1}^d &= u_1 \\ p_{e2}^d &= (1-u_1)u_2 \\ p_{e3}^d &= (1-u_1)(1-u_2)u_3 \\ p_{e4}^d &= (1-u_1)(1-u_2)(1-u_3)u_4 \end{aligned} \tag{4.5}$$

The corresponding time duration of these events are denoted by T_{e1}^d, T_{e2}^d, T_{e3}^d, and T_{e4}^d, respectively. These time durations are calculated as follows:

$$\begin{aligned} T_{e1}^d &= T_{RTS} + T_{CTS} + T_{SIFS} + T_{DIFS} + 2\delta \\ T_{e2}^d &= T_{RTS} + T_{CTS} + T_{SIFS} + T_{DIFS} + 2\delta \\ T_{e3}^d &= T_{RTS} + T_{CTS} + \frac{8L_s}{R_{sd}} + \frac{L_{PLCP}}{R_b} + T_{ACK} + 3T_{SIFS} + T_{DIFS} + 4\delta \\ T_{e4}^d &= T_{RTS} + T_{CTS} + \frac{8L_s}{R_{sd}} + \frac{L_{PLCP}}{R_b} + T_{ACK} + 3T_{SIFS} + T_{DIFS} + 4\delta \end{aligned} \tag{4.6}$$

where δ is the propagation delay, T_{DIFS} is the duration of the Distributed Inter-Frame Space (DIFS), and T_{SIFS} is the duration of Short Inter-

Frame Space (SIFS).

From equation (4.5), the probability $P_{e,i}$ of the node i that uses a single-hop transmission is expressed as follows:

$$P_{e,i} = p_{e1}^{d} + p_{e2}^{d} + p_{e3}^{d} + p_{e4}^{d} \tag{4.7}$$

4.2.1.2 Cooperative Transmission

In this scenario, a source node transmits its data packet to the AP via a relay node. The source node transmits its data packet at a data-rate $R_{sr}\ Mbps$ to the relay node. The relay then forwards the data packet of the source to the AP at a data-rate $R_{rd}\ Mbps$. When a source node is at data-rate $1\ Mbps$, it can use a two-hop data-rates $(R_{sr}, R_{rd}) = \{(11,11),(5.5,11),(11,5.5),(5.5,5.5),(2,11),(11,2),(2,5.5),(5.5,2)\}$. Otherwise, when the data-rate is $2\ Mbps$, a source node uses a two-hop data-rate $(R_{sr}, R_{rd}) = \{(11,11),(5.5,11),(11,5.5),(5.5,5.5)\}$.

In the same manner as the single-hop transmission, after transmitting a CRTS packet with no collision, there are seven events at which the transmission may fail due to imperfect channel conditions. These events are a CRTS, a CCTS, a RRTS, a DATA-S from the source to the relay, a DATA-S from the relay to the AP, a DATA-R from the relay to the AP, and a CACK packets corruption. The probability w_1, that a CRTS is corrupted given that there is exactly one CRTS is transmitted, is calculated as follows:

$$\begin{aligned} w_1 &= Pr(\text{CRTS is corrupted}|\text{no CRTS collision}) \\ &= 1-(1-BER_b)^{8L_{CRTS}} \end{aligned} \tag{4.8}$$

where L_{CRTS} is the CRTS packet length in octets. The probability w_2, that a CCTS is corrupted given no CRTS collision and corruption, is expressed as follows:

$$w_2 = 1 - (1 - BER_b)^{8L_{CCTS}} \quad (4.9)$$

where L_{CCTS} is the CCTS packet length in octets. The probability w_3, that a RRTS is corrupted after receiving both CRTS and CCTS correctly, is as follows:

$$w_3 = 1 - (1 - BER_b)^{8L_{RRTS}} \quad (4.10)$$

where L_{RRTS} is the RRTS packet length in octets. The probability that a DATA-S from the source to the relay is corrupted after correct CRTS, CCTS and RRTS, denoted by w_4, is calculated as follows:

$$w_4 = 1 - (1 - BER_{sr})^{8L_s}(1 - BER_b)^{8L_{PLCP}} \quad (4.11)$$

where BER_{sr} is the bit error rate of the data packet (source-relay) at the data-rate R_{sr}. The probability w_5, that a DATA-S (relay-AP) is corrupted given that CRTS, CCTS, RRTS, and DATA-S (source-relay) are successfully received and given that there is no CRTS collision, is computed as follows:

$$w_5 = 1 - (1 - BER_{rd})^{8L_s}(1 - BER_b)^{8L_{PLCP}} \quad (4.12)$$

where BER_{rd} is the bit error rate between the relay and the AP of the data packet sent at data-rate R_{rd}. The relay node sends a DATA-R

after sending a DATA-S (relay-AP) immediately even if a DATA-S is received incorrectly. The probability w_6, that a DATA-R is not successfully received after receiving CRTS, CCTS, RRTS, DATA-S (source-relay) correctly where it is independent on DATA-S (relay-AP), is expressed as follows:

$$w_6 = 1 - (1 - BER_{rd})^{8L_r}(1 - BER_b)^{8L_{PLCP}} \quad (4.13)$$

where L_r is the data packet length of the relay node in octets. The AP sends a CACK if at least one the two packets DATA-S (relay-AP) and DATA-R is received correctly. The probability w_7, that a CACK is corrupted after receiving CRTS, CCTS, RRTS, DATA-S (source-relay), and at least one of both DATA-S (relay-AP) and DATA-R correctly, is then expressed as follows:

$$w_7 = 1 - (1 - BER_b)^{L_{CACK}} \quad (4.14)$$

where L_{CACK} is the CACK packet length in octets. Let q_{e1}^c be the probability of a CRTS corruption, q_{e2}^c be the probability of a CCTS corruption, q_{e3}^c be the probability of a RRTS corruption, q_{e4}^c be the probability of a DATA-S (from the source to the relay) corruption, q_{e5}^c be the probability of a DATA-S (from the relay to the AP) corruption, q_{e6}^c be the probability of a DATA-R corruption, and q_{e7}^c be the probability of a CACK corruption. These

probabilities are calculated as follows:

$$\begin{aligned}
q_{e1}^c &= w_1 \\
q_{e2}^c &= (1-w_1)w_2 \\
q_{e3}^c &= (1-w_1)(1-w_2)w_3 \\
q_{e4}^c &= (1-w_1)(1-w_2)(1-w_3)w_4 \\
q_{e5}^c &= (1-w_1)(1-w_2)(1-w_3)(1-w_4)w_5 \\
q_{e6}^c &= (1-w_1)(1-w_2)(1-w_3)(1-w_4)w_6 \\
q_{e7}^c &= (1-w_1)(1-w_2)(1-w_3)(1-w_4)(1-w_5w_6)w_7
\end{aligned} \tag{4.15}$$

where $1-w_5w_6$ is the probability that at least one of the DATA-S (relay-AP) and DATA-R packets is received correctly by the AP. The time duration of these seven different events are denoted by T_{e1}^c, T_{e2}^c, T_{e3}^c, T_{e4}^c, T_{e5}^c, T_{e6}^c, and T_{e7}^c, respectively. These time durations are calculated as follows:

$$\begin{aligned}
T_{e1}^c &= T_{CRTS} + T_{CCTS} + T_{SIFS} + T_{DIFS} + 2\delta \\
T_{e2}^c &= T_{CRTS} + T_{CCTS} + T_{SIFS} + T_{DIFS} + 2\delta \\
T_{e3}^c &= T_{CRTS} + T_{CCTS} + T_{RRTS} + 2T_{SIFS} + T_{DIFS} + 3\delta \\
T_{e4}^c &= T_{CRTS} + T_{CCTS} + T_{RRTS} + \frac{8L_s}{R_{sr}} + T_{PLCP} + 4T_{SIFS} + T_{DIFS} + 4\delta \\
T_{e5}^c &= T_{CRTS} + T_{CCTS} + T_{RRTS} + \frac{8L_s}{R_{sr}} + \frac{8(L_s+L_r)}{R_{rd}} + 3T_{PLCP} + T_{CACK} \\
&\quad +6T_{SIFS} + T_{DIFS} + 7\delta \\
T_{e6}^c &= T_{e7}^c = T_{e5}^c
\end{aligned} \tag{4.16}$$

From equation (4.15), the probability $P_{e,i}$ of the node i that uses a

two-hop transmission is calculated as follows:

$$P_{e,i} = q_{e1}^{c} + q_{e2}^{c} + q_{e3}^{c} + q_{e4}^{c} + q_{e5}^{c} + q_{e6}^{c} + q_{e7}^{c} \tag{4.17}$$

4.2.2 Markov Chain Model

In this subsection, a discrete Markov chain model is introduced to study the behaviour of the CARD protocol under assumptions of saturated conditions, multi-rate transmissions, imperfect channel conditions, and IEEE 802.11b physical layer with 4 way (i.e., RTS/CTS) handshaking mechanism. The analysis can be easily extended to IEEE 802.11a/g and later physical layer extensions. Before presenting the analysis of the proposed model, it helps to highlight some of the key differences between the proposed model and other models proposed in the literature.

1. A finite retransmission limit (retry limit) defined in (1,5,6,8) is modelled while the Bianchi's model (27) assumes an infinite retry limit which is not consistent with the IEEE 802.11 standards.

2. In the proposed model, the node suspends its backoff counter decrement if the radio channel becomes busy whereas the Bianchi's model (27) assumes that the backoff counter decreases during a busy slot time.

3. The proposed model in Fig. 4.4 considers the packet transmission failures due to imperfect channel conditions, whereas the Bianchi's model assumes ideal channel transmission.

4. The proposed model takes into account the multi-rate transmissions while Bianchi's model considers a single rate transmission.

5. The Bianchi's model is a two-dimensional model whereas the proposed model introduces a third dimension specifying the remaining time duration during a successful transmission, an unsuccessful transmission including both erroneous and collision transmissions, and frozen transmission due to a busy slot time.

6. In the proposed model the probability that the channel is sensed busy and the probability that the packet is unsuccessful due to erroneous and collision transmissions are different from each other.

Following the same consideration of the Bianchi's model (27), the time is considered to be slotted and at the end of each slot time an event that activates a transition to another state occurs (149). Let $b(t)$ be a stochastic process representing the value of the backoff counter for a given node at time t. Let $s(t)$ be a random process representing the backoff stage j at time t, where $0 \leq j \leq m$, where for each node there are $m+1$ stages of the backoff delay. The third dimension $u(t)$ specify the remaining time during a successful transmission, an unsuccessful transmission including both an erroneous and a collision transmissions, and a frozen transmission due to a busy slot time. The value of the backoff counter in stage j is uniformly chosen in the range of $(0, 1, ..., W_j - 1)$, where W_j is given as follows (5):

$$W_j = \begin{cases} 2^j W_0 & j \leq m' \\ 2^{m'} W_0 & j > m' \end{cases} \tag{4.18}$$

where m' is the maximum number of retries using different contention window (CW) size. All the parameters assigned in this chapter is for the Direct Sequence Spread Spectrum (DSSS) PHY layer in the IEEE 802.11.

$W_0 = CW_{min} + 1$ and $2^{m'}W_0 = CW_{max} + 1$, where $W_{min} = 31$, $W_{max} = 1023$, and $m' = 5$ for the IEEE 802.11b (5). The analysis can be applied in all other IEEE 802.11 PHY layer standards. As shown in Fig. 4.4, the three dimensional process $\{s(t), b(t), u(t)\}$ is a discrete-time Markov chain under assumption that the probability $P_{u,i}$, that the transmitted frame is corrupted due to a collision or an erroneous transmission and the probability $P_{b,i}$, that the channel is sensed busy are independent. It is referred to a generic node with index $i \in S = \{S^d \cup S_1^c \cup S_2^c\}$; where S^d is the set of nodes that employ a single-hop transmission, S_1^c is the set of nodes at a data-rate $1\ Mbps$ and employing a two-hop transmission, and S_2^c is the set of nodes at a data-rate $2\ Mbps$ and employing a two-hop transmission. The details of these node sets is given in Appendix A. The state of each node can be described by $\{j, k, \ell\}$, where j is the backoff stage, $j = 0, 1, ..., m$ ($j = -1$ represents a successful transmission stage) and k is the backoff counter taking values from $[0, W_{j-1}]$ in time slots. The third index ℓ specifies the following:

- The remaining time for the successful transmission states

$$(-1, 0, \ell) \quad 1 \leq \ell \leq N_{s,i}$$

- The remaining time for the unsuccessful transmission states (due to either a collision or an erroneous transmission)

$$(j, 0, \ell) \quad 1 \leq \ell \leq N_{u,i} \quad 0 \leq j \leq m$$

- The remaining time for the frozen transmission period states

$$(j, k, \ell), \quad 1 \leq \ell \leq N_{f,i} \quad 1 \leq k \leq W_j - 1 \quad 0 \leq j \leq m$$

where $N_{s,i}$, $N_{u,i}$, and $N_{f,i}$ stand for a successful transmission period, an unsuccessful transmission period, and a frozen transmission period in a time slot units, respectively. In relation to the generic node i in the network, it is assumed that the collision probability that at least two nodes send in the same slot time is denoted by $P_{c,i}$. The probability $P_{e,i}$, that the transmission is unsuccessful due to imperfect channel conditions, is calculated in equations (4.7) and (4.17) for a single-hop transmission and a two-hop transmission, respectively. It is assumed that both a collision and an erroneous transmission probabilities are statistically independent. The probability $P_{u,i}$, that a transmitted packet from the node i is unsuccessful due to a collision or an erroneous transmission, is calculated as follows:

$$P_{u,i} = 1 - (1 - P_{c,i})(1 - P_{e,i}) = P_{c,i} + (1 - P_{c,i})P_{e,i} \tag{4.19}$$

4.2.2.1 Transition Probabilities

In this model the one step transition probabilities are described as follows:

1. At the beginning of each slot time, the backoff counter freezes for $N_{f,i}$ slots when the channel is sensed busy.

$$P_r\{j, k, N_{f,i}|j, k, 0\} = P_{b,i} \qquad 1 \leq k \leq W_j - 1 \quad 0 \leq j \leq m$$

2. During the frozen period, the counter decreases by one for each slot time.

$$P_r\{j, k, \ell - 1|j, k, \ell\} = 1 \qquad 2 \leq \ell \leq N_{f,i} \quad 0 \leq k \leq W_j - 1 \quad 0 \leq j \leq m$$

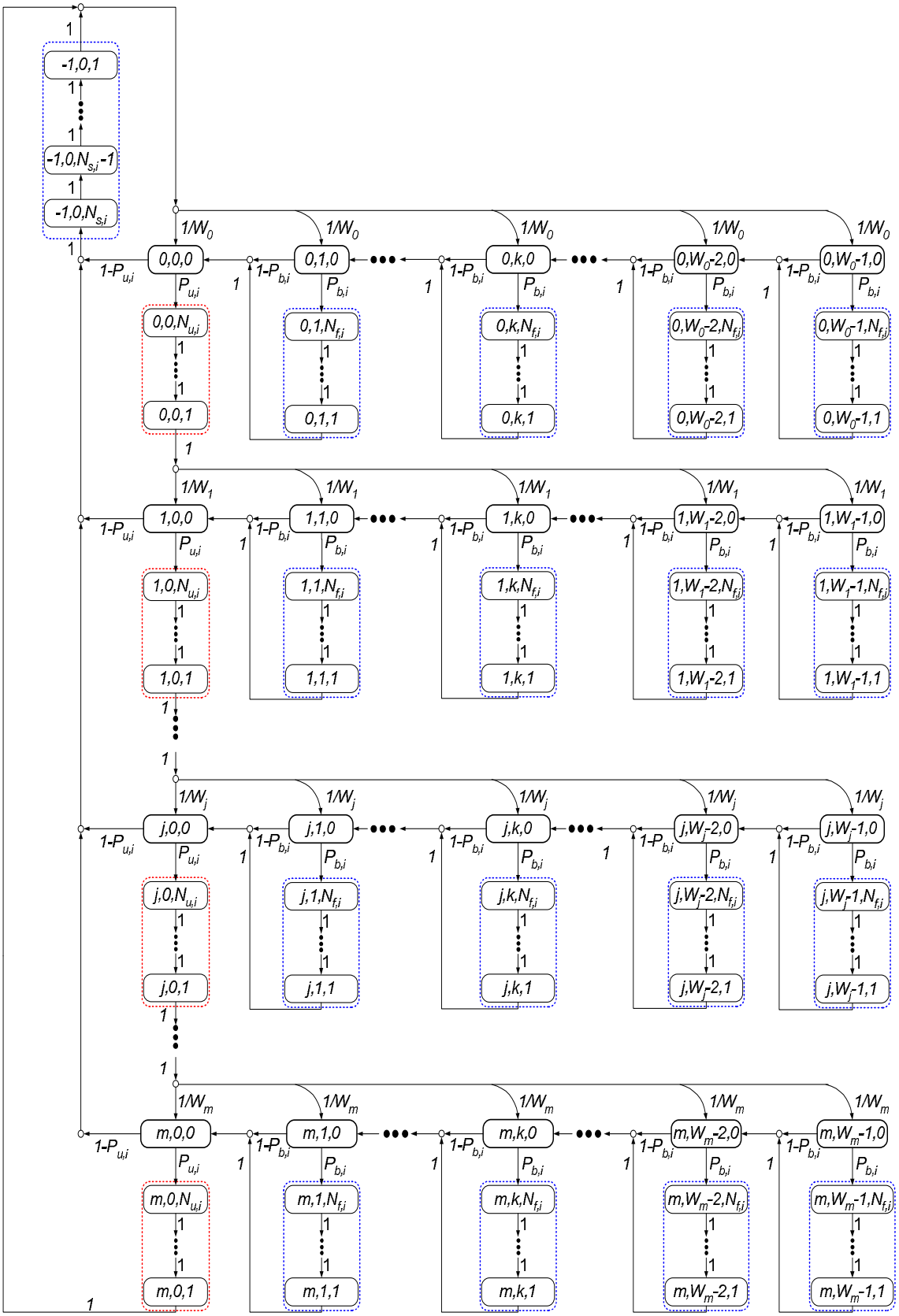

Figure 4.4: CARD protocol Markov chain model.

3. At the end of the frozen period, a node reactivities its backoff counter.

$$P_r\{j, k-1, 0|j, k, 1\} = 1 \qquad 1 \leq k \leq W_j - 1 \quad 0 \leq j \leq m$$

4. The backoff counter decrements when the channel becomes idle.

$$P_r\{j, k-1, 0|j, k, 0\} = 1 - P_{b,i} \qquad 1 \leq k \leq W_j - 1 \quad 0 \leq j \leq m$$

5. When the backoff counter reaches zero and no other node tries to transmit, the transmission is successful.

$$P_r\{-1, 0, N_{s,i}|j, 0, 0\} = 1 - P_{u,i} \qquad 0 \leq j \leq m$$

6. During a successful transmission interval the counter decreases by one for each slot time.

$$P_r\{-1, 0, \ell - 1| - 1, 0, \ell\} = 1 \qquad 2 \leq \ell \leq N_{s,i}$$

7. A new backoff delay of stage 0 is selected after the successful transmission.

$$P\{0, k, 0| - 1, 0, 1\} = \frac{1}{W_0} \qquad 0 \leq k \leq W_0 - 1$$

8. When an unsuccessful transmission occurs due to a collision or an erroneous transmission, a node inters the unsuccessful interval.

$$P_r\{j, 0, N_{u,i}|j, 0, 0\} = P_{u,i} \qquad 0 \leq j \leq m$$

9. During the unsuccessful transmission period the counter decreases by one for each slot time.

$$P\{j, 0, \ell - 1 | j, 0, \ell\} = 1 \qquad 0 \leq j \leq m \quad 2 \leq \ell \leq N_{c,i}$$

10. After the counter of unsuccessful transmission period reaches zero, the node doubles the contention window and inters the next backoff stage.

$$P_r\{j + 1, k, 0 | j, 0, 1\} = \frac{1}{W_{j+1}} \qquad 0 \leq j \leq m - 1$$

11. If there is an unsuccessful transmission after m retries, the current packet is discarded and the node starts a new packet transmission at the end of the unsuccessful transmission period.

$$P_r\{0, k, 0 | m, 0, 1\} = \frac{1}{W_0} \qquad 0 \leq k \leq W_0 - 1$$

4.2.2.2 Steady State Probabilities

At this point, we calculate the steady state probability that a node is at state $\{j, k, \ell\}$. Let $\pi_{j,k,\ell} = lim_{t\to\infty} P\{s(t) = j, b(t) = k, u(t) = \ell\}$ be the stationary distribution of the Markov chain model. In the steady state, similar to (26,27), the following equations hold for the Markov chain model given in Fig. 4.4.

$$\pi_{j-1,0,0} \cdot P_{u,i} = \pi_{j,0,0} \qquad 0 < j \leq m \qquad (4.20)$$

$$\pi_{j,0,0} = P_{u,i}^{j} \cdot \pi_{0,0,0} \qquad 0 \leq j \leq m \tag{4.21}$$

Due to the regularities of the Markov chain, thus for each $1 \leq k \leq W_j - 1$, all the following relations hold:

$$\pi_{j,k,0} = \frac{W_j - k}{W_j} \begin{cases} (1 - P_{u,i}) \sum_{x=0}^{m} \pi_{x,0,0} + P_{u,i}\pi_{m,0,0} & j = 0 \\ P_{u,i}\pi_{j-1,0,0} & 0 < j \leq m \end{cases} \tag{4.22}$$

By substituting equation (4.20) into equations (4.21) and (4.22), and using $\sum_{x=0}^{m-1} \pi_{x,0,0} = \frac{\pi_{0,0,0}(1-P_{u,i}^{m})}{1-P_{u,i}}$, equation (4.22) can be rewritten as follows:

$$\pi_{j,k,0} = \frac{W_j - k}{W_j} P_{u,i}^{j} \pi_{0,0,0} \qquad 0 \leq j \leq m, \quad 0 \leq k \leq W_j - 1 \tag{4.23}$$

For the third dimension, during the successful transmission interval the following relations can be expressed.

$$\pi_{-1,0,\ell} = \pi_{-1,0,N_{s,i}} \qquad 1 \leq \ell \leq N_{s,i} \tag{4.24}$$

$$\pi_{-1,0,N_{s,i}} = \sum_{j=0}^{m} (1 - P_{u,i}) \pi_{j,0,0} \tag{4.25}$$

Substituting equation (4.21) into equation (4.25), we have:

$$\pi_{-1,0,N_{s,i}} = \sum_{j=0}^{m} (1 - P_{u,i}) P_{u,i}^{j} \pi_{0,0,0} = (1 - P_{u,i}^{m+1}) \pi_{0,0,0} \tag{4.26}$$

By substituting equation (4.26) into equation (4.24), we have:

$$\pi_{-1,0,\ell} = (1 - P_{u,i}^{m+1})\pi_{0,0,0} \qquad 1 \leq \ell \leq N_{s,i} \tag{4.27}$$

During the unsuccessful transmission interval, the steady state probabilities can be expressed as follows:

$$\pi_{j,0,\ell} = P_{u,i}\pi_{j,0,0} \qquad 1 \leq \ell \leq N_{u,i} \quad 0 \leq j \leq m \tag{4.28}$$

Similarly, during the frozen transmission period, we have:

$$\pi_{j,k,\ell} = P_{b,i}\pi_{j,k,0} \qquad 1 \leq \ell \leq N_{f,i} \quad 1 \leq k \leq W_j - 1 \quad 0 \leq j \leq m \tag{4.29}$$

Finally, $\pi_{0,0,0}$ can be derived by imposing the normalization condition for the stationary distribution. $\pi_{0,0,0}$ is calculated as follows:

$$1 = \sum_{\ell=1}^{N_{s,i}} \pi_{-1,0,\ell} + \sum_{j=0}^{m} \sum_{\ell=0}^{N_{u,i}} \pi_{j,0,\ell} + \sum_{j=0}^{m} \sum_{k=1}^{W_j-1} \sum_{\ell=0}^{N_{f,i}} \pi_{j,k,\ell} \tag{4.30}$$

From (4.27) and the first term on the R.H.S. of (4.30), we have:

$$\sum_{\ell=1}^{N_{s,i}} \pi_{-1,0,\ell} = N_{s,i}(1 - P_{u,i}^{m+1})\pi_{0,0,0} \tag{4.31}$$

From (4.28), the second term on the R.H.S. of (4.30) is expressed as

follows:

$$\begin{aligned}\sum_{j=0}^{m}\sum_{\ell=0}^{N_{u,i}}\pi_{j,0,\ell} &= \sum_{j=0}^{m}\left[\sum_{\ell=1}^{N_{u,i}}P_{u,i}\pi_{j,0,0}+\pi_{j,0,0}\right] \\ &= (1+N_{u,i}P_{u,i})\sum_{j=0}^{m}\pi_{j,0,0} \\ &= (1+N_{u,i}P_{u,i})\frac{1-P_{u,i}^{m+1}}{1-P_{u,i}}\pi_{0,0,0} \end{aligned} \tag{4.32}$$

From equation (4.29), the third term on the R.H.S. of equation (4.30) can be calculated as follows:

$$\begin{aligned}\sum_{j=0}^{m}\sum_{k=1}^{W_j-1}\sum_{\ell=0}^{N_{f,i}}\pi_{j,k,\ell} &= \sum_{j=0}^{m}\sum_{k=1}^{W_j-1}\left[\sum_{\ell=1}^{N_{f,i}}P_{b,i}\pi_{j,k,0}+\pi_{j,k,0}\right] \\ &= \sum_{j=0}^{m}\sum_{k=1}^{W_j-1}(1+N_{f,i}P_{b,i})\pi_{j,k,0} \end{aligned} \tag{4.33}$$

Substituting equation (4.23) into equation (4.33), we have:

$$\begin{aligned}\sum_{j=0}^{m}\sum_{k=1}^{W_j-1}\sum_{\ell=0}^{N_{f,i}}\pi_{j,k,\ell} &= (1+N_{f,i}P_{b,i})\sum_{j=0}^{m}\sum_{k=1}^{W_j-1}\frac{W_j-k}{W_j}P_{u,i}^{j}\pi_{0,0,0} \\ &= (1+N_{f,i}P_{b,i})\pi_{0,0,0}\sum_{j=0}^{m}\frac{W_j-1}{2}P_{u,i}^{j} \end{aligned} \tag{4.34}$$

By substituting equations (4.31), (4.32), and (4.34) into (4.30), we have:

$$1 = \pi_{0,0,0}\left[N_{s,i}(1-P_{u,i}^{m+1})+(1+N_{u,i}P_{u,i})\frac{1-P_{u,i}^{m+1}}{1-P_{u,i}}+(1+N_{f,i}P_{b,i})\sum_{j=0}^{m}\frac{W_j-1}{2}P_{u,i}^{j}\right]$$

Therefore, $\pi_{0,0,0}$ can be expressed as follows:

$$\pi_{0,0,0} = \left[N_{s,i}(1 - P_{u,i}^{m+1}) + (1 + N_{u,i}P_{u,i})\frac{1 - P_{u,i}^{m+1}}{1 - P_{u,i}} + (1 + N_{f,i}P_{b,i}) \sum_{j=0}^{m} \frac{W_j - 1}{2} P_{u,i}^{j} \right]^{-1} \tag{4.35}$$

4.2.2.3 System Equations

Let τ_i be the probability that the node i transmits during a randomly chosen slot time. The node accesses the medium when its backoff counter reaches zero, regardless of the backoff stage. τ_i can be calculated as follows:

$$\tau_i = \sum_{j=0}^{m} \pi_{j,0,0} = \frac{1 - P_{u,i}^{m+1}}{1 - P_{u,i}} \pi_{0,0,0} \tag{4.36}$$

Substituting equation (4.35) into equation (4.36), τ_i is then calculated as follows:

When $m \leq m'$

$$\tau_i = \frac{2\big(1 - P_{u,i}^{m+1}\big)(1 - 2P_{u,i})}{W_0(1 + N_{f,i}P_{b,i})\big(1 - (2P_{u,i})^{m+1}\big)(1 - P_{u,i}) + \mathcal{A}} \tag{4.37}$$

When $m > m'$

$$\tau_i = \frac{2\big(1 - P_{u,i}^{m+1}\big)(1 - 2P_{u,i})}{W_0(1 + N_{f,i}P_{b,i})\Big[\big(1 - (2P_{u,i})^{m'+1}\big)(1 - P_{u,i}) + \mathcal{B}\Big] + \mathcal{A}} \tag{4.38}$$

where

$$\mathcal{A} = \big(1 - P_{u,i}^{m+1}\big)(1 - 2P_{u,i})\Big[2N_{s,i}(1 - P_{u,i}) + 2(1 + N_{u,i}P_{u,i}) - (1 + N_{f,i}P_{b,i})\Big]$$

$$\mathcal{B} = 2^{m'}(1 - 2P_{u,i})\big(P_{u,i}^{m'+1} - P_{u,i}^{m+1}\big)$$

Therefore, the transmission probability τ_i can be calculated when the values of W_0, m, m', $N_{c,i}$, $N_{f,i}$, $N_{s,i}$, $P_{b,i}$, and $P_{u,i}$ are known. The values of W_0, m, m' are known, but the values of $P_{b,i}$, $P_{u,i}$, $N_{s,i}$, $N_{c,i}$, and $N_{f,i}$ must be calculated.

The probability α_k, that the channel becomes busy due to either an unsuccessful or a successful transmission of a node $k \neq i$, is calculated as follows:

$$\begin{aligned} \alpha_k &= \sum_{\ell=1}^{N_{s,k}} \pi_{-1,0,\ell} + \sum_{j=0}^{m} \sum_{\ell=0}^{N_{u,k}} \pi_{j,0,\ell} \\ &= \tau_k \Big[N_{s,k}(1 - P_{u,k}) + N_{u,k}P_{u,k} + 1\Big] \end{aligned} \tag{4.39}$$

For the node i, the probability $P_{b,i}$, that the channel is sensed busy when it is occupied by at least one node, is calculated as follows:

$$P_{b,i} = 1 - \prod_{\substack{k=1 \\ k \neq i}}^{N} (1 - \alpha_k), \qquad i = 1, 2, ..., N \tag{4.40}$$

The collision probability $P_{c,i}$, that at least one of the $N - 1$ remaining nodes and the node i transmit at the same time slot, is expressed as follows:

$$P_{c,i} = 1 - \prod_{\substack{j=1 \\ j \neq i}}^{N} (1 - \tau_j), \qquad i = 1, 2, ..., N \tag{4.41}$$

By substituting equation (4.7) (or (4.17)) and equation (4.41) into equation (4.19), the unsuccessful probability $P_{u,i}$ is calculated for single-hop (or two-hop) transmission.

The average number of time slots $N_{s,i}$, that represents the successful transmission period, is calculated as follows:

$$N_{s,i} = \left\lceil \frac{I(i \in S^d)T^d_{s,i} + I(i \in S^c)T^c_{s,i}}{\sigma} \right\rceil \tag{4.42}$$

where $\lceil x \rceil$ is the smallest integer larger than x. $I(x)$ is 1 if x is true, and is 0 otherwise. σ is the slot time size. $T^d_{s,i}$ and $T^c_{s,i}$ stand for the successful transmission period for a single-hop and a two-hop transmission, respectively. $T^d_{s,i}$ and $T^c_{s,i}$ is expressed as follows:

$$T^d_{s,i} = T_{RTS} + T_{CTS} + \frac{8L_s}{R^{(i)}_{sd}} + T_{PLCP} + T_{ACK} + 3T_{SIFS} + T_{DIFS} + 4\delta \tag{4.43}$$

$$\begin{aligned} T^c_{s,i} = {} & T_{CRTS} + T_{CCTS} + T_{RRTS} + \frac{8L_s}{R^{(i)}_{sr}} + \frac{8(L_s + L_r)}{R^{(i)}_{rd}} + 3T_{PLCP} + T_{CACK} + 6T_{SIFS} \\ & + T_{DIFS} + 7\delta \end{aligned} \tag{4.44}$$

The average number of time slots $N_{u,i}$ that represents the unsuccessful period can be expressed as follows:

$$N_{u,i} = \left\lceil \frac{T_{u,i}}{\sigma} \right\rceil \tag{4.45}$$

where the unsuccessful transmission period $T_{u,i}$ is calculated as fol-

lows:

$$T_{u,i} = \frac{P_{c,i}}{P_{u,i}} T_{col} + \frac{1 - P_{c,i}}{P_{u,i}} \left[I(i \in S^d) \sum_{j=1}^{4} p_{ei}^d T_{ei}^d + I(i \in S^c) \sum_{j=1}^{7} p_{ei}^c T_{ei}^c \right] \tag{4.46}$$

where T_c is the collision time between at least two nodes. To simplify the analysis, it is assumed that T_c is the same for the single-hop and two-hop transmission and is calculated as follows:

$$T_c = T_{RTS} + T_{CTS} + T_{SIFS} + T_{DIFS} + \delta \tag{4.47}$$

The node i freezes its backoff counter for $N_{f,i}$ slots due to collisions, successful transmissions, and erroneous transmissions. The average number of slots $N_{f,i}$ can then be expressed as follows:

$$N_{f,i} = \left\lceil \frac{T_{f,i}}{\sigma} \right\rceil \tag{4.48}$$

where

$$T_{f,i} = E[T_{C_i}] + E[T_{S_i}] + E[T_{E_i}] \tag{4.49}$$

$E[T_{C_i}]$, $E[T_{S_i}]$, and $E[T_{E_i}]$ stand for the average collision duration, the average successful duration, and the average erroneous transmission duration given that at least one of the $N-1$ nodes transmits during the backoff process of the intended node i. Consequently, we have:

$$E[T_{C,i}] = \left[1 - \sum_{\substack{j=1 \\ j \neq i}}^{N-1} \widehat{P}_{s,j} \right] T_c \tag{4.50}$$

where $\widehat{P}_{s,j}$ is the successful transmission probability of node $j \neq i$ when no other node of the remaining $N-1$ transmits. It is expressed as follows:

$$\widehat{P}_{s,j} = \frac{\prod_{k=1,k\neq j}^{N-1}(1-\alpha_k)}{P_{b,i}} \sum_{\ell=1}^{N_{s,j}} \pi_{-1,0,\ell} = \frac{\prod_{k=1,k\neq j}^{N-1}(1-\alpha_k)}{1-\prod_{k=1,k\neq i}^{N}(1-\alpha_k)} \cdot N_{s,j}(1-P_{u,j})\tau_j \quad (4.51)$$

The average successful duration $E[T_{S,i}]$ is expressed as follows:

$$E[T_{S,i}] = \sum_{\substack{j=1 \\ j\neq i}}^{N-1} \widehat{P}_{s,j}(1-P_{e,j}) \left[I(j \in S^d) T^d_{s,j} + I(j \in S^c) T^c_{s,j} \right] \quad (4.52)$$

where $T^d_{s,j}$ and $T^c_{s,j}$ are given in equations (4.43) and (4.44), respectively. The average erroneous transmission duration $E[T_{E,i}]$ is calculated as follows:

$$E[T_{E,i}] = \sum_{\substack{j=1 \\ j\neq i}}^{N-1} \widehat{P}_{s,j} \left[I(j \in S_d) \sum_{k=1}^{4} p^d_{ek} T^d_{ek} + I(j \in S_c) \sum_{k=1}^{7} q^c_{ek} T^c_{ek} \right] \quad (4.53)$$

Finally, given the set of equations (4.19) and (4.35)-(4.53), a non-linear system can be solved to determine $P_{u,i}$ and τ_i ($\forall\ i = 1, 2, ..., N$). Therefore, in the following sections, we can then derive throughput, energy efficiency, and delay.

4.2.3 Throughput

In this section, we drive an expression for the saturated throughput of CARD protocol in presence of transmission errors. The saturated through-

put $\mathbf{S}$ is defined as a ratio of successfully transmitted payload size over a randomly chosen slot time duration:

$$\mathbf{S} = \frac{E[PL]}{E[T_I] + E[T_C] + E[T_S] + E[T_E]} \tag{4.54}$$

where $E[PL]$ is the average payload size, $E[T_I]$ is the average idle slot duration, $E[T_C]$ is the average collision slot duration, $E[T_S]$ is the average successful transmission slot duration, and $E[T_E]$ is the average slot duration due to erroneous transmission.

Let P_{tr} be the probability that there is at least one transmission occurs in a randomly chosen slot time. Each node occupies the channel with probability α_i, where $i = 1, 2, ..., N$. P_{tr} is calculated as follows:

$$P_{tr} = 1 - \prod_{i=1}^{N}(1 - \alpha_i) \tag{4.55}$$

where α_i is given in equation (4.39). Given a transmission on the channel from a generic node i, the probability $P_{s,i}$, that a transmission is successful, is calculated as follows:

$$\begin{aligned} P_{s,i} &= \sum_{\ell=1}^{N_{s,i}} \pi_{-1,0,\ell} \cdot \prod_{\substack{k=1 \\ k\neq i}}^{N}(1 - \alpha_k) \\ &= N_{s,i}(1 - P_{u,i})\tau_i \cdot \prod_{\substack{k=1 \\ k\neq i}}^{N}(1 - \alpha_k) \end{aligned} \tag{4.56}$$

The average idle slot duration before a transmission takes place is

computed as follows:

$$E[T_I] = (1 - P_{tr})\sigma \tag{4.57}$$

where $1 - P_{tr}$ is the probability that the chosen slot time is empty. In order to calculate the average collision slot duration, let T^d_{col} and T^c_{col} stand for the time duration during which the channel is sensed busy for a single-hop and a two-hop transmission, respectively. T^d_c and T^c_c are computed as follows:

$$T^d_c = T_{RTS} + T_{CTS} + T_{SIFS} + T_{DIFS} + \delta \tag{4.58}$$

$$T^c_c = T_{CRTS} + T_{CCTS} + T_{SIFS} + T_{DIFS} + \delta \tag{4.59}$$

where $T^c_c > T^d_c$. There are two different collisions: (1) the collision occurs with probability P^d_{c1} (or P^c_{c1}) between at least two RTS (or CRTS) packets for a single (or a two)-hop transmission. (2) the collision occurs with probability P^d_{c2} (or P^c_{c2}) between at least one RTS (or CRTS) packet and at least one CRTS (or RTS) packet. Let the number of nodes that employ a single transmission be $N_d = |S^d|$ and those employ a two hop transmission be $N_c = |S^c|$, where $N = N_d + N_c$. The probability $P^{d/c}_{c1}$ is calculated as follows:

$$P^{d/c}_{c1} = \prod_{i \in N_{c/d}} (1 - \tau_i) \left[1 - \left[\prod_{i \in N_{d/c}} (1 - \tau_i) + \sum_{i \in N_{d/c}} \tau_i \prod_{\substack{j \in S^{d/c} \\ j \neq i}} (1 - \tau_j) \right] \right] \tag{4.60}$$

where the right hand side is the probability that the nodes employing a single/two hop transmission do not transmit times the probability that

there are at least two nodes using single/two hop transmission transmit on the channel at the same time. The collision probability P_{c2}^{c} between at least one CRTS packet and at least one RTS packet is calculated as follows:

$$P_{c2}^{c} = \left[1 - \prod_{i \in N_c} (1 - \tau_i)\right]\left[1 - \prod_{k \in N_d} (1 - \tau_k)\right] \tag{4.61}$$

The collision duration in this case is T_{col}^{c}. In the case of single-hop, the probability $P_{c2}^{d} = 0$. The probabilities P_{c}^{d} and P_{c}^{c} are calculated as follows:

$$P_{c}^{d} = P_{c1}^{d} \tag{4.62}$$

$$P_{c}^{c} = P_{c1}^{c} + P_{c1}^{c} \tag{4.63}$$

The average collision slot duration $E[T_C]$ is calculated as follows:

$$E[T_C] = P_{c}^{d} T_{c}^{d} + P_{c}^{c} T_{c}^{c} \tag{4.64}$$

The average slot duration of a successful transmission $E[T_S]$ depends on the transmission technique (single or two hop). In the case of a single-hop transmission, i.e. the nodes in zone I and II, and those in zones III and IV with no relay node available, the average successful transmission period $E[T_S^d]$ is expressed as follows:

$$E[T_S^d] = \sum_{j=1}^{4} T_{s,j}^{d} \sum_{k=1}^{N_i^d} P_{s,k}(1 - P_{e,k}) \tag{4.65}$$

where $T_{s,j}^{d}$ is given in equation (4.43). The remaining nodes in zone

III and IV employ a two-hop transmission to deliver their packet to the AP. Let $E[T^c_{S1}]$ and $E[T^c_{S2}]$ are the average slot duration of a successful two-hop transmission of nodes located in zone IV and III, respectively. $E[T^c_{S1}]$ and $E[T^c_{S2}]$ are expressed as follows:

$$E[T^c_{S1}] = \sum_{i=1}^{3}\sum_{j=1}^{3}\left[\sum_{k=1}^{N_{4(i,j)}} T^c_{s,k}P_{s,k}(1-P_{e,k})\right], \quad at\ i=3\ \ j\neq 3 \tag{4.66}$$

$$E[T^c_{S2}] = \sum_{i=1}^{2}\sum_{j=1}^{2}\left[\sum_{k=1}^{N_{3(i,j)}} T^c_{s,k}P_{s,k}(1-P_{e,k})\right] \tag{4.67}$$

where $T^c_{s,i}$ is given in equation (4.44). Therefore, the average slot duration of a successful transmission is computed as follows:

$$E[T_S] = E[T^d_S] + E[T^c_{S1}] + E[T^c_{S2}] \tag{4.68}$$

The average duration of the slot due to erroneous transmissions is:

$$E[T_E] = \sum_{i=1}^{N} P_{s,i}\left[I(i\in S^d)\sum_{k=1}^{4} p^d_{ei}T^d_{ei} + I(i\in S^c)\sum_{k=1}^{7} q^c_{ei}T^c_{ei}\right] \tag{4.69}$$

In the case of a single-hop transmission p_{ei} and T^d_{ei} are given in equations (4.5) and (4.6) respectively. On the other hand for a two-hop transmission q^c_{ei} and T^c_{ei} are given in equations (4.15) and (4.16), respectively.

The average payload size $E[PL]$ is calculated as follows:

$$E[PL] = 8L_s \sum_{i=1}^{4} \sum_{j=1}^{N_i^d} P_{s,j}(1-P_{e,j}) + 8(L_s+L_r)\left[\sum_{i=1}^{3}\sum_{j=1}^{3}\sum_{k=1}^{N_{4(i,j)}} P_{s,k}(1-P_{e,k}) + \sum_{i=1}^{2}\sum_{j=1}^{2}\sum_{k=1}^{N_3(i,j)} P_{s,k}(1-P_{e,k})\right] \quad (4.70)$$

Given the average slot durations and average payload size derived in above, the saturated throughput is calculated from equation (4.54).

4.2.4 Energy Efficiency

The energy efficiency η, is defined as the ratio of the successfully transmitted data bits to the total energy consumed (99, 100). η, is written as follows:

$$\eta = \frac{E[L]}{\sum_{i=1}^{N}\left(E_B^{(i)} + E_C^{(i)} + E_O^{(i)} + E_E^{(i)} + E_S^{(i)}\right)} \quad (4.71)$$

where $E_B^{(i)}$ is the energy consumption during the backoff period. $E_C^{(i)}$ is the energy consumption during the collision transmission period. $E_O^{(i)}$ is the energy consumption during the overhearing transmission period. $E_E^{(i)}$ is the energy consumption during the erroneous transmission period. $E_S^{(i)}$ is the energy consumption during the successful transmission period. $E[L]$ is the average payload size.

The probability $P(s = j)$, that the generic node i accesses the channel when the backoff counter in stage j reaches zero as shown in

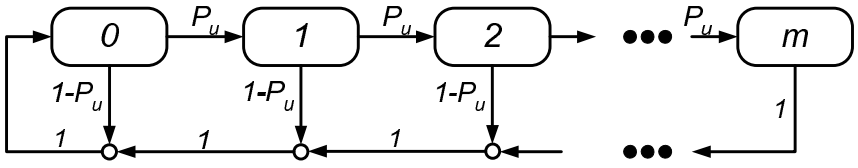

Figure 4.5: Markov chain for backoff stage

Fig. 4.5, is calculated as follows:

$$P(s=j) = P_{u,i}^{j} \cdot P(s=0)$$

where

$$\begin{aligned} \sum_{i=0}^{m} P(s=j) &= \sum_{k=0}^{m} P_{u,i}^{k} \cdot P(s=0) = 1 \\ P(s=0) &= \frac{1-P_{u,i}}{1-P_{u,i}^{m+1}} \end{aligned}$$

The probability $P(s=j)$ is then computed as follows:

$$P(s=j) = \frac{P_{u,i}^{j}(1-P_{u,i})}{1-P_{u,i}^{m+1}} \tag{4.72}$$

where $1-P_{u,i}^{m+1}$ is the probability that the packet is not dropped. It is assumed that $\overline{N_{b,i}}$ is the average total number of time slots during the backoff duration, and it is expressed as follows:

$$\overline{N_{b,i}} = \sum_{j=0}^{m} \frac{P_{u,i}^{j}(1-P_{u,i})}{1-P_{u,i}^{m+1}} \sum_{x=0}^{j} \frac{W_x - 1}{2}, \quad i = 1, 2, ..., N \tag{4.73}$$

where $\sum_{x=0}^{j} \frac{W_x-1}{2}$ is the average number of backoff slots that the intended node i needs to transmit its packet successfully after j retries.

$P_{u,i}^{j}(1 - P_{u,i})$ is the probability that the transmission of the node i is successful after j retries (backoff stages). Consequently, given the duration of an empty slot σ and the idle power consumption P_{IX}, the energy that the node i consumes during the backoff stage, is calculated as follows:

$$E_B^{(i)} = \sigma \cdot P_{IX} \cdot \overline{N_{b,i}}, \quad i = 1, 2, ..., N \tag{4.74}$$

Notice that in equation (4.73) only the successful packet transmissions are considered. Let $\overline{N}_{idle,i}$ be the average number of consecutive idle slots between two consecutive busy slots of the $N-1$ remaining nodes. $\overline{N}_{idle,i}$ is then calculated as follows:

$$\overline{N}_{idle,i} = \sum_{j=0}^{\infty} j(1 - P_{b,i})^j P_{b,i} = \frac{1}{P_{b,i}} - 1 \tag{4.75}$$

The average number of transmissions $\overline{N_{o,i}}$ overheard by the generic node i from the other $N-1$ nodes during the backoff process is calculated as follows:

$$\overline{N_{o,i}} = \frac{\overline{N_{b,i}}}{\overline{N}_{idle,i}} = \frac{\overline{N_{b,i}}}{1 - P_{b,i}} P_{b,i} \tag{4.76}$$

where $P_{b,i}$ is given in equation (4.40). Both $\overline{N_{b,i}}$ and $\overline{N_{o,i}}$ can be treated as the total number of idle and busy slots that a packet encounters during the backoff stages, respectively. The intended node i overhears the collisions, the successful transmissions, and the erroneous transmissions of the $N-1$ nodes. Therefore, the energy that the node i consumes in overhearing other nodes transmission during the backoff stages is calculated

as follows:

$$E_O^{(i)} = \overline{N_{o,i}} P_{RX} T_{f,i} \tag{4.77}$$

where $T_{f,i}$ is given in equation (4.49), and P_{RX} is the receiving power consumption. The average number of retries $\overline{N_{r_i}}$ that the node i encounters before delivering its packet correctly to its destination, is calculated as follows:

$$\overline{N_{r_i}} = \sum_{i=0}^{m} \frac{i P_{u,i}^{i}(1 - P_{u,i})}{1 - P_{u,i}^{m+1}} = \frac{1 - P_{u,i}}{1 - P_{u,i}^{m+1}} \left[\frac{P_{u,i}}{(1 - P_{u,i})^2}(1 - P_{u,i}^{m}) - \frac{m P_{u,i}^{m+1}}{1 - P_{u,i}} \right] \tag{4.78}$$

The $\overline{N_{r_i}}$ is the sum of retries due to both collision and erroneous transmission. From equation (4.19), $\frac{P_{c,i}}{P_{u,i}}$ is the fraction of the total retries due to a collision transmission, and the average number of retries $\overline{N_{c_i}}$ that is due to a collision transmission in the total retries is calculated as follows:

$$\overline{N_{c_i}} = \overline{N_{r_i}} \frac{P_{c,i}}{P_{u,i}} \tag{4.79}$$

Consequently, the energy consumption due to collision is computed as follows:

$$E_C^{(i)} = \overline{N_{c_i}} \Big[P_{TX} T_{RTS/CRTS} + P_{RX} T_{CTS/CCTS} + P_{IX}(T_{DIFS} + T_{SIFS}) \Big] \tag{4.80}$$

where P_{TX} is the power consumption during transmission. The fraction of the total retries due to an erroneous transmission is: $\frac{(1-P_{c,i})q_{ek}^{c}}{P_{u,i}}$, where $k \in (1, 7)$ for a two-hop transmission, and $\frac{(1-P_{c,i})p_{ek}}{P_{u,i}}$, where $k \in (1, 4)$ for a single-hop transmission. Let $\overline{N_{ek}^{c}}$, where $k = 1, 2, ..., 7$ be the average num-

ber of retries due to the corruption of CRTS, CCTS, RRTS, DATA-S (source-relay), DATA-S (relay-AP), DATA-R, and ACK, respectively. It is then calculated as follows:

$$\overline{N_{ek}^{c}} = \overline{N_{r_i}} \frac{(1 - P_{c,i}) q_{ek}^{c}}{P_{u,i}}, \qquad k = 1, 2, ...7 \tag{4.81}$$

Similarly, in the case of a single-hop transmission $\overline{N_{ek}^{d}}$, where $k \in (1, 4)$ stands for the average number of retries due to the corruption of RTS, CTS, DATA-S (source-AP), and ACK, respectively given that exactly one RTS is transmitted. Thus, we have:

$$\overline{N_{ek}^{d}} = \overline{N_{r_i}} \frac{(1 - P_{c,i}) p_{ek}}{P_{u,i}}, \qquad k = 1, 2, 3, 4 \tag{4.82}$$

To calculate the energy consumption during an erroneous transmission, it is assumed that E_{ek}^{d}, where $k = 1, 2, ...4$ is the erroneous energy consumption during the corruption transmission of RTS, CTS, DATA-S (source-AP), and ACK packets, respectively under a single-hop transmission. E_{ek}^{d} is expressed as follows:

$$\begin{aligned}
E_{e1}^{d} &= P_{TX} T_{RTS} + P_{IX}(T_{CTS} + T_{SIFS} + T_{DIFS} + 2\delta) \\
E_{e2}^{d} &= P_{TX} T_{RTS} + P_{RX} T_{CTS} + P_{IX}(T_{SIFS} + T_{DIFS} + 2\delta) \\
E_{e3}^{d} &= P_{TX}(T_{RTS} + \frac{8L_s}{R_{sd}} + T_{PLCP}) + P_{RX} T_{CTS} + P_{IX}(T_{ACK} + 3T_{SIFS} + T_{DIFS} + 4\delta) \\
E_{e4}^{d} &= P_{TX}(T_{RTS} + \frac{8L_s}{R_{sd}} + T_{PLCP}) + P_{RX} T_{CTS} + P_{IX}(T_{ACK} + 3T_{SIFS} + T_{DIFS} + 4\delta)
\end{aligned} \tag{4.83}$$

Similarly, if the intended node i employs a two-hop transmission, the energy consumption during an erroneous transmission is defined as E_{ek}^{c},

where $k = 1, 2, ...7$. It is the energy consumption during the corruption transmission of CRTS, CCTS, RRTS, DATA-S (source-relay), DATA-S (relay-AP), DATA-R, and CACK, respectively. E^c_{ek} is expressed as follows:

$$\begin{aligned}
E^c_{e1} &= P_{TX}T_{CRTS} + P_{IX}(T_{CCTS} + T_{SIFS} + T_{DIFS} + 2\delta) \\
E^c_{e2} &= P_{TX}T_{CRTS} + P_{RX}T_{CCTS} + P_{IX}(T_{SIFS} + T_{DIFS} + 2\delta) \\
E^c_{e3} &= P_{TX}T_{CRTS} + P_{RX}(T_{CCTS} + T_{RRTS}) + P_{IX}(2T_{SIFS} + T_{DIFS} + 3\delta) \\
E^c_{e4} &= P_{TX}(T_{CRTS} + \frac{8L_s}{R_{sr}} + T_{PLCP}) + P_{RX}(T_{CCTS} + T_{RRTS}) \\
&\quad + P_{IX}(4T_{SIFS} + T_{DIFS} + 5\delta) \\
E^c_{e5} &= P_{TX}(T_{CRTS} + \frac{8L_s}{R_{sr}} + T_{PLCP}) + P_{RX}(T_{CCTS} + T_{RRTS} + \frac{8L_s}{R_{rd}} \\
&\quad + \frac{8L_r}{R_{rd}} + 2T_{PLCP}) + P_{IX}(T_{CACK} + 6T_{SIFS} + T_{DIFS} + 7\delta) \\
E^c_{e6} &= P_{TX}(T_{CRTS} + \frac{8L_s}{R_{sr}} + T_{PLCP}) + P_{RX}(T_{CCTS} + T_{RRTS} + \frac{8L_s}{R_{rd}} \\
&\quad + \frac{8L_r}{R_{rd}} + 2T_{PLCP}) + P_{IX}(T_{CACK} + 6T_{SIFS} + T_{DIFS} + 7\delta) \\
E^c_{e7} &= P_{TX}(T_{CRTS} + \frac{8L_s}{R_{sr}} + T_{PLCP}) + P_{RX}(T_{CCTS} + T_{RRTS} + \frac{8L_s}{R_{rd}} \\
&\quad + \frac{8L_r}{R_{rd}} + 2T_{PLCP} + T_{CACK}) + P_{IX}(6T_{SIFS} + T_{DIFS} + 7\delta)
\end{aligned} \tag{4.84}$$

Therefore, the total energy consumption $E^{(i)}_E$, that the intended node i contends successfully but the packet is corrupted at the receiver, is calculated as follows:

$$E^{(i)}_E = I(i \in S^d) \sum_{i=1}^{4} \overline{N^d_{ek}} E^d_{ek} + I(i \in S^c) \sum_{i=1}^{7} \overline{N^c_{ek}} E^c_{ek} \tag{4.85}$$

The energy consumption for a successful single-hop transmission, E^d_S,

is computed as follows:

$$E_S^d = P_{TX}(T_{RTS} + \frac{8L_s}{R_{sd}} + T_{PLCP}) + P_{RX}T_{CTS} + P_{IX}(T_{ACK} + 3T_{SIFS} + T_{DIFS} + 4\delta) \tag{4.86}$$

for a successful two-hop transmission, we have:

$$\begin{aligned} E_S^c &= P_{TX}(T_{CRTS} + \frac{8L_s}{R_{sr}} + T_{PLCP}) + P_{RX}(T_{CCTS} + T_{RRTS} + \frac{8L_s}{R_{rd}} \\ &\quad + \frac{8L_r}{R_{rd}} + 2T_{PLCP}) + P_{IX}(T_{CACK} + 6T_{SIFS} + T_{DIFS} + 7\delta) \end{aligned} \tag{4.87}$$

The energy consumption during a successful transmission of the intended node i is computed as follows:

$$E_S^{(i)} = I(i \in S^d)E_S^d + I(i \in S^c)E_S^c \tag{4.88}$$

Finally the average payload size $E[L]$ is given as follows:

$$E[L] = 8L_s \sum_{i=1}^{4} N_i^d + 8(L_s + L_r)\left[\sum_{i=1}^{3}\sum_{j=1}^{3} N_{4(i,j)} + \sum_{i=1}^{2}\sum_{j=1}^{2} N_{3(i,j)}\right] \tag{4.89}$$

4.2.5 Delay

The average packet delay is the time interval between two successful transmissions at a node. If the packet is discarded because it has reached the retry limit, the delay for this packet will not be included in the computing of the average delay. Let D_i $(i = 1, 2, ..., N)$ denote a random variable representing a packet delay of the intended node i. Thus, the average packet delay $E[D_i]$ is expressed as follows:

$$E[D_i] = E[D_{b,i}] + E[D_{c,i}] + E[D_{o,i}] + E[D_{e,i}] + E[D_{s,i}] \tag{4.90}$$

where $E[D_{b,i}]$, $E[D_{c,i}]$, $E[D_{o,i}]$, $E[D_{e,i}]$, and $E[D_{s,i}]$ stand for the average delay during decreasing the backoff counter, the average delay due to a collision transmission, the average delay due to freezing the backoff counter during the transmissions of the other nodes, the average delay due to an erroneous transmission, and the average delay of a successful transmission, respectively. These average delay values are calculated as follows:

$$\begin{aligned}
E[D_{b,i}] &= \sigma\overline{N_{b,i}} \\
E[D_{c,i}] &= \overline{N_{c,i}}T_c \\
E[D_{o,i}] &= \overline{N_{o,i}}T_{f,i} \\
E[D_{e,i}] &= \widehat{P}_{s,i}\left[I(i \in S_d)\sum_{k=1}^{4}\overline{N}_{ek}p_{ek}T_{ek} + I(i \in S_c)\sum_{k=1}^{7}\overline{N_{ek}^c}q_{ek}^c T_{ek}^c\right] \\
E[D_{s,i}] &= I(i \in S^d)T_{s,i}^d + I(i \in S^c)T_{s,i}^c
\end{aligned} \tag{4.91}$$

where $\overline{N_{b,i}}$ and $\overline{N_{o,i}}$ are given in equations (4.73) and (4.76), respectively. $T_{f,i}$ is given in equation (4.48). $T_{s,i}^d$, $T_{s,i}^c$, and T_c are given in (4.43), (4.44), and (4.47), respectively. T_{ek}^d and T_{ek}^c are given in (4.6) and (4.16), respectively. N_{ek}^c and N_{ek}^d are given in (4.81) and (4.82), respectively. Therefore, the total average delay of the network is calculated as follows:

$$E[D_T] = \frac{1}{N}\sum_{i=1}^{N} E[D_i] \tag{4.92}$$

Parameter	Value	Parameter	Value
MAC header	272 bits	Slot time	20 μs
PHY header	192 bits	SIFS	10 μs
RTS	352 bits	DIFS	50 μs
CTS	304 bits	CRTS	400 bits μs
ACK	304 bits	CCTS	306 bits
CW_{min}	31 slots	RRTS	304 bits
CW_{max}	1023 slots	CACK	306 bits
PLCP rate	1 Mbps	P_{IX}, P_{RX}, P_{TX}	0.8,0.8,1.0 Watt

Table 4.2: PHY and MAC setup of the CARD protocol.

4.3 Analytical and Simulation results

To validate the above analysis, a custom event driven simulator developed by using the Mobile Framework (MF) of the OMNET++ (148) package written in C++ programming language. The parameters used in simulation and analysis are set to the default values specified in IEEE 802.11b standard which are summarized in Table 4.2. The network setting is the same as given in (Chapter 3, Section 3.4). In all following figures, solid lines are results of the analytical model results through Matlab software package. Whereas dot-dashed lines are for the simulation results through OMNET++ software package.

4.3.1 Throughput Results

In Fig. 4.6, we compare the saturated throughput achieved by the CARD, CoopMAC, and IEEE 802.11b protocols under ideal channel conditions. As the network size, i.e. number of nodes, increases, the throughput for 802.11b decreases due to collisions. This is because of increasing the number of nodes causes increasing the collision probability, and

hence the overall throughput degrades. On the other hand, the throughput achieved by both the CARD and CoopMAC protocols increases exponentially as the number of nodes increases. The reason is that as the number of nodes increases, the probability of a low data-rate node finding a relay node increases. The two-hop transmission between a source node and the AP can be established via a relay node, and the data-rate from a source node to the AP increases. Therefore, the cooperative transmission not only compensates the collision probability caused by increasing the number of nodes, but also solves the performance anomaly caused by the low data-rate nodes; for this reason the throughput of both the CARD and CoopMAC protcols increases as the number of nodes increases. However, the CARD protocol achieves a higher throughput than the CoopMAC protocol.

As shown in Fig. 4.6, the CARD protocol can achieve throughput up to 42% more than that can be achieved by the CoopMAC protocol when the number of nodes is more than 30 nodes. This is because the CARD protocol achieves both cooperative diversity gain and cooperative multiplexing gain. The relay node shares the handshake procedure between a source node and the AP and transmits its own data immediately after forwarding the source station's information to the AP. On the contrary, the CoopMAC protocol achieves only cooperative diversity gain; where the relay node forwards only the information of the source node to the AP.

The channel conditions is one of the critical parameters that can affect the performance of the WLANs. It is then important to study the effect of the imperfect channel conditions on the throughput that can be achieved by the CARD protocol. Fig. 4.7 shows the relationship between throughput and network size under different channel conditions for the

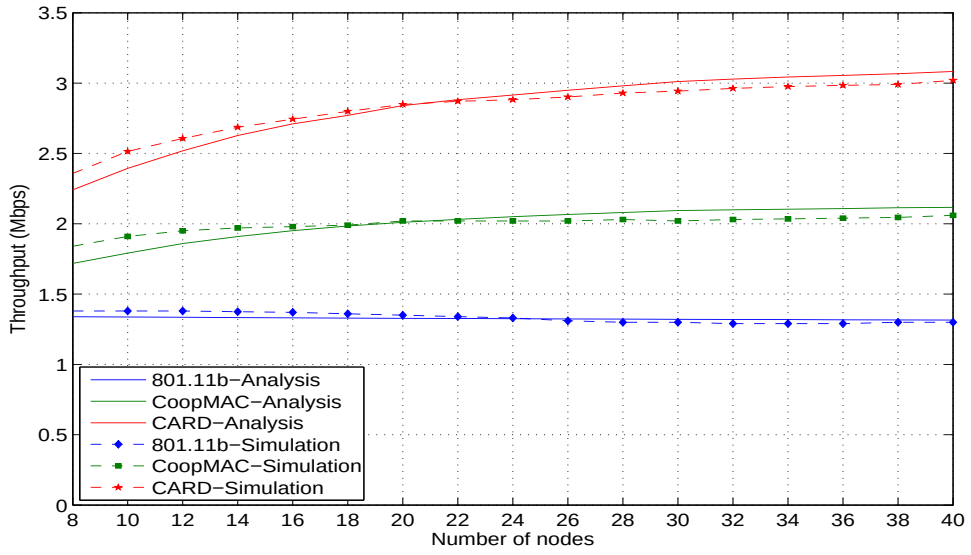

Figure 4.6: Throughput vs. number of nodes under ideal channel, L = 1024 bytes.

802.11b, CoopMAC, and CARD protocols. The throughput performance under $BER = 2 \times 10^{-5}$ and under $BER = 6 \times 10^{-5}$ is given in Fig. 4.7(a) and Fig. 4.7(b), respectively. As the channel quality becomes poor, the throughput of the three protocols decreases. The reason is that the probability of packet errors increases as the channel conditions becomes poor. Consequently, the number of retransmission retries, and the transmission time to deliver the data packet to the AP also increases. Even if the channel conditions becomes imperfect, the CARD protocol outperforms both the 802.11b and CoopMAC protocols. For example the throughput that can be achieved by the CARD when the $BER = 6 \times 10^{-5}$ is higher than the throughput that can be achieved by the CoopMAC protocol under ideal channel conditions. Therefore, the CARD protocol is more reliable than the existing 802.11b and CoopMAC protocols.

It is well known that the packet length has a major effect on the performance of any MAC protocol. Therefore, in Fig. 4.8, we study the effect of the packet length on the throughput performance of the 802.11b,

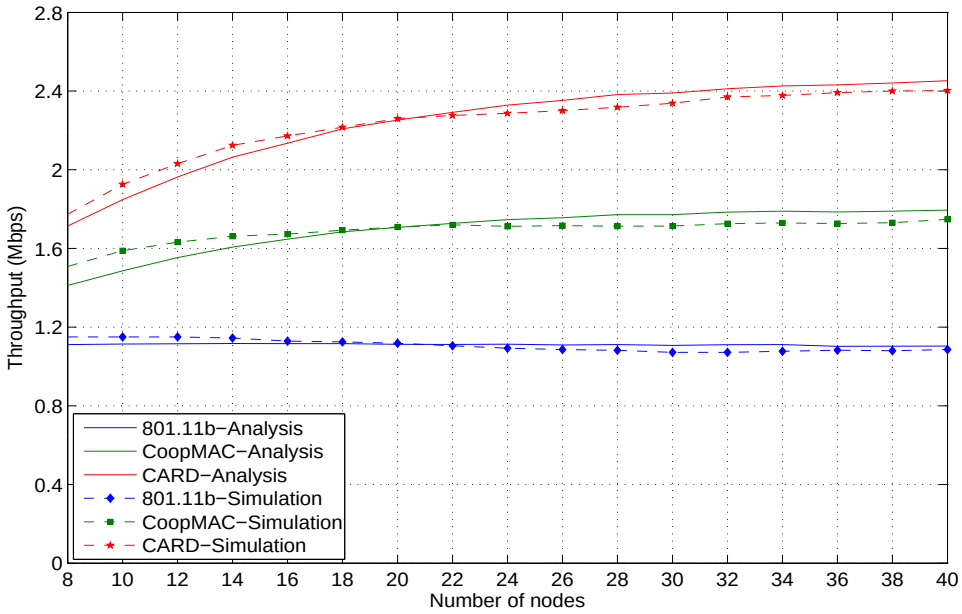

(a) Throughput vs. number of nodes at $BER = 2 * 10^{-5}$.

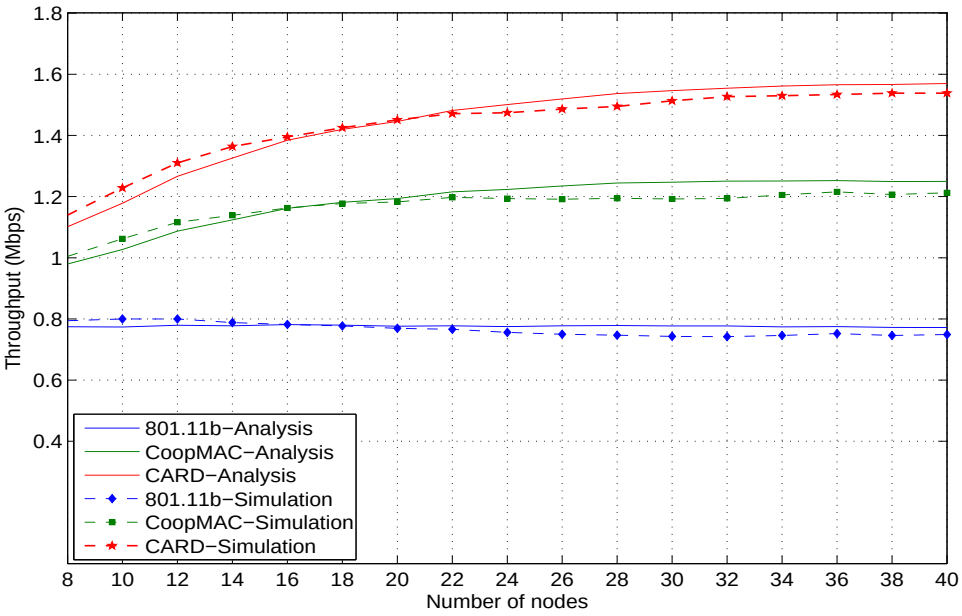

(b) Throughput vs. number of nodes at $BER = 6 * 10^{-5}$.

Figure 4.7: Throughput vs. number of nodes under imperfect channel, L=1024 byte.

CoopMAC, and CARD protocols under ideal channel conditions and a fixed number of nodes which is selected to be 30 nodes. The packet size is changed from 400 bytes, at which the RTS/CTS transmission technique can be used in the standard IEEE 802.11b, to 2000 byte which is approximately the maximum packet length supported by the IEEE 802.11b. When the packet length increases, the throughput that can be achieved by the 802.11b, CoopMAC, and CARD protocols increases. The reason is that the overhead including the PLCP header and control frames is reduced when the packet length increases. The CARD protocol outperforms the 802.11b and CoopMAC protocols under different packet lengths from the minimum to the maximum value.

As shown in Fig. 4.8, the throughput achieved by the CARD protocol is up to 155% more than the 802.11b throughput and is up to 35% more the CoopMAC throughput. In addition the throughput of the CARD protocols is close to the maximum throughput (which is 5 Mbps) that can be achieved when all of the nodes are running at the maximum transmission rate which is 11 Mbps.

Fig. 4.9 shows the throughput of the 802.11b, CoopMAC, and CARD protocols versus the packet length under imperfect channel conditions and a fixed number of nodes at 30 nodes. The throughput when the $BER = 2 \times 10^{-5}$ and the $BER = 6 \times 10^{-5}$ is shown in Fig. 4.9(a) and Fig. 4.9(b), respectively. As discussed before, when the channel condition becomes poor, the throughput of the three protocols comes down. However, the CARD outperforms the CoopMAC even if the channel condition becomes imperfect. For example, when the $BER = 2 \times 10^{-5}$, the throughput of the CARD is degraded by 14% when the packet length is 400 byte, and is degraded by 45% when the packet length is 2000 byte. The reason is

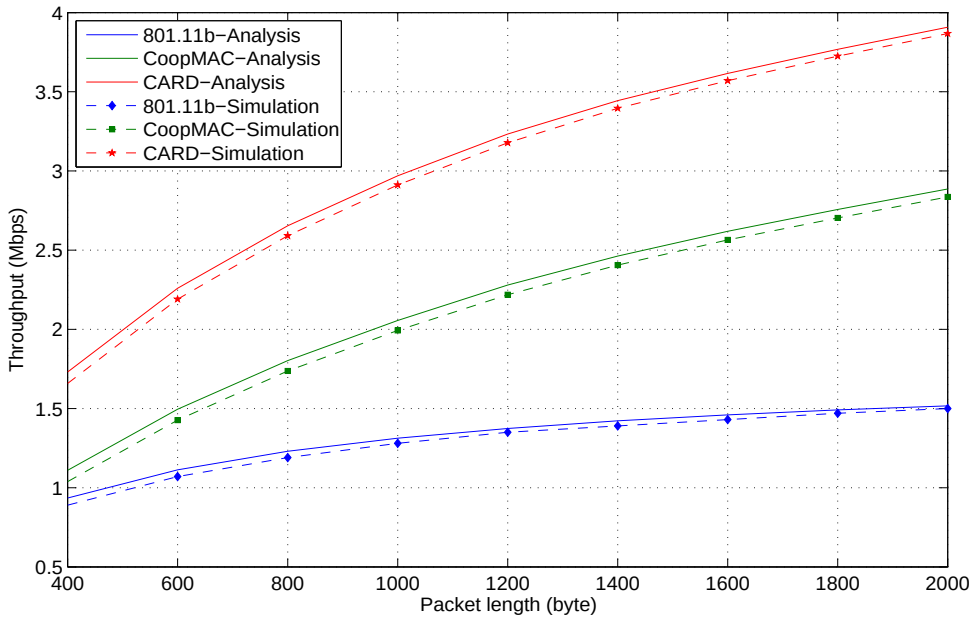

Figure 4.8: Throughput versus packet length under ideal channel, N=30 nodes.

that as the packet length increases, the probability of packet error rate also increases, and hence the number retransmission retries increases. As a result, the throughput is degraded as the packet length increases. As show also in Fig. 4.9(b), as the packet length increases the throughput increases until the packet length becomes around 1200 byte, after that the throughput decreases as the packet length increases. As the packet length increases, the throughput increases and also the packet error rate also increases, and then the throughput decreases. For this reason, the throughput improvement is reduced by the packet error as the packet length increases. Under all the channel conditions, the CARD protocol outperforms the CoopMAC protocol.

The throughput versus number of nodes under ideal channel conditions of both BTAC and CARD protocols is shown in Fig. 4.10. The CARD protocol outperforms the BTAC protocol, since the throughput of the CARD

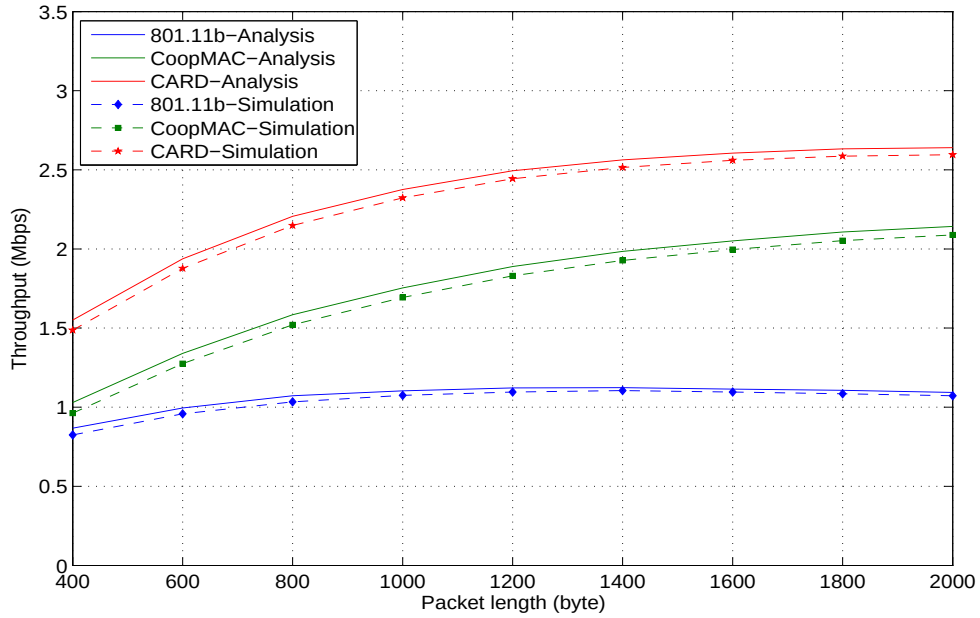

(a) Throughput vs. packet length at $BER = 2 * 10^{-5}$.

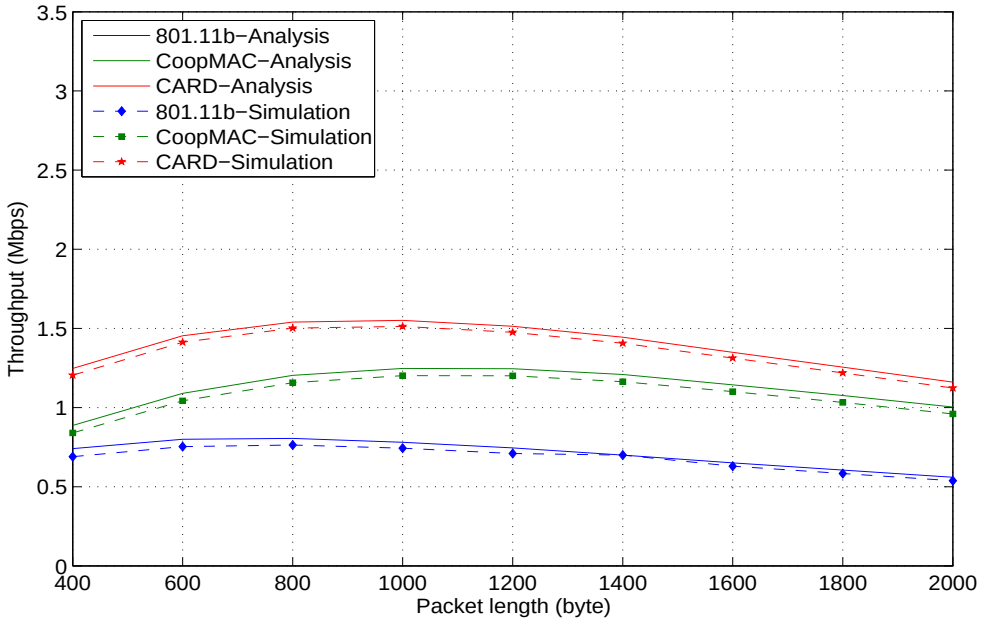

(b) Throughput vs. packet length at $BER = 6 * 10^{-5}$.

Figure 4.9: Throughput vs. packet length under imperfect channel, N=30.

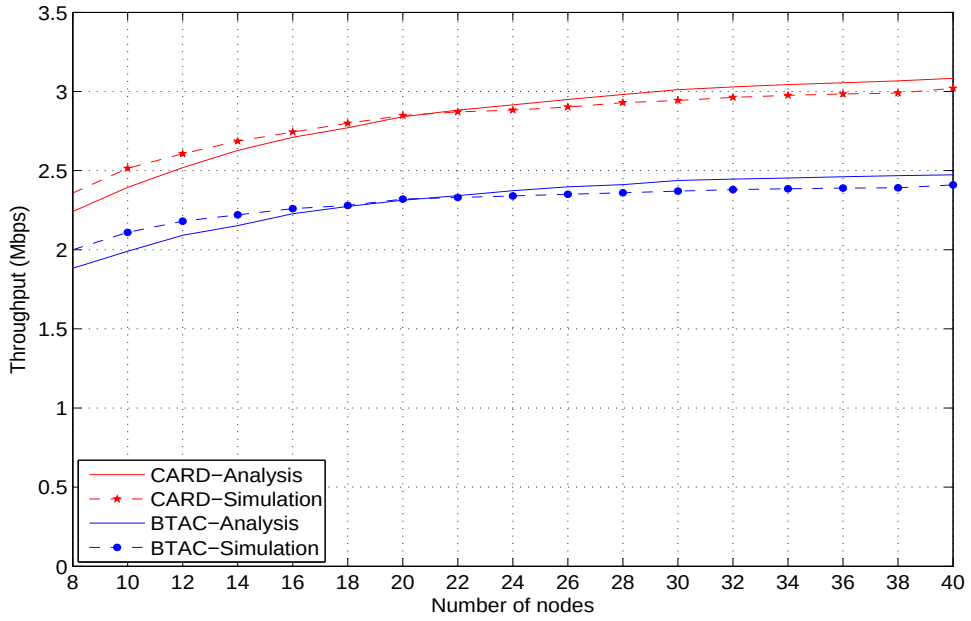

Figure 4.10: Throughput versus number of nodes under ideal channel, L=1024 byte.

protocol is up to 25% higher than the BTAC protocol.. This is because the CARD protocol achieves both cooperative diversity gain and cooperative multiplexing gain. The relay node shares the handshake procedure between a source node and the AP and transmits its own data immediately after forwarding the source station's information to the AP. On the contrary, the BTAC protocol achieves only cooperative diversity gain; where the relay node forwards only the information of the source node to the AP.

4.3.2 Energy Efficiency Results

The Energy efficiency is considered as one of the most critical requirements to design an efficient MAC protocol. Fig. 4.11 compare the energy efficiency of the 802.11b, CoopMAC, and CARD protocols under ideal channel conditions and a fixed packet length at 1024 byte. The

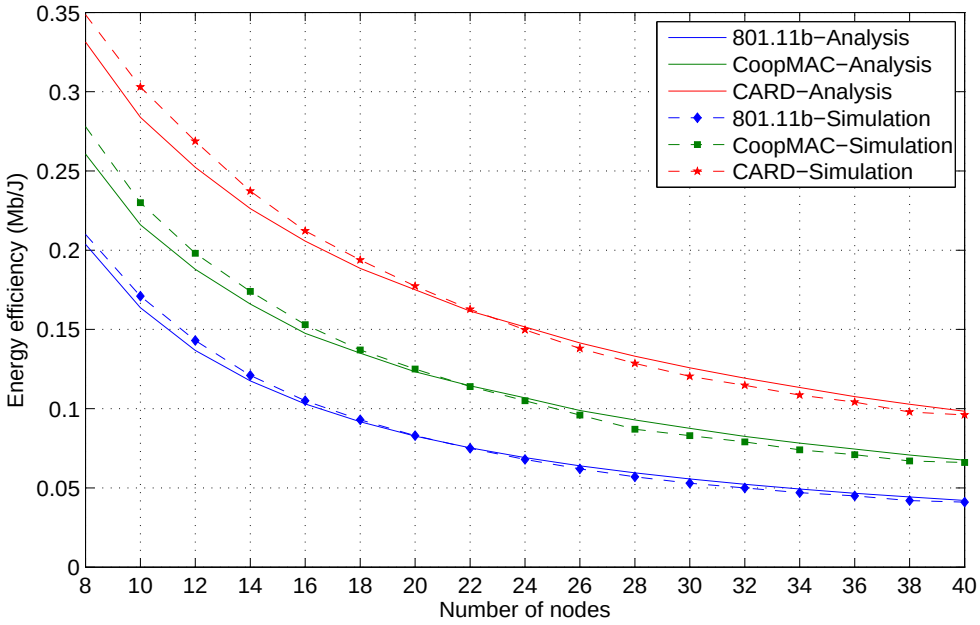

Figure 4.11: Energy efficiency vs. number of nodes under ideal channel, L=1024 bytes.

CARD protocol outperforms both the 802.11b and CoopMAC protocols. Since the energy efficiency of the CARD protocol is up to 30% and up to 80% higher than the CoopMAC and 802.11b protocols, respectively. As shown in Fig. 4.11, when the number of nodes increases, the energy efficiency decreases. The energy efficiency decreases as the number of node increases due to increasing the probability of collisions. Whereas the number of retransmissions increases as the collision probability increases. Hence, a node consumes more energy on the retransmission, receiving, overhearing, and sensing the medium.

The effect of the medium status on the energy efficiency versus the number of nodes is shown in Fig. 4.12 at a fixed packet length 1024 byte. As the medium becomes worst, the energy efficiency of the 802.11b, CoopMAC, and CARD protocols decreases, where the number of retransmission retries increases and a node consumes more energy on the retransmission,

overhearing, receiving, and sensing the medium. The CARD protocol is better than the 802.11b and CoopMAC protocols under different channel conditions. The CARD at $BER = 6 \times 10^{-5}$, shown in Fig. 4.12(b) has energy efficiency higher than that of the CoopMAC protocol at $BER = 2 \times 10^{-5}$ shown in Fig. 4.12(a). Therefore, the CARD protocol is more reliable than the CoopMAC protocol against the channel conditions.

The effect of packet length on the energy efficiency at a fixed number of nodes (30 nodes) is studied in Fig. 4.13 and Fig. 4.14 under ideal and imperfect channel conditions, respectively. As the packet size increases, the energy efficiency of the 802.11, CoopMAC, and CARD protocols increases. The reason is that the overhead including the PLCP header and control frames is reduced when the packet length increases. Therefore, more energy is saved, and the energy efficiency is then increases. The energy efficiency decreases as the channel becomes poor. This is because the number retransmissions increases and a node consumes more energy to deliver its data packets to the AP. Consequently, the energy efficiency decreases. As shown in Fig. 4.14, the energy efficiency of the CARD protocol at $BER = 6 \times 10^{-5}$ shown in Fig. 4.12(b) is approximately equal to the energy efficiency of the CoopMAC protocol at the ideal channel conditions.

Fig. 4.15 compare the energy efficiency of both BTAC and CARD protocols under ideal channel conditions and a fixed packet length at 1024 byte. The CARD protocol outperforms BTAC protocol. Since the energy efficiency of the CARD protocol is up to 20% higher than the BTAC protocol.

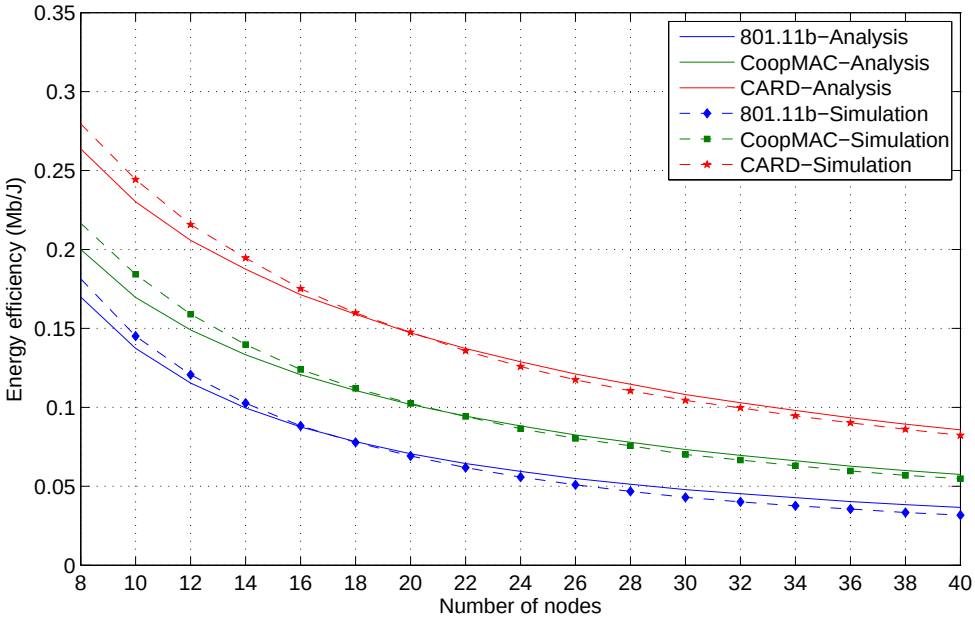

(a) Energy vs. number of nodes at $BER = 2 * 10^{-5}$.

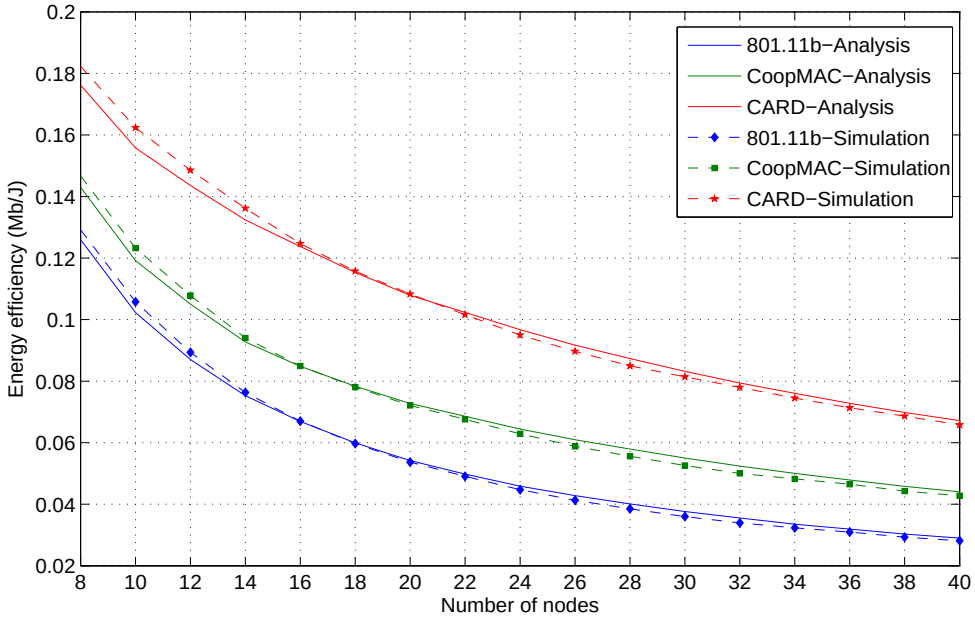

(b) Energy vs. number of nodes at $BER = 6 * 10^{-5}$.

Figure 4.12: Energy vs. number of nodes under imperfect channel, L=1024 byte.

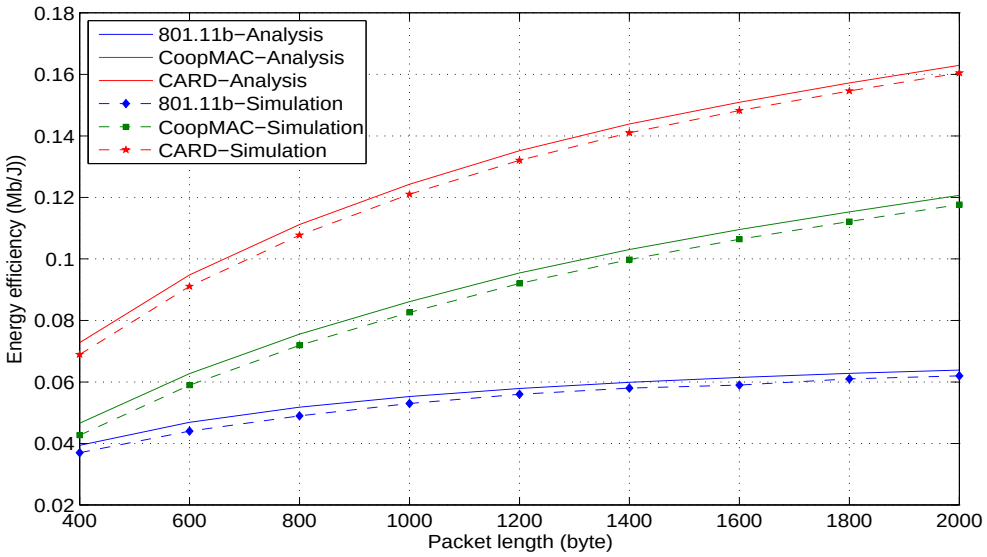

Figure 4.13: Energy efficiency vs. packet length under ideal channel, N=30.

4.3.3 Delay Results

The improvement in system throughput also transforms into a better a packet delay performance. The relation between the service delay and the number of nodes for a successful packet transmission and a fixed packet length (1024 byte) is shown in Fig. 4.16. As the number of nodes increases, the service delay also increases. This is due to the collision probability increases as the number of node increases, and hence the number of retries increases. As a result, the service delay which is the time required to deliver the packet to the AP increases. However, the service delay for the CARD protocol is substantially lower than that for both the 802.11b MAC and CoopMAC protocols under ideal channel conditions. As shown in Fig. 4.16, the service delay of the CARD protocol is up to 150% and up to 50% less than the service delay of the 802.11b and CoopMAC protocols, respectively. This is because the CARD protocol achieves both cooperative diversity gain and cooperative multiplexing gain. On the con-

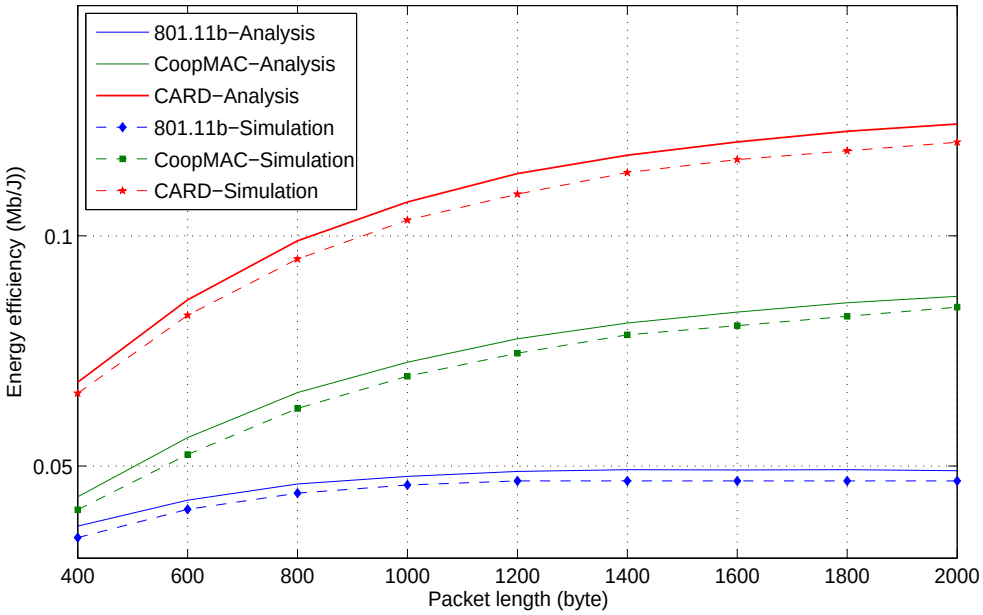

(a) Energy vs. packet length at $BER = 2 * 10^{-5}$.

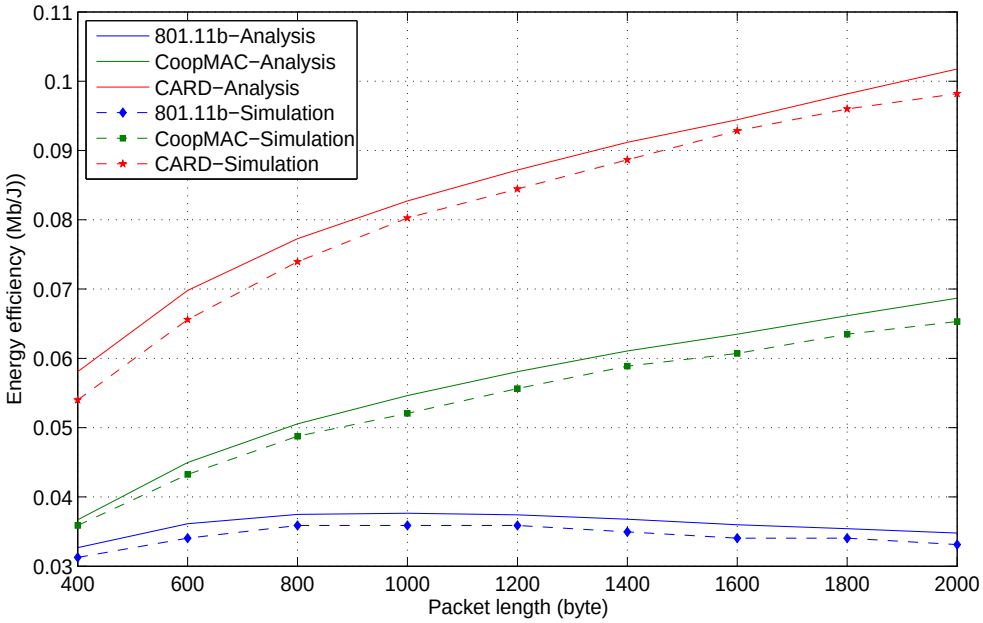

(b) Energy vs. packet length at $BER = 6 * 10^{-5}$.

Figure 4.14: Energy vs. packet length under imperfect channel, N=30.

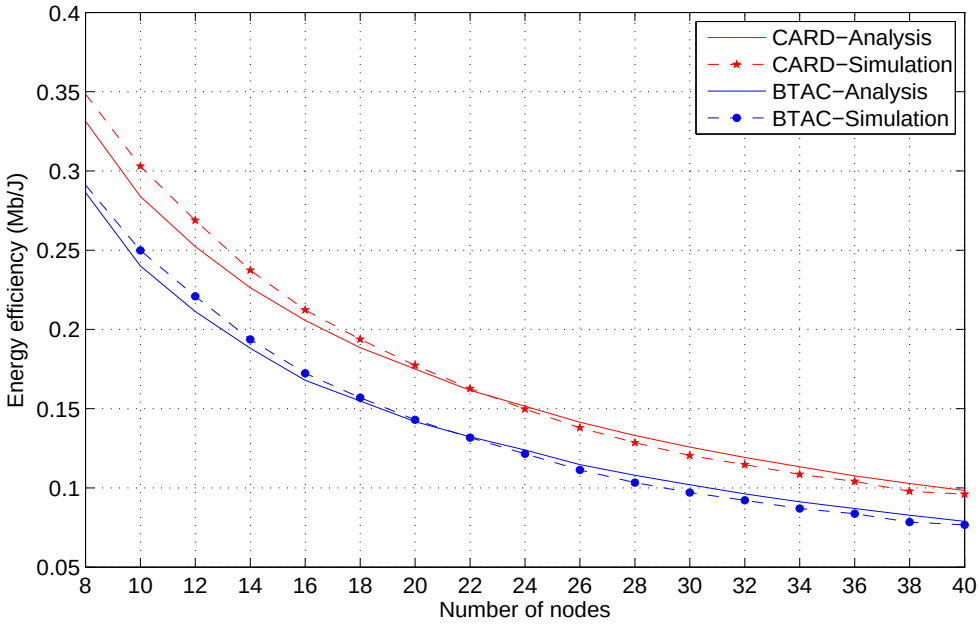

Figure 4.15: Energy efficiency versus number of nodes under ideal channel, L=1024 byte.

trary, the CoopMAC protocol achieves only cooperative diversity gain.

Fig. 4.17 illustrates the service delay of the 802.11b, CoopMAC, and CARD protocols versus the number of nodes under dynamic channel conditions and a fixed packet length which is 1024 byte. As the medium quality becomes poor, the service delay of the three protocols increases but with different values. The reason is that the number of retransmission retries increases not only due to increasing the collision probability as the number of node increases, but also due to increasing the packet error rate as the medium quality becomes poor. Consequently, the service delay increases as the channel condition becomes poor. The service delay of CARD protocol is lower than the service delay of both the 802.11b and the CoopMAC protocols under the imperfect channel conditions.

The effect of packet length on the service delay under ideal and imperfect channel conditions is given in Fig. 4.18 and Fig. 4.19 for a fixed

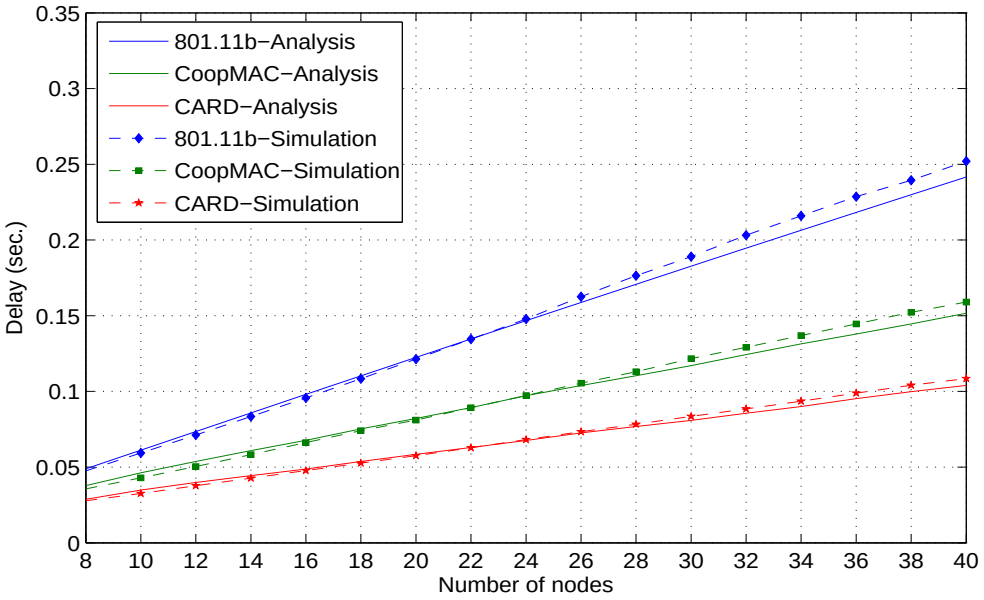

Figure 4.16: Service delay vs. number of nodes under ideal channel, L = 1024 bytes.

number of nodes which is 30 nodes. As the packet length increases, the service delay of the three protocols increases. The reason is that the transmission time increases as the packet length increases, and hence the service delay increases. The service delay of the CARD protocol is lower than that the service delay of both the 802.11b and CoopMAC protocols under different channel conditions.

The relation between the service delay and the number of nodes for a successful packet transmission and a fixed packet length (1024 byte) is shown in Fig. 4.20. The service delay for the CARD protocol is substantially lower than that for both the BTAC protocol under ideal channel conditions. As shown in Fig. 4.20, the service delay of the CARD protocol is up to 32% less than the service delay of the BTAC protocol. This is because the CARD protocol achieves both cooperative diversity gain and cooperative multiplexing gain. On the contrary, the BTAC protocol achieves only

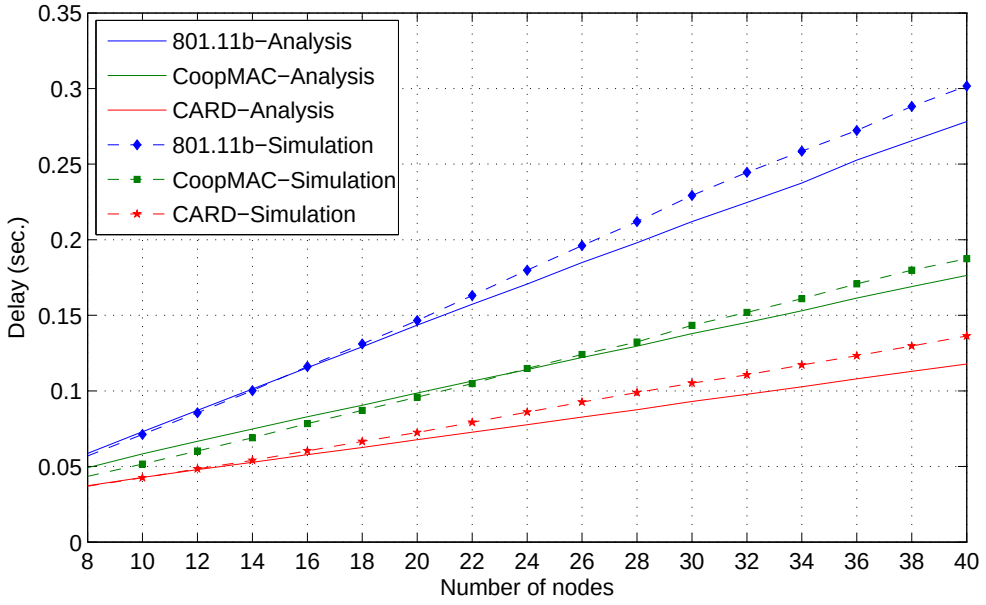

(a) Delay vs. number of nodes at $BER = 2 * 10^{-5}$.

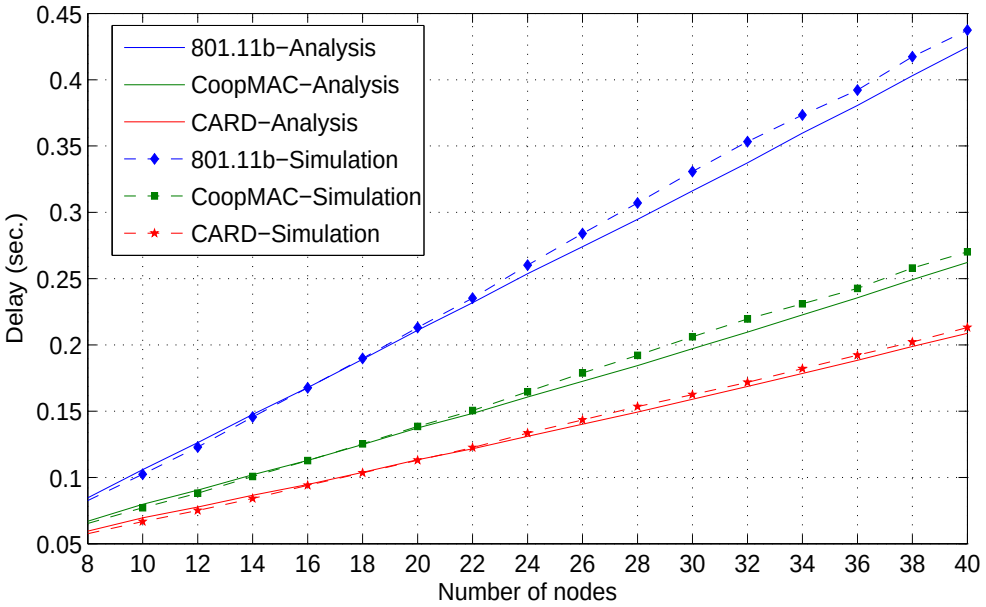

(b) Delay vs. number of nodes at $BER = 6 * 10^{-5}$.

Figure 4.17: Delay vs. number of nodes under imperfect channel, L=1024 byte.

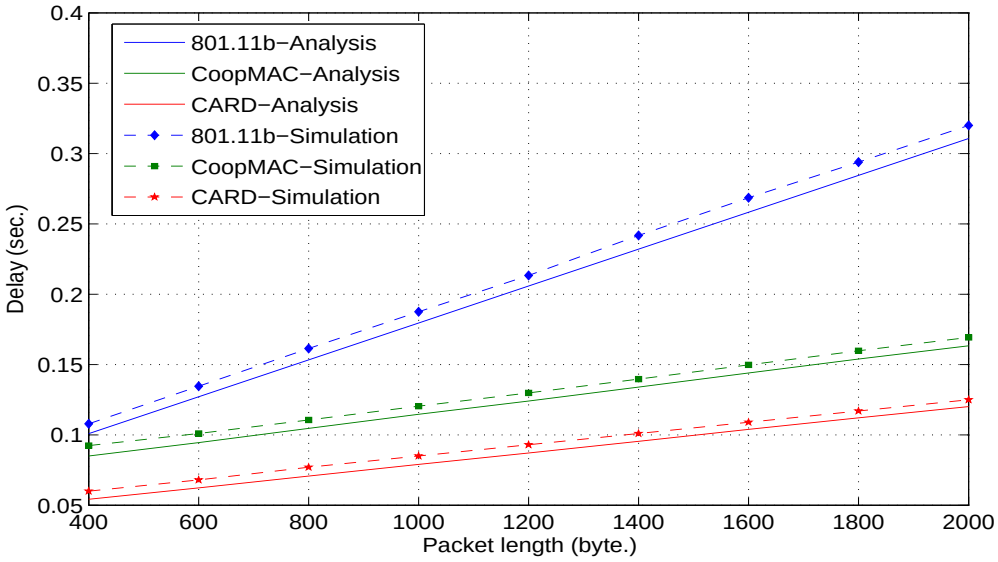

Figure 4.18: Service delay vs. packet length under ideal channel, N=30.

cooperative diversity gain.

4.4 Conclusions

In this chapter, we propose a new MAC protocol, called Cooperative Access with Relay's Data (CARD) for multi-rate WLANs. CARD uses the best relay node to improve the overall transmission rate for low data-rate nodes. More importantly, CARD enables a relay node to transmit its own data packet without the handshake procedure for accessing the channel. In doing so, CARD for first time provides a novel transmission mechanism for the relay node and therefore can achieve both cooperative diversity gain and multiplexing gain. Compared with the IEEE 802.11b standard, the signalling changes and overheads in CARD are minimum, thus making CARD fully compatible with the IEEE 802.11b standard and suitable for coexisting with the standard DCF protocols.

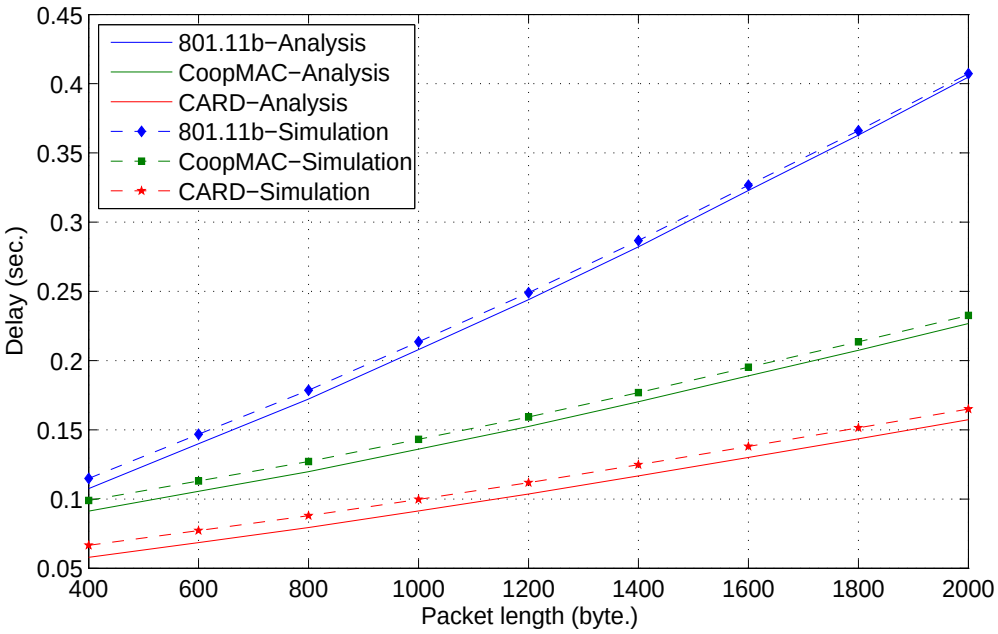

(a) Delay vs. packet length at $BER = 2 * 10^{-5}$.

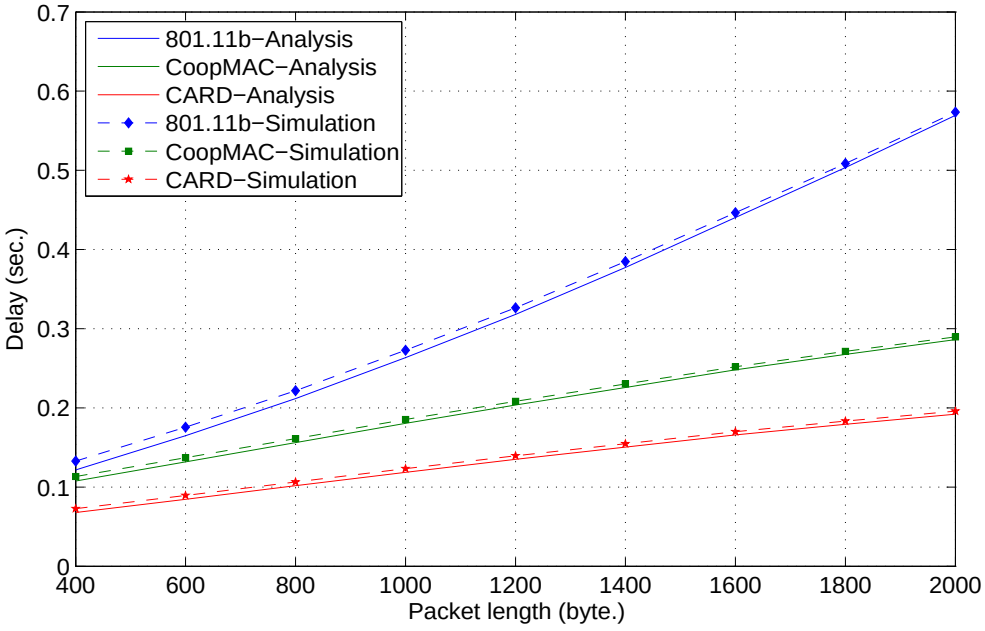

(b) Delay vs. packet length at $BER = 6 * 10^{-5}$.

Figure 4.19: Delay vs. packet length under imperfect channel, N=30.

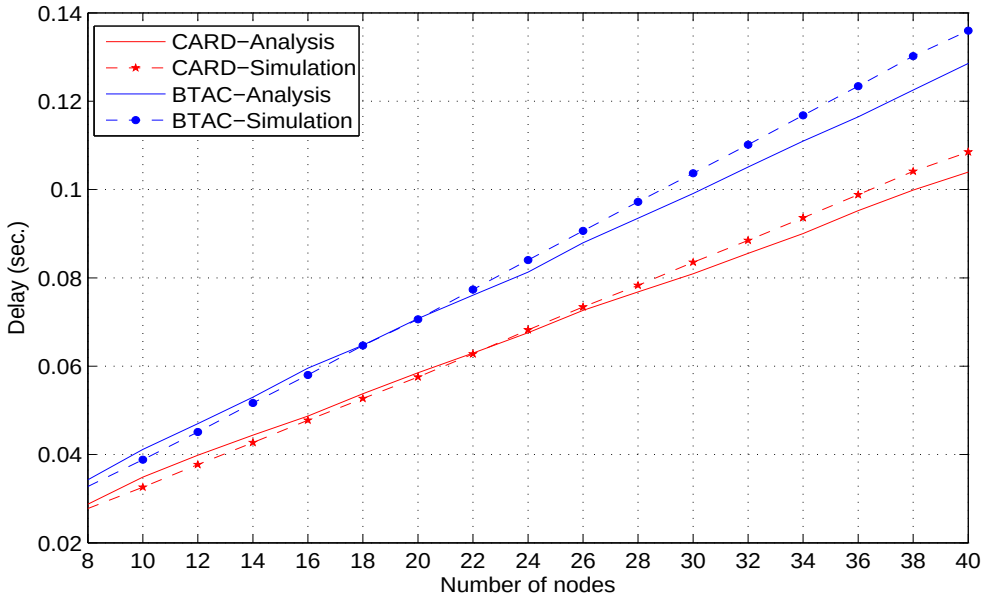

Figure 4.20: Delay versus number of nodes under ideal channel, L=1024 byte.

A new cross-layer analytical approach is developed to evaluate the performance of CARD under dynamic wireless channel conditions. Analytical and simulation results show that, compared with other cooperative MAC protocols, under the CARD protocol the overall system throughput, service delay, and energy efficiency can be significantly improved under different channel conditions. Since the throughput achieved by the CARD protocol is up to 155% more than the 802.11b throughput, is up to 35% more than the CoopMAC throughput, and is up to 25% more than the BTAC throughput under ideal channel conditions. In addition the throughput of the CARD protocols is close to the maximum throughput (which is 5 Mbps) that can be achieved when all of the nodes are running at the maximum transmission rate, i.e. 11 Mbps. On the other hand, the service delay of the CARD protocol is up to 150%, up to 50%, and up to 32% less than the service delay of the 802.11b, CoopMAC, and BTAC protocols, re-

spectively under ideal channel conditions. The energy efficiency of the CARD protocol under ideal channel conditions is up to 20%, up to 30%, and up to 80% higher than the BTAC, the CoopMAC, and 802.11b protocols, respectively. The CARD protocol achieves better throughput, service delay, and energy efficiency than the CoopMAC protocol under imperfect channel conditions. As a result, the CARD protocol is more reliable than the CoopMAC protocol under dynamic channel conditions.

Chapter 5

Unsaturated Analysis of Cooperative MAC protocols

In chapters 3 and 4 both the BTAC and CARD protocols are studied assuming saturated conditions, i.e. each node always has a packet waiting for transmission. The studies on saturated conditions are essential for gaining insights into the behavior of both protocols. However, the saturated assumption is impractical for networks providing real-time applications such as web, email and voice. In such cases, a saturated assumption is not appropriate (150–152). Therefore, the aim of this chapter is to propose a mathematical model for both the BTAC and the standard IEEE 802.11 protocols under unsaturated conditions.

The remainder of the chapter is organized as follows. Section 5.1 presents the proposed Markov chain model for the unsaturated conditions. Throughput, energy efficiency, and delay analysis are given in Section 5.2. In Section 5.3 the analytical model is validated using OMNET++ (148) simulations. Finally, some conclusion remarks are given in Section 5.4.

5.1 Non-saturated Markov Chain model

The Markov chain model given in (Sec. 4.2.2, pp. 133) is modified to study the behaviour of the DCF under the assumption of unsaturated conditions, error free channel, and multi-rate transmissions. Under the IEEE 802.11 standard, it is mandatory that the backoff mechanism is performed after each successful transmission even if there is no other MAC Service Data Unit (MSDU) to be transmitted. This referred to as "post-backoff". The post-backoff guarantees that there is always at least one backoff interval preceding a packet transmission. Alternatively, there is an exception to the essential rule that an MSDU from the upper layer has to be transmitted after performing the backoff mechanism. The MSDU arriving from the upper layer may be transmitted immediately without waiting any time if the transmission queue is empty, the latest post-backoff is finished, and at the same time the channel has been idle for at least one DCF interval. In the proposed model this exceptional case and the unsaturated traffic conditions are taken into account by introducing a new state (idle state) labelled $(0, -1, 0)$ explained later.

Let m' be the maximum number of retransmissions using different contention window (CW) size. Let m be the maximum number of retries after which the packet is discarded even if it is not received correctly. Let $s(t)$ be a random process representing the backoff stage j at time t, where $0 \leq j \leq m$. Let $b(t)$ be a stochastic process representing the value of the backoff counter for a given node at time t. The value of the backoff

counter is uniformly chosen from $[0, W_j - 1]$; W_j is given as follows (1):

$$W_j = \begin{cases} 2^j W_0 & j \leq m' \\ 2^{m'} W_0 & j > m' \end{cases} \tag{5.1}$$

The third dimension $u(t)$ specify the remaining time during a successful transmission, a collision transmission, and a frozen transmission. As shown in Fig. 5.1, the three dimensional process $\{s(t), b(t), u(t)\}$ is a discrete-time Markov chain under assumption that the collision probability $P_{c,i}$ and the probability $P_{b,i}$, that the channel is busy are independent. It is referred to a generic node with index $i \in S = \{S^d \cup S_1^c \cup S_2^c\}$; where S^d is the set of nodes that employ a single-hop transmission, S_1^c is the set of nodes at rate 1 Mbps and employing a two-hop transmission, and S_2^c is the set of nodes at rate 2 Mbps and employing a two-hop transmissions. The details of these sets are given in Appendix A. The state of each node can be described by $\{j, k, \ell\}$. j is the backoff stage, $j = 0, 1, ..., m$, and $j = -1$ represents a successful transmission stage. k is the backoff counter taking values from $[0, W_{j-1}]$ in time slots, and $k = -1$ stands for idle state (i.e. empty queue) during the backoff stage 0. The third index ℓ specifies the following:

- The remaining time for the successful transmission states

$$(-1, 0, \ell) \quad 1 \leq \ell \leq N_{s,i}$$

- The remaining time for the collision transmission states

$$(j, 0, \ell) \quad 1 \leq \ell \leq N_{c,i} \quad 0 \leq j \leq m$$

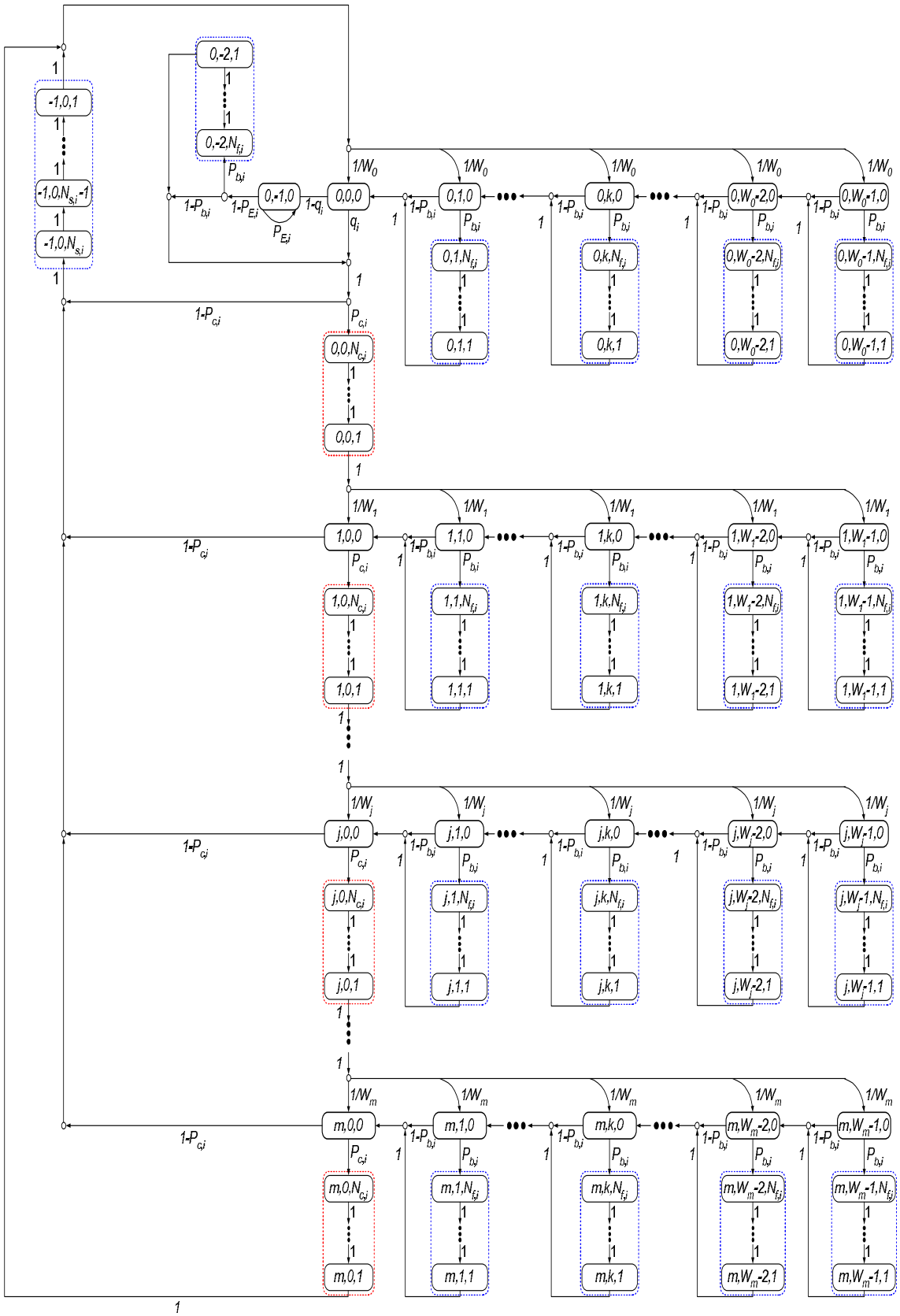

Figure 5.1: Unsaturated Markov chain model.

- The remaining time for the frozen transmission period states

$$(j, k, \ell), \quad 1 \leq \ell \leq N_{f,i} \quad 1 \leq k \leq W_j - 1 \quad 0 \leq j \leq m$$

$$(0, -1, \ell), \quad 1 \leq \ell \leq N_{f,i}$$

where $N_{s,i}$, $N_{c,i}$, and $N_{f,i}$ stand for a successful transmission period, a collision transmission period, and a frozen transmission period in a slot time units, respectively.

5.1.1 Transition Probabilities

In this model the one step transition probabilities are expressed as follows:

1. At the beginning of each slot time, the backoff counter freezes for $N_{f,i}$ slots when the channel becomes busy.

$$P_r\{j, k, N_{f,i} | j, k, 0\} = P_{b,i} \qquad 1 \leq k \leq W_j - 1 \quad 0 \leq j \leq m$$

2. The node suspends its transmission for $N_{f,i}$ slots during a busy channel while the node resides in the idle state and at least one packet arrives with probability $1 - P_{E,i}$

$$P_r\{0, -1, N_{f,i} | 0, -1, 0\} = P_{b,i}(1 - P_{E,i})$$

3. During the frozen period, the counter decreases by one for each slot

time.

$$P_r\{j,k,\ell-1|j,k,\ell\}=1 \qquad 2\leq\ell\leq N_{f,i} \quad 0\leq k\leq W_j-1 \quad 0\leq j\leq m$$

$$P_r\{0,-1,\ell-1|0,-1,\ell\}=1 \qquad 2\leq\ell\leq N_{f,i}$$

4. At the end of the frozen period, the node reactivities its backoff counter.

$$P_r\{j,k-1,0|j,k,1\}=1 \qquad 1\leq k\leq W_j-1 \quad 0\leq j\leq m$$

5. The node accesses the medium at the end of the frozen interval of the idle state after receiving at least one packet from the upper layer. The transmission is successful if there is no other node tries to transmit.

$$P_r\{-1,0,N_{s,i}|0,-1,1\}=1-P_{c,i}$$

6. If the node's buffer is not empty, the transmission is unsuccessful due to a collision with other nodes at the end of the frozen period.

$$P_r\{0,0,N_{c,i}|0,-1,1\}=P_{c,i}$$

7. The node stays in the idle state if the buffer is empty.

$$P_r\{0,-1,0|0,-1,0\}=P_{E,i}$$

8. If the channel is idle and there is at least one packet arrival during

the idle state, the transmission is unsuccessful due to a collision.

$$P_r\{0, 0, N_{c,i}|0, -1, 0\} = (1 - P_{E,i})(1 - P_{b,i})P_{c,i}$$

9. During the idle state if there is at least one packet arrival from the upper layer and the channel becomes idle, the transmission is successful when other nodes are listening.

$$P_r\{0, 0, N_{s,i}|0, -1, 0\} = (1 - P_{E,i})(1 - P_{b,i})(1 - P_{c,i})$$

10. When the backoff counter reaches zero in stage 0, the node inters the idle state if its buffer is empty.

$$P_r\{0, -1, 0|0, 0, 0\} = 1 - q_i$$

11. The transmission is successful at the end of stage 0 if the channel is idle and the buffer is not empty.

$$P_r\{-1, 0, N_{s,i}|0, 0, 0\} = q_i(1 - P_{c,i})$$

12. When the node's buffer is not empty at the end of backoff stage 0, the transmission is unsuccessful due to a collision with other nodes.

$$P_r\{0, 0, N_{c,i}|0, 0, 0\} = q_i P_{c,i}$$

13. The backoff counter is decrementing when the channel is sensed idle.

$$P_r\{j, k-1, 0|j, k, 0\} = 1 - P_{b,i} \qquad 1 \leq k \leq W_j - 1 \quad 0 \leq j \leq m$$

14. When the backoff counter reaches zero and no other node tries to transmit, the transmission is successful.

$$P_r\{-1, 0, N_{s,i}|j, 0, 0\} = 1 - P_{c,i} \qquad 1 \leq j \leq m$$

15. During a successful transmission interval the counter decreases by one for each slot time.

$$P_r\{-1, 0, \ell - 1| - 1, 0, \ell\} = 1 \qquad 2 \leq \ell \leq N_{s,i}$$

16. A new backoff delay of stage 0 is selected after the successful transmission.

$$P\{0, k, 0| - 1, 0, 1\} = \frac{1}{W_0} \qquad 0 \leq k \leq W_0 - 1$$

17. When an unsuccessful transmission occurs due to a collision, the node inters the unsuccessful interval.

$$P_r\{j, 0, N_{c,i}|j, 0, 0\} = P_{c,i} \qquad 1 \leq j \leq m$$

18. During the unsuccessful transmission period the counter decreases by one for each slot time.

$$P\{j, 0, \ell - 1|j, 0, \ell\} = 1 \qquad 0 \leq j \leq m \quad 2 \leq \ell \leq N_{c,i}$$

19. After the counter of unsuccessful transmission period reaches zero,

the node doubles the contention window and inters the next backoff stage.

$$P_r\{j+1,k,0|j,0,1\} = \frac{1}{W_{j+1}} \qquad 0 \leq j \leq m-1$$

20. If there is an unsuccessful transmission after m retries, the current packet is discarded and the node starts a new packet transmission at the end of the unsuccessful transmission period.

$$P_r\{0,k,0|m,0,1\} = \frac{1}{W_0} \qquad 0 \leq k \leq W_0 - 1$$

where q_i is the probability that there is at least one packet waiting for transmission in the queue of the generic node i after completing the post-backoff of a pervious transmission. At the idle state (i.e. empty queue), $P_{E,i}$ is the probability that the generic node i stays in the idle state until at least one packet arrives from the upper layer.

5.1.2 System Equations

Let $\pi_{j,k,\ell} = lim_{t\to\infty} P\{s(t) = j, b(t) = k, u(t) = \ell\}$ be the stationary distribution of the model. In the steady state, the following equations hold for the Markov chain model given in Fig. 5.1.

$$\begin{aligned} \pi_{0,-1,1} &= P_{b,i}(1 - P_{E,i})\pi_{0,-1,0} \\ (1 - P_{E,i})\pi_{0,-1,0} &= (1 - q_i)\pi_{0,0,0} \end{aligned} \tag{5.2}$$

From which, we have:

$$\pi_{0,-1,1} = P_{b,i}(1 - q_i)\pi_{0,0,0} \tag{5.3}$$

From the model we also have:

$$\pi_{0,0,N_{c,i}} = P_{c,i}\Big[q_i\pi_{0,0,0} + (1-P_{b,i})(1-P_{E,i})\pi_{0,-1,0} + \pi_{0,-1,1}\Big] \tag{5.4}$$

By substituting equations (5.2) and (5.3) into equation (5.4) we have:

$$\pi_{0,0,N_{c,i}} = P_{c,i}\pi_{0,0,0} \tag{5.5}$$

where

$$\pi_{j,0,\ell} = \pi_{j,0,N_{c,i}} \qquad 0 \le j \le m \quad 1 \le \ell < N_{c,i} \tag{5.6}$$

and

$$\pi_{1,0,0} = \pi_{0,0,1} \tag{5.7}$$

Substituting equations (5.5) and (5.6) into equation (5.7), we have:

$$\pi_{1,0,0} = P_{c,i}\pi_{0,0,0} \tag{5.8}$$

Thus, we have:

$$\pi_{j,0,0} = P_{c,i}\cdot\pi_{j-1,0,0} \quad \rightarrow \quad \pi_{j,0,0} = P_{c,i}^{j}\pi_{0,0,0} \qquad 0 \le j \le m \tag{5.9}$$

Due to the regularities of the Markov chain, thus for each $1 \le k \le$

$W_j - 1$, all the following relations hold:

$$\pi_{j,k,0} = \frac{W_j - k}{W_j} \begin{cases} (1 - P_{c,i}) \sum_{x=0}^{m} \pi_{x,0,0} + P_{c,i}\pi_{m,0,0} & j = 0 \\ P_{c,i}\pi_{j-1,0,0} & 0 < j \leq m \end{cases} \tag{5.10}$$

By substituting equation (5.9) into equation (5.10), and using $\sum_{x=0}^{m} \pi_{x,0,0} = \frac{\pi_{0,0,0}(1-P_{c,i}^{m+1})}{1-P_{c,i}}$, equation (5.10) is rewritten as follows:

$$\pi_{j,k,0} = \frac{W_j - k}{W_j} P_{c,i}^{j} \pi_{0,0,0} \qquad 0 \leq j \leq m, \quad 0 \leq k \leq W_j - 1 \tag{5.11}$$

For the third dimension, during the successful transmission interval the following relation is expressed:

$$\pi_{-1,0,\ell} = \sum_{j=0}^{m} (1 - P_{c,i})\pi_{j,0,0} \qquad 1 \leq \ell \leq N_{s,i} \tag{5.12}$$

By substituting equation (5.9) into equation (5.12), we have:

$$\begin{aligned} \pi_{-1,0,\ell} &= \sum_{j=0}^{m} (1 - P_{c,i}) P_{c,i}^{j} \pi_{0,0,0} \\ &= (1 - P_{c,i}^{m+1})\pi_{0,0,0} \qquad 1 \leq \ell \leq N_{s,i} \end{aligned} \tag{5.13}$$

Du to the collision transmission, we have:

$$\pi_{j,0,\ell} = P_{c,i}\pi_{j,0,0} \qquad 1 \leq \ell \leq N_{c,i} \quad 0 \leq j \leq m \tag{5.14}$$

Due the frozen transmission and the node has a packet ready for

transmission, we have:

$$\pi_{j,k,\ell} = P_{b,i}\pi_{j,k,0} \qquad 1 \leq \ell \leq N_{f,i} \quad 1 \leq k \leq W_j - 1 \quad 0 \leq j \leq m \tag{5.15}$$

On the other hand, if the node's buffer is empty and at least one packet arrives from the upper layer, and at the same time the channel becomes busy, we have:

$$\begin{aligned} \pi_{0,-1,\ell} &= P_{b,i}(1 - P_{E,i})\pi_{0,-1,0} \\ &= P_{b,i}(1 - q_i)\pi_{0,0,0} \qquad\qquad 1 \leq \ell \leq N_{f,i} \end{aligned} \tag{5.16}$$

Thus, $\pi_{j,k,\ell}$ can be expressed as a function of $\pi_{0,0,0}$. By imposing the normalization condition for the stationary distribution, $\pi_{0,0,0}$ is calculated as follows:

$$1 = \sum_{\ell=1}^{N_{s,i}} \pi_{-1,0,\ell} + \sum_{\ell=0}^{N_{f,i}} \pi_{0,-1,\ell} + \sum_{j=0}^{m} \sum_{\ell=0}^{N_{c,i}} \pi_{j,0,\ell} + \sum_{j=0}^{m} \sum_{k=1}^{W_j-1} \sum_{\ell=0}^{N_{f,i}} \pi_{j,k,\ell} \tag{5.17}$$

From equation (5.13) and the first term on the R.H.S. of equation (5.17), we have:

$$\begin{aligned} \sum_{\ell=1}^{N_{s,i}} \pi_{-1,0,\ell} &= \sum_{\ell=1}^{N_{s,i}} (1 - P_{c,i}^{m+1})\pi_{0,0,0} \\ &= N_{s,i}(1 - P_{c,i}^{m+1})\pi_{0,0,0} \end{aligned} \tag{5.18}$$

From equations (5.2) and (5.16), and the second term on the R.H.S. of equation (5.17), we have:

$$\sum_{\ell=0}^{N_{f,i}} \pi_{0,-1,\ell} = \sum_{\ell=1}^{N_{f,i}} \pi_{0,-1,\ell} + \pi_{0,-1,0}$$
$$= \frac{1-q_i}{1-P_{E,i}} \Big[N_{f,i} P_{b,i} (1-P_{E,i}) + 1 \Big] \pi_{0,0,0} \tag{5.19}$$

From equation (5.14), the third term on the R.H.S. of equation (5.17) can be expressed as follows:

$$\begin{aligned} \sum_{j=0}^{m} \sum_{\ell=0}^{N_{c,i}} \pi_{j,0,\ell} &= \sum_{j=0}^{m} \Big[\sum_{\ell=1}^{N_{c,i}} P_{c,i} \pi_{j,0,0} + \pi_{j,0,0} \Big] \\ &= \sum_{j=0}^{m} (1 + N_{c,i} P_{c,i}) \pi_{j,0,0} \\ &= \frac{1 - P_{c,i}^{m+1}}{1 - P_{c,i}} (1 + N_{c,i} P_{c,i}) \pi_{0,0,0} \end{aligned} \tag{5.20}$$

From equation (5.15), the fourth term on the R.H.S. of equation (5.17) can be calculated as follows:

$$\begin{aligned} \sum_{j=0}^{m} \sum_{k=1}^{W_j - 1} \sum_{\ell=0}^{N_{f,i}} \pi_{j,k,\ell} &= \sum_{j=0}^{m} \sum_{k=1}^{W_j - 1} \Big[\sum_{\ell=1}^{N_{f,i}} P_{b,i} \pi_{j,k,0} + \pi_{j,k,0} \Big] \\ &= \sum_{j=0}^{m} \sum_{k=1}^{W_j - 1} (1 + N_{f,i} P_{b,i}) \pi_{j,k,0} \end{aligned} \tag{5.21}$$

Substituting equation (5.11) into equation (5.21), we have:

$$\begin{aligned} \sum_{j=0}^{m} \sum_{k=1}^{W_j - 1} \sum_{\ell=0}^{N_{f,i}} \pi_{j,k,\ell} &= (1 + N_{f,i} P_{b,i}) \sum_{j=0}^{m} \sum_{k=1}^{W_j - 1} \frac{W_j - k}{W_j} P_{c,i}^{j} \pi_{0,0,0} \\ &= (1 + N_{f,i} P_{b,i}) \pi_{0,0,0} \sum_{j=0}^{m} \frac{W_j - 1}{2} P_{c,i}^{j} \end{aligned} \tag{5.22}$$

By substituting equations (5.18), (5.19), (5.20), and (5.22) into equa-

tion (5.17), we have:

$$\pi_{0,0,0} = \left[(1-P_{c,i}^{m+1})N_{s,i} + \frac{1-q_i}{1-P_{E,i}}\Big(1+(1-P_{E,i})N_{f,i}P_{b,i}\Big) + (1+N_{c,i}P_{c,i})\frac{1-P_{c,i}^{m+1}}{1-P_{c,i}} + (1+N_{f,i}P_{b,i})\sum_{j=0}^{m}\frac{W_j-1}{2}P_{c,i}^{j}\right]^{-1} \tag{5.23}$$

Let τ_i be the probability that the generic node i transmits during a slot time. The node transmits when its backoff counter reaches zero and there is a packet in its queue regardless of the backoff stage. The node accesses the channel also from the idle state when a packet arrives from the upper layer and at the same time the channel is idle. Consequently, we have:

$$\tau_i = \sum_{j=1}^{m}\pi_{j,0,0} + q_i\pi_{0,0,0} + (1-P_{E,i})(1-P_{b,i})\pi_{0,-1,0} + \pi_{0,-1,1} \tag{5.24}$$

From equations (5.4) and (5.5), we have:

$$q_i\pi_{0,0,0} + (1-P_{E,i})(1-P_{b,i})\pi_{0,-1,0} + \pi_{0,-1,1} = \pi_{0,0,0} \tag{5.25}$$

By substituting equation (5.25) into equation (5.24), we have:

$$\tau_i = \sum_{j=0}^{m}\pi_{j,0,0} = \frac{1-P_{c,i}^{m+1}}{1-P_{c,i}}\pi_{0,0,0} \tag{5.26}$$

Substituting equation (5.23) into equation (5.26), τ_i is then calculated as follows:

When $m \leq m'$

$$\tau_i = \frac{2\big(1 - P_{c,i}^{m+1}\big)(1 - 2P_{c,i})}{W_0(1 + N_{f,i}P_{b,i})\big(1 - (2P_{c,i})^{m+1}\big)(1 - P_{c,i}) + \mathcal{A} + \mathcal{B}} \tag{5.27}$$

When $m > m'$

$$\tau_i = \frac{2\big(1 - P_{c,i}^{m+1}\big)(1 - 2P_{c,i})}{W_0(1 + N_{f,i}P_{b,i})\Big[\big(1 - (2P_{c,i})^{m'+1}\big)(1 - P_{c,i}) + \mathcal{C}\Big] + \mathcal{A} + \mathcal{B}} \tag{5.28}$$

where

$$\mathcal{A} = \big(1 - P_{c,i}^{m+1}\big)(1 - 2P_{c,i})\Big[2N_{s,i}(1 - P_{c,i}) + 2(1 + N_{c,i}P_{c,i}) - (1 + N_{f,i}P_{b,i})\Big]$$

$$\mathcal{B} = \frac{2(1 - q_i)(1 - P_{c,i})(1 - 2P_{c,i})}{1 - P_{E,i}}\Big(1 + (1 - P_{E,i})N_{f,i}P_{b,i}\Big)$$

$$\mathcal{C} = 2^{m'}(1 - 2P_{c,i})\big(P_{c,i}^{m'+1} - P_{c,i}^{m+1}\big)$$

Therefore, the transmission probability τ_i can be calculated when the values of W_0, m, m', $N_{c,i}$, $N_{f,i}$, $N_{s,i}$, $P_{b,i}$, $P_{E,i}$, q_i, and $P_{c,i}$ are known. The values of W_0, m, m' are known, but the values of $P_{b,i}$, $P_{c,i}$, $N_{s,i}$, $N_{c,i}$, $N_{f,i}$, $P_{E,i}$, and q_i must be calculated. The probability α_k, that the channel is busy due to either a collision transmission or a successful transmission of a node $k \neq i$, is calculated as follows:

$$\begin{aligned} \alpha_k &= (q_k\pi_{0,0,0} + (1 - P_{E,k})(1 - P_{b,k})\pi_{0,-1,0} + \pi_{0,-1,1}) + \sum_{\ell=1}^{N_{c,k}} \pi_{0,0,\ell} \\ &\quad + \sum_{\ell=1}^{N_{s,k}} \pi_{-1,0,\ell} + \sum_{j=1}^{m}\sum_{\ell=0}^{N_{c,k}} \pi_{j,0,\ell} \end{aligned} \tag{5.29}$$

Substituting equation (5.25) into equation (5.29), we have:

$$\begin{aligned}\alpha_k &= \sum_{\ell=1}^{N_{s,k}} \pi_{-1,0,\ell} + \sum_{j=0}^{m}\sum_{\ell=0}^{N_{c,k}} \pi_{j,0,\ell} \\ &= \tau_k\Big[N_{s,k}(1-P_{c,k}) + N_{c,k}P_{c,k} + 1\Big] \end{aligned} \tag{5.30}$$

For the node i, the probability $P_{b,i}$, that the channel is sensed busy when it is occupied by at least one node, is calculated as follows:

$$P_{b,i} = 1 - \prod_{\substack{k=1 \\ k\neq i}}^{N}(1-\alpha_k), \qquad i = 1, 2, ..., N \tag{5.31}$$

The collision probability $P_{c,i}$, that at least one of the $N-1$ remaining nodes and the node i transmit at the same time slot, is expressed as follows:

$$P_{c,i} = 1 - \prod_{\substack{j=1 \\ j\neq i}}^{N}(1-\tau_j), \qquad i = 1, 2, ..., N \tag{5.32}$$

The average number of time slots $N_{c,i}$ that represents the collision period can be expressed as follows:

$$N_{c,i} = \left\lceil \frac{T_c}{\sigma} \right\rceil \tag{5.33}$$

where $\lceil x \rceil$ is the smallest integer larger than x. σ is the slot time size. T_c is the collision time between at least two nodes. The value of T_c depends on the employed MAC protocol. In this chapter the analysis is based on the BTAC protocol. The analysis can be easily extended for the CARD protocol and the other MAC protocols. However, the simulation results in addition to the BTAC protocol can be applied to both the IEEE 802.11b (5)

and the CARD protocols. Therefore, T_c is computed as follows:

$$T_c = T_{MRTS} + T_{CTS} + T_{SIFS} + T_{DIFS} + \delta \tag{5.34}$$

where T_{MRTS}, T_{CTS}, T_{SIFS}, and T_{DIFS} stand for the time duration of MRTS, CTS, SIFS, and DIFS, respectively. δ is the channel propagation delay. The number of time slots $N_{s,i}$, that represents the successful transmission period, is calculated as follows:

$$N_{s,i} = \left\lceil \frac{I(i \in S^d)T^d_{s,i} + I(i \in S^c)T^c_{s,i}}{\sigma} \right\rceil \tag{5.35}$$

where $I(x)$ is 1 if x is true, and is 0 otherwise. $T^d_{s,i}$ and $T^c_{s,i}$ stand for the successful transmission period for a single-hop and a two-hop transmission, respectively. $T^d_{s,i}$ and $T^c_{s,i}$ can be expressed as follows:

$$T^d_{s,i} = T_{RTS} + T_{CTS} + \frac{8L}{R_{sd}} + T_{PLCP} + T_{ACK} + 3T_{SIFS} + T_{DIFS} + 4\delta \tag{5.36}$$

$$\begin{aligned} T^c_{s,i} = {} & T_{MRTS} + T_{CTS} + T_{BTS} + \frac{8L}{R_{sr}} + \frac{8L}{R_{rd}} + 2T_{PLCP} + T_{ACK} + 5T_{SIFS} \\ & + T_{DIFS} + 6\delta \end{aligned} \tag{5.37}$$

where L is the data packet length in octets, R_{sd} is the data-rate between a source node i and the AP. T_{PLCP} is the time duration of the PLCP header, and T_{ACK} is the time duration of the ACK packet. T_{BTS} is the time duration of the Busy-Tone-Signal (BTS). R_{sr} and R_{rd} are the data-rate between the source and the relay and between the relay and the AP, respectively. S^d and S^c are the set of nodes employing a single-hop and a

two-hop transmission, respectively.

The generic node i freezes its backoff counter for $N_{f,i}$ time slots due to collision and successful transmissions of the other $N-1$ nodes under condition that the channel is sensed busy. The average number of slots $N_{f,i}$ can be expressed as follows:

$$N_{f,i} = \left\lceil \frac{T_{f,i}}{\sigma} \right\rceil \tag{5.38}$$

where T_f is the freezing duration during which the backoff counter is frozen, and it is computed as follows:

$$T_{f,i} = E[T_{C_i}] + E[T_{S_i}] \tag{5.39}$$

$E[T_{C_i}]$ and $E[T_{S_i}]$ stand for the average collision duration and the average successful duration under condition that the channel is busy, respectively. Consequently, we have:

$$E[T_{C,i}] = \left[1 - \sum_{\substack{j=1 \\ j \neq i}}^{N} \widehat{P}_{s,j}\right] T_c \tag{5.40}$$

where $\widehat{P}_{s,j}$ is the successful transmission probability of node $j \neq i$ when no other node of the remaining $N-1$ transmits. It is expressed as follows:

$$\widehat{P}_{s,j} = \frac{\prod_{k=1,k\neq j}^{N-1}(1-\alpha_k)}{P_{b,i}} \sum_{\ell=1}^{N_{s,j}} \pi_{-1,0,\ell} = \frac{\prod_{k=1,k\neq j}^{N-1}(1-\alpha_k)}{1 - \prod_{k=1,k\neq i}^{N}(1-\alpha_k)} \cdot N_{s,j}(1-P_{c,j})\tau_j \tag{5.41}$$

The average successful duration $E[T_{S,i}]$ is expressed as follows:

$$E[T_{S,i}] = \sum_{\substack{j=1 \\ j \neq i}}^{N} \widehat{P}_{s,j} \Big[I(j \in S^d) T^d_{s,j} + I(j \in S^c) T^c_{s,j} \Big] \tag{5.42}$$

where $T^d_{s,j}$ and $T^c_{s,j}$ are given in equations (5.36) and (5.37), respectively. The next step is to calculate the values of q_i and $P_{E,i}$. In this chapter, it is assumed that the packet arrivals at each node follow the Poisson process with a mean rate λ packet per second equal for all nodes. Let $E[T_{service,i}]$ is the average MAC service time of the generic node i. The MAC service time is the time interval from the time instant that a packet becomes the head of the queue to the time instant when the post-backoff completed by reaching either the state $(0,0,0)$ or $(-1,0,0)$ if the queue is either busy or empty, respectively. Notice that the service time considers the time either the packet is acknowledged for a successful transmission or the packet is discarded. It is shown in (153) that the exponential distribution is a good approximation model for the MAC layer service time. Consequently, a single node could be represented as an $M/M/1/K$ queuing system, in which K is the maximum queue length. Thus, the probability q_i, that there is at least one packet available at the end of the post-backoff stage, is given as follows (154):

$$q_i = \begin{cases} 1 - \frac{1-\rho_i}{1-\rho_i^{K-1}} & \rho_i < 1 \\ 1 & \rho_i \geq 1 \end{cases} \tag{5.43}$$

where ρ_i is the utilization factor and is given as follows:

$$\rho_i = \lambda E[T_{service,i}] \tag{5.44}$$

This requires knowing the average service time $E[T_{service,i}]$, which is derived in Section 5.2.2. Assuming the packets arrive at the MAC in a Poisson process with rate λ, the probability $P_{E,i}$, that the MAC queue is empty the following generic time slot conditioning that the queue is empty at the beginning of the slot, is calculated as follows:

$$P_{E,i} = P_{b,i}\left[\left(\frac{1}{P_{b,i}} - 1\right)e^{-\lambda\sigma} + \sum_{\substack{j=1 \\ j\neq i}}^{N} \widehat{P}_{s,j} e^{-\lambda T_{s,j}} + \left(1 - \sum_{\substack{j=1 \\ j\neq i}}^{N} \widehat{P}_{s,j}\right)e^{-\lambda T_c}\right] \tag{5.45}$$

5.2 Performance Analysis

In this section the throughput, delay, and energy efficiency are studied under unsaturated conditions. The analysis could be applied to the IEEE 802.11 standard protocols, the BTAC protocol, the CARD protocol, and any other MAC protocols. In this chapter the BTAC protocol is considered.

5.2.1 Throughput Analysis

The throughput S is calculated as follows:

$$\mathrm{S} = \frac{E[PL]}{E[T_I] + E[T_C] + E[T_S]} \tag{5.46}$$

where $E[PL]$ is the average payload size, $E[T_I]$ is the average idle slot duration, $E[T_C]$ is the average collision slot duration, and $E[T_S]$ is the

average successful transmission slot duration

Let P_{tr} be the probability that there is at least one transmission occurs in a randomly chosen time slot. Each node occupies the channel with probability α_i, where $i = 1, 2, ..., N$. P_{tr} is then calculated as follows:

$$P_{tr} = 1 - \prod_{i=1}^{N}(1 - \alpha_i) \tag{5.47}$$

where α_i is given in equation (5.30). Given a transmission on the channel from any node i, the probability $P_{s,i}$, that the transmission is successful, is calculated as follows:

$$\begin{aligned} P_{s,i} &= \sum_{\ell=1}^{N_{s,i}} \pi_{-1,0,\ell} \cdot \prod_{\substack{k=1 \\ k\neq i}}^{N}(1 - \alpha_k) \\ &= N_{s,i}(1 - P_{c,i})\tau_i \cdot \prod_{\substack{k=1 \\ k\neq i}}^{N}(1 - \alpha_k) \end{aligned} \tag{5.48}$$

The average idle slot duration before a transmission takes place is computed as follows:

$$E[T_I] = (1 - P_{tr})\sigma \tag{5.49}$$

where $1 - P_{tr}$ is the probability that the chosen slot time is empty. The average collision slot duration $E[T_C]$ is expressed as follows:

$$E[T_C] = \Big(P_{tr} - \sum_{i=1}^{N} P_{s,i}\Big)T_c \tag{5.50}$$

where T_c is given in equation (5.34). The average successful duration

$E[T_S]$ is expressed as follows:

$$E[T_S] = \sum_{i=1}^{N} P_{s,i} \Big[I(i \in S^d) T_{s,i}^d + I(i \in S^c) T_{s,i}^c \Big] \tag{5.51}$$

where $T_{s,i}^d$ and $T_{s,i}^c$ are given in equations (5.36) and (5.37), respectively. For a fixed packet length L, the average payload size $E[PL]$ is computed as follows:

$$E[PL] \;=\; 8L \sum_{i=1}^{N} P_{s,i} \tag{5.52}$$

Finally, the throughput $\mathbf{S}$ can calculated by substituting equations (5.49), (5.50), (5.51), and (5.52) into equation (5.46).

5.2.2 Delay Analysis

In this subsection two kinds of delay are studied. The first kind is the average service delay $E[T_{service,i}]$ that is used to calculate ρ_i in equation (5.44). The second kind is the average medium access delay $E[D_i]$ that is defined as the time interval from the time instant the packet becomes head of the queue ready for transmission to the time instant when the packet is acknowledged for a successful transmission. Let D_i $(i = 1, 2, ..., N)$ denote a random variable representing a packet delay of a generic node i. Thus, the average packet delay $E[D_{suc,i}]$ is expressed as follows:

$$E[D_{suc,i}] = E[D_{b,i}] + E[D_{c,i}] + E[D_{o,i}] + E[D_{s,i}] \tag{5.53}$$

where $E[D_{b,i}]$, $E[D_{c,i}]$, $E[D_{o,i}]$, and $E[D_{s,i}]$ stand for the average delay during decreasing backoff counter, the average delay due to a collision transmission, the average delay due to freezing the backoff counter during the transmissions of the other nodes, and the average delay of a successful transmission, respectively. These average delay values are calculated as follows:

$$\begin{aligned} E[D_{b,i}] &= \overline{N_{b,i}}\sigma \\ E[D_{c,i}] &= \overline{N_{c,i}}T_c \\ E[D_{o,i}] &= \overline{N_{o,i}}T_{f,i} + (1 - P_{E,i})P_{b,i}T_{f,i} \\ E[D_{s,i}] &= I(i \in S^d)T^d_{s,i} + I(i \in S^c)T^c_{s,i} \end{aligned} \tag{5.54}$$

where T_c, $T^d_{s,i}$, $T^c_{s,i}$, and $T_{f,i}$ are given in (5.34), (5.36), (5.37), and (5.39), respectively. $\overline{N_{b,i}}$ is the average number of backoff slots that the node i needs to transmit its packet successfully, without taking into account the time the counter is stopped. $\overline{N_{c,i}}$ is the average number of collisions that the node i encounters before the packet is sent successfully. $\overline{N_{o,i}}$ is the average number of transmissions overheard by the node i during the backoff process. The average number $\overline{N_{b,i}}$ is calculated as follows:

$$\overline{N_{b,i}} = \sum_{j=0}^{m} \frac{P^j_{c,i}(1 - P_{c,i})}{1 - P^{m+1}_{c,i}} \sum_{k=0}^{j} \frac{W_k - 1}{2} \tag{5.55}$$

where $\frac{P^j_{c,i}(1-P_{c,i})}{1-P^{m+1}_{c,i}}$ is the successful transmission probability after the jth backoff stage conditioned that the packet is not dropped, and the corresponding average number of the backoff slots is $\sum_{k=0}^{j} \frac{W_k-1}{2}$. The average number of collisions $\overline{N_{c,i}}$ is calculated as follows:

$$\overline{N_{c,i}} = \sum_{i=0}^{m} \frac{iP_{c,i}^{i}(1-P_{c,i})}{1-P_{c,i}^{m+1}} = \frac{1-P_{c,i}}{1-P_{c,i}^{m+1}} \left[\frac{P_{c,i}}{(1-P_{c,i})^2}(1-P_{c,i}^{m}) - \frac{mP_{c,i}^{m+1}}{1-P_{c,i}} \right] \quad (5.56)$$

Let $\overline{N}_{idle,i}$ be the average number of consecutive idle slots between two consecutive busy slots of the $N-1$ remaining nodes. $\overline{N}_{idle,i}$ is calculated as follows:

$$\overline{N}_{idle,i} = \sum_{j=0}^{\infty} j(1-P_{b,i})^{j} P_{b,i} = \frac{1}{P_{b,i}} - 1 \quad (5.57)$$

Consequently, the average number of transmissions $\overline{N_{o,i}}$ overheard by the node i is calculated as follows:

$$\overline{N_{o,i}} = \frac{\overline{N_{b,i}}}{\max(\overline{N}_{idle,i}, 1)} - 1 \quad (5.58)$$

Therefore, the delay $E[D_{suc,i}]$ can be calculated by substituting equations (5.55), (5.56), and (5.58) into equation (5.53). For the reason that $E[T_{service,i}]$ includes the time duration of the successful and dropped packets, $E[T_{service,i}]$ is calculated as follows:

$$E[T_{service,i}] = (1-P_{c,i}^{m+1})E[D_{suc,i}] + P_{c,i}^{m+1}E[D_{drop,i}] \quad (5.59)$$

where $E[D_{drop,i}]$ is the average delay in the case of the packet being dropped. Hence, $E[D_{drop,i}]$ is computed as follows:

$$E[D_{drop,i}] = \sum_{j=0}^{m} \frac{W_j - 1}{2} \Big(\sigma + \frac{P_{b,i}}{1-P_{b,i}} T_{f,i} \Big) + (1-P_{E,i})P_{b,i} + (m+1)T_c \quad (5.60)$$

Finally, the total average medium access delay is calculated as fol-

lows:

$$E[D_T] = \frac{1}{N}\sum_{i=1}^{N} E[D_{suc,i}] \tag{5.61}$$

5.2.3 Energy Efficiency

The energy efficiency η, is defined as the ratio of the successfully transmitted data bits to the total energy consumed (99,100). η is written as follows:

$$\eta = \frac{E[L]}{\sum_{i=1}^{N}\left(E_B^{(i)} + E_C^{(i)} + E_O^{(i)} + E_S^{(i)}\right)} \tag{5.62}$$

where $E_B^{(i)}$ is the energy consumption during the backoff period. $E_C^{(i)}$ is the energy consumption during the collision transmission period. $E_O^{(i)}$ is the energy consumption during the overhearing transmission period. $E_S^{(i)}$ is the energy consumption during the successful transmission period. $E[L]$ is the average payload size.

Given the duration of an empty slot σ and the idle power consumption P_{IX}, the energy, that the node i consumes during the backoff stage, is calculated as follows:

$$E_B^{(i)} = \sigma \cdot P_{IX} \cdot \overline{N_{b,i}}, \quad i = 1, 2, ..., N \tag{5.63}$$

where $\overline{N_{b,i}}$ is given in equation (5.55). The node i overhears the collision and the successful transmissions. Therefore, the energy, that the node

i consumes in overhearing other nodes transmission during the backoff stages, is calculated as follows:

$$E_O^{(i)} = P_{RX}\left[\overline{N_{o,i}}T_{f,i} + (1 - P_{E,i})P_{b,i}T_{f,i}\right] \tag{5.64}$$

where P_{bi}, $T_{f,i}$, $P_{E,i}$, , and $\overline{N_{o,i}}$ are given in equations (5.31), (5.39), (5.45), and (5.58), respectively. P_{RX} is the receiving power consumption. The energy consumption due to collision is calculated as follows:

$$E_C^{(i)} = \overline{N_{c,i}}\Big[P_{TX}T_{RTS} + P_{RX}T_{CTS} + P_{IX}(T_{DIFS} + T_{SIFS})\Big] \tag{5.65}$$

where P_{TX} is the power consumption during transmission, and $\overline{N_{c,i}}$ is the average number of collisions given in equation (5.56). The energy consumption for a successful single-hop transmission, $E_{S,i}^d$, is computed as follows:

$$E_{S,i}^d = P_{TX}\Big(T_{RTS} + \frac{8L}{R_{sd}} + T_{PLCP}\Big) + P_{RX}T_{CTS} + P_{IX}\Big(T_{ACK} + 3T_{SIFS} + T_{DIFS} + 4\delta\Big) \tag{5.66}$$

For a successful two-hop transmission, the energy consumption $E_{S,i}^c$ is computed as follows:

$$\begin{aligned} E_{S,i}^c \;=\; & P_{TX}\Big(T_{MRTS} + \frac{8L}{R_{sr}} + T_{PLCP}\Big) + P_{RX}\Big(T_{CTS} + T_{BTS} + \frac{8L}{R_{rd}} + T_{PLCP}\Big) \\ & + P_{IX}\Big(T_{ACK} + 5T_{SIFS} + T_{DIFS} + 6\delta\Big) \end{aligned} \tag{5.67}$$

The energy consumption during a successful transmission of the

Parameter	Value	Parameter	Value
MAC header	272 bits	Slot time	20 μs
PHY header	192 bits	SIFS	10 μs
RTS	352 bits	DIFS	50 μs
CTS	304 bits	Busy Tone	20 μs
ACK	304 bits	CW_{min}	31 slots
PLCP data-rate	1 Mbps	CW_{max}	1023 slots
Data-rate	1, 2, 5.5, 11 Mbps	P_{IX}, P_{RX}, P_{TX}	0.8, 0.8, 1.0 Watt

Table 5.1: System parameters under unsaturated conditions.

generic node i is then computed as follows:

$$E_S^{(i)} = I(i \in S^d)E_{S,i}^d + I(i \in S^c)E_{S,i}^c \tag{5.68}$$

Finally, the average packet length $E[L] = \sum_{i=1}^{N} 8L$ assuming a fixed packet length. Therefore, the energy efficiency η can be calculated using equation (5.62).

5.3 Analytical and Simulation Results

To validate the above analysis, a custom event driven simulator developed by using the Mobile Framework (MF) of the OMNET++ (148) package written in C++ programming language. The parameters used in simulation and analysis are set to the default values specified in IEEE 802.11b standard which are summarized in Table 5.1. The network setting is the same as given in (Chapter 3, Section 3.4). In all following figures, solid lines are for the analytical model results through Matlab software package. Whereas dot-dashed lines are for the simulation results through OMNET++ software package.

5.3.1 Throughput Results

Fig. 5.2 shows the relationship between the total mean offered load, the number of nodes, and the overall throughput of both the 802.11b and the BTAC protocols at a fixed payload size which is 1024 byte. Since Fig. 5.2(a) and Fig. 5.2(b) show the results for 10 and 30 nodes, respectively. Under 802.11b protocol, the relationship between throughput and offered load is linear when $\lambda_{totoal} \leq 120$ and throughout is saturated when $\lambda_{totoal} \geq 300$ when the number of nodes is 10 or 30 nodes. On the other hand, the relationship between throughput of the BTAC protocol and offered load is linear when $\lambda_{totoal} \leq 200$ and $\lambda_{totoal} \leq 300$ for the number of node 10 and 30 nodes, respectively, whereas throughput is saturated at $\lambda_{totoal} \geq 400$ for both $N = 10$ and $N = 30$ nodes.

The reason of the linear relationship between throughput and a low offered load is that at a low offered load the probability of accessing the medium is low, the collision probability then becomes negligible. Therefore, the probability to send a data packet successfully is very high and then the overall throughput is equal to $\lambda_{total} \times L$, where L is the packet length in bits. As the number of nodes increases, the linear relationship between throughput and offered load also increases under the BTAC protocol and becomes constant under the 802.11b protocol. This is because the probability of finding relay node increases as the number of nodes increases. Consequently, the time required to send a data packet from the source to the AP decreases due to the high data rate through the two-hop transmission. Therefore, the occupation time of channel becomes less than the arrival rate of data packets at each node. For this reason, the collision probability decrease and hence the relationship between throughput and offered load is linear.

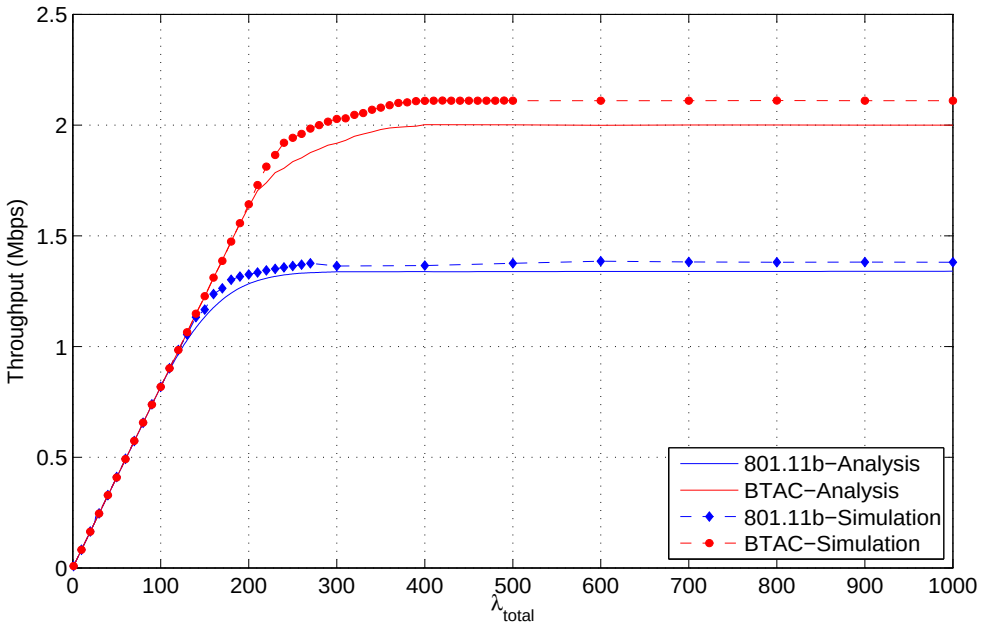

(a) Throughput vs. total traffic load at $N = 10$.

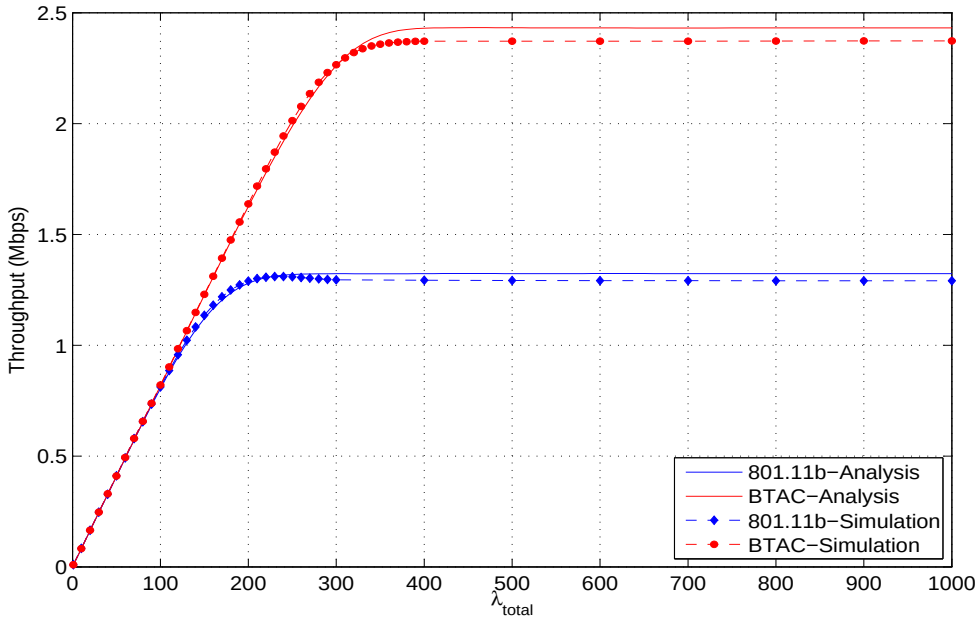

(b) Throughput vs. total traffic load at $N = 30$.

Figure 5.2: Throughput performance versus total traffic load and number of nodes, $L = 1024\ byte$.

Fig. 5.3 shows the results for $L = 1024$ and $L = 1500$ byte of throughout versus offered load at a fixed number of nodes which is 30 nodes. In Fig. 5.3(a), the BTAC is saturated at $\lambda_{total} = 400$, where in Fig. 5.3(b), it is saturated at $\lambda_{total} = 300$. The reason is that as the packet length increases, the occupation time of the medium increases. Hence, probability of node to have a packet in its queue increases and the probability to access the medium also increases. For this reason the collision probability increases and causes the throughput to saturated at a low traffic load as the packet length increases. As the packet length increases, the saturated throughput increases. This because the effect of the control overhead becomes noneligible as the packet length increases, the saturated throughout then increases as the packet length increases.

5.3.2 Energy Efficiency Results

The energy efficiency is counted as one of the most important requirements to design an efficient MAC protocol. Hence, the energy efficiency of the 802.11b and BTAC protocols versus the offered load under different number of nodes and fixed packet length and under different packet length and fixed number of nodes is shown in Fig. 5.4 and Fig. 5.5, respectively. As the offered load increases, the collision probability increases. As a result, the number of retries to deliver a data packet from source node to the AP increases. This causes increasing in the transmission, the receiving, overhearing, and sensing energy. Therefore, the node consumes more energy on the retransmissions, receiving and sensing the medium. Consequently, the energy efficiency decreases as the offered load increases. The BTAC protocol achieves higher energy efficiency than the 802.11b protocol due to advantage of using a two-hop

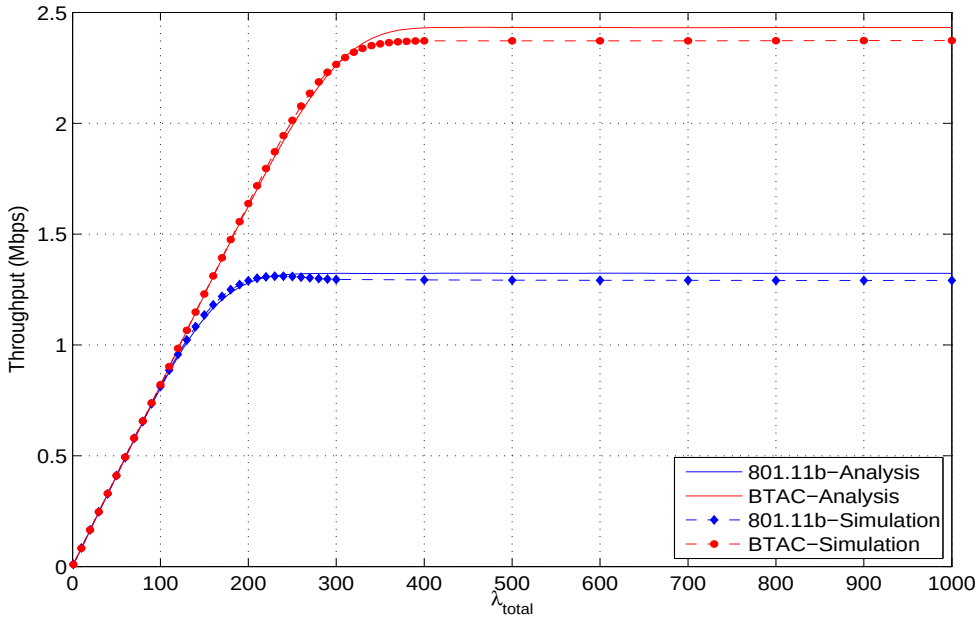

(a) Throughput vs. total traffic load at $L = 1024$.

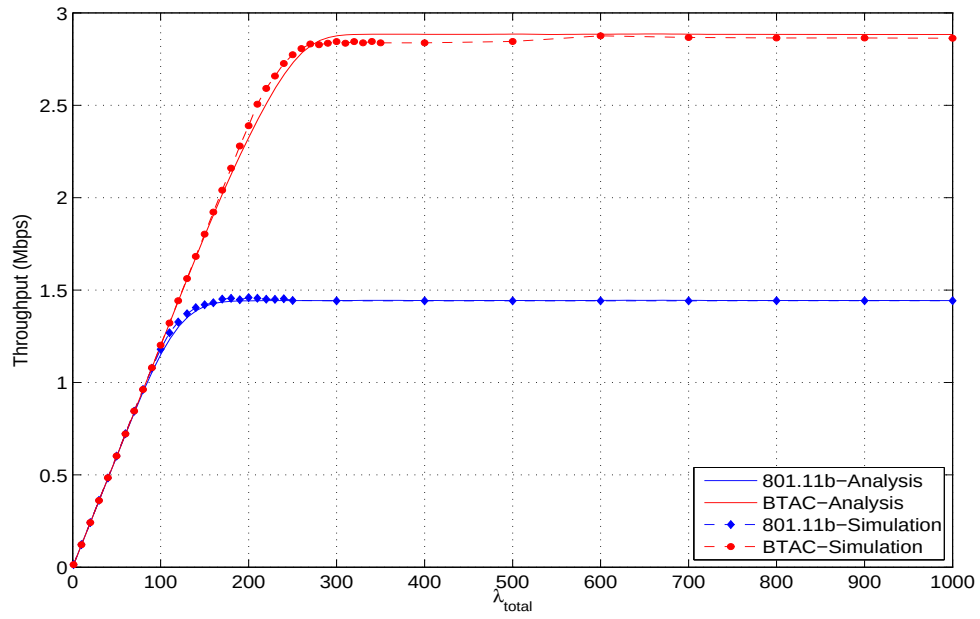

(b) Throughput vs. total traffic load at $L = 1500$.

Figure 5.3: Throughput performance versus total traffic load and packet length, $N = 30$.

transmission.

5.3.3 Delay Results

It is important to consider the delay experienced by a data packet in the MAC layer as well as throughput. Fig. 5.6 and Fig. 5.7 show the results of delay versus offered load at $N = 10$, $N = 30$ and $L = 1024$ and at $L = 1024,\ L = 1500$ byte and $N = 30$, respectively. As the offered load increases, the collision probability increases, and hence the delay (associated with medium contention and collisions) increases. The BTAC protocol outperforms the 802.11b protocol under all traffic conditions, number of nodes, and packet length. This is due to using the tow-hop transmission.

5.4 Conclusions

In this chapter, a Markov chain model is proposed taking the traffic characteristic and multi-rate transmissions into account. The model also considers the post-backoff that there is always at least one backoff interval preceding a packet transmission. Alternatively, there is an exception to the essential rule that an a packet from the upper layer has to be transmitted after performing the backoff mechanism. The packet arriving from the upper layer may be transmitted immediately without waiting any time if the transmission queue is empty, the latest post-backoff is finished, and at the same time the channel has been idle for at least one DCF interval. In the proposed model this exceptional case is considered. The $M/M/1/K$ queuing model is introduced in this chapter to study the various performance metrics of WLAN in the non-saturated state which is the desired

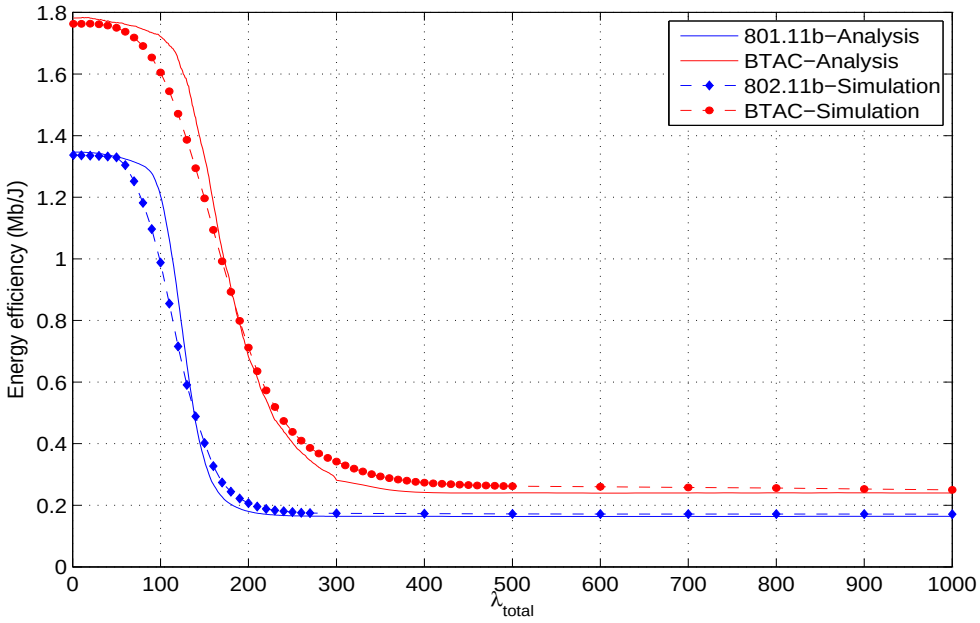

(a) Energy efficiency vs. total traffic load at $N = 10$.

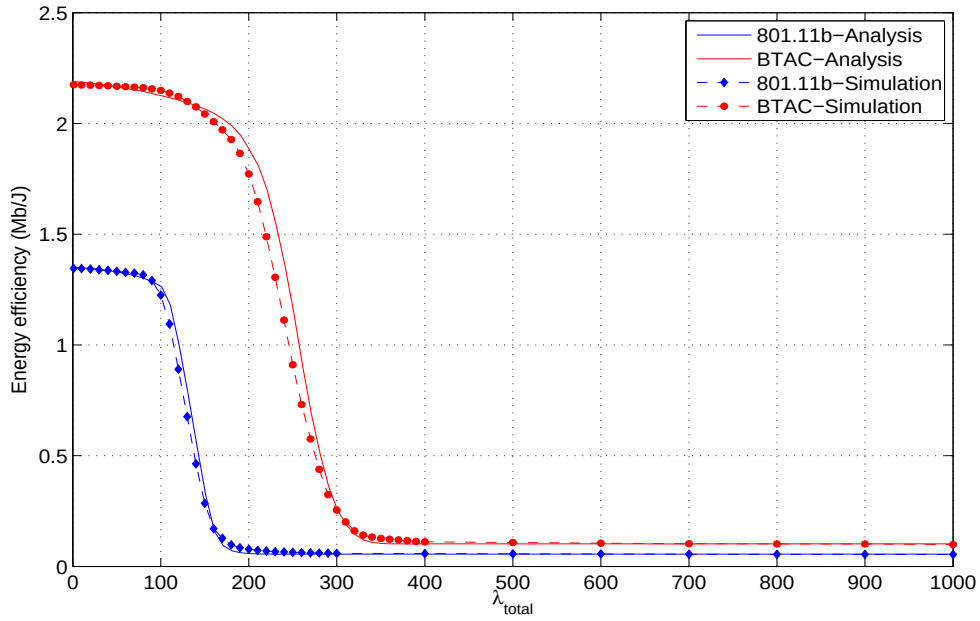

(b) Energy efficiency vs. total traffic load at $N = 30$.

Figure 5.4: Energy efficiency performance versus total traffic load and number of nodes, $L = 1024\ byte$.

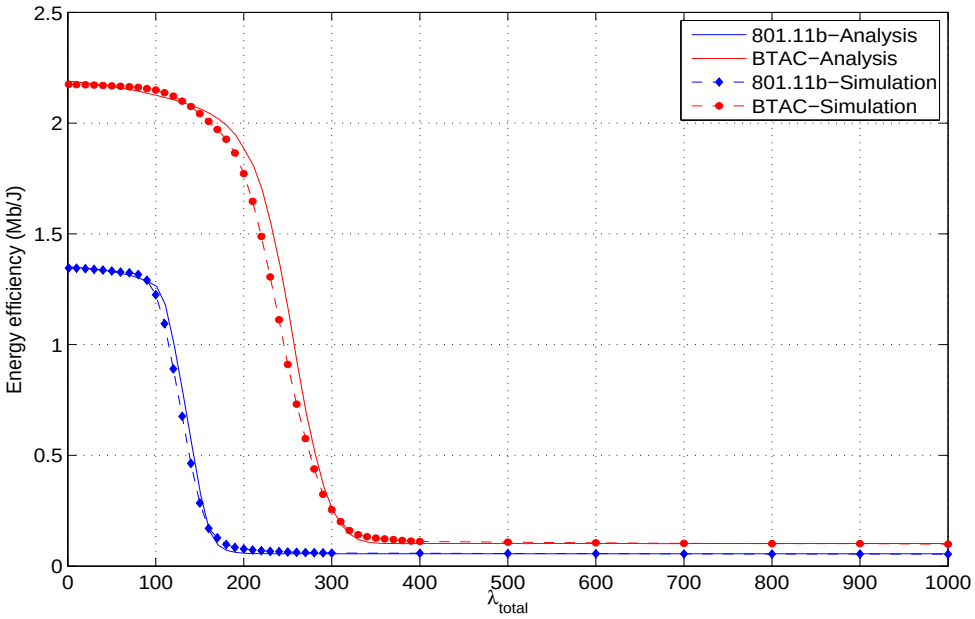

(a) Energy efficiency vs. total traffic load at $L = 1024$.

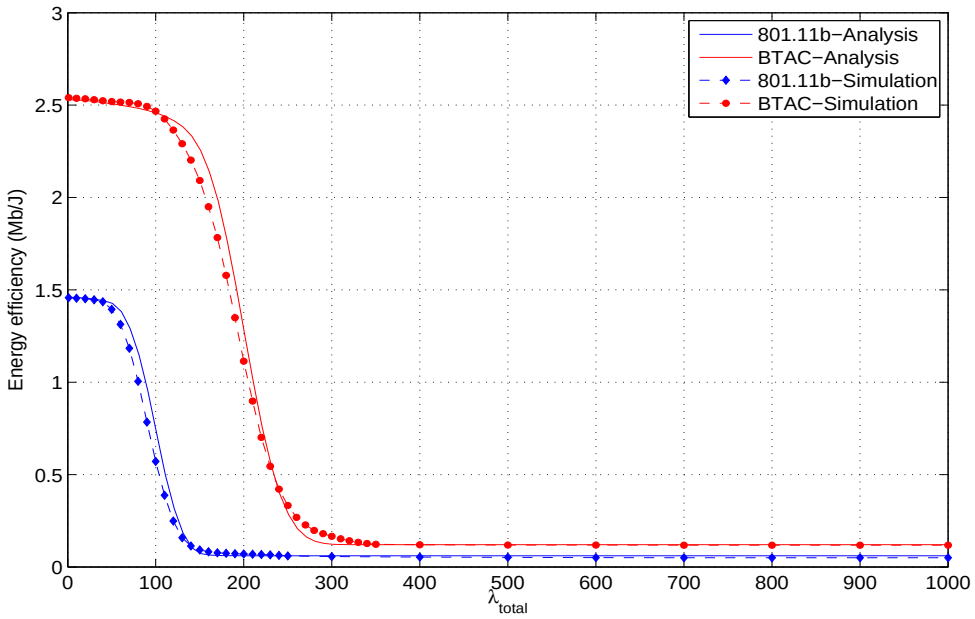

(b) Energy efficiency vs. total traffic load at $L = 1500$.

Figure 5.5: Energy efficiency performance versus total traffic load and packet length, $N = 30$.

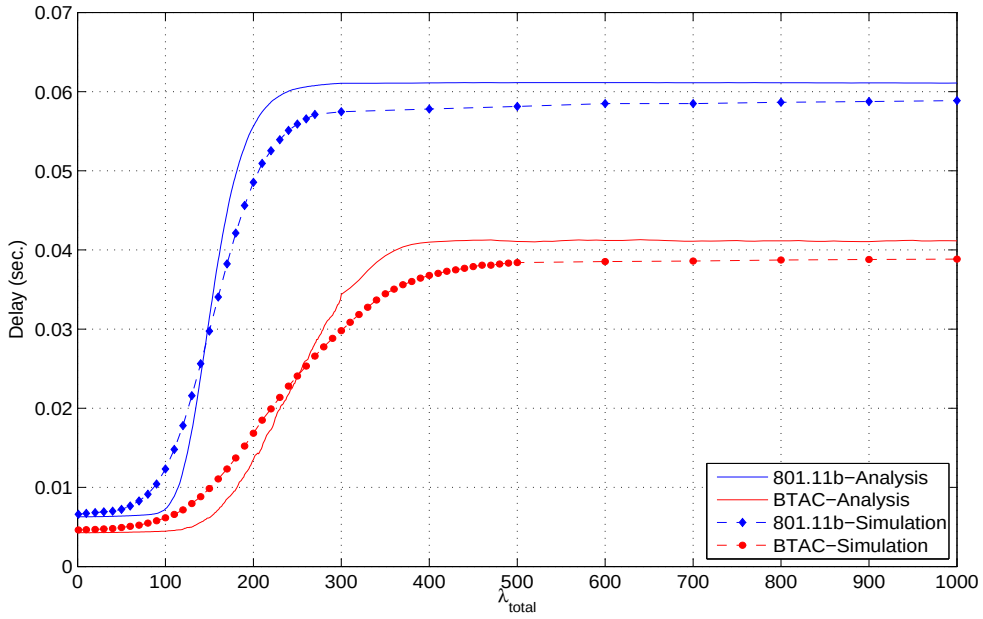

(a) Delay vs. total traffic load at $N = 10$.

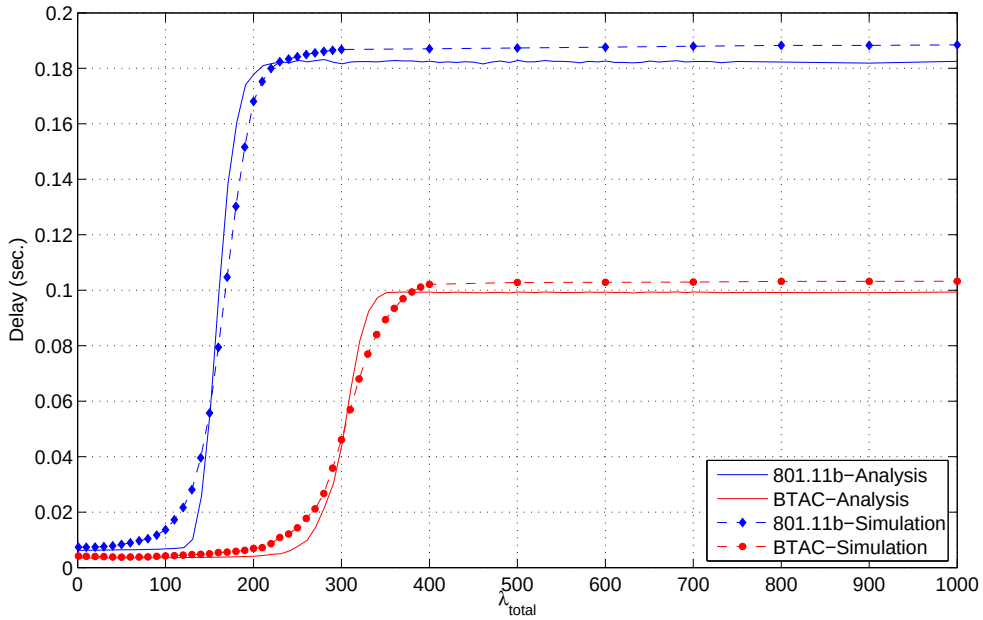

(b) Delay vs. total traffic load at $N = 30$.

Figure 5.6: Delay performance versus total traffic load and number of nodes, $L = 1024\ byte$.

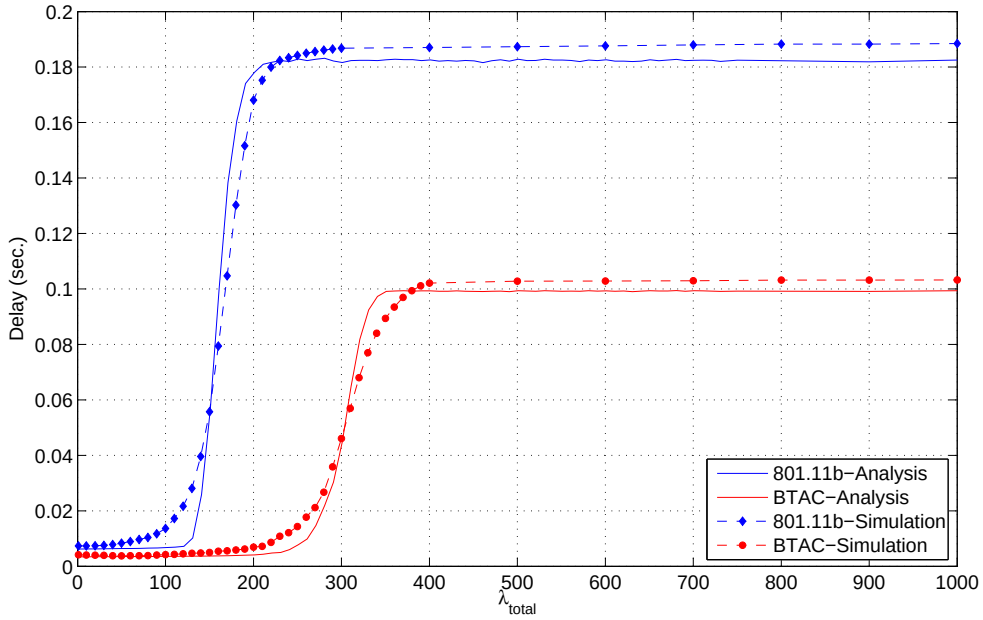

(a) Delay vs. total traffic load at $L = 1024$.

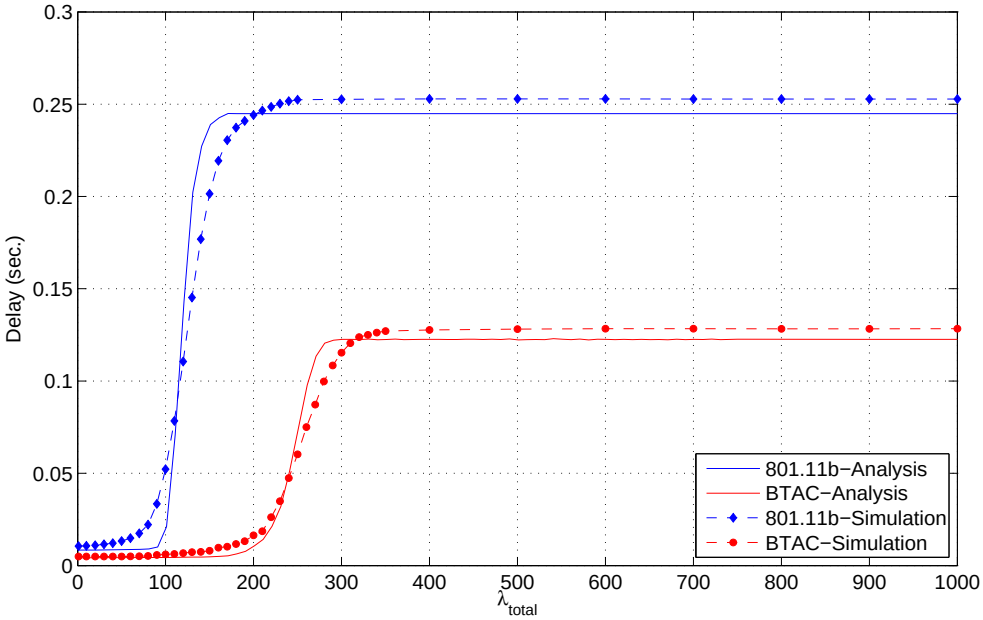

(b) Delay vs. total traffic load at $L = 1500$.

Figure 5.7: Delay performance versus total traffic load and packet length, $N = 30$.

state for some applications.

An analytical model is then presented to study the performance of the IEEE 802.11 and BTAC protocols under non-saturation traffic conditions in terms of throughput, medium access and service delay, and energy efficiency. The results show that the performance of both the 802.11b and the BTAC protocols depends on the traffic conditions. Since under the very low offered load, the throughput performance of the BTAC protocol is similar to the 802.11b, whereas the delay and energy efficiency of the BTAC protocol is better than that of the 802.11b protocol. On the other hand, the BTAC protocol outperforms the 802.11b under a medium and high offered load in terms of throughput, delay, and energy efficiency. Therefore, the two-hop transmission technique used by the BTAC protocol is suitable to apply under both light and heavy traffic load.

Chapter 6

Conclusions and Future Work

6.1 Conclusions

According to the IEEE 802.11 standards, Wireless Local Area Networks (WLANs) can support multiple transmission data rates depending on the instantaneous channel conditions between the source station and the Access Point (AP). To achieve the target Packet Error Rate (PER) in data transmissions, a source station transmits its data packets to the AP at a low date rate when the channel quality is poor. In such a multi-rate WLAN, those low data-rate stations will occupy the shared communication channel for a longer period for packet transmissions, thus reducing the channel efficiency and overall system performance.

Performance degradation can be mitigated by using the concept of cooperative communication at Medium Access Control (MAC) layer. A source station can use a neighbouring node, called relay, which has high quality communication channels to both source station and the AP. This relay-based cooperative communication can effectively improve net-

work coverage, transmission data rate, reliability, and overall system performance.

This thesis addresses the channel efficiency problem in multi-rate WLANs by adopting the concept of cooperative communications in the development and evaluation of two cooperative Medium Access Control (MAC) protocols, namely Busy Tone based Cooperative MAC (BTAC) protocol and Cooperative Access with Relay's Data (CARD) protocol. Under BTAC, a low data-rate source station uses a close-by intermediate station as its relay to forward its data packets at higher data-rates to the AP through a two-hop path. In this way, BTAC can achieve cooperative diversity gain in multi-rate WLANs. Furthermore, the proposed CARD protocol enables a relay station to transmit its own data packets to the AP immediately after forwarding its neighbour's packets, thus saving the handshake procedure and overheads for sensing and reserving the common channel. In doing so, CARD can achieve both cooperative diversity gain and cooperative multiplexing gain. Both BTAC and CARD protocols are backward compatible with the existing IEEE 802.11 standards.

Accordingly, new cross-layer analytical approaches have been developed in this thesis to study the performance of BTAC and CARD under different channel conditions and traffic loads, i.e. saturated and unsaturated traffics. Analytical results, verified by extensive simulation results, show that BTAC and CARD protocols can significantly improve system throughput, service delay, and energy efficiency performance in realistic communication scenarios. Compared with traditional IEEE 802.11b MAC protocol, BTAC can greatly improve system performance by up to 88%, 40% and 84% in terms of throughput, energy efficiency and service delay, respectively. Further, by enabling relay nodes to insert their own

packet transmissions without an additional handshake procedure, CARD can achieve up to 165% throughput gain over the IEEE 802.11b MAC protocol. In addition, the throughput of CARD is approaching the maximum value (i.e. 5 Mbps) when all the nodes have high-quality communication channels for packet transmissions, i.e. 11 Mbps. In addition, the energy efficiency and service delay performance of CARD are about 90% and 140% better than those of the IEEE 802.11b MAC protocol.

In order to support both BTAC and CARD protocols in real WLAN implementations, some minor modifications related to relay packet transmissions and control frames (e.g. BTS under BTAC and RRTS under CARD) are needed to enhance the current IEEE 802.11 standards. However, this implementation complexity is considered quite low compared to the significant performance gains of BTAC and CARD protocols. A general drawback of relay-based cooperative MAC protocols is the power consumption of a relay station, which may consume much more energy than other stations in receiving and forwarding neighbouring stations' data packets at high data rates. This problem is partially offset in CARD protocol by enabling a relay station to transmit its own data packets to the AP immediately after forwarding its neighbour's packets, thus saving handshake procedure and power consumption of a relay station. To further reduce the energy consumption of a relay in BTAC and CARD protocols, when multiple relay stations are available, we can use their remaining energy levels to make a choice of the most suitable relay station.

6.2 Future Work

A number of possible areas are identified for future work of this research.

It will be important to extend the study of BTAC and CARD protocols under more realistic channel models, e.g. Rayleigh fading channel model (155). In this thesis, the same bit error rate (BER) is assumed for different data transmission rates. In reality, BER performance depends on channel models, data rates, modulation and coding schemes. In addition to the Poisson traffic model used in this thesis, it will be useful to evaluate the performance of BTAC and CARD protocols under unsaturated conditions with more sophisticated traffic models, such as Markov Modulated Poisson Process (MMPP) model (156). Further, research may be extended to the newly emerging IEEE 802.11n standard, which has a different MAC layer comparing to the IEEE 802.11a/b/g standards.

In this thesis the BTAC and CARD protocols were examined in two-hop networks. The schemes and analytical methods presented here can be extended to more complicated multi-hop scenarios and with mobile relays. Also, it will be interesting to study the system performance of BTAC and CARD protocols under real time applications such as video traffic. These results will help in developing a deeper understanding of BTAC and CARD protocols and their superior performance.

The security issue of MAC protocols is not considered in this research. The proposed BTAC and CARD protocols may suffer from security attacks. For example, a malicious relay station could drop some to-be-forwarded data packets. On the other hand, a malicious relay station could modify the data packets received from the source station before forwarding it to the AP. Therefore, it is very important to develop a secure protection

mechanism for supporting reliable data transmissions in BTAC and CARD protocols.

Appendix A

Node Distribution Probability

In the following paragraphes the average number of nodes located in different zones is derived. Let N_1^d, N_2^d, N_3^d, and N_4^d stand for the average number of nodes in zones I, and II, III, and IV operating at the direct transmission data-rates 1, 2, 5.5, and 11 Mbps, respectively. These average number of nodes are computed as follows:

$$N_u^d = NP_u \tag{A.1}$$

where P_u, $u = 1, 2, 3, 4$ is the fraction of nodes in zones I, II, III, and IV, respectively that communicate directly with the AP. It is assumed that only the nodes in zone III and IV can benefit from cooperative transmission. If a source node is located in zone IV (at data-rate 1 Mbps) and there is relay node available, this source node can employ a two-hop transmission. Depending on the channel quality, the supported data-rates are given by the set $(R_{sr}, R_{rd}) = \{(11, 11), (5.5, 11), (11, 5.5), (5.5, 5.5), (2, 11), (11, 2), (2, 5.5), (5.5, 2)\}$.

Let $N_{4(u,v)}$ be the average number of nodes in zone IV at first-hop rate R_u Mbps and second-hop rate R_v Mbps. The average number $N_{4(u,v)}$ is then expressed as follows.

$$N_{4,(u,v)} = NP_{4(u,v)} \qquad u, v = 1, 2, 3 \quad at \quad u = 3 \quad v \neq 3 \tag{A.2}$$

where $P_{4(u,v)}$ is the fraction of nodes in zone IV employing a two-hop transmission at data-rates R_u and R_v. Similarly, if a source node is located in zone III (at data-rate 2 Mbps) and there is a relay node available, the set of supported data-rates is given by $(R_{sr}, R_{rd}) = \{(11, 11), (5.5, 11), (11, 5.5), (5.5, 5.5)\}$.

The average number of nodes $N_{3(u,v)}$ in zone III at two-hop data rates R_u and R_v, is then calculated as follows.

$$N_{3,(u,v)} = NP_{3(u,v)} \qquad u, v = 1, 2 \tag{A.3}$$

where $P_{3(u,v)}$ is the fraction of nodes in zone IV using two-hop transmission at rates R_u and R_v. P_u, $P_{3(u,v)}$, and $P_{4(u,v)}$ are given in Appendix B.

Therefore, the total set of nodes $S = \{S^d, S_1^c, S_2^c\}$ includes three different sets of nodes. The set $S^d = \{N_u^d \quad \forall \quad u = 1, 2, 3, 4\}$ contains the nodes that use a direct transmission scheme. The set $S_1^c = \{N_{4(u,v)} \quad \forall \quad u, v = 1, 2, 3\}$ contains the nodes at data-rate 1 Mbps and are located in zone IV. These nodes use a two-hop transmission scheme. Finally, the set $S_2^c = \{N_{3(u,v)} \quad \forall \quad u, v = 1, 2\}$ is the set of nodes that are located in zone

III (at data-rate 2Mbps) and use a two-hop transmission. Notice that $|S^d| + |S_1^c| + |S_2^c| = N$, where $|\cdot|$ is the cardinality of the set.

Appendix B

Relay Probability

Consider a one cell wireless local area network (WLAN) consisting of an access point (AP) and N nodes. The network supports M different data-rates, denoted by R_m, where $m = 1, 2, ..., M$, and $R_1 > R_2 > ...R_M$. For simplicity, we only consider path loss (155), which means that the signal strength mainly depends on the distance between the transmitter and the receiver for a given transmission power. The maximum transmission radius of a node at data-rate R_m is r_m, where $r_1 < r_2 < ... < r_M$. The AP is located at the center of the cell of a radius R, where $R = r_M$. The nodes are assumed to be uniformly distributed within the coverage area of the cell. In this work, we consider the case of one relay node and four different transmission data-rates (M=4), where the analysis can be extended to larger number of data-rates.

We define $A_{x,y}(r)$ as the area of a region in which a node must be located to work as a relay for another node (source node) which at a distance r from the AP. As shown in Fig. B.1, the relay node is within a distance r_x from the source node and within a distance r_y from the AP; the data rate of the first hop (source to relay) is R_x and of the second hop

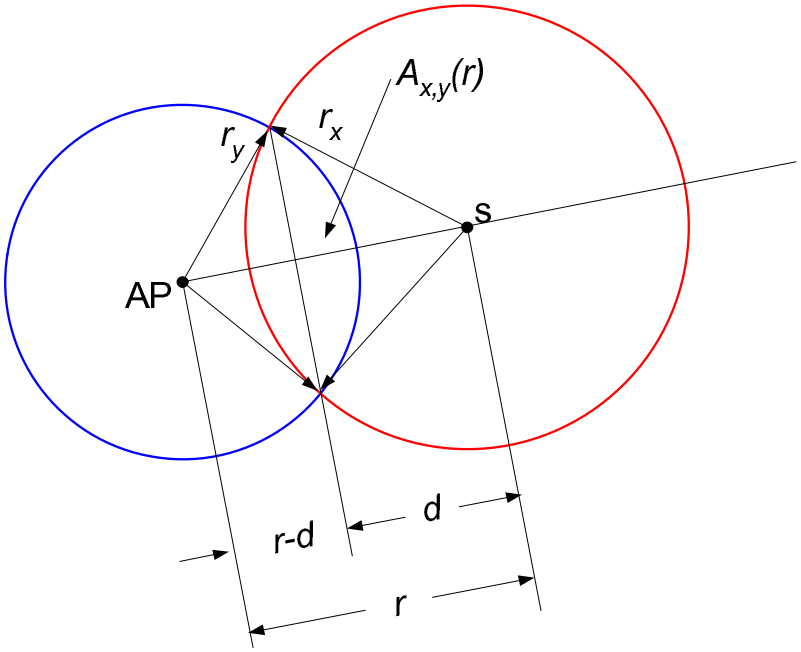

Figure B.1: Intersection area of two circles.

(relay to AP) is R_y. For example, $A_{1,2}(r)$ is the area that a relay has to be located so that it can provide data rate R_1 (source-relay link), and data rate R_2 (relay-AP link) for a node at a distance r from the AP.

The area $A_{x,y}(r)$ between the two circles can be divided into two circular segments: $A_x(r)$ is the segment from the circle s, and $A_y(r)$ is the segment from the circle AP. The area $A_y(r)$ is given by:

$$\begin{aligned} A_y(r) &= \int_{y=-\sqrt{r_y^2-(r-d)^2}}^{y=\sqrt{r_y^2-(r-d)^2}} \int_{x=r-d}^{\sqrt{r_y^2-y^2}} dxdy \\ &= r_y^2 \cos^{-1}\left(\frac{r-d}{r_y}\right) - (r-d)\sqrt{r_y^2-(r-d)^2} \end{aligned} \tag{B.1}$$

Similarly, the second part $A_x(r)$ from circle s can be calculated as

follows:

$$\begin{aligned} A_x(r) &= \int_{y=-\sqrt{r_x^2-d^2}}^{y=\sqrt{r_x^2-d^2}} \int_{x=d}^{\sqrt{r_x^2-y^2}} dxdy \\ &= r_x^2 \cos^{-1}\left(\frac{d}{r_x}\right) - d\sqrt{r_x^2-d^2} \end{aligned} \tag{B.2}$$

where $d = \frac{r^2+r_y^2-r_x^2}{2r}$. Therefore, from (B.1) and (B.2) the intersection area $A_{x,y}(r)$ can be calculated as follows:

$$\begin{aligned} A_{x,y}(r) &= A_x(r) + A_y(r) \\ &= r_x^2 \cos^{-1}\left(\frac{r^2+r_x^2-r_y^2}{2r_x r}\right) + r_y^2 \cos^{-1}\left(\frac{r^2-r_x^2+r_y^2}{2r_y r}\right) \\ &\quad -\frac{1}{2}\sqrt{(r_x+r_y-r)(r_x-r_y+r)(r_y-r_x+r)(r_x+r_y+r)} \end{aligned} \tag{B.3}$$

The probability that a source node can be able to send its information to the AP via a relay node, is equivalent to to the probability that there is at least one node in its relay area $A_{x,y}(r)$. Assuming the data-rate from source node to relay node (first hop) is R_x, the data-rate from relay node to the AP (second hop) is R_y, and the data-rate from source node to the AP (direct transmission) is R_z. Consequently, in order for a node to act as a relay for a source node, the following condition must be satisfied, the source to relay transmission time ($1/R_x$) plus the relay to the AP transmission time ($1/R_y$) is less than the transmission time ($1/R_z$) from the source to the AP. Then, we have:

$$\frac{1}{R_x} + \frac{1}{R_y} < \frac{1}{R_z} \tag{B.4}$$

where the packet length is assumed to be fixed. Assuming the N nodes are uniformly distributed within the cell, then the probability density function (PDF) of a node at a distance r from the AP is given by:

$$p_r(r) = \frac{2r}{R^2}, \qquad 0 \leq r \leq R \tag{B.5}$$

and the node's angle is uniformly distributed between $[0, \pi)$. Fig. B.2 shows the relaying regions for our proposed method, where the analysis given in (157) is extended for four transmission data-rates. It is assumed that nodes located only in zone-3 ($r_2 \leq r < r_3$) and zone-4 ($r_3 \leq r < r_4$) can benefits from relaying, where nodes in zone-1 ($0 \leq r < r_1$) and zone-2 ($r_1 \leq r < r_2$) transmit directly at a high data-rate to the AP. Then, the fraction of nodes at data-rate R_1 and R_2 is given, respectively as follows:

$$\begin{aligned} P_1 &= \int_{r=0}^{r_1} \frac{2r}{R^2}\, dr &= \frac{r_1^2}{R^2} \\ P_2 &= \int_{r=r_1}^{r_2} \frac{2r}{R^2}\, dr &= \frac{r_2^2 - r_1^2}{R^2} \end{aligned} \tag{B.6}$$

We define $P_{4(x,y)}$ as the expected fraction of nodes in zone-4 that can benefit from relaying provided by a relay node placed within area $A_{x,y}(r)$. Not that this for a first hop data-rate R_x and a second hop data-rate R_y. Analogously, $P_{3(x,y)}$ gives the proportion of nodes in zone-3 that can benefit from a relay within area $A_{x,y}(r)$ with data-rate R_x for first hop and data-rate R_y for second hop. For instant, $P_{4(2,1)}$ is the fraction of nodes in zone-4 uses a relay node with a first hop (source-relay) data-rate R_2 and second hop (relay-AP) data-rate R_1. where $P_{3(1,2)}$ is the fraction of nodes in zone-3 that benefits from relaying with data-rate R_1 for the first hop and

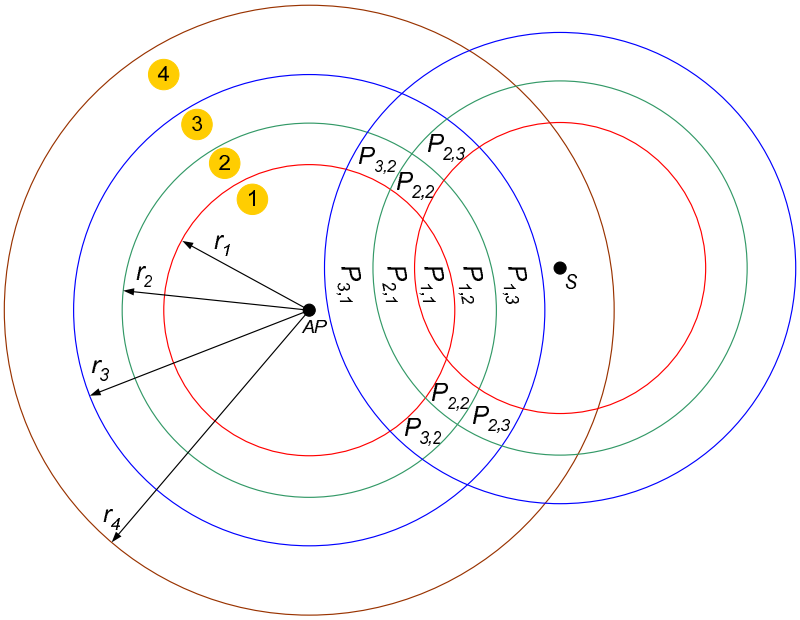

Figure B.2: Relay regions of a node in zone-4.

data-rate R_2 for the second hop. Therefore, we have

$P_{4(1,1)}$ is given as follows:

$$P_{4(1,1)} = I(r_3 < 2r_1)\left[\int_{r=r_3}^{min(2r_1,R)} \frac{2r}{R^2}\left(1-\left(1-\frac{A_{1,1}(r)}{\pi R^2}\right)^{N-1}\right)dr\right] \tag{B.7}$$

where $I(x)$ is 1 if x is true, and is 0 otherwise. The fraction $P_{4(2,1)}$ is given as:

$$P_{4(2,1)} = I(r_3 < r_1 + r_2)\left[\int_{r=r_3}^{min(r1+r2,R)} \frac{2r}{R^2}\left(1-\left(1-\frac{A_{2,1}(r)}{\pi R^2}\right)^{N-1}\right)dr\right] - P_{1,1} \tag{B.8}$$

$P_{4(1,2)}$ is calculated by:

$$\begin{aligned} P_{4(1,2)} &= I(r_3 < 2r_1)\left[\int_{r=r_3}^{2r_1}\frac{2r}{R^2}\left(1-\left(1-\frac{2A_{1,2}(r)-A_{1,1}(r)}{\pi R^2}\right)^{N-1}\right)dr\right. \\ &\quad \left.+\int_{r=2r_1}^{min(r_1+r_2,R)}\frac{2r}{R^2}\left(1-\left(1-\frac{2A_{1,2}(r)}{\pi R^2}\right)^{N-1}\right)dr\right] \\ &\quad +I(2r_1 < r_3 < r_1+r_2)\left[\int_{r=r_3}^{min(r_1+r_2,R)}\frac{2r}{R^2}\left(1-\left(1-\frac{2A_{1,2}(r)}{\pi R^2}\right)^{N-1}\right)dr\right] \\ &\quad -\Big[P_{1,1}+P_{2,1}\Big] \end{aligned} \tag{B.9}$$

$P_{4(2,2)}$ is given as follows:

$$\begin{aligned} P_{4(2,2)} &= I(r_3 < 2r_2)\left[\int_{r=r_3}^{min(2r_2,R)}\frac{2r}{R^2}\left(1-\left(1-\frac{A_{2,2}(r)}{\pi R^2}\right)^{N-1}\right)dr\right] \\ &\quad -\Big[P_{4(1,1)}+P_{4(2,1)}+P_{4(1,2)}\Big] \end{aligned} \tag{B.10}$$

$P_{4(3,1)}$ is calculated as follows:

$$
\begin{aligned}
P_{4(3,1)} \quad = \quad & I(r_3 < r_1 + r_2)\Bigg[\int_{r=r_3}^{r_1+r_2} \frac{2r}{R^2}\left(1-\left(1-\frac{A_{2,2}(r)+A_{3,1}(r)-A_{2,1}(r)}{\pi R^2}\right)^{N-1}\right)dr \\
& + I(2r_2 < r_1 + r_3)\Bigg[\int_{r=r_1+r_2}^{2r_2} \frac{2r}{R^2}\left(1-\left(1-\frac{A_{2,2}(r)+A_{3,1}(r)}{\pi R^2}\right)^{N-1}\right)dr \\
& + \int_{r=2r_2}^{min(r_1+r_3,R)} \frac{2r}{R^2}\left(1-\left(1-\frac{A_{3,1}(r)}{\pi R^2}\right)^{N-1}\right)dr\Bigg] \\
& + I(2r_2 > r_1 + r_3)\Bigg[\int_{r=r_1+r_2}^{r_1+r_3} \frac{2r}{R^2}\left(1-\left(1-\frac{A_{2,2}(r)+A_{3,1}(r)}{\pi R^2}\right)^{N-1}\right)dr \\
& + \int_{r=r_1+r_3}^{min(2r_2,R)} \frac{2r}{R^2}\left(1-\left(1-\frac{A_{2,2}(r)}{\pi R^2}\right)^{N-1}\right)dr\Bigg]\Bigg] \\
& + I(r_3 > r_1 + r_2)\Bigg[I(2r_2 < r_1 + r_3)\Bigg[\int_{r=r_3}^{2r_2} \frac{2r}{R^2}\left(1-\left(1-\frac{A_{2,2}(r)+A_{3,1}(r)}{\pi R^2}\right)^{N-1}\right)dr \\
& + \int_{r=2r_2}^{min(r_1+r_3,R)} \frac{2r}{R^2}\left(1-\left(1-\frac{A_{3,1}(r)}{\pi R^2}\right)^{N-1}\right)dr\Bigg] \\
& + I(2r_2 > r_1 + r_3)\Bigg[\int_{r=r_3}^{r_1+r_3} \frac{2r}{R^2}\left(1-\left(1-\frac{A_{2,2}(r)+A_{3,1}(r)}{\pi R^2}\right)^{N-1}\right)dr \\
& + \int_{r=r_1+r_3}^{min(2r_2,R)} \frac{2r}{R^2}\left(1-\left(1-\frac{A_{2,2}(r)}{\pi R^2}\right)^{N-1}\right)dr\Bigg]\Bigg] \\
& - \Big[P_{4(1,1)} + P_{4(2,1)} + P_{4(1,2)} + P_{4(2,2)}\Big] \qquad \text{(B.11)}
\end{aligned}
$$

$P_{4(1,3)}$ is given by:

$$
\begin{aligned}
P_{4(1,3)} \;=\;& I(r_3 < r_1 + r_2)\Bigg[\int_{r=r_3}^{r_1+r_2} \frac{2r}{R^2}\left(1-\left(1-\frac{A_{2,2}(r)+2A_{1,3}(r)-2A_{1,2}(r)}{\pi R^2}\right)^{N-1}\right)dr \\
&+I(2r_2 < r_1 + r_3)\Bigg[\int_{r=r_1+r_2}^{2r_2} \frac{2r}{R^2}\left(1-\left(1-\frac{A_{2,2}(r)+2A_{1,3}(r)}{\pi R^2}\right)^{N-1}\right)dr \\
&+\int_{r=2r_2}^{min(r_1+r_3,R)} \frac{2r}{R^2}\left(1-\left(1-\frac{2A_{1,3}(r)}{\pi R^2}\right)^{N-1}\right)dr\Bigg] \\
&+I(2r_2 > r_1 + r_3)\Bigg[\int_{r=r_1+r_2}^{r_1+r_3} \frac{2r}{R^2}\left(1-\left(1-\frac{A_{2,2}(r)+2A_{1,3}(r)}{\pi R^2}\right)^{N-1}\right)dr \\
&+\int_{r=r_1+r_3}^{min(2r_2,R)} \frac{2r}{R^2}\left(1-\left(1-\frac{A_{2,2}(r)}{\pi R^2}\right)^{N-1}\right)dr\Bigg]\Bigg] \\
&+I(r_3 > r_1 + r_2)\Bigg[I(2r_2 < r_1 + r_3)\Bigg[\int_{r=r_3}^{2r_2} \frac{2r}{R^2}\left(1-\left(1-\frac{A_{2,2}(r)+2A_{1,3}(r)}{\pi R^2}\right)^{N-1}\right)dr \\
&+\int_{r=2r_2}^{min(r_1+r_3,R)} \frac{2r}{R^2}\left(1-\left(1-\frac{2A_{1,3}(r)}{\pi R^2}\right)^{N-1}\right)dr\Bigg] \\
&+I(2r_2 > r_1 + r_3)\Bigg[\int_{r=r_3}^{r_1+r_3} \frac{2r}{R^2}\left(1-\left(1-\frac{A_{2,2}(r)+2A_{1,3}(r)}{\pi R^2}\right)^{N-1}\right)dr \\
&+\int_{r=r_1+r_3}^{min(2r_2,R)} \frac{2r}{R^2}\left(1-\left(1-\frac{A_{2,2}(r)}{\pi R^2}\right)^{N-1}\right)dr\Bigg]\Bigg] \\
&-\Big[P_{4(1,1)}+P_{4(2,1)}+P_{4(1,2)}+P_{4(2,2)}+P_{4(3,1)}\Big]
\end{aligned}
\tag{B.12}
$$

$P_{4(3,2)}$ is given as follows:

$$\begin{aligned}
P_{4(3,2)} &= I(r_3 < r_1 + r_2)\left[\int_{r=r_3}^{r_1+r_2} \frac{2r}{R^2}\left(1-\left(1-\frac{A_{3,2}(r)+A_{3,1}(r)-A_{1,2}(r)}{\pi R^2}\right)^{N-1}\right)dr\right. \\
&+\int_{r=r_1+r_2}^{r_1+r_3} \frac{2r}{R^2}\left(1-\left(1-\frac{A_{3,2}(r)+A_{3,1}(r)}{\pi R^2}\right)^{N-1}\right)dr \\
&\left.+\int_{r=r_1+r_3}^{min(r_2+r_3,R)} \frac{2r}{R^2}\left(1-\left(1-\frac{A_{3,2}(r)}{\pi R^2}\right)^{N-1}\right)dr\right] \\
&+I(r_3 > r_1 + r_2)\left[\int_{r=r_3}^{r_1+r_3} \frac{2r}{R^2}\left(1-\left(1-\frac{A_{3,2}(r)+A_{3,1}(r)}{\pi R^2}\right)^{N-1}\right)dr\right. \\
&\left.+\int_{r=r_1+r_3}^{min(r_2+r_3,R)} \frac{2r}{R^2}\left(1-\left(1-\frac{A_{3,2}(r)}{\pi R^2}\right)^{N-1}\right)dr\right] \\
&-\Big[P_{4(1,1)}+P_{4(1,2)}+P_{4(2,1)}+P_{4(2,2)}+P_{4(3,1)}+P_{4(1,3)}\Big] \qquad \text{(B.13)}
\end{aligned}$$

$P_{4(2,3)}$ is calculated as follows:

$$\begin{aligned}
P_{4(2,3)} &= I(r_3 < 2r_2)\left[\int_{r=r_3}^{2r_2} \frac{2r}{R^2}\left(1-\left(1-\frac{2A_{2,3}(r)-A_{2,2}(r)}{\pi R^2}\right)^{N-1}\right)dr\right. \\
&\left.+\int_{r=2r_2}^{min(r_2+r_3,R)} \frac{2r}{R^2}\left(1-\left(1-\frac{2A_{2,3}(r)}{\pi R^2}\right)^{N-1}\right)dr\right] \\
&+I(r_3 > 2r_2)\left[\int_{r=r_3}^{min(r_2+r_3,R)} \frac{2r}{R^2}\left(1-\left(1-\frac{2A_{3,2}(r)}{\pi R^2}\right)^{N-1}\right)dr\right] \\
&-\Big[P_{4(1,1)}+P_{4(2,1)}+P_{4(1,2)}+P_{4(2,2)}+P_{4(3,1)}+P_{4(1,3)}+P_{4(3,2)}\Big] \qquad \text{(B.14)}
\end{aligned}$$

Finally, the fraction of nodes P_4 in zone-4 that can not benefit from relaying is given as follows:

$$P_4 = \frac{r_4^2-r_3^2}{R^2} - \Big[P_{4(1,1)}+P_{4(2,1)}+P_{4(1,2)}+P_{4(2,2)}+P_{4(3,1)}+P_{4(1,3)}+P_{4(3,2)}+P_{4(2,3)}\Big] \qquad \text{(B.15)}$$

In a similar way, the fraction of nodes in zone-3 that can take the advantage of relaying can be calculated as follows.

$P_{3(1,1)}$ is calculated by:

$$P_{3(1,1)} = I(r_2 < 2r_1)\left[\int_{r=r_2}^{min(2r_1,r_3)} \frac{2r}{R^2}\left(1-\left(1-\frac{A_{1,1}(r)}{\pi R^2}\right)^{N-1}\right)dr\right] \quad \text{(B.16)}$$

$P_{3(2,1)}$ is given as:

$$P_{3(2,1)} = \int_{r=r_2}^{min(r_1+r_2,r_3)} \frac{2r}{R^2}\left(1-\left(1-\frac{A_{2,1}(r)}{\pi R^2}\right)^{N-1}\right)dr - P_{3(1,1)} \quad \text{(B.17)}$$

$P_{3(1,2)}$ is given as follows:

$$\begin{aligned} P_{3(1,2)} = {} & I(r_2 < 2r_1)\left[\int_{r=r_2}^{2r_1} \frac{2r}{R^2}\left(1-\left(1-\frac{2A_{1,2}(r)-A_{1,1}(r)}{\pi R^2}\right)^{N-1}\right)dr\right. \\ & \left.+\int_{r=2r_1}^{min(r_1+r_2,r_3)} \frac{2r}{R^2}\left(1-\left(1-\frac{2A_{1,2}(r)}{\pi R^2}\right)^{N-1}\right)dr\right] \\ & +I(r_2 > 2r_1)\left[\int_{r=r_2}^{min(r_1+r_2,r_3)} \frac{2r}{R^2}\left(1-\left(1-\frac{2A_{1,2}(r)}{\pi R^2}\right)^{N-1}\right)dr\right] - \\ & \left[P_{3(1,1)}+P_{3(2,1)}\right] \end{aligned} \quad \text{(B.18)}$$

$P_{3(1,2)}$ is given as follows:

$$P_{3(2,2)} = \int_{r=r_2}^{min(2r_2,r_3)} \frac{2r}{R^2}\left(1-\left(1-\frac{A_{2,2}(r)}{\pi R^2}\right)^{N-1}\right)dr - \left[P_{3(1,1)}+P_{3(2,1)}+P_{3(1,2)}\right] \quad \text{(B.19)}$$

Finally, the fraction of nodes P_3 that uses direct transmission at data

rate R_3 is given as follows:

$$P_3 = \frac{r_3^2 - r_2^2}{R} - \left[P_{3(1,1)} + P_{3(2,1)} + P_{3(1,2)} + P_{3(2,2)} \right] \quad \text{(B.20)}$$

Bibliography

(1) *IEEE Std. 802.11-1999, Part 11: Wireless LAN Medium Access Control (MAC) and Physical Layer (PHY) specifications*, 1999.

(2) ETSI, *ETS, Radio Equipment and Systems (RES); High Performance Radio Local Area Network (HIPERLAN), Type 1 Functional Specification*, 1st ed., 1996.

(3) *ABIresearch*. (Online). Available: http://www.abiresearch.com/press/1570-Mobile+Device+Shipments+Will+Nearly+Double+Before+2015

(4) M. Heusse, F. Rousseau, G. Berger-Sabbatel, and A. Duda, "Performance anomaly of 802.11b," in *Proc. INFOCOM 2003. Twenty-Second Annual Joint Conference of the IEEE Computer and Communications. IEEE Societies*, vol. 2, 2003, pp. 836–843 vol.2.

(5) *IEEE Std. 802.11b-1999, Part 11: Wireless LAN Medium Access Control (MAC) and Physical Layer (PHY) specifications: High-Speed Physical Layer Extension in the 2.4GHz Band*, 1999.

(6) *IEEE Std 802.11a-1999, Part 11: Wireless LAN Medium Access Control (MAC) and Physical Layer (PHY) specifications: High Speed Physical Layer in the 5GHz Ban*, 1999.

(7) *IEEE Std 802.11d-2001, Part 11: Wireless LAN Medium Access Control (MAC) and Physical Layer (PHY) Specifications*, 2001.

(8) *IEEE Std 802.11e-2005, Part 11: Wireless Medium Access Control (MAC) and physical layer (PHY) specifications: Medium Access Conitrol (MAC) Enthancements for Quality of Service (QoS)*, 2005.

(9) *IEEE Std 802.11g-2003, Part 11: Wireless LAN Medium Access Control (MAC) and Physical Layer (PHY) specifications: Further Higher Data Rate Extension in the 2.4GHz Band*, 2003.

(10) *IEEE Std 802.11h-2003, Part 11: Wireless LAN Medium Access Control (MAC) and Physical Layer (PHY) Specifications: Spectrum and Transmit Power Management extensions in the 5 GHz band in Europe*, 2003.

(11) *IEEE Std 802.11i-2004, Part 11: Wireless Medium Access Control (MAC) and physical layer (PHY) specifications: Medium Access Conitrol (MAC) Enthancements for Quality of Service (QoS)*, 2005.

(12) *IEEE Std 802.11j-2004, Part 11: Wireless LAN Medium Access Control (MAC) and Physical Layer (PHY) specifications: 4.9 GHz - 5 GHz Operation in Japan*, 2004.

(13) *IEEE Std 802.11-2007, Part 11: Wireless LAN Medium Access Control (MAC) and Physical Layer (PHY) Specifications*, 2007.

(14) *IEEE Std 802.11n-2009, Part 11: Wireless LAN Medium Access Control (MAC) and Physical Layer (PHY) specifications: Enhancements for Higher Throughput*, 2009.

(15) M. S. Gast, *802.11 Wireless Networks: The Definitive Guide*. O'Reilly, 2005.

(16) (Online). Available: http://www.cisco.com/en/US/products/hw/wireless/ps4570/products_white_paper09186a00801d61a3.shtml

(17) S. M. Lars Berlemann, *Cognitive Radio and Dynamic Spectrum Access*. John Wiley & Sons, Ltd, 2009.

(18) W. Stallings, *Data and Computer Communications*, 8th ed., 2007.

(19) P. Karn, "MACA a new channel access method for packet radio," in *Computer Networking Conference*, vol. 9th, 1990, pp. 134–140.

(20) V. Bharghavan, A. Demers, S. Shenker, and L. Zhang, "MACAW: a media access protocol for wireless LAN's," in *SIGCOMM '94: Proceedings of the conference on Communications architectures, protocols and applications*. New York, NY, USA: ACM, 1994, pp. 212–225.

(21) F. Tobagi and L. Kleinrock, "Packet Switching in Radio Channels: Part II–The Hidden Terminal Problem in Carrier Sense Multiple-Access and the Busy-Tone Solution," *IEEE Trans. Commun.*, vol. 23, no. 12, pp. 1417–1433, 1975.

(22) M. Natkaniec and A. R. Pach, "A Performance Analysis of IEEE 802.11 Networks in the Presence of Hidden Stations," in *PWC '00: Proceedings of the IFIP TC6/WG6.8 Working Conference on Personal Wireless Communications*. Deventer, The Netherlands, The Netherlands: Kluwer, B.V., 2000, pp. 157–168.

(23) C. Fullmer and J. Garcia-Luna-Aceves, "Complete single-channel solutions to hidden terminal problems in wireless LANs," in *Proc. 'Towards the Knowledge Millennium' Communications ICC 97 Montreal 1997 IEEE International Conference on*, vol. 2, 1997, pp. 575–579 vol.2.

(24) C. L. Fullmer and J. J. Garcia-Luna-Aceves, "Solutions to hidden terminal problems in wireless networks," *SIGCOMM Comput. Commun. Rev.*, vol. 27, no. 4, pp. 39–49, 1997.

(25) H. Zhai and Y. Fang, "A Solution to Hidden Terminal Problem Over a Single Channel in Wireless AD HOC Networks," in *Proc. IEEE Military Communications Conference MILCOM 2006*, 2006, pp. 1–7.

(26) G. Bianchi, "IEEE 802.11-saturation throughput analysis," *IEEE Commun. Lett.*, vol. 2, no. 12, pp. 318–320, 1998.

(27) ——, "Performance Analysis of the IEEE 802.11 Distributed Coordination Function," *IEEE Journal on Selected Areas in Communications*, vol. 18, no. 3, pp. 535–547, March 2000.

(28) G. Bianchi and I. Tinnirello, "Remarks on IEEE 802.11 DCF Performance Analysis," *IEEE Communications Letters*, vol. 9, no. 8, pp. 765–767, August 2005.

(29) S. M. Bernhard H. Walke and L. Berlemann, *IEEE 802 Wireless Systems: Protocols, Multi-Hop Mesh/Relaying, Performance and Spectrum Coexistence*. John Wiley & Sons,Ltd, 2006.

(30) D. D. Coleman and D. A. Westcott, *CWNA Certified Wireless Network Administrator Official Study Guide: Exam PW0-104*, 1st ed. John Wiley & Sons,Ltd, 2009.

(31) D. Bantz and F. Bauchot, "Wireless LAN design alternatives," *IEEE Network*, vol. 8, no. 2, pp. 43–53, March–April 1994.

(32) K.-C. Chen, "Medium access control of wireless LANs for mobile computing," *IEEE Network*, vol. 8, no. 5, pp. 50–63, Sept.–Oct. 1994.

(33) R. Kohno, R. Meidan, and L. Milstein, "Spread spectrum access methods for wireless communications," *IEEE Commun. Mag.*, vol. 33, no. 1, pp. 58–67, Jan. 1995.

(34) B. Crow, I. Widjaja, L. Kim, and P. Sakai, "IEEE 802.11 Wireless Local Area Networks," *IEEE Commun. Mag.*, vol. 35, no. 9, pp. 116–126, Sept. 1997.

(35) F. J. L.-H. Asuncion Santamaria, *Wireless LAN Standards and Applications*, 1st ed. Artech House Publishers, 2001.

(36) J. N. Laneman and G. W. Wornell, "Distributed space-time coded protocols for exploiting cooperative diversity in wireless networks," *IEEE Trans. Inform. Theory*, vol. 49, pp. 2415–2425, Oct. 2003.

(37) J. N. Laneman, D. N. C. Tse, and G. W. Wornel, "Cooperative diversity in wireless networks: efficient protocols and outage behavior," *IEEE Trans. Inf. Theory*, vol. 50, no. 12, pp. 3062–3080, Dec 2004.

(38) A. Sendonaris, E. Erkip, and B. Aazhang, "User cooperation diversity-Part I: system description," *IEEE Trans. Comm.*, vol. 51, pp. 1927–1938, Nov. 2003.

(39) ——, "User cooperation diversity- Part II: implementation aspects and performance analysis," *IEEE Trans. Comm.*, vol. 51, pp. 1939–1948, Nov. 2003.

(40) T. E. Hunter and A. Nosratinia, "Cooperation diversity through coding," in *Proc. IEEE ISIT*, Laussane, Switzerland, July 2002, p. 220.

(41) M. Janani, A. Hedayat, T. E. Hunter, and A. Nostratinia, "Coded cooperation in wireless communications: space-time transmission and

iterative decoding," *IEEE Trans. Signal Processing*, vol. 52, no. 1, pp. 362–371, Feb. 2004.

(42) T. Hunter and A. Nosratinia, "Coded cooperation under slow fading, fast fading and power control," *Asilomar Conferencce on Signals, Systems, and Computers*, Nov. 2002.

(43) T. Hunter, S. Sanayei, and A. Nosratinia, "Outage analysis of coded cooperation," *IEEE Trans. Info. Theory*, vol. 52, pp. 375–391, Feb. 2006.

(44) G. Kramer, I. Marić, and R. D. Yates, "Cooperative Communications," *Found. Trends Netw.*, vol. 1, no. 3, pp. 271–425, 2006.

(45) J.-S. Liu and Y. chang Wong, "A relay-based multirate protocol in infrastructure wireless LANs," in *Proc. 12th IEEE International Conference on Networks (ICON 2004)*, vol. 1, 16–19 Nov. 2004, pp. 201–206.

(46) H. Zhu and G. Cao, "On Improving the Performance of IEEE 802.11 with Relay-Enabled PCF," *Mobile Networking and Applications (MONET)*, vol. 9, pp. 423–434, 2004.

(47) ——, "rDCF: a relay-enabled medium access control protocol for wireless ad hoc networks," in *Proc. IEEE 24th Annual Joint Conference of the IEEE Computer and Communications Societies INFOCOM 2005*, vol. 1, 2005, pp. 12–22 vol. 1.

(48) ——, "rDCF: A Relay-Enabled Medium Access Control Protocol for Wireless Ad Hoc Networks," vol. 5, no. 9, pp. 1201–1214, 2006.

(49) P. Liu, Z. Tao, and S. Panwar, "A cooperative MAC protocol for wireless local area networks," in *Proc. IEEE International Conference on Communications ICC 2005*, vol. 5, 2005, pp. 2962–2968 Vol. 5.

(50) P. Liu, Z. Tao, S. Narayanan, T. Korakis, and S. S. Panwar, "CoopMAC: A Cooperative MAC for Wireless LANs," *IEEE Journal on Selected Areas in Communications*, vol. 25, no. 2, pp. 340–354, February 2007.

(51) C.-T. Chou, J. Yang, and D. Wang, "Cooperative MAC Protocol with Automatic Relay Selection in Distributed Wireless Networks," in *PERCOMW '07: Proceedings of the Fifth IEEE International Conference on Pervasive Computing and Communications Workshops*. Washington, DC, USA: IEEE Computer Society, 2007, pp. 526–531.

(52) H. Shan, W. Zhuang, and Z. Wang, "Distributed cooperative MAC for multihop wireless networks," *IEEE Commun. Mag.*, vol. 47, no. 2, pp. 126–133, February 2009.

(53) T. Korakis, S. Narayanan, A. Bagri, and S. Panwar, "Implementing a Cooperative MAC Protocol for Wireless LANs," in *Proc. IEEE International Conference on Communications ICC '06*, vol. 10, 2006, pp. 4805–4810.

(54) O. Alay, Z. Xu, T. Korakis, Y. Wang, and S. Panwar, "Implementing a Cooperative MAC Protocol for Wireless Video Multicast," in *Proc. IEEE Wireless Communications and Networking Conference WCNC 2009*, 2009, pp. 1–6.

(55) A. Bletsas, A. Khisti, D. Reed, and A. Lippman, "A simple Cooperative diversity method based on network path selection," *IEEE J. Select. Areas Commun.*, vol. 24, no. 3, pp. 659–672, 2006.

(56) E. Ziouva and T. Antonakopoulos, "CSMA/CA performance under high traffic conditions: throughput and delay analysis," *Computer Communications*, vol. 25, no. 3, pp. 313–321, Feb. 2002.

(57) Y. Xiao, "A simple and effective priority scheme for IEEE 802.11," *IEEE Commun. Lett.*, vol. 7, no. 2, pp. 70–72, 2003.

(58) M. Ergen and P. Varaiya, "Throughput analysis and admission control for IEEE 802.11a," *Mob. Netw. Appl.*, vol. 10, no. 5, pp. 705–716, 2005.

(59) H. Wu, Y. Peng, K. Long, S. Cheng, and J. Ma, "Performance of reliable transport protocol over IEEE 802.11 wireless LAN: analysis and enhancement," in *Proc. IEEE Twenty-First Annual Joint Conference of the IEEE Computer and Communications Societies INFOCOM 2002*, vol. 2, 2002, pp. 599–607.

(60) P. Chatzimisios, A. Boucouvalas, and V. Vitsas, "Influence of channel BER on IEEE 802.11 DCF," *Electronics Letters*, vol. 39, no. 23, pp. 1687–9–, 2003.

(61) N. Gupta and P. R. Kumar, "A performance analysis of the 802.11 wireless LAN medium access control," *Communications in Information and Systems*, vol. 3, no. 4, pp. 279–304, September 2004.

(62) X. Dong and P. Varaiya, "Saturation throughput analysis of IEEE 802.11 wireless LANs for a lossy channel," *IEEE Commun. Lett.*, vol. 9, no. 2, pp. 100–102, 2005.

(63) Q. Ni, T. Li, T. Turletti, and Y. Xiao, "Saturation throughput analysis of error-prone 802.11 wireless networks: Research Articles," *Wirel. Commun. Mob. Comput.*, vol. 5, no. 8, pp. 945–956, 2005.

(64) H. C. Lee, "Impact of Bit Errors on the DCF Throughput in Wireless LAN over Ricean Fading Channels," in *Proc. International Conference on Digital Telecommunications, ICDT '06*, 2006, pp. 37–37.

(65) Y. Zheng, K. Lu, D. Wu, and Y. Fang, "Performance Analysis of IEEE 802.11 DCF in Imperfect Channels," *IEEE Trans. Veh. Technol.*, vol. 55, no. 5, pp. 1648–1656, 2006.

(66) F. Daneshgaran, M. Laddomada, F. Mesiti, M. Mondin, and M. Zanolo, "Saturation throughput analysis of IEEE 802.11 in the presence of non ideal transmission channel and capture effects," *IEEE Trans. Commun.*, vol. 56, no. 7, pp. 1178–1188, 2008.

(67) G. R. Cantieni, Q. Ni, C. Barakat, and T. Turletti, "Performance analysis under finite load and improvements for multirate 802.11," *Comput. Commun.*, vol. 28, no. 10, pp. 1095–1109, 2005.

(68) K. Duffy, D. Malone, and D. Leith, "Modeling the 802.11 distributed coordination function in non-saturated conditions," *IEEE Commun. Lett.*, vol. 9, no. 8, pp. 715–717, Aug 2005.

(69) Y. S. Liaw, A. Dadej, and A. Jayasuriya, "Performance Analysis of IEEE 802.11 DCF under Limited Load," in *Proc. Asia-Pacific Conference on Communications*, 5–5 Oct. 2005, pp. 759–763.

(70) J. Sudarev, L. White, and S. Perreau, "Performance analysis of 802.11 CSMA/CA for infrastructure networks under finite load conditions," in *Proc. 14th IEEE Workshop on Local and Metropolitan Area Networks LANMAN 2005*, 18–18 Sept. 2005, pp. 6pp.–6.

(71) F. Daneshgaran, M. Laddomada, F. Mesiti, and M. Mondin, "On the Linear Behaviour of the Throughput of IEEE 802.11 DCF in Non-Saturated Conditions," *IEEE Commun. Lett.*, vol. 11, no. 11, pp. 856–858, November 2007.

(72) E. Daneshgaran, M. Laddomada, F. Mesiti, and M. Mondin, "A Model of the IEEE 802.11 DCF in Presence of Non Ideal Transmission Channel and Capture Effects," in *Proc. IEEE Global Telecommunications Conference GLOBECOM '07*, 26–30 Nov. 2007, pp. 5112–5116.

(73) D. Malone, K. Duffy, and D. Leith, "Modeling the 802.11 Distributed Coordination Function in Nonsaturated Heterogeneous Conditions," *IEEE/ACM Trans. Networking*, vol. 15, no. 1, pp. 159–172, Feb. 2007.

(74) N. Dao and R. Malaney, "A New Markov Model for Non-Saturated 802.11 Networks," in *Proc. 5th IEEE Consumer Communications and Networking Conference CCNC 2008*, 10–12 Jan. 2008, pp. 420–424.

(75) F. Daneshgaran, M. Laddomada, F. Mesiti, and M. Mondin, "Unsaturated Throughput Analysis of IEEE 802.11 in Presence of Non Ideal Transmission Channel and Capture Effects," *IEEE Trans. Wireless Commun.*, vol. 7, no. 4, pp. 1276–1286, April 2008.

(76) K. Ghaboosi, M. Latva-aho, and Y. Xiao, "Finite Load Analysis of IEEE 802.11 Distributed Coordination Function," in *Proc. IEEE International Conference on Communications ICC '08*, 19–23 May 2008, pp. 2561–2565.

(77) H. Y. Hwang, J. K. Kwon, J. W. Yang, and D. K. Sung, "Goodput analysis of a WLAN with hidden nodes under a non-saturated condition," *IEEE Trans. Wireless Commun.*, vol. 8, no. 5, pp. 2259–2264, May 2009.

(78) F. Cali, M. Conti, and E. Gregori, "Dynamic tuning of the IEEE 802.11 protocol to achieve a theoretical throughput limit," *IEEE/ACM Trans. Networking*, vol. 8, no. 6, pp. 785–799, Dec. 2000.

(79) A. Khalaj, N. Yazdani, and M. Rahgozar, "The effect of decreasing CW size on performance IEEE 802.11 DCF," in *Proc. 13th IEEE International Conference on Networks Jointly held with the 2005 IEEE 7th Malaysia International Conference on Communication*, vol. 1, 16–18 Nov. 2005, p. 5pp.

(80) Y. Peng, S.-D. Cheng, and J.-L. Chen, "RSAD: a robust distributed contention-based adaptive mechanism for IEEE 802.11 wireless LANs," *J. Comput. Sci. Technol.*, vol. 20, no. 2, pp. 282–288, 2005.

(81) Q. Xia and M. Hamdi, "Contention Window Adjustment for IEEE 802.11 WLANs: A Control-Theoretic Approach," in *Proc. IEEE International Conference on Communications*, vol. 9, June 2006, pp. 3923–3928.

(82) H. Anouar and C. Bonnet, "Optimal Constant-Window Backoff Scheme for IEEE 802.11 DCF in Single-Hop Wireless Networks Under Finite Load Conditions," *Wirel. Pers. Commun.*, vol. 43, no. 4, pp. 1583–1602, 2007.

(83) A. Khalaj, N. Yazdani, and M. Rahgozar, "Effect of the contention window size on performance and fairness of the IEEE 802.11 standard," *Wirel. Pers. Commun.*, vol. 43, no. 4, pp. 1267–1278, 2007.

(84) S. Choudhury and J. Gibson, "Throughput Optimization for Wireless LANs in the Presence of Packet Error Rate Constraints," *IEEE Commun. Lett.*, vol. 12, no. 1, pp. 11–13, January 2008.

(85) Y. Xiao and J. Rosdahl, "Throughput and delay limits of IEEE 802.11," *IEEE Commun. Lett.*, vol. 6, no. 8, pp. 355–357, Aug. 2002.

(86) M. M. Carvalho and J. J. Garcia-Luna-Aceves, "Delay Analysis of IEEE 802.11 in Single-Hop Networks," in *ICNP '03: Proceedings of the 11th IEEE International Conference on Network Protocols*. Washington, DC, USA: IEEE Computer Society, 2003, p. 146.

(87) P. Chatzimisios, A. Boucouvalas, and V. Vitsas, "IEEE 802.11 packet delay–a finite retry limit analysis," in *IEEE Global Telecommunications Conference (GLOBECOM '03)*, vol. 2, San Francisco, Calif, USA, December 2003., Dec. 2003, pp. 950–954.

(88) Z. Hadzi-Velkov and B. Spasenovski, "Saturation throughput - delay analysis of IEEE 802.11 DCF in fading channel," in *Proc. IEEE International Conference on Communications ICC '03*, vol. 1, 2003, pp. 121–126 vol.1.

(89) G. Wang, Y. Shu, L. Zhang, and O. Yang, "Delay analysis of the IEEE 802.11 DCF," in *Proc. 14th IEEE on Personal, Indoor and Mobile Radio Communications PIMRC 2003*, vol. 2, 2003, pp. 1737–1741.

(90) H. Zhai and Y. Fang, "Performance of wireless LANs based on IEEE 802.11 MAC protocols," in *Proc. 14th IEEE on Personal, Indoor and Mobile Radio Communications PIMRC 2003*, vol. 3, 2003, pp. 2586–2590.

(91) I. Vukovic and N. Smavatkul, "Delay analysis of different backoff algorithms in IEEE 802.11," in *Proc. VTC2004-Fall Vehicular Technology Conference 2004 IEEE 60th*, vol. 6, 2004, pp. 4553–4557 Vol. 6.

(92) P. Raptis, V. Vitsas, K. Paparrizos, P. Chatzimisios, and A. C. Boucouvalas, "Packet Delay Distribution of the IEEE 802.11 Distributed Coordination Function," in *WOWMOM '05: Proceedings of the Sixth IEEE*

International Symposium on World of Wireless Mobile and Multimedia Networks. Washington, DC, USA: IEEE Computer Society, 2005, pp. 299–304.

(93) A. Zanella and F. De Pellegrini, "Statistical characterization of the service time in saturated IEEE 802.11 networks," *IEEE Commun. Lett.*, vol. 9, no. 3, pp. 225–227, March 2005.

(94) A. Banchs, P. Serrano, and A. Azcorra, "End-to-end delay analysis and admission control in 802.11 DCF WLANs," *Comput. Commun.*, vol. 29, no. 7, pp. 842–854, 2006.

(95) B. Sikdar, "An Analytic Model for the Delay in IEEE 802.11 PCF MAC-Based Wireless Networks," *IEEE Trans. Wireless Commun.*, vol. 6, no. 4, pp. 1542–1550, April 2007.

(96) G. Sun and B. Hu, "Delay Analysis of IEEE 802.11 DCF with Back-off Suspension," in *FGCN '07: Proceedings of the Future Generation Communication and Networking*. Washington, DC, USA: IEEE Computer Society, 2007, pp. 148–151.

(97) J. S. Vardakas, I. Papapanagiotou, M. D. Logothetis, and S. A. Kotsopoulos, "On the End-to-End Delay Analysis of the IEEE 802.11 Distributed Coordination Function," in *ICIMP '07: Proceedings of the Second International Conference on Internet Monitoring and Protection*. Washington, DC, USA: IEEE Computer Society, 2007, p. 16.

(98) O. Tickoo and B. Sikdar, "Modeling queueing and channel access delay in unsaturated IEEE 802.11 random access MAC based wireless networks," *IEEE/ACM Trans. Netw.*, vol. 16, no. 4, pp. 878–891, 2008.

(99) A. Chockalingam, W. Xu, M. Zorzi, and L. Milstein, "Energy efficiency analysis of a multichannel wireless access protocol," *Proceedings of IEEE International Symposium Personal, Indoor and Mobile Radio Communications (PIMRC)*, vol. 3, pp. 1096–1100, 1998.

(100) P. Lettieri and M. Srivastava, "Adaptive frame length control for improving wireless network link throughput, range and energy efficiency," *Proceedings of the IEEE INFOCOM*, vol. 2, pp. 564–571, 1998.

(101) R. Bruno, M. Conti, and E. Gregori, "Optimization of efficiency and energy consumption in p-persistent CSMA-based wireless LANs," vol. 1, no. 1, pp. 10–31, Jan.–March 2002.

(102) A. Zanella and F. D. Pellegrini, "Mathematical Analysis of IEEE 802.11 Energy Efficiency," in *Wireless Personal Multimedia Communications WPMC'04*, Abano Terme (Padova), Sept. 2004.

(103) J. Yin, X. Wang, and D. Agrawal, "Energy efficiency evaluation of wireless LAN over bursty error channel," in *Global Telecommunications Conference, 2005. GLOBECOM '05. IEEE*, vol. 6, 2-2 Dec. 2005, pp. 5pp.–3632.

(104) A. M. Tsung-Han Lee and B. Zhou, "Modeling Energy Consumption in error-prone IEEE 802.11-based Wireless Ad-Hoc Networks," in *9th IFIP/IEEE International Conference on Management of Multimedia and Mobile Networks & Services, MMNS 2006*, Dublin, Ireland, 25-27 Oct. 2006.

(105) X. Wang and D. Agrawal, "Analysis and optimization of energy efficiency in 802.11 distributed coordination function," in *Proc. IEEE In-*

ternational Conference on Performance, Computing, and Communications, 2004, pp. 707–712.

(106) X. Wang, J. Yin, and D. P. Agrawal, "Analysis and optimization of the energy efficiency in the 802.11 DCF," *Mob. Netw. Appl.*, vol. 11, no. 2, pp. 279–286, 2006.

(107) O. Bouattay, T. Chahed, M. Frikha, and S. Tabbane, "Modeling and Analysis of Energy Consumption in IEEE802.11e Networks," in *Proc. Fourth European Conference on Universal Multiservice Networks ECUMN '07*, Feb. 2007, pp. 145–151.

(108) W.-K. Kuo, "Energy efficiency modeling for IEEE 802.11 DCF system without retry limits," *Comput. Commun.*, vol. 30, no. 4, pp. 856–862, 2007.

(109) E. Rantala, A. Karppanen, S. Granlund, and P. Sarolahti, "Modeling energy efficiency in wireless internet communication," in *MobiHeld '09: Proceedings of the 1st ACM workshop on Networking, systems, and applications for mobile handhelds*. New York, NY, USA: ACM, 2009, pp. 67–68.

(110) Y. Xu, J. C. S. Lui, and D.-M. Chiu, "Improving energy efficiency via probabilistic rate combination in 802.11 multi-rate wireless networks," *Ad Hoc Netw.*, vol. 7, no. 7, pp. 1370–1385, 2009.

(111) Y. Xiao, "Enhanced DCF of IEEE 802.11e to support QoS," in *Proc. IEEE Wireless Communications and Networking WCNC 2003*, vol. 2, 2003, pp. 1291–1296 vol.2.

(112) Z.-n. Kong, D. Tsang, B. Bensaou, and D. Gao, "Performance analysis of IEEE 802.11e contention-based channel access," *IEEE J. Select. Areas Commun.*, vol. 22, no. 10, pp. 2095–2106, 2004.

(113) J. Robinson and T. Randhawa, "Saturation throughput analysis of IEEE 802.11e enhanced distributed coordination function," *IEEE J. Select. Areas Commun.*, vol. 22, no. 5, pp. 917–928, 2004.

(114) I. Inan, F. Keceli, and E. Ayanoglu, "Saturation Throughput Analysis of the 802.11e Enhanced Distributed Channel Access Function," in *Proc. IEEE International Conference on Communications ICC '07*, 2007, pp. 409–414.

(115) S. Mangold, G. Hiertz, and B. Walke, "IEEE 802.11e wireless LAN - resource sharing with contention based medium access," in *Proc. 14th IEEE on Personal, Indoor and Mobile Radio Communications PIMRC 2003*, vol. 3, 2003, pp. 2019–2026 vol.3.

(116) Y. Xiao, "Performance analysis of IEEE 802.11e EDCF under saturation condition," in *Proc. IEEE International Conference on Communications*, vol. 1, 2004, pp. 170–174.

(117) Q. Ni, "Performance analysis and enhancements for IEEE 802.11e wireless networks," *IEEE Network*, vol. 19, no. 4, pp. 21–27, 2005.

(118) Y. Xiao, "Performance analysis of priority schemes for IEEE 802.11 and IEEE 802.11e wireless LANs," *IEEE Trans. Wireless Commun.*, vol. 4, no. 4, pp. 1506–1515, 2005.

(119) Y. Chen, Q.-A. Zeng, and D. Agrawal, "Performance analysis of IEEE 802.11e enhanced distributed coordination function," in *Proc.*

ICON2003 Networks The 11th IEEE International Conference on, 2003, pp. 573–578.

(120) H. Zhu and I. Chlamtac, "An analytical model for IEEE 802.11e EDCF differential services," in *Proc. 12th International Conference on Computer Communications and Networks ICCCN 2003*, 2003, pp. 163–168.

(121) J. Hui and M. Devetsikiotis, "Performance analysis of IEEE 802.11e EDCA by a unified model," in *Proc. IEEE Global Telecommunications Conference GLOBECOM '04*, vol. 2, 2004, pp. 754–759 Vol.2.

(122) ——, "A unified model for the performance analysis of IEEE 802.11e EDCA," *IEEE Trans. Commun.*, vol. 53, no. 9, pp. 1498–1510, 2005.

(123) J. Tantra, C. H. Foh, and A. Mnaouer, "Throughput and delay analysis of the IEEE 802.11e EDCA saturation," in *Proc. IEEE International Conference on Communications ICC 2005*, vol. 5, 2005, pp. 3450–3454.

(124) H. Zhu and I. Chlamtac, "Performance analysis for IEEE 802.11e EDCF service differentiation," *IEEE Trans. Wireless Commun.*, vol. 4, no. 4, pp. 1779–1788, 2005.

(125) Z. Tao and S. Panwar, "Throughput and delay analysis for the IEEE 802.11e enhanced distributed channel access," *IEEE Trans. Commun.*, vol. 54, no. 4, pp. 596–603, April 2006.

(126) L. Xiong and G. Mao, "Performance Analysis of IEEE 802.11 DCF with Data Rate Switching," *IEEE Commun. Lett.*, vol. 11, no. 9, pp. 759–761, 2007.

(127) ——, "Saturated throughput analysis of IEEE 802.11e EDCA," *Comput. Netw.*, vol. 51, no. 11, pp. 3047–3068, 2007.

(128) X. Ma and X. Chen, "Performance Analysis of IEEE 802.11 Broadcast Scheme in Ad Hoc Wireless LANs," *IEEE Trans. Veh. Technol.*, vol. 57, no. 6, pp. 3757–3768, 2008.

(129) H. Y. Hwang, S. J. Kim, D. K. Sung, and N.-O. Song, "Performance Analysis of IEEE 802.11e EDCA With a Virtual Collision Handler," *IEEE Trans. Veh. Technol.*, vol. 57, no. 2, pp. 1293–1297, 2008.

(130) A. Kamerman and L. Monteban, "WaveLAN-II: A High-Performance Wireless LAN for the Unlicensed Band," *Bell Labs Technical Journal*, vol. 2, no. 3, pp. 118–133, August 1997.

(131) G. Holland, N. Vaidya, and P. Bahl, "A rate-adaptive MAC protocol for multi-Hop wireless networks," in *MobiCom '01: Proceedings of the 7th annual international conference on Mobile computing and networking*. New York, NY, USA: ACM, 2001, pp. 236–251.

(132) D. Qiao and S. Choi, "Goodput enhancement of IEEE 802.11a wireless LAN via link adaptation," in *Proc. IEEE International Conference on Communications ICC 2001*, vol. 7, 11–14 June 2001, pp. 1995–2000.

(133) D. Qiao, S. Choi, and K. Shin, "Goodput analysis and link adaptation for IEEE 802.11a wireless LANs," vol. 1, no. 4, pp. 278–292, Oct.–Dec. 2002.

(134) J.-L. Wu, H.-H. Liu, and Y.-J. Lung, "An adaptive multirate IEEE 802.11 wireless LAN," in *Proc. 15th International Conference on Information Networking*, 31 Jan.–2 Feb. 2001, pp. 411–418.

(135) B. Sadeghi, V. Kanodia, A. Sabharwal, and E. Knightly, "Opportunistic media access for multirate ad hoc networks," in *MobiCom '02:*

Proceedings of the 8th annual international conference on Mobile computing and networking. New York, NY, USA: ACM, 2002, pp. 24–35.

(136) ——, "OAR: An Opportunistic Autorate Media Access Protocol for Ad Hoc Networks," *Wireless Networks*, vol. 11, no. 1-2, pp. 39–53, 2005.

(137) M. Lacage, M. H. Manshaei, and T. Turletti, "IEEE 802.11 rate adaptation: a practical approach," in *MSWiM '04: Proceedings of the 7th ACM international symposium on Modeling, analysis and simulation of wireless and mobile systems*. New York, NY, USA: ACM, 2004, pp. 126–134.

(138) L.-C. Wang, Y.-W. Lin, and W.-C. Liu, "Cross-layer goodput analysis for rate adaptive IEEE 802.11a WLAN in the generalized Nakagami fading channel," in *Proc. IEEE International Conference on Communications*, vol. 4, 20–24 June 2004, pp. 2312–2316.

(139) E. Ancillotti, R. Bruno, and M. Conti, "Design and performance evaluation of throughput-aware rate adaptation protocols for IEEE 802.11 wireless networks," *Perform. Eval.*, vol. 66, no. 12, pp. 811–825, 2009.

(140) Y. Rong, A. Y. Teymorian, L. Ma, X. Cheng, and H.-A. Choi, "A novel rate adaptation scheme for 802.11 networks," *Trans. Wireless. Comm.*, vol. 8, no. 2, pp. 862–870, 2009.

(141) H. Wang and C.-C. Tsou, "A Rate Adaptation Scheme with Loss Differentiation for WLAN," in *HIS '09: Proceedings of the 2009 Ninth International Conference on Hybrid Intelligent Systems*. Washington, DC, USA: IEEE Computer Society, 2009, pp. 108–112.

(142) P. Liu, Z. Tao, Z. Lin, E. Erkip, and S. Panwar, "Cooperative Wireless Communications: A cross-Layer Approach," *IEEE Wireless Commun. Mag.*, vol. 13, no. 4, pp. 84–92, Aug. 2006.

(143) W. Z. H. Shan, P. Wang and Z. Wang, "Cross-layer cooperative triple busy tone multiple access for wireless networks," in *Proc. IEEE Globecom'08*, Nov.-Dec. 2008.

(144) F. Daneshgaran, M. Laddomada, F. Mesiti, and M. Mondin, "Modelling and Analysis of the Distributed Coordination Function of IEEE 802.11 with Multirate Capability," in *Proc. IEEE Wireless Communications and Networking Conference WCNC 2008*, 2008, pp. 1344–1349.

(145) E. N. Gilbert, *Capacity of a burst-noise channel*. Bell Syst. Tech. J., Sept. 1960, vol. 39.

(146) E. O. Elliott, *Estimates of error rates for codes on burst-noise channels*. Bell Syst. Tech. J., Sept. 1963, vol. 42.

(147) J. Norris, *Markov Chains, Cambridge Series in Statistical and Probabilistic Mathematics*. Cambridge U. Press, 1997.

(148) *Objective Modular Network Testbed in C++ (OMNET++)*. (Online). Available: http://www.omnetpp.org/index.php

(149) T. G. Robertazzi, *Computer Networks and Systems Queueing Theory and Performance Evaluation*, 3rd ed. Springer-Verlag, 2000.

(150) L. Cai, X. Shen, J. Mark, L. Cai, and Y. Xiao, "Voice capacity analysis of WLAN with unbalanced traffic," *IEEE Trans. Veh. Technol.*, vol. 55, no. 3, pp. 752–761, May 2006.

(151) A. Chan and S. C. Liew, "VoIP Capacity over Multiple IEEE 802.11 WLANs," in *Proc. IEEE International Conference on Communications ICC '07*, 24–28 June 2007, pp. 3251–3258.

(152) S. Ahmed, X. Jiang, and S. Horiguchi, "Voice Capacity Analysis and Enhancement in Wireless LAN," in *Proc. IEEE Wireless Communications and Networking Conference WCNC 2008*, March 31 2008–April 3 2008, pp. 2153–2157.

(153) Y. K. Hongqiang Zhai and Y. Fang, "Performance analysis of IEEE 802.11 MAC protocols in wireless LANs:Research Articles," *Wireless Communications and Mobile Computing*, vol. 4, pp. 917–931, 2004.

(154) D. Bertsekas and R. Gallager, *Data Networks*, 2nd ed. Prentice Hall, 1992.

(155) T. Rappaport, *Wireless Communications: Principle and Practice*. Prentice Hall, 1996.

(156) O. C. Ibe, *Markov Processes for Stochastic Modeling*. Academic Press, September 2008.

(157) L. M. Feeney, D. Hollos, M. Kubisch, S. Mengesha, and H. Karl, "A Geometric Derivation of the Probability of Finding a Relay in Multi-rate Networks," *Networking 2004, networking technologies, services, and protocols; performance of computer and communication networks; mobile and wireless communications*, pp. 1312–1317, 2004.